2-2011

Advanced Oxidation of Drinking Water using Ultraviolet Light and Alternative Solid Forms of Hydrogen Peroxide

Zachary F. Monge

ADVANCED OXIDATION OF DRINKING WATER USING ULTRAVIOLET LIGHT
AND ALTERNATIVE SOLID FORMS OF HYDROGEN PEROXIDE

A Masters Project Presented

By

ZACHARY F. MONGE

Submitted to the Department of Civil and Environmental Engineering of the University
of Massachusetts Amherst in partial fulfillment of the requirements for the degree of

MASTER OF SCIENCE IN ENVIRONMENTAL ENGINEERING

February 2011

Department of Environmental and Water Resources Engineering

ADVANCED OXIDATION OF DRINKING WATER USING ULTAVIOLET LIGHT AND ALTERNATIVE SOLID FORMS OF HYDROGEN PEROXIDE
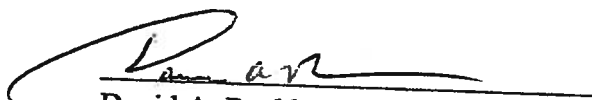
A Masters Project Presented

By

ZACHARY F. MONGE

Approved as to style and content by:

_____
Erik J. Rosenfeldt, Chairperson

_____
David A. Reckhow, Member

_____
Chul Park, Member

_____
David P. Ahlfeld
Graduate Program Direction, MSEVE
Civil and Environmental Engineering Department

ACKNOWLEDGEMENTS

ABSTRACT

ADVANCED OXIDATION OF DRINKING WATER USING ULTRAVIOLET LIGHT

AND ALTERNATIVE SOLID FORMS OF HYDROGEN PEROXIDE

FEBRUARY 2011

ZACHARY F. MONGE

B.S. ENVIRONMENTAL ENGINEERING, UNIVERSITY OF CONNECTICUT

M.S. ENVIRONMENTAL ENGINEERING CANDIDATE, UNIVERSITY OF

MASSACHUSETTS AMHERST

Directed by: Professor Erik J. Rosenfeldt

With the increasing focus on removing emerging, unregulated drinking water contaminants, the use of advanced oxidation processes (AOPs) has become more prevalent. A commonly used AOP is the ultraviolet light/hydrogen peroxide (UV/H_2O_2) AOP. This process utilizes the formation of hydroxyl radicals to oxidize contaminants to less harmful forms. In this analysis, two alternative solid forms of H_2O_2, sodium perborate (SPB) and sodium percarbonate (SPC) were used as sources of H_2O_2 in the UV/H_2O_2 AOP. The potential advantage of SPB and SPC is that they are solids in nature, and as a result, the shipping costs and shipping energy requirements can be reduced significantly compared to that of liquid H_2O_2.

The yields of active H_2O_2 via SPB and SPC were investigated in deionized (DI) water and three natural water sources from the Northampton, MA Water Filtration Plant. In DI water, the active yields of H_2O_2 via SPB and SPC were much higher than in the

natural water sources. The findings of this analysis indicate that both SPB and SPC are viable sources of H_2O_2, especially in waters that are treated to reduce the background carbonate concentration.

In highly finished waters similar to DI water, it is expected that the use of SPB and SPC will result in reduced oxidation rates of drinking water contaminants. Therefore, the use of SPB and SPC as H_2O_2 sources in the UV/H_2O_2 AOP in highly finished waters is not encouraged. In natural water sources, SPB and SPC appear to be viable alternatives to liquid H_2O_2 for use in the UV/H_2O_2 AOP up to active H_2O_2 concentrations of 5mg/L.

Using SPB and SPC has the potential for significant cost savings depending on the source of the water used in the drinking water treatment process. For facilities with surface waters as the source water, significant cost savings are possible. However water reclamation and reuse facilities have high purity source waters and SPB and SPC as sources of H_2O_2 are more costly alternatives. The reduction in treatment facilities carbon footprints' associated with shipping H_2O_2 is largely dependent on the location of the chemical production facilities of each reagent.

TABLE OF CONTENTS

LIST OF TABLES

LIST OF FIGURES

LIST OF SYMBOLS

A = ultraviolet absorbance of sample (cm^{-1})

Alk = measured alkalinity of sample (M)

b = pathway length of cuvette (cm)

c = concentration of absorbing species (M)

C_t/C_0 = relative concentration (unitless)

d = depth of exposed sample in UV exposure dish (cm)

DF = dilution factor of active hydrogen peroxide yield determinations (unitless)

e = measured irradiance by radiometer (W/m^2)

E = intensity of UV light on exposed samples (W/m^2)

$\bar{E}$ = average intensity of UV light on exposed samples (W/m^2)

K_w = acid dissociation constant of water (10^{-14})

K_2 = second acid dissociation constant of carbonic acid ($10^{-10.3}$)

$k_{x,\cdot OH}$ = rate of hydroxyl radical scavenging by species x ($M^{-1}s^{-1}$)

k' = methylene blue first order decay rate constant (cm^2mJ^{-1})

PF = Petri Factor of UV exposure dish (unitless)

pH = measured pH of sample (pH units)

RF = Reflection Factor of UV exposure dish (unitless)

SF = radiometer Sensor Factor (unitless)

t = time (s)

UV_{254} = ultraviolet light absorbance at 254nm (cm^{-1})

λ_{max} = maximum wavelength (cm)

ε_{max} = maximum molar absorptivity (Mcm^{-1})

[x] = concentration of species x (M)

LIST OF ABBREVIATIONS

AOPs = advanced oxidation processes

CCL2 = US EPA's Second Drinking Water Contaminant Candidate List

BAC = biological activated carbon

BDOC = biodegradability

BO_3^{3-} = borate ion

B_T = total borate

Cl^- = chloride ion

CO_3^{2-} = carbonate ion

C_T = total carbonate

DBP = disinfection byproduct

DI = deionized

GAC = granular activated carbon

HCO_3^- = bicarbonate ion

HOO^- = deprotonated form of hydrogen peroxide

H_2O_2 = hydrogen peroxide

H_3BO_3 = boric acid

$H_2BO_3^-$ = deprotonated form of boric acid

H_2TiO_4 = pertitanic acid

HCl = hydrochloric acid

H_2CO_3 = carbonic acid

H^+ = hydrogen ion

HRL = health reference level

$h\nu$ = ultraviolet irradiation

I_2 = iodine

I⁻ = iodine ion

I_3^- = tri-iodide ion

KI = potassium iodide

$KMnO_4$ = potassium permanganate

KHP = potassium phthalate

LP-UV = low pressure ultraviolet light

MB = methylene blue

n-BuCl = n-butyl chloride

$NaBO_2$ = sodium metaborate

$NaBO_3$ = sodium perborate

Na_2CO_3 = sodium carbonate

$Na_2CO_3\text{-}1.5H_2O_2$ = sodium percarbonate

NaOH = sodium hydroxide

$(NH_4)_6Mo_7O_{24}$ = ammonium molybdate

NOM = natural organic matter

NPDWR = national public drinking water regulation

O_2 = oxygen

·OH = hydroxyl radical

$·OH_2$ = peroxyl radical

SDWRP = South District Water Reclamation Plant

SPB = sodium perborate

SPC = sodium percarbonate

TiO_2 = titanium dioxide

TOC = total organic carbon

UV = ultraviolet light

CHAPTER 1: INTRODUCTION

Advanced Oxidation Processes (AOPs) have been identified as an effective way to control emerging unregulated contaminants in drinking water. One AOP used in drinking water and water reuse is a combination of ultraviolet (UV) light and hydrogen peroxide (H_2O_2). This combination yields hydroxyl radicals ($\cdot OH$) which are powerful oxidants capable of transforming harmful drinking water contaminants into potentially less harmful forms. It has been shown that the UV/H_2O_2 AOP has the potential to oxidize many organic and inorganic contaminants including disinfection byproduct (DBP) precursors, infectious organisms and humic acids. (Toor and Mohseni, 2006, Wang et al., 1999, Hsiang and Gurol, 1995 and US EPA, 2007). Complete oxidation of contaminants to carbon dioxide, water, and inorganic ions rarely occurs in practice; rather less harmful intermediates are formed.

An issue with the UV/H_2O_2 AOP is the treatment costs. Rosenfeldt et al. (2006, 2008) found that the energy requirements of UV light and H_2O_2 contribute equally to production of hydroxyl radicals. Therefore, it is potentially possible to decrease the energy requirements and treatment costs associated with H_2O_2 by using alternative solid forms of H_2O_2. The purpose of this study is to examine if this cost can be significantly reduced by using two solid chemicals, sodium perborate ($NaBO_3$, abbreviated as SPB) and sodium percarbonate (Na_2CO_3-$1.5H_2O_2$, abbreviated as SPC), that when dissolved in water form H_2O_2 active species.

1.0 Sodium Perborate and Sodium Percarbonate

SPB and SPC are two granular solid chemicals that when added to water yield H_2O_2. Compared to liquid hydrogen peroxide, SPB and SPC have exceptional storage stability and no shock sensitivity (McKillop and Sanderson, 1995). McKillop and Sanderson (1995) also report that both reagents are non-toxic and neither reagent nor their resulting products are considered harmful to humans or the environment in low concentrations. SPB is used in many commonly used household materials, including mouth washes, cleaning fluids and bleaches (Borax, 2005 and European Chemical Industry Council, 1997). SPC also has many household uses including detergents and toothpaste (McKillop and Sanderson, 1995 and US Department of Health and Human Services, 2010).

SPB is available in mono-, tri- and tetra-hydrate forms, but for the purposes of this discussion and experimentation the mono-hydrate form was focused on. Unlike SPC, SPB does not contain H_2O_2 in its solid state. In fact, the borate (BO_3^{3-}) ion is not present in SPB, rather the $B_2O_4(OH)_4^{2-}$ ion is present and connected with two peroxo bridges. **Figure 1-1** shows the chemical structure of SPB (McKillop and Sanderson, 1995).
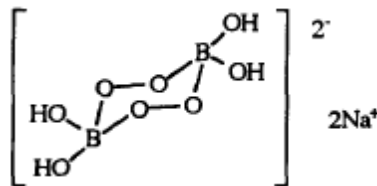
Figure 1-1: Chemical Structure of SPB (Reprinted from McKillop and Sanderson, 1995)

SPB undergoes hydrolysis in contact with water, producing H_2O_2 and sodium metaborate ($NaBO_2$), as in **Reaction 1-1**. In alkaline water solutions, $NaBO_2$ reacts and

forms boric acid, H_3BO_3, and sodium hydroxide (NaOH) as shown in **Reaction 1-2** (Goel, 2007). The combination of **Reaction 1-1** and **1-2** results in **Reaction 1-3**, which can be used to relate the addition of SPB to borate yield.

$$NaBO_3 + H_2O \rightarrow H_2O_2 + NaBO_2 \; \boldsymbol{Reaction\ 1-1}$$

$$NaBO_2 + 2H_2O \rightarrow H_3BO_3 + NaOH \; \boldsymbol{Reaction\ 1-2}$$

$$NaBO_3 + 3H_2O \rightarrow H_2O_2 + H_3BO_3 + NaOH \; \boldsymbol{Reaction\ 1-3}$$
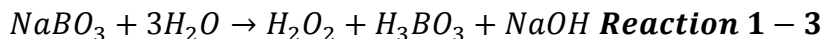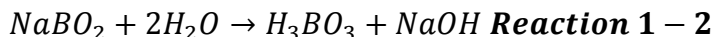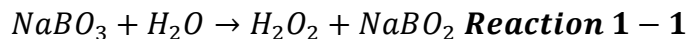
H_3BO_3 is the main byproduct of the dissolution of SPB in water. The speciation of borate in water depends on the pH. H_3BO_3 is a polyprotic acid, and disassociates to $H_2BO_3^-$, HBO_3^{2-} and BO_3^{3-}. The pK_a's of the disassociation of H_3BO_3 are 9.24, 12.40 and 13.40, respectively (Perelygin and Chistyakov, 2006). H_3BO_3 is a weak acid and is also commonly used as a pH buffer in the pH range of 7.5-9.2 (Vela et al., 1986). Borate scavenging of hydroxyl radicals has been studied by Buxton and Sellers (1987). They report a hydroxyl radical scavenging rate of $5 \times 10^3 M^{-1}sec^{-1}$ for H_3BO_3. This is significantly less than that of H_2O_2, NOM, and carbonate species. As a result, it is expected that hydroxyl radical scavenging by H_3BO_3 will be minimal.

One potential issue with the use of SPB in drinking water is drinking water standards for boron. Boron is listed on the US EPA's Second Drinking Water Contaminant Candidate List (CCL2). As such, its effects upon consumption by humans were examined. Based on the typical reference dose to humans, the US EPA has set a health reference level (HRL) for boron of 1.4mg/L (US EPA, 2008a). A study by Frey et al. (2004) found that out of 228 drinking water suppliers with groundwater source water, 7 exceeded the HRL. Additionally, it was found that out of 113 surface water sources,

none exceeded the HRL. Based on these findings, the US EPA determined not to regulate

boron with a national primary drinking water regulation (NPDWR). However, the states

of CA, FL, ME, MN, NH and WI have set their own standards for boron ranging from

0.6-1.0mg/L.

The chemical structure of SPC is shown in **Figure 1-2** (Muzart, 1995), and SPC

dissolves in water according to **Reaction 1-4.**
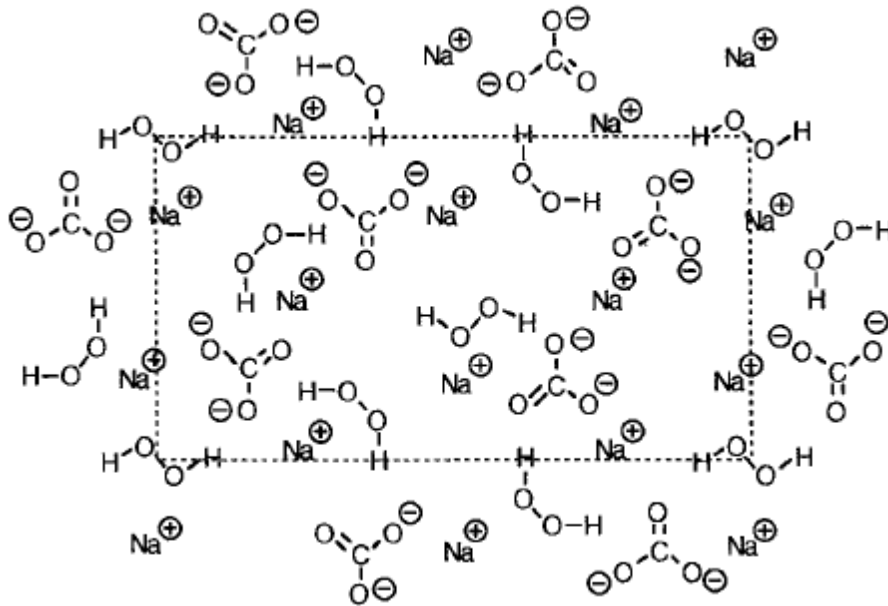
Figure 1-2: Chemical Structure of SPC (Reprinted from Muzart, 1995). Hydrogen bonds
have been removed for clarity.

$$2(Na_2CO_3 \cdot 1.5H_2O_2) \rightarrow 2Na_2CO_3 + 3H_2O_2 \; \boldsymbol{Reaction\; 1-4}$$
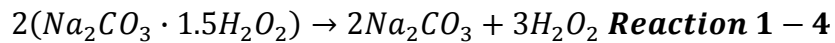
The main byproduct of SPC dissolution in water besides H_2O_2 is sodium

bicarbonate (Na_2CO_3). The addition of Na_2CO_3 to water will increase the alkalinity which

will increase the buffering capacity of the water. As a result, it is expected that the pH of

the sample will increase when SPC is added to the water samples. Like SPB, SPC is very

stable when dry; however, once it becomes wet it will readily decompose to hydrogen

4

peroxide. A potential side effect of using SPC as an alternative to liquid H_2O_2 in the UV/H_2O_2 AOP is that the additional carbonate yield may scavenge hydroxyl radicals. Bicarbonate (HCO_3^-) and carbonate (CO_3^{2-}) have hydroxyl radical scavenging rates of $8.5 \times 10^6 M^{-1}sec^{-1}$ and $3.9 \times 10^8 M^{-1}sec^{-1}$, respectively (Buxton et al., 1988). These rates are significantly greater than that of published borate species. It is expected that hydroxyl radical scavenging by carbonate species will reduce the efficiency of the UV/H_2O_2 AOP at high concentrations of SPC.

Unlike boron, there are no drinking water standards for carbonate species. However, it is desirable to limit the alkalinity concentration found in drinking water to between 30 and 400 mg/L (Illinois Department of Public Health, Undated). Alkalinity concentrations are expected to stay within this range for the intended SPC concentrations. Additionally, there are no human health effects related to carbonate concentration.

Both SPB and SPC are classified as strong oxidizers, and as such they must be handled and shipped accordingly (Acros Organics, 2009). Typically, SPB and SPC are shipped in 1 ton "super-sacks," 50lb bags and 88lb drums (OCI Chemical Company, 2010a). McKillop and Sanderson (1995) reported that if excessive amounts of SPC are mixed with highly oxidative substances violent exothermic reactions may occur. Due to the presence of H_2O_2 when SPB is dissolved in water, explosive reactions are also possible with SPB. However, explosive reactions only occur in the presence of highly reduced compounds such as ferrous sulfide or lead (II or IV) oxide (National Research Council. 1995). Grades of H_2O_2 from 28.1% to 52% are considered Class 2 oxidizers, corrosives and Class 1 unstable reactives (US Peroxide, 2009). This grade of H_2O_2 is

typically used in the UV/H_2O_2 AOP. Therefore, SPB and SPC used in the UV/H_2O_2 AOP will fall under the same hazard ratings as liquid H_2O_2.

As Class 2 oxidizers, SPB, SPC and liquid H_2O_2 may cause spontaneous ignition of combustible materials with which they come into contact with (US Peroxide, 2009). The primary storage requirement of Class 2 oxidizers is that they must be stored away from materials that may cause combustible reactions to occur when mixed (Magnussen, 1997). H_2O_2 is incompatible with copper, chromium, iron, most metals and their salts, flammable fluids, aniline and nitromethane; and should be isolated from these materials (Argonne National Laboratory, Undated). As corrosives, SPB, SPC and liquid H_2O_2 can burn skin and tissues when contact occurs. Furthermore, as Class 1 unstable reactives, these substances can become unstable at increased temperatures and pressures (US Peroxide, 2009). SPC is also listed under the Toxic Substances Control Act, and as such specific reporting, record keeping and testing requirements are necessary during its manufacturing, importation and use (US EPA, 1976).

McKillop and Sanderson (1995 and 1999) have performed extensive research on SPB and SPC and their ability to oxidize various organics in aqueous and non-aqueous conditions in the presence of various activator species. They have found that in the presence of activator species, SPB is able to oxidize thiols and selenols, carbonyl derivatives and organophosphorus wastes more effectively than SPC. On the other hand, SPC oxidizes cyclic ketones, alcohols, and azo dyes. It was also noted that SPB and SPC were not able to significantly oxidize alkynes and aliphatic nitriles.

CHAPTER 2: RESEARCH OBJECTIVES

The hypothesis driving this research is that the active forms of peroxide formed with the dissolution of SPB and SPC in water will react similarly to hydrogen peroxide. As such, because SPB and SPC can be shipped in solid form and dissolved on-site, significant savings in chemical costs and shipping energy will be realized as compared to H_2O_2, which must be shipped in 30% or 50% solution. The hypothesis will be explored through completion of the following tasks.

1. Determine the yield of active H_2O_2 of SPB and SPC in DI water and three natural water samples from the Northampton, MA Water Filtration Plant.

2. Examine the ability of active H_2O_2 from the three substances (liquid H_2O_2, SPB and SPC) to produce hydroxyl radicals when exposed to UV light.

3. Examine or calculate the yields of borate and carbonate upon addition of SPB and SPC to each water, and quantify associated impact on AOP efficiency.

4. Compare shipping costs and energy consumption associated with using liquid H_2O_2, SPB and SPC.

CHAPTER 3: LITERATURE REVIEW

3.0 UV Light Used for Drinking Water Treatment

Since the beginning of the 20th century, UV light has been used for disinfecting drinking water. Although early attempts at using this technology were rather unsuccessful, UV disinfection has once again become a popular treatment method. This is due to the fact that other disinfection technologies can produce cancer causing DBPs and they can be ineffective at removing *Giardia* and *Cryptosporidium* cysts (Carlson et al., 1985).

Recent research in using UV light in water treatment has focused on using UV in combination with chemicals for the advanced oxidation of drinking water to control emerging contaminants such as DBP precursors, halogenated organics and pharmaceuticals (Toor and Mohseni, 2006, Ince and Apikyan, 1999 and Andreozzi et al., 2004).

3.1 UV Advanced Oxidation Processes (AOPs)

3.1.1 Hydroxyl Radical

The powerful oxidant that is the result of the reaction between UV light and H_2O_2 is the hydroxyl radical. H.J.H. Fenton first discovered the hydroxyl radical in 1894 via the oxidation of malic acid by hydrogen peroxide (Walling, 1975). Since that time significant research has been completed into further understanding the ability of the hydroxyl radical. The term used to describe the ability of an oxidant to oxidize contaminants in drinking water is oxidation potential. An oxidant with a high oxidation potential will degrade a contaminant at a faster rate than a weaker oxidant. **Figure 3-1**

below compares the oxidation potentials of commonly used oxidants in water treatment (ITT Water and Wastewater, Undated).
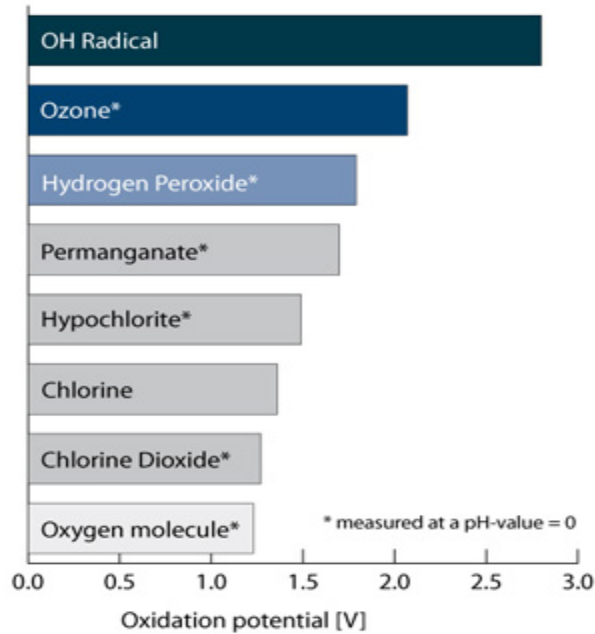
Figure 3-1: Oxidation Potential of Common Oxidants (Adapted from ITT Water and Wastewater)

Clearly, the hydroxyl radical is the most powerful oxidant that is used in water treatment processes. However, Legrini et al. (1993) report that fluorine has a higher oxidation potential than the hydroxyl radical (3.03V vs. 2.80V), but the use of fluorine in water treatment is undesirable due to its adverse effects on humans and the environment.

3.1.2   UV/H_2O_2 AOP

UV light can be used in combination with multiple substances for the advanced oxidation of drinking water. The mechanism behind the combination of UV and H_2O_2 for treating drinking water is the formation of hydroxyl radicals which can oxidize contaminants. In the UV/H_2O_2 AOP, the cleavage of H_2O_2 with UV light produces a quantum yield of two hydroxyl radicals per unit of radiation absorbed (Glaze et al., 1987), as in **Reaction 3-1**.

$$H_2O_2 + hv \rightarrow 2 \cdot OH \; \boldsymbol{Reaction\; 3-1}$$
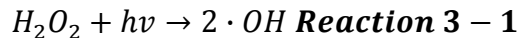
The sequence of reactions of hydroxyl radicals with organic matter in drinking water is highlighted in Legrini et al. (1993). Hydroxyl radicals formed react with organic compounds to produce organic radicals. These radicals then proceed to react with dissolved oxygen to form peroxyl radicals which initiate thermal oxidation reactions to produce less harmful contaminants such as superoxide anions and carbonyl compounds. This process is similar for most contaminants that are oxidized by hydroxyl radicals.

One issue with the UV/H_2O_2 AOP is the reaction of hydroxyl radicals with other constituents found in drinking water, referred to as scavengers. When radical scavenging occurs, less hydroxyl radicals are available to oxidize contaminants of concern. Known scavengers of hydroxyl radicals are natural organic matter (NOM), carbonate (CO_3^{2-}), bicarbonate (HCO_3^-) and chlorine (Cl^-) ions (Gultekin and Ince, 2004 and Liao et al., 2000). For waters with high concentrations of these scavengers, pre-treatment processes to reduce the chemical concentrations are necessary to improve the performance and decrease the cost of the UV/H_2O_2 AOP.

Another drawback of the UV/H_2O_2 AOP is the relatively small molar extinction coefficient of H_2O_2 (19.6$M^{-1}cm^{-1}$). The low molar extinction coefficient is an indication that less UV light is absorbed by H_2O_2 and subsequently less hydroxyl radicals are formed. This results in the need for relatively high concentrations of H_2O_2 used in the UV/H_2O_2 AOP (Glaze et al, 1987). As a result of the high cost of liquid H_2O_2 and the lower molar extinction coefficient, costs can be substantially increased. On the other hand, if alternative solid forms of H_2O_2 can be used to treat drinking water with the same

efficiency as liquid H_2O_2, the costs of treatment can be significantly reduced and the UV/H_2O_2 AOP can become more desirable.

3.1.2.1 H_2O_2 Concentration Used in UV/H_2O_2 AOP

The most important parameter in the UV/H_2O_2 AOP is the concentration of H_2O_2 used (Modrzejewska et al., 2006). Studies have shown that above 8.2mM (approximately 280mg/L) H_2O_2, hydroxyl radical scavenging by the hydroperoxyl radical occurs (Gultekin and Ince, 2004). Rosenfeldt et al. (2006) used H_2O_2 concentrations of 2, 10 and 50mg/L, which are more indicative of concentrations that would be used in actual drinking water treatment processes.

Due to the fact that limited amounts of H_2O_2 are consumed in typical AOP applications (<10%), significant H_2O_2 residuals can exist, and consideration of the use of the UV/H_2O_2 AOP must include a method to quench H_2O_2 residuals to less than 0.5mg/L (National Research Council, 1999). Some common quenchers used are types of granular activated carbon (GAC) and sodium hypochlorite (Pantin, 2009). The GAC will remove most of the remaining H_2O_2 residual by internal and external mass transfer mechanisms, and the stoichiometric mass ratio of free chlorine to H_2O_2 is 2:1 for quenching purposes (Doom, 2008 and Pantin, 2009).

3.1.2.2 Grade of H_2O_2 Used

There are several grades of H_2O_2 that are available for purchase and use in a variety of sectors ranging from household uses to rocket fuel. The common household H_2O_2 is typically 3-6% H_2O_2 by weight. On the other hand, when used in water treatment, food grade H_2O_2 is used and is usually 30-70% H_2O_2 by weight (Drink H_2O_2, Undated). The increased percentage of the solution is necessary so that enough oxidation power is

11

available to oxidize contaminants. However with the increased percentage of H_2O_2 in solution, the stability of the solution decreases, and safety procedures with storing and using H_2O_2 must be carefully followed. **Figure 3-2** below (Solvay Chemicals, 2005) shows that as the purity of a solution of H_2O_2 is increased, the pH of the solution decreases dramatically. This is another reason why high purity H_2O_2 is not used in water treatment.

* No stabilizers added
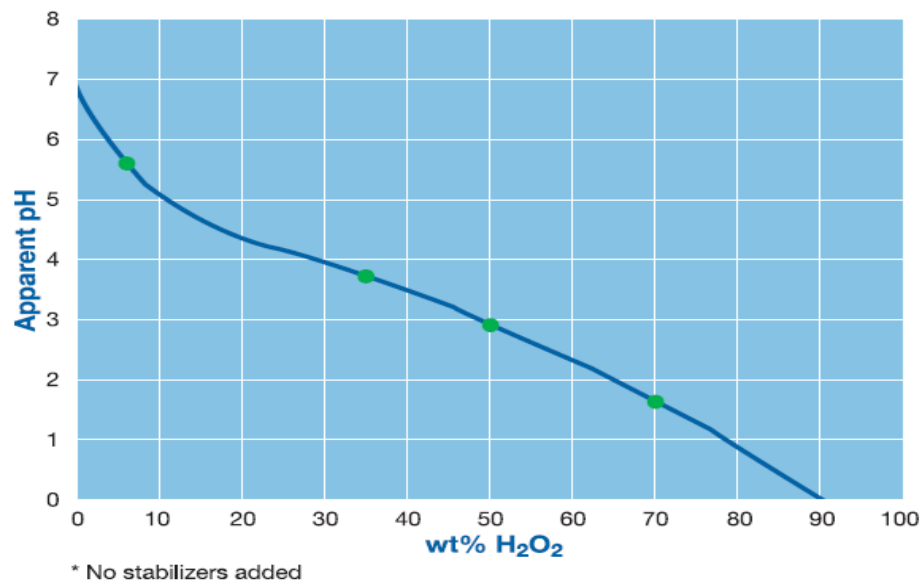
Figure 3-2: Apparent pH of solutions of H_2O_2 (Solvay Chemicals, 2005)

Pure grade H_2O_2 (100%) rarely exists due to its extreme pH and oxidative powers. However, 90% H_2O_2 is used by military institutions in rocket fuel. The use of high grade H_2O_2 in rocket fuel has been common since World War II in planes, torpedoes and rockets (General Kinetics, LLC, 1999). Currently, high grade H_2O_2 is used in gas generators and thrusters for spacecraft (Wernimont and Durant, 2004 and Wernimont and Ventura, 2009).

3.2 Hydroxyl Radical Scavenging

The main disadvantage of the use of hydroxyl radicals as oxidizers in water treatment is the non-selectivity of the hydroxyl radical in solution. This mechanism is called scavenging and is the result of non-target species attacking and using the hydroxyl radical's oxidative ability. Numerous species found in water can scavenge hydroxyl radicals including CO_3^{2-}, HCO_3^-, Cl^-, NOM and humic acids (Glaze et al., 1995, Gulteskin and Ince, 2004, and Liao et al., 2000). The scavenging of these species drastically limits the ability of hydroxyl radicals to react with contaminants, because scavengers are typically present at orders of magnitude greater concentrations than the target contaminants.

Much research has been done on the matter of carbonate scavenging (scavenging by carbonate species) due to its prevalence in all water supplies. As previously mentioned, Buxton et al. (1988) have developed second order rate constants for the reaction of carbonate and bicarbonate with hydroxyl radicals. Carbonate is a 46 times stronger hydroxyl radical scavenger than bicarbonate. This is important, and can potentially be avoided in water treatment by lowering the pH below the pK_a between bicarbonate and carbonate (10.3). Below this pH, bicarbonate is the dominant species, and less scavenging will occur as a result. Carbonic acid (H_2CO_3) also scavenges hydroxyl radicals, but Liao and Gurol (1995) have shown that scavenging by H_2CO_3 is negligible. Liao et al. (2000) have shown that as the pH of a solution is increased, the hydroxyl radical concentration decreases in the presence of carbonate species. Furthermore, Gultekin and Ince (2000) discovered that only low concentrations of CO_3^{2-}

are necessary to inhibit the decay of azo dyes, while the inhibition of azo dyes only occurs when the concentration of HCO_3^- is greater than 5mM.

Research on the ability of chloride to scavenge hydroxyl radicals has indicated that chloride concentration between 100 and 1250mM as Cl^- will restrict the availability of hydroxyl radicals to decay azo dyes (Gultekin and Ince, 2000). Liao et al. (2000) confirmed this in their experiments with the decay of n-chlorobutane (BuCl). They also found, similar to the carbonate species, that pH is important in the amount of scavenging that occurs. The amount of scavenging of hydroxyl radicals that occurs in the pH range of 2 to 6 is less than that when the pH is less than 2 or more than 6. This information is important in the placement of the UV/H_2O_2 AOP in a water treatment plant. For the optimum amount of oxidation of targeted contaminants in drinking water, the UV/H_2O_2 AOP should be placed before the addition of any chlorine disinfection mechanisms.

Another interesting scavenger of hydroxyl radicals is H_2O_2 when excessive H_2O_2 concentrations are used. Gultekin and Ince (2000) found that above a concentration of 8.2mM the rate of color removal of azo dyes decreased. This is the result of scavenging by the hydroperoxyl radical ($\cdot OH_2$). The formation of the hydroperoxyl radical is presented in **Reaction 3-8** below.

$$\cdot OH + H_2O_2 \rightarrow \cdot OH_2 + H_2O \ \textbf{\textit{Reaction 3} } - \textbf{8}$$
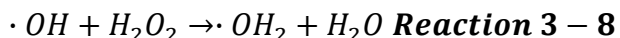
Buxton et al. (1988) report the rate constant of this reaction to be $2.7 \times 10^7 M^{-1}s^{-1}$ which is comparable to that of HCO_3^- and CO_3^{2-}. In combination with these and the numerous other scavengers found in drinking water supplies an excessive concentration of H_2O_2 used in treatment can inhibit rather than help the oxidation processes.

3.3 UV-AOPs Used in Combination with Other Treatment Processes

The combination of the UV/H_2O_2 AOP and activated carbon has been studied for the removal pollutants found in drinking water. Ince and Apikyan (1999) studied the effects of simultaneous activated carbon adsorption and UV/H_2O_2 AOP on the removal of phenol and organic carbon as model compounds for drinking water contaminants. Additionally, the "destructive regeneration" of the activated carbon by advanced oxidation was also examined. Through their experiments it was determined that the H_2O_2 did not adsorb to the carbon in the presence of UV light, rather it was found to yield hydroxyl radicals. Also it was found that there is no reaction between UV light and the activated carbon.

The results of phenol removal in the system indicated that phenol was completely removed in the first stage of the process, mainly through the reaction with hydroxyl radicals. The removal of organic carbon on the other hand was slightly less (87.5%) and was due to both advanced oxidation and adsorption to the activated carbon. An interesting finding of this research was that spent activated carbon was regenerated using the UV/H_2O_2 AOP. Ninety-two and a half percent (92.5%) mineralization was accomplished using the UV/H_2O_2 AOP. This was accomplished at lower energy and H_2O_2 consumption rates than it would if treatment were completed with adsorption alone. This study indicates that the UV/H_2O_2 AOP can be used in conjunction with traditional treatment processes and effectively lower treatment costs with an increased treatment level.

Toor and Mohseni (2006) studied the effects of the UV/H_2O_2 AOP when used in conjunction with biological activated carbon (BAC) on the removal of DBPs. In this study the BAC treatment was placed downstream of the UV/H_2O_2 AOP. One potential benefit of separating the two processes is that any intermediates formed during the UV/H_2O_2 AOP can be removed via adsorption. Without the presence of BAC the concentration of H_2O_2 needed to cause significant reductions in DBPs would need to be approximately 23mg/L and a UV fluence rate of more than 1000mJ/cm^2 is required. This could be quite expensive if used in the treatment process.

Once the BAC was added downstream of the UV exposure, significant DBP removal can be accomplished with a moderate UV fluence of approximately 500mJ/cm^2. Additionally, the TOC and UV_{254} of the water treated were significantly decreased with the combination of the UV/H_2O_2 AOP and BAC. The main reason for this is the increased biodegradability (BDOC) of the water after the UV/H_2O_2 AOP. When just the UV/H_2O_2 AOP was used in the treatment process, the BDOC of the sample water was 60%. However, when BAC was included with the UV/H_2O_2 AOP, the BDOC was decreased to 40%. This reduction is desired, due to the potential re-growth of pathogens in water distribution systems with high BDOC. The findings of this research indicate enhanced drinking water treatment is possible when activated carbon is added downstream of the UV/H_2O_2 AOP.

CHAPTER 4: METHODS OF INVESTIGATION

The purpose of this investigation is to determine the active H_2O_2 yield of SPB and SPC and compare the ability of SPB and SPC to decay methylene blue (MB) when used in combination with LP-UV light to that of 30% liquid H_2O_2.

4.0 Materials

Analytical grade 95% sodium perborate monohydrate and sodium percarbonate were acquired from Acros Organics (Belgium) and 30% liquid H_2O_2 was purchased from Ricca Chemical Company (Texas). Potassium iodide (KI) purchased from EM Science (New Jersey) Ammonium molybdate tetrahydrate $((NH_4)_6Mo_7O_{24})$, sodium hydroxide (NaOH) and potassium hydrogen phthalate (KHP) (Acros Organics, Belgium) were used in the determination of the active yield of H_2O_2 of each sample. MB powder purchased from Fisher Scientific (Pennsylvania) was used to create a 10^{-2}M stock solution of MB, which was further diluted to $1\square$M in the tested water for use in the UV exposure experiments. Additionally, bromcresol green obtained from Fisher Scientific (Pennsylvania) was used as an indicator of the endpoint pH of alkalinity analyses.

4.1 Waters Used in Analyses

Deionized (DI) water and three natural water samples were used in the comparison of the abilities of SPB and SPC to liquid H_2O_2 in degrading MB under the presence of UV light. The three natural water samples were collected in June and July 2010 from the Northampton, MA Water Filtration Plant. The samples were collected from pre-treatment water, treated water before chlorination, and post-treatment finished water. Natural water samples were filtered with a 0.45µM filter to remove and

particulates. Total organic carbon (TOC) analysis was performed on the three natural water samples using a Shimadzu (Maryland) TOC-5000A Total Organic Carbon Analyzer. The values obtained were significantly greater than the typical TOC of the Northampton Water Filtration Plant treatment water, and were thus called into question. For calculations, TOC concentrations for each source water were assumed to be the average TOC concentration of the source water for the month of collection as obtained from the Northampton Water Filtration Plant. Alkalinity was also measured using standard methods (APHA, 1992) in each natural water source. pH was measured using a Thermo Electron Corporation (Illinois) Orion 410A+ pH meter. The water quality parameters of the natural water sources are presented in **Table 4-1**. TOC values presented are the monthly average TOC concentrations for the months of collection of each water source.

Table 4-1: Water Quality Parameters of the Natural Waters

Source Water	Measured DOC (mg/L)	Average Monthly TOC(mg/L)	pH	Alkalinity (mg/L as CaCO$_3$)	Total Carbonate (mg/L)
Pre-Treatment Water	9.11	2.50	6.67	15.0	18.31
Treated, Unchlorinated	2.42	1.70	7.11	7.5	9.15
Post-Treatment, Finished Water	1.85	Non-Detectable	7.14	22.0	26.86

4.2 Analytical Methods

4.2.1 Active Hydrogen Peroxide Determination Method

The active H_2O_2 of each sample was determined using the I_3^- Method outlined by Klassen et al. (1994) which is accurate to H_2O_2 concentrations as low as 1μM. This

method was chosen over several other peroxide detection methods, described in

Appendix A, due to previous laboratory experience and successful application of the

method. This method utilizes an ammonium molybdate catalyzed reaction between H_2O_2

and the I^- ion to form I_2 (iodine) (**Reaction 4-1**). I_2 then reacts with free I^- ions in

solution to form the I_3^- ion (**Reaction 4-2**) which can be measured using optical

absorption.

$$H_2O_2 + 2I^- + 2H^+ \rightarrow I_2 + 2H_2O \; \textbf{\textit{Reaction 4} - 1}$$

$$I_2 + I^- \leftrightarrow I_3^- \; \textbf{\textit{Reaction 4} - 2}$$
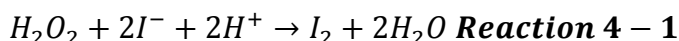
Two solutions (A and B) were prepared for the I_3^- Method. Solution A consisted

of 33g of KI, 1g of NaOH and 0.1g of ammonium molybdate diluted to 500mL with de-

ionized water. Solution A was stirred for approximately 10 minutes to dissolve all of the

ammonium molybdate. Additionally, Solution A was kept refrigerated in a dark bottle to

inhibit photo-oxidation of I^- to I_2. Solution B was a mixture of 10g of KHP per 500mL. It

was also kept in a dark bottle and refrigerated between uses.

The I_3^- Method can be completed with a small volume of sample (less than 1mL)

that is mixed with equivalent volumes of Solutions A and B. For the experiments

discussed here, 0.25mL of Solutions A and B were mixed in a microcentrifuge cuvette

and a sample containing H_2O_2 was added and diluted accordingly to bring the total

volume of mixed solution to 1mL. Typical dilutions used in this experiment ranged from

dilution factors of 0 to 10. The samples were allowed to react with the equivolume

mixture of Solutions A and B for a short period of time (approximately 5 minutes) and

then analyzed with the ThermoSpectronic (Illinois) Genesys 10UV spectrophotometer at

352nm with a 1cm Plastibrand (Missouri) plastic cuvette. The same cuvette was used for

all samples to eliminate absorption measurement errors associated with using multiple cuvettes. Additionally, a blank absorbance was determined for a mixture of 0.25mL of Solutions A and B and 0.5mL of DI water. The absorbance of this mixture was assumed to be the result of background formation of I_3^-. The actual absorbance of each of the samples is calculated by subtracting the blank absorbance from the absorbance of the sample.

The concentration of active H_2O_2 was determined from the generation of I_3^-, with a molar absorption coefficient of 26,400 $M^{-1}cm^{-1}$. Beer's Law can be used to relate absorbance (A) and concentration (c) of active H_2O_2 in molar units via the molar absorption coefficient, dilution factor (DF) and pathway length (b) (Swinehart, 1962). This is shown in equation format below. (**Equation 4-1**)

$$c = \frac{A}{26400 \times b} \times DF \quad \textbf{\textit{Equation 4} - 1}$$

4.2.2 Determination of Active Hydrogen Peroxide Yield

The active H_2O_2 yield of liquid H_2O_2, SPB and SPC in each of the water samples was determined using the I_3^- Method. Stock solutions of $10^{-2}M$ Liquid H_2O_2, SPB and SPC were created in DI water. The stock solutions were then diluted to theoretical H_2O_2 concentrations ranging from 0 to 15mg/L in each water sample. These solutions of active H_2O_2 were continuously stirred to promote the complete mixing of the reagent in the water sample. The active H_2O_2 concentration of the solution was then determined using the previously presented I_3^- Method.

4.2.3 Methylene Blue as a Model Compound

MB is commonly used as model compounds in testing the ability of the UV/H_2O_2 AOP to oxidize contaminants found in water due to its observed non-reactivity with UV light or H_2O_2 alone, and susceptibility to AOP conditions. A study by Georgiou et al. (2001) examined the ability of the UV/H_2O_2 AOP to remove various azo dyes, including MB. In their work they demonstrated that the MB does not decay in the presence of UV light or H_2O_2 alone. Upon the addition of 1g/L of H_2O_2, complete destruction of MB was found after 20-30 minutes of irradiation, attributed to the reaction between MB and hydroxyl radical. Furthermore, they applied the UV/H_2O_2 AOP to cotton textile wastewater and found the same results to be true in a slightly longer time (1 hour). Additionally, Tayade et al. (2009) and Yao and Wang (2010) have shown that MB does not decay appreciably in the presence of UV light alone. Both studies demonstrated that MB only slightly decays in the presence of UV light, but decays significantly upon the addition of titanium dioxide (TiO_2) and H_2O_2 to the UV process.

4.2.4 Collimated Beam, Low Pressure UV Reactor

The bench-scale LP-UV reactor consists of black painted walls, 4-15W germicidal mercury UV lamps, an adjustable stand, stir plate and a shutter which allows for control of when the samples are exposed to the UV light. Two collimating plates filter stray light, creating a "quasi-collimated" beam of UV light that is used to irradiate each of the solutions of peroxide and MB (Bolton, 2010). The adjustable stand allows for varying the height of the exposed sample which will affect the intensity of UV light that the exposed sample is subject to. Furthermore, the stir plate was utilized to ensure that the

exposed sample was well mixed at all times during the exposure process. A photograph

of the reactor is provided in **Figure 4-1**.

Figure 4-1: Photograph of LP-UV Reactor

UV irradiance was measured with a Mannix Testing and Measurement UV Light

Meter for each run of samples tested. The sample height was adjusted for all experiments

such that the applied incident UV intensity was approximately $1mW/cm^2$. In addition to

the UV light intensity, the UV_{254} absorbance of each sample was determined using a 1cm

cuvette and the ThermoSpectronic Genesys 10UV spectrophotometer. This allowed for

the determination of the UV dose based on the exposure time of the sample. The formula

for calculating the UV dose is presented in **Equation 4-2**, where $\bar{E}$ is the average

intensity of UV light and t is the exposure time.

$$UV\ Dose = \bar{E} \times t \ \textbf{Equation 4} - \textbf{2}$$

Using the measured irradiance (e), the incident irradiance (E) can be calculated

with **Equation 4-3**, where PF is the petri factor of the glass exposure dish, RF is the

reflection factor of incident UV light and SF is the radiometer sensor factor.

$$E = \frac{(e \times PF \times RF)}{SF} \ \textbf{Equation 4} - \textbf{3}$$

The values of PF, RF and SF were determined prior to experimentation, and the

values used were 0.94, 0.975 and 0.45, respectively. $\bar{E}$ can then be determined from the

calculated I using **Equation 4-4** below; where UV_{254} is the UV absorbance of the

exposed sample at 254nm and d is the depth of the exposed sample in the exposure dish.

$$\bar{E} = E \times \frac{(1 - e^{(-2.303 \times UV_{254} \times d)})}{(2.303 \times UV_{254} \times d)} \ \textbf{Equation 4} - \textbf{4}$$

The depth of the sample (d) in the exposure dish was 2.04cm for each sample

because the same exposure dish (50x35mm) and volume of sample (40mL) were used for

each exposure.

4.2.5 AvaSpec System Used to Determine Methylene Blue Decay Rate

Another factor for using MB as a hydroxyl radical probe compound is the ease

with which sample analysis can be performed. MB readily absorbs visible light at

664nm, so nearly continuous MB detection could be made utilizing an AvaSpec-2048

fiber optic spectrophotometer. Absorbance measurements were exported to an Excel

spreadsheet file via the USB2.0 interface at approximately 2mJ/cm^2 intervals.

A schematic of this process is presented in **Figure 4-2**. Complete instructions for

the operation of the AvaSoft software is presented in **Appendix B**, from Hross (2010).
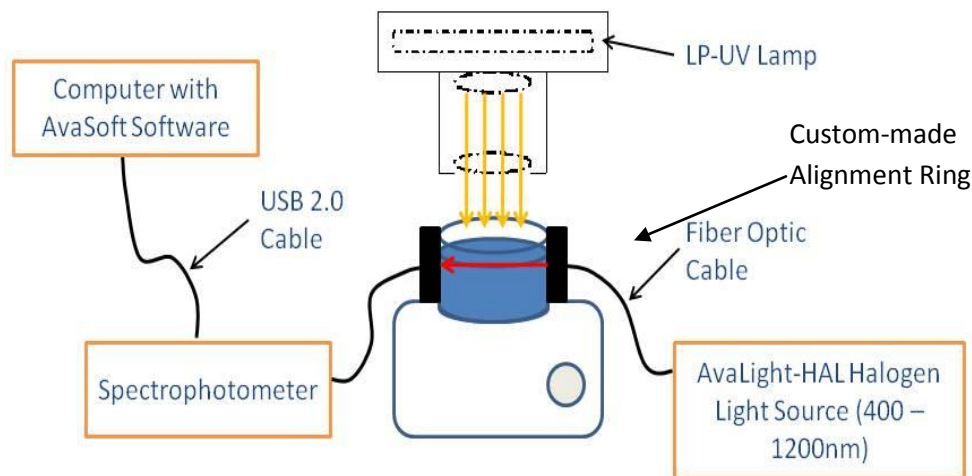
Figure 4-2: Schematic of UV Exposure Process

The AvaLight-HAL halogen lamp source was connected via a fiber optic cable to

one side of the custom made alignment ring, and another fiber optic cable was connected

from the other side of the ring to the AvaSpec-2048 spectrophotometer. The alignment

ring served to hold the sample dish, and ensure proper alignment of the light source and

detector. Additionally, a light attenuator was used to dim the light source from the

AvaLight-HAL halogen lamp to prevent detector saturation. In this manner, visible light

from the halogen lamp was delivered to the exposed sample and the wavelength specific

light that passed through the sample was measured via the AvaSpec-2048. For these

experiments, absorbance at 664nm was continuously measured for MB detection for the

duration of the exposures. Blanking the spectrophotometer required 40mL of DI water in

a 50x35mm exposure dish. The process of exposing each sample required that 40mL of each sample be placed in an exposure dish which was placed within the alignment ring on top of the stir plate. The same exposure dish was cleaned and reused for each of the experiments and the placement of the dish in the collimating piece was the same for each experiment to minimize differential glass effects.

MB absorbance values recorded during the LP-UV exposure were converted to concentrations using a calibration curve relating MB concentration and absorbance. The calibration curve was developed by measuring the absorbance of 0.5, 1.0, 1.5, 2.0, 2.5 and 5.0μM solutions of MB several times to determine an average absorbance at 664nm for each concentration. The calibration curve is presented in **Figure 4-3**.
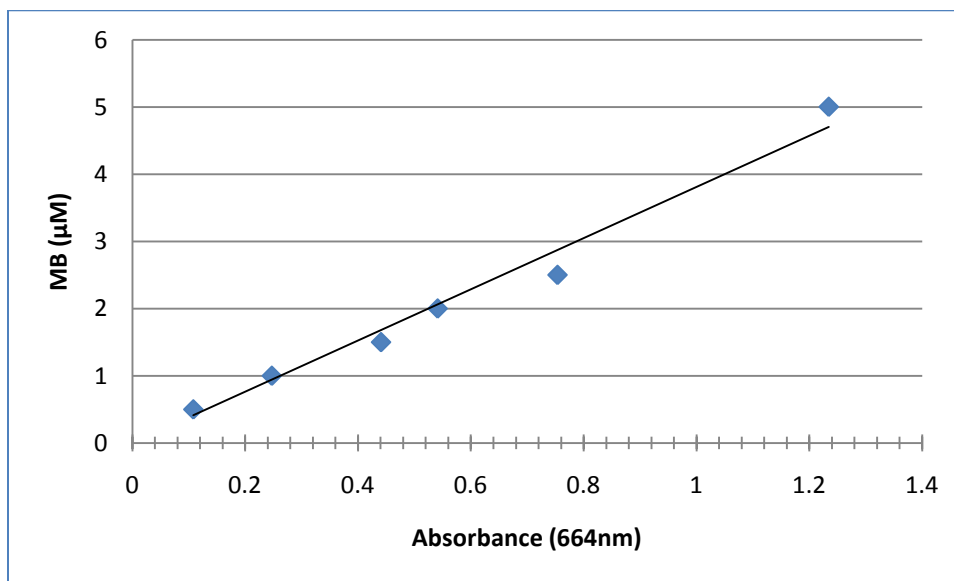
Figure 4-3: Methylene Blue Calibration Curve

The equation of the linear best fit trendline for the data is $y = 3.8092x$ with an R^2 correlation value of 0.9785. The trendline was forced to go through the origin to prevent negative concentrations from occurring due to low measured absorbances.

4.3 General Experiment Design

Experiments involved exposing solutions of SPB, SPC and liquid H_2O_2 to approximately 300mJ/cm^2 of UV radiation using a low pressure UV lamp. Stock solutions of SPB, SPC and liquid H_2O_2 used in the analysis were diluted in DI water and three natural water samples to create theoretical active H_2O_2 concentrations of 0, 1, 2, 3, 4, 5, 7, 10 and 15mg/L. The actual active H_2O_2 concentration of the samples was measured at this time. MB was also added from a 10^{-2}M stock solution in DI to a concentration of 1µM in each sample. After the addition of the constituents to each sample the UV absorbance at 254nm and pH of each sample was determined. Forty milliliters (40mL) of each samples was then exposed to approximately 300mJ/cm^2 of LP-UV radiation at approximately 1mW/cm^2 in the UV apparatus designed in detail by Hross, 2010. A schematic of this process is presented below. (**Figure 4-4**)
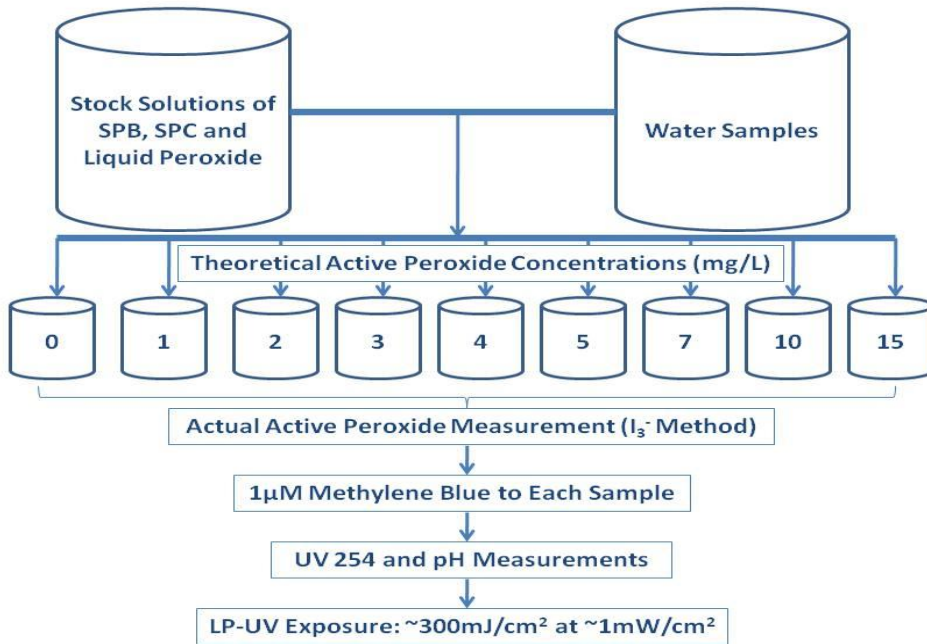
Figure 4-4: Schematic of General Experiment

The LP-UV exposure duration for each sample was approximately 3 minutes. This allowed for sufficient time for the decay of MB via hydroxyl radicals which was recorded at approximately 5mJ/cm^2 intervals by the AvaSpec spectrophotometer and exported to Excel spreadsheet format via the USB2.0 interface. The comparison between liquid H_2O_2, SPB and SPC on decaying MB was examined while varying the pH. When pH adjustment was required, solutions of 0.1N hydrochloric acid (HCl) and NaOH were used. HCl and NaOH were added to the samples in a dropwise manner using a polyethylene transfer pipette to the desired pH. For this experiment the pH's examined were 5, 7 and 8.5; in addition to the natural pH of the sample.

4.4 Carbonate Yield

The carbonate yield of the samples dosed with SPC was determined using the alkalinity determination method set forth by the Standard Methods of Water and Wastewater (APHA, 1992). Alkalinity in most waters is controlled by carbonate, bicarbonate and hydroxide and thus the concentration of total carbonates in a water sample can be determined by determining the alkalinity of the water. In this experiment the water samples dosed with SPC were titrated to the end-point pH of bromcresol green, 4.5. Bromcresol green was used as an indicator to determine when the pH approached 4.5. Additionally, the Thermo Electron Corporation Orion 410A+ pH meter was used to accurately end the titration at pH 4.5.

Once the total alkalinity of the sample was determined the total carbonate yield was calculated by summing the amount of bicarbonate (HCO_3^-) and carbonate (CO_3^{2-}). These were determined with the below equations; where K_w is the acid dissociation

constant for water (10^{-14}), Alk is the measured alkalinity of the sample and K_2 is the

second acid dissociation constant for carbonic acid ($10^{-10.3}$). (**Equations 4-5** and **4-6**)

$$[HCO_3^-] = \frac{2Alk - 10^{K_w - pH}}{1 + 2K_2 10^{-pH}} \quad \textbf{\textit{Equation 4 - 5}}$$

$$[CO_3^{2-}] = \frac{[HCO_3^-]K_2}{10^{-pH}} \quad \textbf{\textit{Equation 4 - 6}}$$

CHAPTER 5: RESULTS AND DISCUSSION

5.0 Active H_2O_2 Yield

5.0.1 DI Water

The active H_2O_2 yield of 30% liquid H_2O_2 was examined in DI water to test the use of the I_3^- Method to determine H_2O_2 concentrations in water. The results are presented in **Figure 5-1** below.
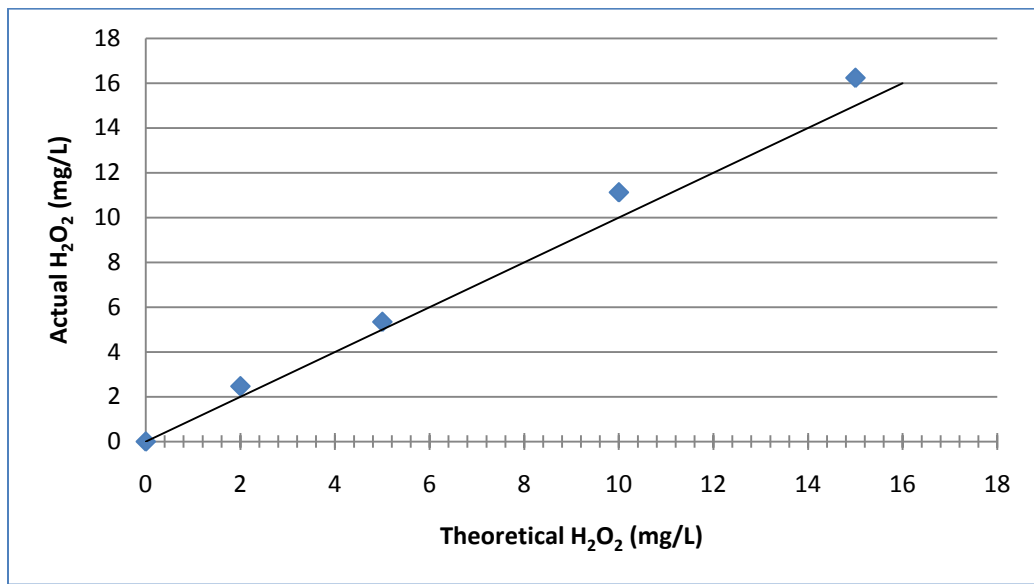
Figure 5-1: Theoretical H_2O_2 and Actual H_2O_2 Yield of 30% liquid H_2O_2 in DI Water

Ideally, the theoretical H_2O_2 concentration and actual active H_2O_2 yield should be a 1:1 ratio (i.e. 100% yield). This is presented in **Figure 5-1** with a solid line with a slope of 1. A trendline was applied to the relationship between the theoretical and actual H_2O_2 yields, the slope of the line would be 1.09, less than 10% different from what was expected. Additionally, the average error in the I_3^- Method compared to the theoretical concentrations of H_2O_2 was 10.8%. Based upon this analysis, the I_3^- Method was determined to be an acceptable method for the determinations of active H_2O_2

concentrations. **Figure 5-2** below displays the relationship between theoretical H_2O_2 and active H_2O_2 yield for SPB and SPC in DI water. Also shown in **Figure 5-2** is a solid line indicating a 1:1 ratio (100% yield) between theoretical H_2O_2 concentration and active H_2O_2 yield.
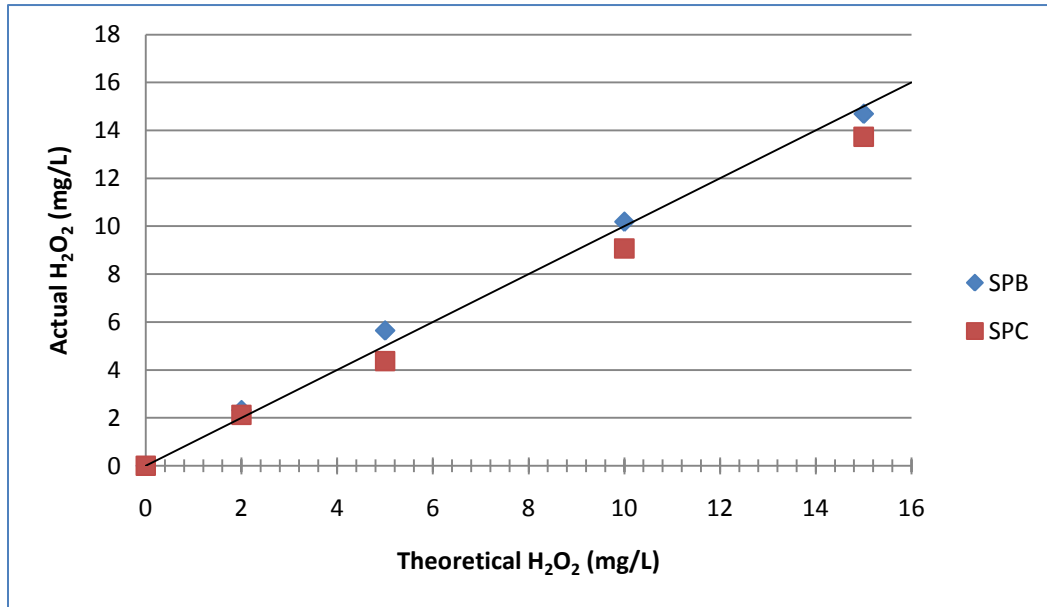
Figure 5-2: Theoretical H_2O_2 and Active H_2O_2 Yield of SPB and SPC in DI Water

The active H_2O_2 yield of both SPB and SPC in DI water is similar to the ideal 1:1 ratio for each concentration studied. Both reagents have a slightly lower yield than liquid H_2O_2. SPC has a slightly lower yield of active H_2O_2 than SPB. These suppositions were confirmed by examining the percent yield. SPB added to water resulted in a 92.7% ($\pm 6.1\%$) active peroxide yield, while for SPC, the yield was 93.9% ($\pm 8.1\%$). From these experiments, it can be expected that highly treated waters with compositions similar to DI water will have high yields of active H_2O_2 from SPB and SPC.

5.0.2 Pre-Treatment Water

The yield of active H_2O_2 via liquid H_2O_2, SPB and SPC in pre-treatment water from the Northampton, MA Water Filtration Plant is presented in **Figure 5-3** below. Also shown is a solid line indicating 100% theoretical yield.
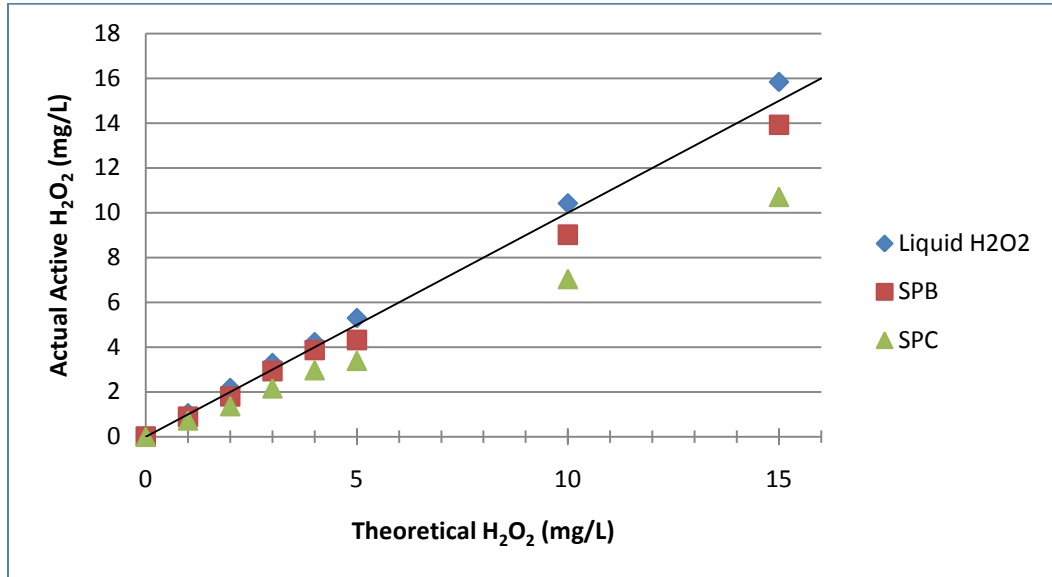
Figure 5-3: Yield of Active H_2O_2 in Pre-Treatment Water

Liquid H_2O_2 produced approximately 100% yield of active H_2O_2 in the pre-treatment water for all concentrations considered. SPB and SPC yield lesser amounts of active H_2O_2. SPB produced an average yield of 91.7% ($\pm3.1\%$) and SPC generated a 71.1% ($\pm1.8\%$) yield in the pre-treatment water.

5.0.3 Treated, Unchlorinated Water

The location of a UV light source for UV AOP should be downstream of treatment to remove particulates and some scavengers has occurred. Treated, unchlorinated water (post-pre treatment and filtration) was collected from the

Northampton Water Filtration Plant to simulate this location. The results of yield analysis in this water are presented in **Figure 5-4**. Again, a solid line was included to indicate 100% active H_2O_2 yield.
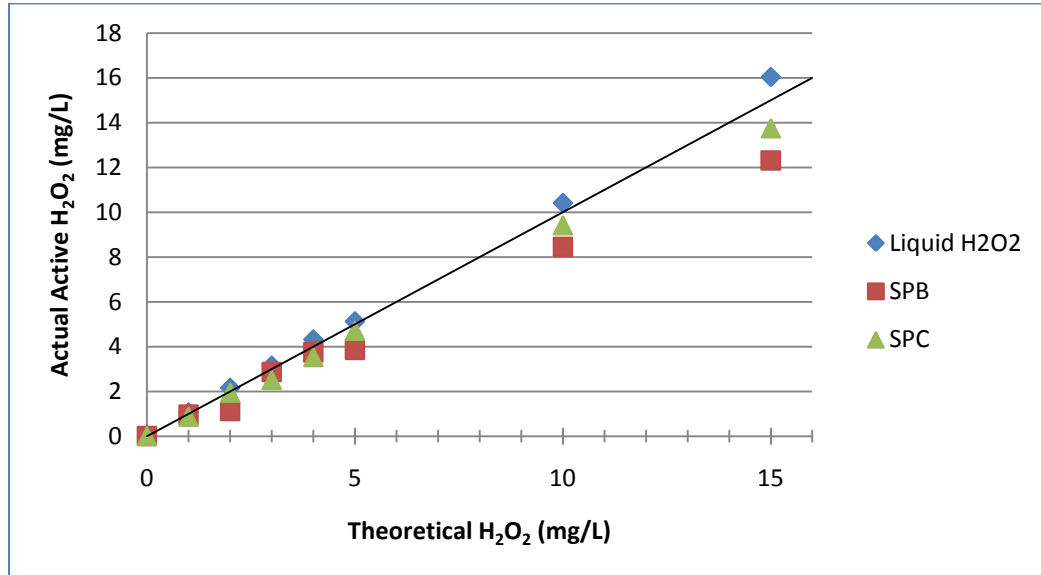
Figure 5-4: Yield of Active H_2O_2 in Treated, Unchlorinated Water

As was the case with DI water and pre-treatment water, the yield of active H_2O_2 upon addition of liquid H_2O_2 to this water source was approximately 100%. Also, the yield of active H_2O_2 via SPB addition to the water source was similar to the pre-treatment water source. For the treated, unchlorinated water source, the yield was 83.5% ($\pm$10.4%). Unlike in the pre-treatment water source, the yield of SPC in the treated, unchlorinated water source was significantly higher (90.8% $\pm$3.5%).

5.0.4 Post-Treatment Water

The post-treatment water source is the result of further treatment of the unchlorinated water source. This included chlorination and the addition of a sodium bicarbonate buffer to adjust the pH of the water to the desired range. The active H_2O_2

yield upon the addition of liquid H_2O_2, SPB and SPC is shown in **Figure 5-5**. Again, a

solid line was included to indicate 100% active H_2O_2 yield is also shown.
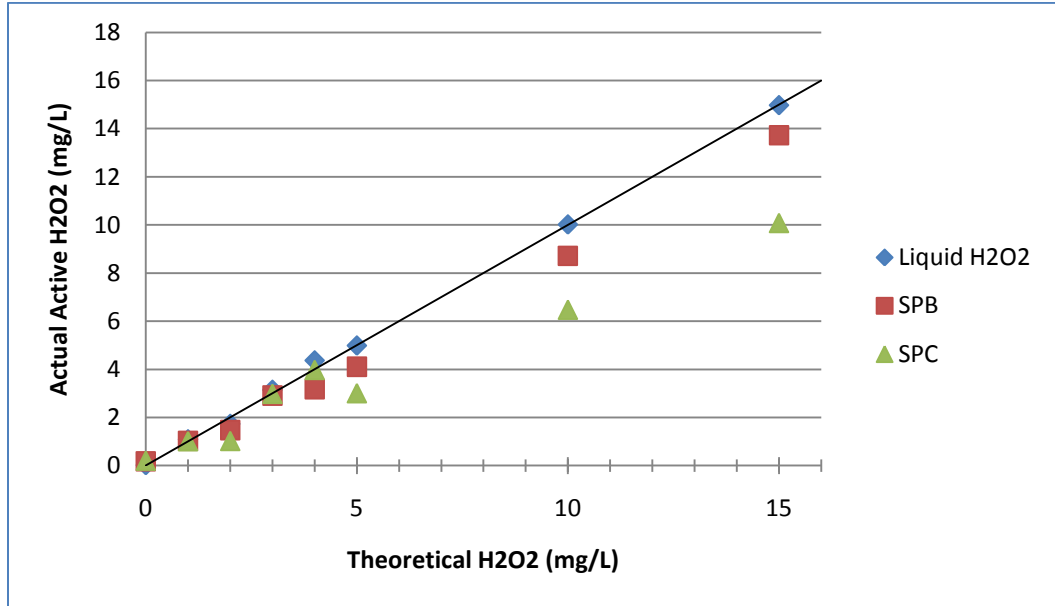
Figure 5-5: Yield of Active H_2O_2 in Post-Treatment, Finished Water

The addition of liquid H_2O_2 to this water source resulted in approximately 100%

yield of active H_2O_2. This was expected based on the high finished quality of the water.

Similar to the yield of active H_2O_2 found in the other water samples tested, the active

H_2O_2 yield due to SPB addition was 87.7% ($\pm$7.5%). The yield of active H_2O_2 via SPC

addition to this water source was 77.7% ($\pm$16.0%). The low yield of active H_2O_2 via SPC

is similar to that found in the pre-treatment water source (71.1%).

5.0.5 Summary of Active H_2O_2 Yields

A summary of the percent yields with 95% confidence intervals of active H_2O_2

upon via addition of liquid H_2O_2, SPB and SPC to the waters examined is presented in

Table 5-1.

Table 5-1: Summary of Percent Yields with 95% Confidence Intervals of Active H_2O_2 in Source Waters

Water Source	Percent Yield of Active H_2O_2 upon Liquid H_2O_2 Addition	Percent Yield of Active H_2O_2 upon SPB Addition	Percent Yield of Active H_2O_2 upon SPC Addition
Deionized	100%	92.7% ($\pm$6.1%)	93.9% ($\pm$8.1%)
Pre-Treatment	100%	91.7% ($\pm$3.1%)	71.1% ($\pm$1.8%)
Treated, Unchlorinated	100%	83.5% ($\pm$10.4%)	90.8% ($\pm$3.5%)
Post-Treatment, Finished	100%	87.7% ($\pm$7.5%)	77.7% ($\pm$16.0%)

It is apparent that the yield of active H_2O_2 from the addition of liquid H_2O_2 to each of the water sources is unaffected by the composition of the waters However, the yield of active H_2O_2 is slightly decreased when SPB is used as the source of H_2O_2 The observed yield upon SPC addition seems to be greatly impacted by water quality. A potential explanation for the observed trend links decreased yield with increased concentrations of background carbonate. The total carbonate concentration of the finished water is highest in the pre-treatment (18.31 mg/L) and post-treatment water (26.86 mg/L), and lowest in the treated, unchlorinated water. Total carbonate in the pre-treatment water is due to the presence of naturally occurring alkalinity, which is reduced in the plant treatment, and reintroduced into the post-treatment, finished water after chlorination in the form of a sodium carbonate buffer used for pH adjustment. The higher carbonate concentration of the pre- and post-treatment water sources limits the dissolution of SPC in water, thus limiting the formation of active H_2O_2. This is because the rate of dissolution of carbonate species will decrease as saturation is approached (Caldeira and Rau, 2000).

5.1 Carbonate and Borate Yields Via SPB and SPC Addition

5.1.1 Carbonate Yield

The expected total carbonate (C_T) to active H_2O_2 molar ratio in samples dosed with SPC is 2:3 (0.67). **Table 5-2** lists the C_T to active H_2O_2 molar ratios in each of the sample waters.

Table 5-2: C_T to Active H_2O_2 Molar Ratio in Each Water Sample Dosed with SPC

Sample Water	C_T to Active H_2O_2 Molar Ratio
DI Water	0.61 ($\pm$0.15)
Pre-Treatment Water	0.38 ($\pm$0.01)
Treated, Unchlorinated Water	0.41 ($\pm$0.07)
Post-Treatment Water	0.30 ($\pm$0.01)

Compared to the theoretical ratio, the actual C_T to active H_2O_2 ratio in DI water is approximately the same. This was expected given that the initial concentration of carbonate in DI water is minimal, which allows for the near completion of the dissolution of SPC forming H_2O_2 and Na_2CO_3. In contrast, in natural waters which have higher initial concentrations of total carbonate, the molar ratio of C_T to active H_2O_2 is less than the theoretical ratio. This can be directly attributed to the presence of carbonate species in the water samples preventing the dissolution of SPC in water to going to completion. This was also seen in the active H_2O_2 yields of each of the water samples (**Table 5-1**). A higher active H_2O_2 yield was found in the treated, unchlorinated water sample which had the lowest C_T of all of the natural water samples. This reaffirms the notion that SPC is a viable alternative to liquid H_2O_2, especially in waters with lower C_T concentrations.

5.1.2   Borate Yield

Determining the actual borate yield upon addition of SPB to the water sources studied was not possible due to analytical limitations. As a result, the theoretical borate yield was determined based on the reaction of SPB in water forming H_2O_2, H_3BO_3 and NaOH (**Reaction 1-4**, repeated below).

$$NaBO_3 + 3H_2O \rightarrow H_2O_2 + H_3BO_3 + NaOH \quad \boldsymbol{Reaction\ 1-4}$$
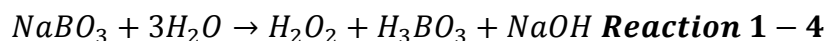
It was then assumed that the total borate yield (B_T) upon SPB addition to water was equal to the concentration of H_3BO_3 based on the stoichiometry of **Reaction 1-4**. This is justifiable based on the results of the total carbonate yield upon SPC addition to DI water. Based on stoichiometry, the ratio of total carbonate (C_T) to active H_2O_2 is 2:3 (0.67). The experimental results of the carbonate yield in DI water resulted in an average C_T to active H_2O_2 molar ratio of 0.61. Borate would be present mainly as $H_2BO_3^-$ in waters at pH's above 9.24. Furthermore, presenting the borate yield in terms of mg-Boron/L for comparison to water quality standards can be accomplished by multiplying the molar concentration of B_T by the molecular weight of boron, 10.81g/mol.

The theoretical total borate (B_T) yield upon addition of SPB to each of the water sources is presented for known active H_2O_2 concentrations in **Tables 5-3** to **5-6**. B_T values are presented as mg-Boron/L.

Table 5-3: Theoretical Borate Yield upon SPB Addition to DI Water

Active H_2O_2 (mg/L)	B_T (mg-B/L)
0	0
2.13	0.68
5.22	1.66
10.07	3.20
15.04	4.78

Table 5-4: Theoretical Borate Yield upon SPB Addition to Pre-Treatment Water

Active H_2O_2 (mg/L)	B_T (mg-B/L)
0	0
1.30	0.41
3.25	1.03
6.81	2.16
10.12	3.22

Table 5-5: Theoretical Borate Yield upon SPB Addition to Treated, Unchlorinated Water

Active H_2O_2 (mg/L)	B_T (mg-B/L)
0	0
1.58	0.50
4.92	1.56
9.67	3.08
14.11	4.49

Table 5-6: Theoretical Borate Yield upon SPB Addition to Post-Treatment Water

Active H_2O_2 (mg/L)	B_T (mg-B/L)
0	0
0.86	0.27
2.33	0.74
5.37	1.71
8.02	2.55

The initial B_T concentration of the natural water sources was assumed to be negligible. The borate yields in all water sources are expected to be similar. This can be explained by a comparison to SPC addition to water and the additional carbonate yield. The carbonate yields in the natural water sources occurred at a slower rate than the theoretical expected rate due to the presence of background carbonate species. In contrast, the borate concentration of the natural water samples is typically very low (US EPA, 2008a).

However, it is assumed that the addition of SPB to drinking water sources at concentrations of 5mg/L or less will not violate the health reference level for boron of 1.4mg/L set by the EPA. Also, some states have drinking water standards for boron ranging from 0.6-1.0mg/L (US EPA, 2008b). Based on this information the use of SPB as an alternative to liquid H_2O_2 is viable up to concentrations of approximately 5mg/L. Above this concentration, the addition of SPB to water will cause excessive boron concentrations to develop which could be harmful to human health or the environment.

5.2 Methodology for Comparing UV/H_2O_2 AOP Efficiency

5.2.1   MB Decay as a Function of Applied UV Dose

The ability of each reagent to produce hydroxyl radicals from the reaction between active H_2O_2 and UV light was determined by measuring the decay of MB as a function of applied UV dose. MB was used as a hydroxyl radical probe compound based upon the fact that it does not decay appreciably when exposed to UV light or hydrogen peroxide directly, but is readily degraded when hydroxyl radicals are present in solution.

As outlined in **Chapter 3**, the decay of MB absorbance at 664nm as a function of UV dose was continuously measured using the AvaSpec-2048 spectrophotometer, and

imported directly into an Excel® spreadsheet at one second intervals over the duration of the UV exposure (corresponding to approximately 2 mJ/cm^2 UV dose intervals). Plots were then be generated showing the decay of MB as a function of UV dose. **Figures 5-6** through **5-9** are examples of this type of plot in each of the waters tested. Plots of each reagent in the four sample waters at each concentration tested are available **Appendix C**. Relative MB concentration (C_t/C_0) of each sample over time was plotted rather than the actual concentration to account for any slight differences in initial MB concentration.
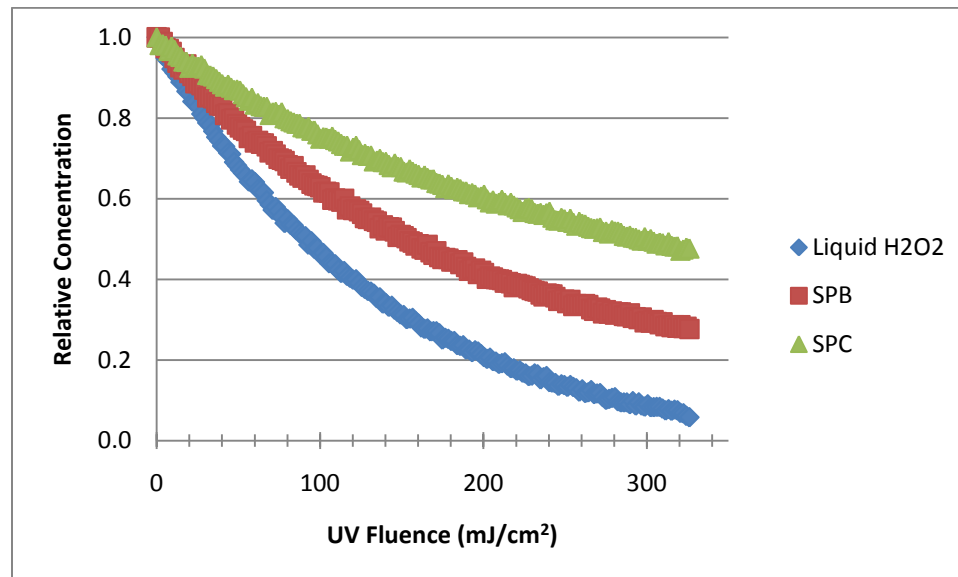
Figure 5-6: Decay of MB as a Function of UV Dose; Sample in DI Water; Reagents are Theoretical 10mg/L H_2O_2
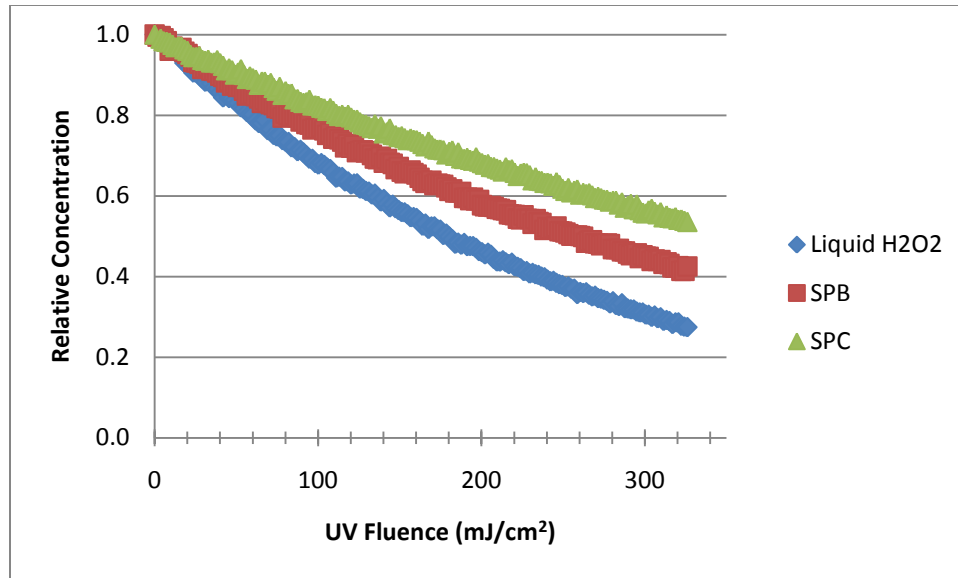
Figure 5-7: Decay of MB as a Function of UV Dose; Sample in Pre-Treatment Water; Reagents are Theoretical 10mg/L H_2O_2
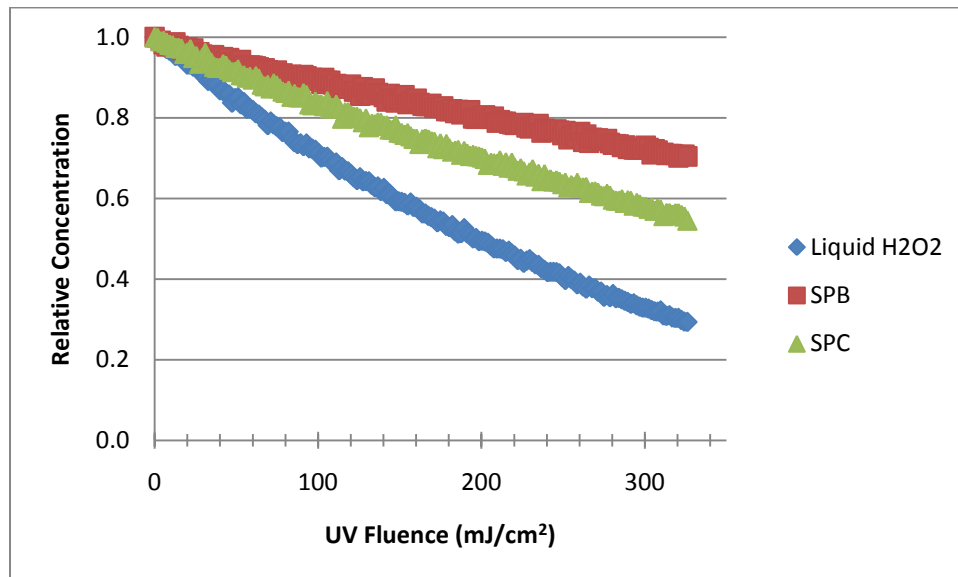
Figure 5-8: Decay of MB as a Function of UV Dose; Sample in Treated, Unchlorinated Water; Reagents are Theoretical 10mg/L H_2O_2
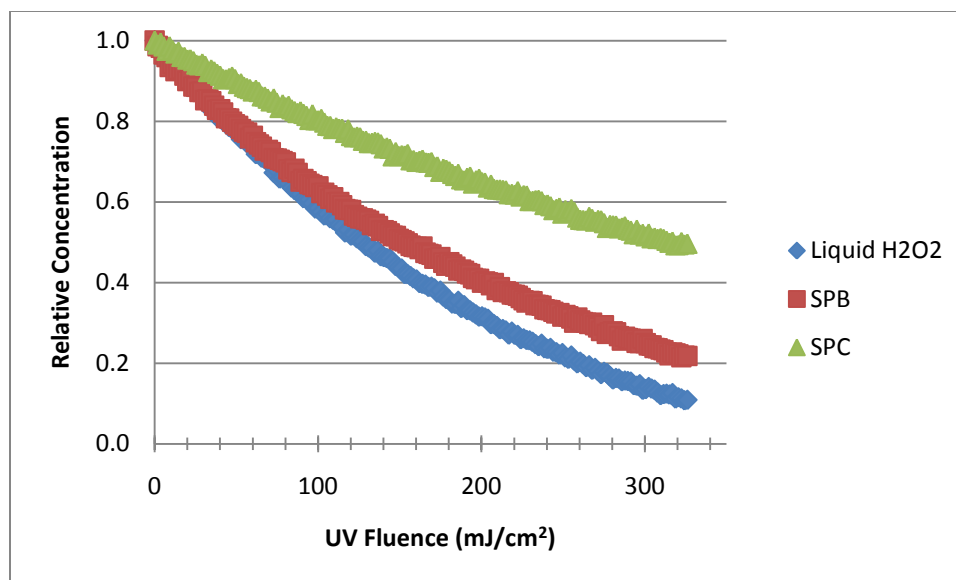
Figure 5-9: Decay of MB as a Function of UV Dose; Sample in Post-Treatment Water; Reagents are Theoretical 10mg/L H_2O_2

The rate of MB destruction was fastest for liquid H_2O_2, followed by SPB and SPC when a theoretical H_2O_2 concentration of 10mg/L was used. This is an indication that liquid H_2O_2 produced the greatest amount of hydroxyl radicals followed by SPB and then SPC. This was true for all water samples except the treated, unchlorinated water sample in which SPC produced more hydroxyl radicals than SPB. However, comparing the performance of the three reagents in the four sample waters using this method does not account for the varying yields of active H_2O_2. A lower active H_2O_2 concentration will produce less hydroxyl radicals and vice versa.

The parameter best suited for comparing the amenability of liquid H_2O_2, SPB, and SPC for UV AOP calculations is the pseudo first order decay rate of 1μM MB, plotted as a function of initial, measured, active peroxide. The dose-based pseudo first order rate constant (k') was determined by plotting the natural log of the MB concentration as a function of UV Dose, and calculating the negative of the slope of the linear best fit trendline, with units of inverse UV dose (cm^2 mJ^{-1}). An example of the calculation is

presented in **Figure 5-10**, for the case of liquid H_2O_2 at 2 mg/L active H_2O_2 in DI water.

Similar plots of each of the samples tested are available in **Appendix D**.
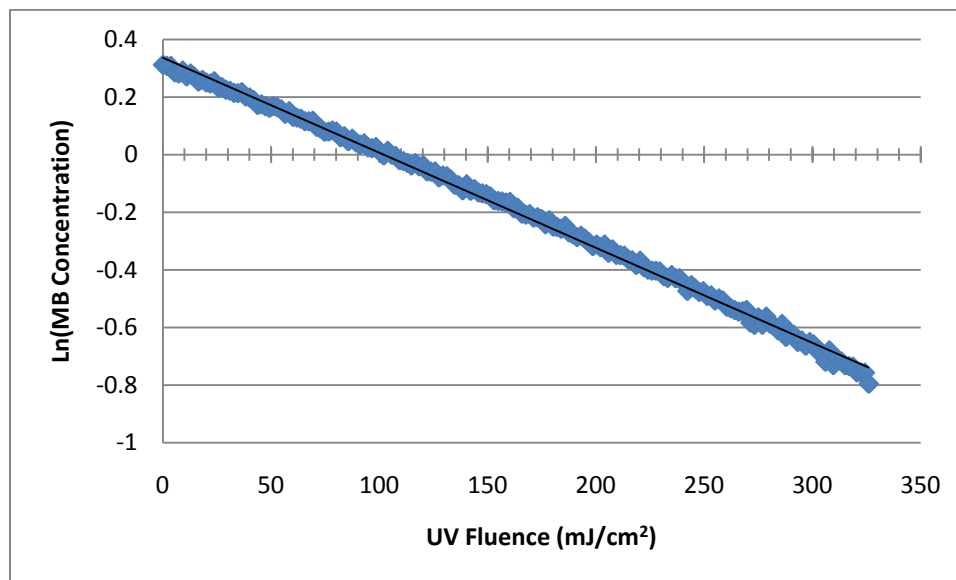
Figure 5-10: Example of Plot Used to Determine Pseudo First Order MB Decay Rate

For this sample the equation of the linear best fit trendline was $y = -0.0033x + 0.3357$, indicating that the pseudo first order decay rate of MB (k') in this sample of $0.0033 \pm 2.5 \times 10^{-5}$ cm^2 mJ^{-1}.

5.2.2 Replicate Analysis of MB Decay

Replicates of theoretical 2 and 15mg/L H_2O_2 samples of liquid H_2O_2, SPB and SPC were completed to examine variability in the MB AOP oxidation methodology. **Figure 5-11** displays one example of replicate MB decay plots for theoretical 2mg/L active H_2O_2 concentrations in DI water. Similar results were observed for each water sample tested, and replicate comparison plots are available in **Appendix E**.
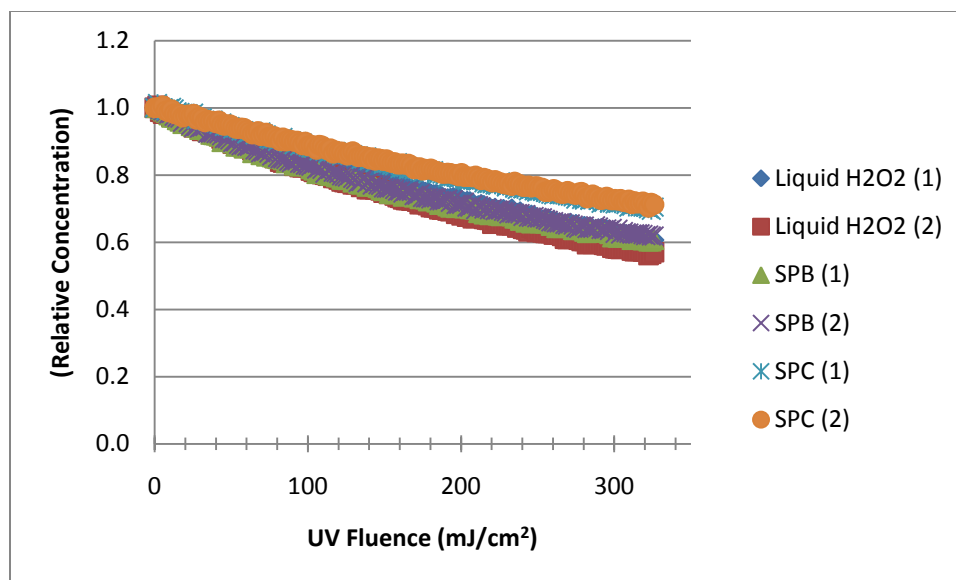
Figure 5-11: Replicates of UV Exposures

As seen in **Figure 5-11**, the replicates indicate that the method used to analyze the decay of MB over time while exposed to UV light can be reproduced without significant differences in the results. **Table 5-7** displays the MB decay rates of each of the samples shown in **Figure 5-11** along with their 95% confidence intervals.

Table 5-7: MB Decay Rate and 95% Confidence Intervals for Replicate Analysis

Sample	MB Decay Rate (cm^2/mJ)
Liquid H$_2$O$_2$ (1)	0.473 ($\pm$.001)
Liquid H$_2$O$_2$ (2)	0.474 ($\pm$.001)
SPB (1)	0.393 ($\pm$.001)
SPB (2)	0.401 ($\pm$.002)
SPC (1)	0.337 ($\pm$.001)
SPC (2)	0.376 ($\pm$.002)

5.3 Liquid H$_2$O$_2$, SPB and SPC for UV-AOP in DI Water

The dose based MB decay rate constants for solutions of liquid H$_2$O$_2$, SPB, and SPC in DI water are shown as a function of measured active H$_2$O$_2$ in **Figure 5-12**.
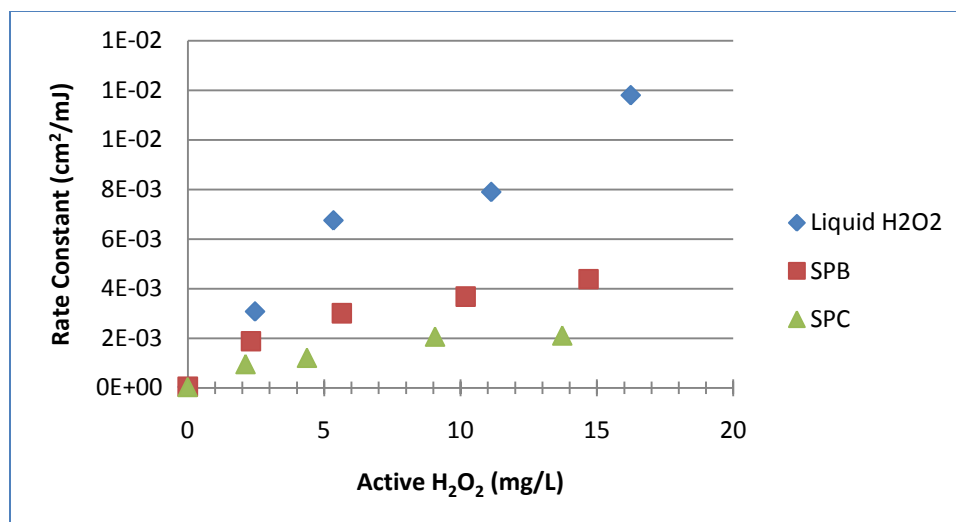
Figure 5-12: MB Decay Rates in DI Water as a Function of Active H_2O_2 in DI Water

Figure 5-12 shows that the fastest decay of MB occurred when liquid H_2O_2 was used as the source of hydroxyl radicals. Also, the rate of MB destruction is directly proportional to the active H_2O_2 concentration. Since MB decay is used as a surrogate for hydroxyl radical production it can be concluded that up to an active H_2O_2 concentration of 15mg/L, the concentration of hydroxyl radicals produced in DI water from liquid H_2O_2 is directly proportional to the liquid H_2O_2 concentration. This linear nature is due to the fact that there is a very low concentration of hydroxyl radical scavengers present in DI water, and liquid H_2O_2 contributes little scavenging to the solution.

A 47.2% ($\pm$16.2%) decrease in MB destruction rate occurred when SPB was used as the source of hydroxyl radicals. Furthermore, when SPC was used as the source of hydroxyl radicals in solution, there was a 75.5% ($\pm$12.9%) decrease in the MB decay rate. This shows that in DI water, where there are very low concentrations of constituents that may interfere with the UV/H_2O_2 AOP, liquid H_2O_2 and SPB greatly outperform SPC in terms of hydroxyl radical production.

5.3.1   The Effect of pH on MB Decay

The effect of pH on the decay rate of MB by hydroxyl radicals produced from the reaction of UV light with liquid H_2O_2, SPB and SPC in DI water was examined and the results are shown in **Figure 5-13**. The relationship between the pH upon addition of the three reagents used as sources of H_2O_2 to DI water and active H_2O_2 concentration is shown in **Figure 5-14**.
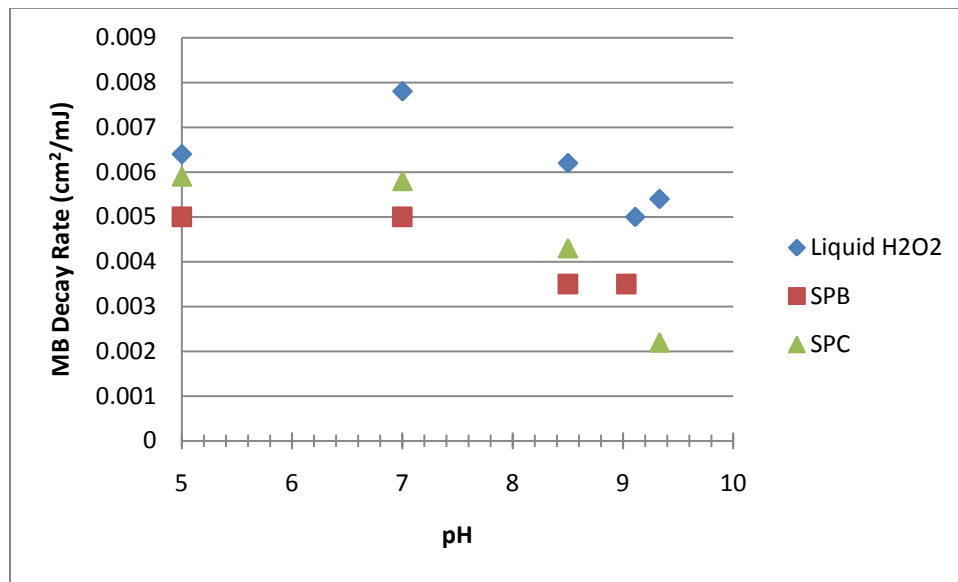
Figure 5-13: MB Decay Rate as a Function of pH in DI Water; All Samples are approximately 10mg/L H_2O_2
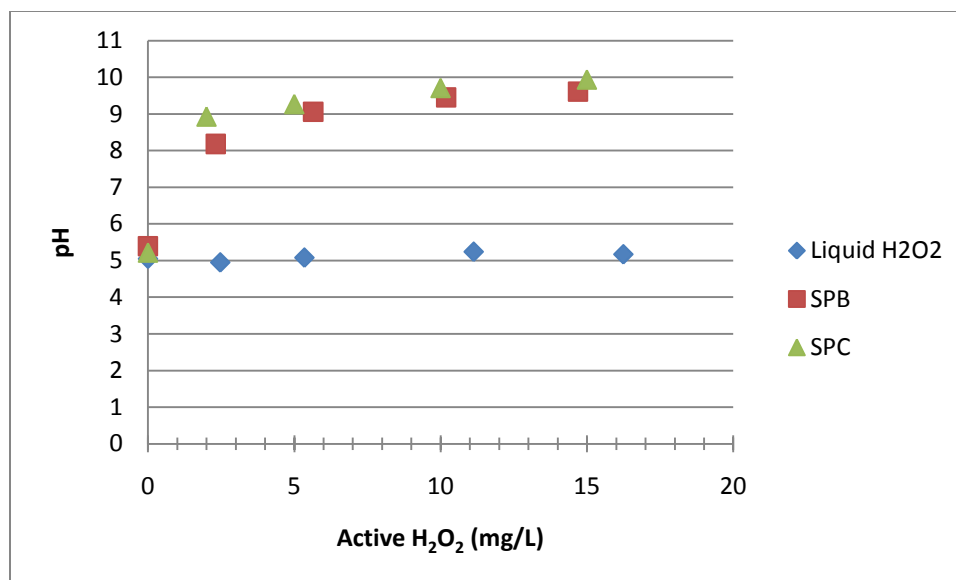
Figure 5-14: pH as a Function of Active H_2O_2 Concentration after Addition of Each Reagent to DI Water

When liquid H_2O_2 was used as the source of active H_2O_2, increased pH resulted in slower MB decay rates. A plausible explanation for this involves the deprotonation of hydrogen peroxide (H_2O_2) into the peroxyl (HO_2^-) ion, which is a much stronger hydroxyl radical scavenger (hydroxyl radical scavenging rate of $7.5 \times 10^9 M^{-1}s^{-1}$ (Buxton et al., 1988). As the rate constant is several orders greater for the deprotonated peroxyl ion, even a small amount of the compound present has the ability to increase background scavenging significantly. The peroxyl ion is present at higher concentrations as the pH approaches pK_a of H_2O_2 (11.62). For the case of the liquid H_2O_2 samples, there was a 20.5% loss in MB decay rate from pH 7 to pH 8.5. The increase in total scavenging caused by deprotonation of only 0.07% of the initial H_2O_2 to HO_2^- ion was 17.4%. The same trend was observed in the SPB and SPC samples. Therefore, it can be assumed that the formation of the peroxyl ion slows MB decay for each species in an equivalent fashion as the pH increases. These results are similar to the findings of Chang et al.

(2010), who found that above pH 7, the formation of the peroxyl ion results in a slower dye degradation rate.

The rate of MB destruction with SPB and SPC as the H_2O_2 source is lower than that for liquid peroxide at each pH value, and is directly attributable to the presence of additional scavengers in the system, derived from the solid oxidant itself. The greater decrease in MB decay at higher pH's in the SPC dosed samples compared to the SPB dosed samples can be attributed to the faster scavenging rate of the carbonate ion compared to that of the $H_2BO_3^-$ ion. Therefore, controlling the pH of the liquid H_2O_2, SPB and SPC dosed samples to 7 or less can increase the efficiency of the UV/H_2O_2 AOP.

Figure 5-14 shows that the addition of liquid H_2O_2 to DI water did not cause an increase in the pH of the water sample. However, when SPB and SPC were used as alternative sources of H_2O_2 in DI water, the pH increased as the concentration of reagent used increased. Above active H_2O_2 concentrations of approximately 5mg/L the use of SPB and SPC in highly finished waters may cause undesirable pH increases, reducing the efficiency of the UV/H_2O_2 AOP.

5.3.2   MB Decay in the UV/SPC AOP

The observed rates for MB decay by SPC increase linearly, but at a depressed rate when compared to liquid peroxide (**Figure 5-12**). This can be explained by scavenging introduced by SPC dissolution to CO_3^{2-} and HCO_3^- ions. The total amount of hydroxyl radical scavenging ($S._{OH}$) by H_2O_2, NOM and carbonate species in DI water is calculated using **Equation 5-1**; where $k_{x,·OH}$ is the rate of hydroxyl radical scavenging by species x and the concentrations of H_2O_2, NOM and the carbonate species are in molar units.

$$S_{\cdot OH} = k_{H_2O_2,\cdot OH} \times [H_2O_2] + k_{HO_2^-,\cdot OH} \times [HO_2^-] + k_{CO_3^{2-},\cdot OH} \times [CO_3^{2-}] + k_{HCO_3^-,\cdot OH}$$
$$\times [HCO_3^-] + k_{NOM,\cdot OH} \times [NOM] \ \boldsymbol{Equation\ 5-1}$$

The rates of hydroxyl radical scavenging of H_2O_2, CO_3^{2-} and HCO_3^- were reported

by Buxton et al. (1988). The rate used for background NOM was 2.5×10^4 L-mg^{-1}sec^{-1}.

However, the scavenging by NOM was only considered for the natural water sources. For

the use of SPC as the source of hydroxyl radicals in DI water, the theoretical percentage

of scavenging by H_2O_2 and HO_2^- and by added carbonate species is shown in **Table 5-8**.

Table 5-8: Total Scavenging Theoretical Percent Hydroxyl Radical Scavenging for SPC
Samples in DI Water

Active H_2O_2 Concentration (mg/L)	Total Scavenging (s^{-1})	% Hydroxyl Radical Scavenging by H_2O_2 and HO_2^-	% Hydroxyl Radical Scavenging by CO_3^{2-} and HCO_3^-
0	0	0%	0%
2.13	3.75×10^3	49.9%	50.1%
5.22	2.70×10^4	37.5%	62.5%
10.07	1.02×10^5	36.1%	63.9%
15.04	4.22×10^5	33.6%	66.4%

It was found that theoretical hydroxyl radical scavenging by CO_3^{2-} and HCO_3^-

accounted for the consumption of more than half of the hydroxyl radicals produced. This

indicates the importance of not using excessive SPC in the UV/SPC AOP. Using higher

concentrations of SPC can result in an unintended decrease in the efficiency of the

UV/SPC AOP.

5.3.3   MB Decay in the UV/SPB AOP

The observed rates of MB decay by the UV/SPB derived active H_2O_2 increases

linearly with active H_2O_2, but at a depressed rate when compared with liquid peroxide

(**Figure 5-12**). While not as depressed as SPC, a similar analysis was performed to investigate borate scavenging of hydroxyl radicals when SPB is used as the H_2O_2 source. Buxton and Sellers (1987) report a hydroxyl radical scavenging rate ($k_{H_3BO_3,\cdot OH}$) of $5 \times 10^4 M^{-1}sec^{-1}$ for boric acid (H_3BO_3). The scavenging by the deprotonated form of boric acid ($H_2BO_3^-$) was not reported, and as such, necessitated an estimation of the rate. This was accomplished as follows.

Step 1: Create a plot relating k' retardation with increased total scavenging.

The rate of MB decay (k') was determined with 10 mg/L active H_2O_2 derived from SPC in DI water at pH values 5, 7, 8.5 and 9.33, along with liquid H_2O_2 with pH adjusted to 9.33. The relative k' of each SPC sample was determined by dividing the k' of each SPC sample by the k' of the liquid H_2O_2 sample. Also, the total scavenging by carbonate and H_2O_2 was determined using **Equation 5-1**. The relationship between the relative k' and total scavenging was plotted on a log-log scale (**Figure 5-15**).
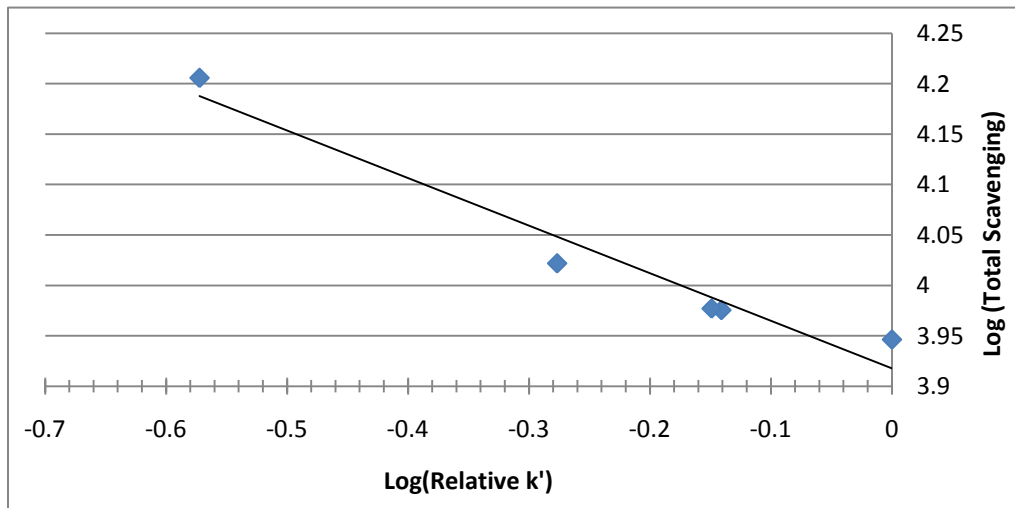
Figure 5-15: Relationship between Total Scavenging and Relative k' for SPC Samples in DI Water

The equation of the line of best fit is $log(Total\ Scavenging) = -0.4721 \times log(Relative\ k') + 3.9176$. **Figure 5-15** can then be used to relate the relative k' of a sample to an unknown total scavenging rate.

Step 2: Calculate relative k' for each SPB pH sample, compared with liquid H_2O_2.

The rate of MB decay (k') was determined with approximately 10 mg/L active H_2O_2 derived from SPB in DI water at pH values of 5, 7, 8.5, and 9.1, along with approximately 10 mg/L liquid H_2O_2 with pH adjusted to 9.1. Relative k' values were determined for each SPB sample by dividing the k' of each SPB sample by the k' of the liquid H_2O_2 sample. By using the equation of the line of best fit in **Figure 5-15**, the logarithm of the relative k' of the SPB samples could be converted to the logarithm of the total scavenging value.

Step 3: Calculate borate species scavenging.

Once the total scavenging of the sample was determined, the scavenging by borate species (H_3BO_3 and $H_2BO_3^-$) was determined by subtracting the known scavenging by H_2O_2 from the total scavenging. The scavenging rate by $H_2BO_3^-$ was then determined by subtracting the total borate scavenging by the scavenging by H_3BO_3 and dividing by the concentration of $H_2BO_3^-$ in solution. This resulted in an estimated $H_2BO_3^-$ hydroxyl radical scavenging rate ($k_{H_2BO_3^-,\cdot OH}$) of 4.27×10^7 ($\pm 3.79 \times 10^7$)$M^{-1}sec^{-1}$. This value is significantly higher than that of H_3BO_3, indicating that the deprotonated form of boric acid is the main scavenger of hydroxyl radicals in water. The scavenging rate by $H_2BO_3^-$

50

is similar to the scavenging rates of HCO_3^- and CO_3^{2-}, however, its effects are less profound due to the typical low concentrations of borate in water at typical pH (pKa = 9.24).

Equation 5-1 can then be modified for borate species for use in the determination of the theoretical percent of hydroxyl radical scavenging by borate. (**Equation 5-2**)

$$S._{OH} = k_{H_2O_2,·OH} \times [H_2O_2] + k_{HO_2^-,·OH} \times [HO_2^-] + k_{H_3BO_3,·OH} \times [H_3BO_3] + k_{H_2BO_3^-,·OH}$$
$$\times [H_2BO_3^-] + k_{NOM,·OH} \times [NOM] \quad \boldsymbol{Equation\ 5-2}$$

Again, the contributions of background alkalinity were only considered in the natural water sources. **Table 5-9** shows the total scavenging and the theoretical percentage of scavenging by H_2O_2 and borate species in DI water.

Table 5-9: Total Scavenging and Theoretical Percent Hydroxyl Radical Scavenging for SPB Samples in DI Water

Active H_2O_2 (mg/L)	Total Scavenging (s^{-1})	% Hydroxyl Radical Scavenging by H_2O_2 and HO_2^-	% Hydroxyl Radical Scavenging by H_3BO_3 and $H_2BO_3^-$
2.32	1.86x103	89.5%	10.5%
5.64	4.76x103	73.7%	26.3%
10.19	8.88x103	74.6%	25.4%
14.69	1.30x104	77.0%	23.0%

Scavenging by borate species is approximately 70% of the scavenging that was seen by carbonate species in the SPC dosed samples. $H_2BO_3^-$ scavenges hydroxyl radicals at a rate comparable to that of HCO_3^- and CO_3^{2-}. Therefore, the main reason behind the decreased theoretical percent of scavenging by borate species is the low concentration of borate in the water samples. Also, in comparison to the total scavenging by H_2O_2 and

carbonate species (**Table 5-8**), the total scavenging by H_2O_2 and borate species is approximately an order of magnitude less.

The above analysis allows for the conclusion that SPB and SPC are not viable alternative sources of H_2O_2 for use in the UV/H_2O_2 AOP in highly finished waters similar to DI water. Due to the purity of the water, hydroxyl radical scavenging by carbonate and borate species may limit the performance of the UV/H_2O_2 AOP. Also unintended pH increase may occur even at low SPB and SPC concentrations.

5.4 Liquid H_2O_2 for UV-AOP in Natural Waters

5.4.1 Pre-Treatment Water

Figure 5-16 is a comparison of the MB destruction rates when liquid H_2O_2, SPB and SPC are used as H_2O_2 sources in the pre-treatment water sample.
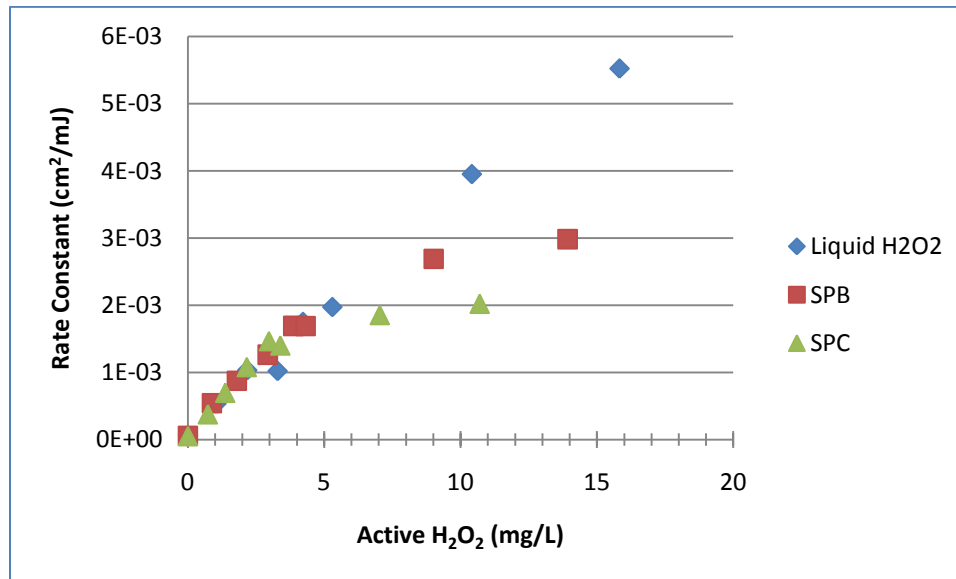
Figure 5-16: MB Decay Rates in Pre-Treatment Water as a Function of Active H_2O_2

The linear proportionality of liquid H_2O_2 concentration to MB destruction rate found in DI water was again found in the pre-treatment water source. However,

compared to DI water, the rate of MB destruction using liquid H_2O_2 as the source of active H_2O_2 in the pre-treatment water was 60.1% ($\pm$9.9%) less than those in DI water. The same leveling off trend present in DI water with SPB and SPC as the H_2O_2 source occurred in the pre-treatment water. The percent reduction of MB destruction rates in pre-treatment water compared to DI water was 39.1% ($\pm$11.7%) for SPB and 14.1% ($\pm$13.3%) for SPC. These reductions can be attributed to the presence of background scavengers and UV light absorbers found in the pre-treatment water.

Specifically, background alkalinity scavenges hydroxyl radicals at a faster rate than other typical drinking water contaminants. Based on this fact, it can be assumed that background alkalinity species are the main scavengers of hydroxyl radicals in the pre-treatment water. From **Figure 5-16**, it can be inferred that the borate scavenging will occur at a slower rate compared to the rate of carbonate scavenging. This explains why the rate of MB decay due to SPB is not decreased as much as with liquid H_2O_2 in the post treatment water compared to DI water.

Typically in the UV/H_2O_2 AOP, H_2O_2 concentrations do not exceed 5mg/L in drinking water applications. For this reason, the region of active H_2O_2 concentrations up to 5mg/L is examined in greater detail in **Figure 5-17**.
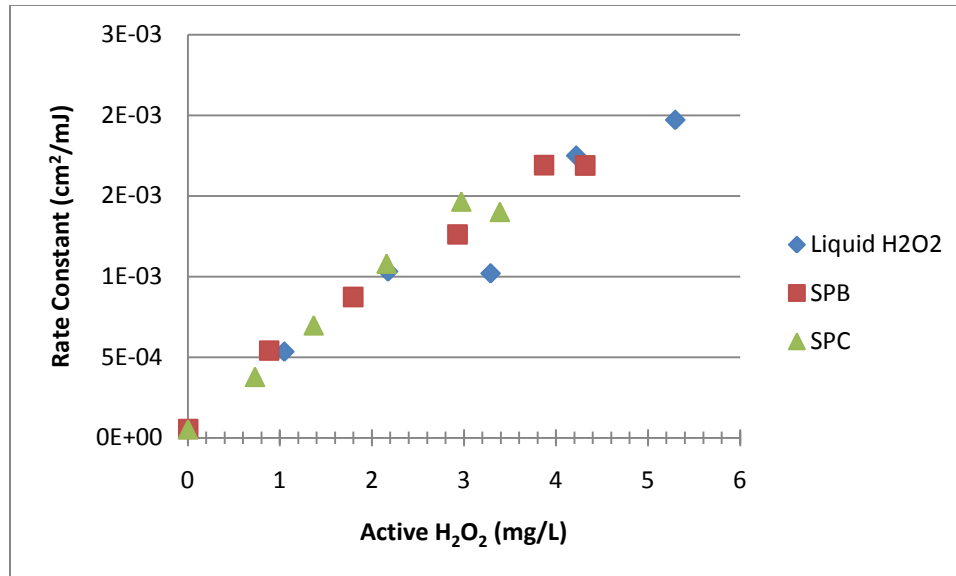
Figure 5-17: MB Decay Rates in Pre-Treatment Water as a Function of Active H_2O_2 up to 5mg/L

Up to an active H_2O_2 concentration of 5mg/L the MB destruction rates are similar for each of the reagents used. This is the result of the fact that scavenging by background alkalinity present in the water sample far outweighs any contributions provided by SPB or SPC breakdown products. When SPC is used as the source of hydroxyl radicals, a slight leveling off of the rate of decay of MB occurs above approximately 3mg/L. This is the result of added carbonate species from SPC breakdown beginning to contribute significant scavenging. Based on the results shown in **Figure 4-20**, if the UV/H_2O_2 AOP occurs in pre-treatment water sources, SPB and SPC can be used as viable alternatives to liquid H_2O_2 as a source of active H_2O_2 up to concentrations of approximately 5mg/L. The effects of additional hydroxyl radical scavenging resulting from SPC and SPB derived carbonate and borate species is seen in **Tables 5-10** and **5-11**.

Table 5-10: Total Scavenging and Theoretical Percent Hydroxyl Radical Scavenging for SPC Samples in Pre-Treatment Water

Active H_2O_2 Concentration (mg/L)	Total Scavenging (s^{-1})	% Hydroxyl Radical Scavenging by H_2O_2 and HO_2^-	% Hydroxyl Radical Scavenging by SPC Derived CO_3^{2-} and HCO_3^-	% Hydroxyl Radical Scavenging by NOM and Background Alkalinity
0	3.75×10^5	0%	0%	100%
1.30	3.80×10^5	0.3%	0.9%	98.8%
3.25	3.87×10^5	0.9%	2.4%	96.7%
6.81	4.10×10^5	2.6%	7.0%	90.4%
10.12	4.34×10^5	4.6%	11.4%	84.0%

Table 5-11: Total Scavenging and Theoretical Percent Hydroxyl Radical Scavenging for SPB Samples in Pre-Treatment Water

Active H_2O_2 (mg/L)	Total Scavenging (s^{-1})	% Hydroxyl Radical Scavenging by H_2O_2 and HO_2^-	% Hydroxyl Radical Scavenging by SPB Derived H_3BO_3 and $H_2BO_3^-$	% Hydroxyl Radical Scavenging by NOM and Background Alkalinity
0.01	3.75×10^5	0%	0%	100%
0.89	3.76×10^5	0.19%	0%	99.81%
1.80	3.76×10^5	0.38%	0.01%	99.61%
2.93	3.77×10^5	0.66%	0.06%	99.28%
3.87	3.78×10^5	0.90%	0.11%	98.99%
4.32	3.78×10^5	1.03%	0.16%	98.81%
9.02	3.82×10^5	1.95%	0.11%	97.93%
13.92	3.87×10^5	4.25%	1.38%	94.36%

Similar to DI water, as the concentration of SPC used is increased; the theoretical percent of carbonate scavenging also increases. However, the increase in carbonate scavenging is not as high as in DI water. This is the result of scavenging by background alkalinity initially present in the pre-treatment water. The effects of excessive carbonate scavenging due to SPC addition are not seen until the concentration of SPC used is above

approximately 7mg/L. Additionally, compared to DI water, the total scavenging is approximately an order of magnitude greater in the pre-treatment water, which is an indication of the increased background alkalinity. Typically, the use of the UV/H_2O_2 AOP does not occur in pre-treatment waters because of this high concentration of NOM and background alkalinity.

The minimal effect of borate species scavenging is seen in **Table 5-11**. Unlike with carbonate species, the borate species have little scavenging effects. At high concentrations of SPB borate scavenging slightly reduces the efficiency of the UV/H_2O_2 AOP. This is the result of increasing borate concentration in the water as the concentration of SPB is increased. Borate scavenging does explain why the trend in MB destruction rate levels off as the active H_2O_2 concentration increases.

The pH dependence of the performance of MB destruction when each reagent is used as a H_2O_2 source is shown in **Figure 5-18**. **Figure 5-19** shows the pH increase as a function of active H_2O_2 concentration for each reagent used in the pre-treatment water source.
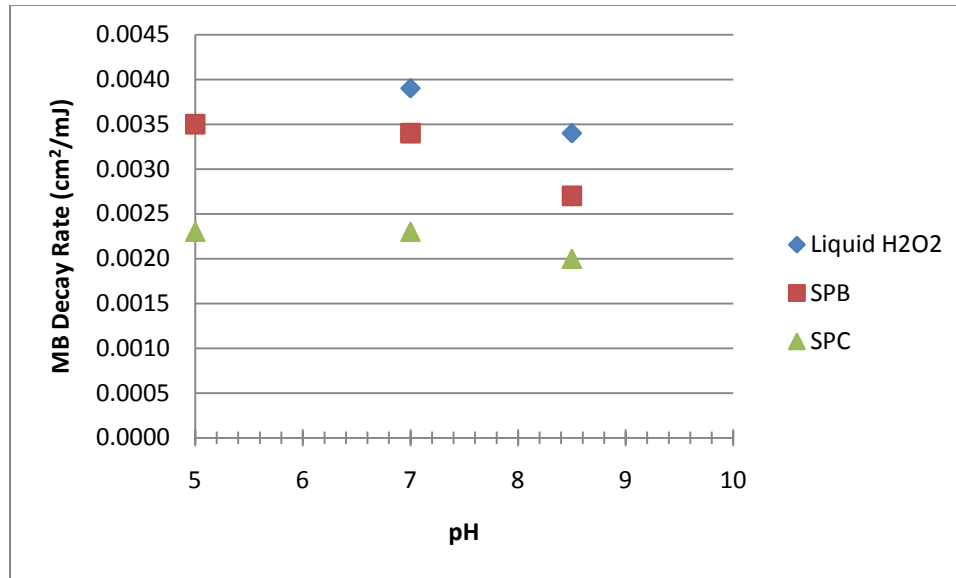
Figure 5-18: MB Decay Rate as a Function of pH in Pre-Treatment Water; All Samples are approximately 10mg/L H_2O_2
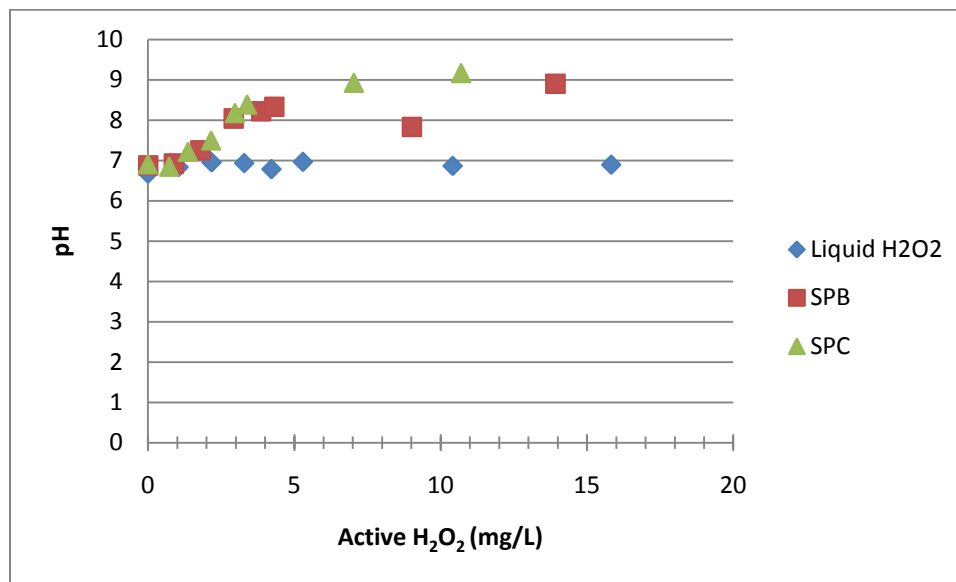
Figure 5-19: pH as a Function of Active H_2O_2 after Liquid H_2O_2, SPB and SPC Addition to Pre-Treatment Water

Similar to DI water the MB destruction rate when liquid H_2O_2 is used as the H_2O_2 source is only slightly effected by increases in the pH of the water. However, the pH increases minimally upon liquid H_2O_2 addition to the pre-treatment water. Also, a slight reduction in the MB destruction rate is seen at higher pH's when SPB and SPC are used

as H_2O_2 sources. This can be attributed the formation of the peroxyl ion at increased pH's. Additionally, the pH increase after adding SPB and SPC to the pre-treatment water was not as high as in DI water due to the presence of added buffering capacity by background alkalinity present in the pre-treatment water. Excessive pH increase is not seen at active H_2O_2 concentrations of 5mg/L or less, which reaffirms the conclusion that SPB and SPC are viable alternatives to liquid H_2O_2 in pre-treatment water sources.

5.4.2 Treated, Unchlorinated Water

The decay rates of MB when the three reagents used as sources of H_2O_2 are added to the treated, unchlorinated water sample and exposed to UV light are shown in **Figure 5-20**.
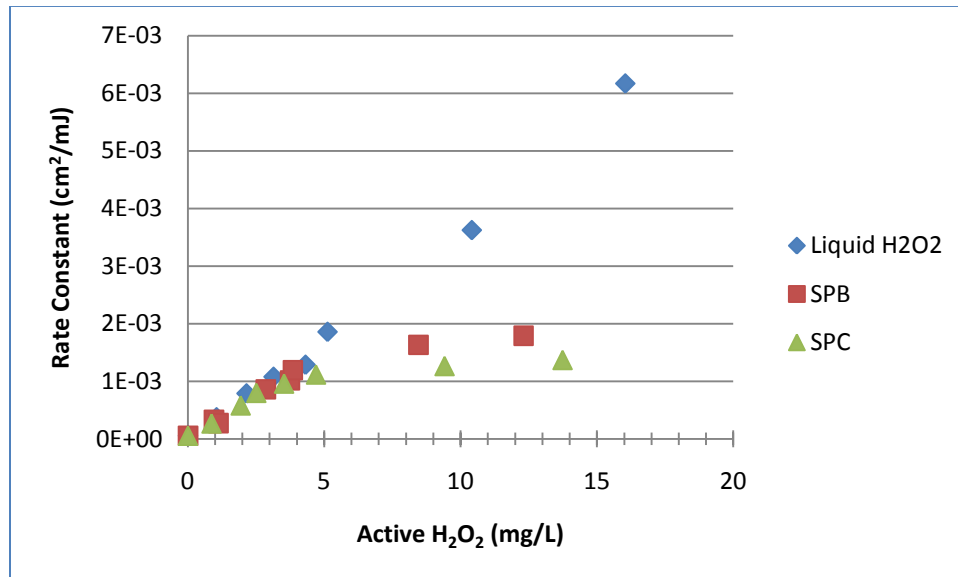
Figure 5-20: MB Decay Rates in Treated, Unchlorinated Water as a Function of Active H_2O_2

The ability of liquid H_2O_2 to produce hydroxyl radicals is not affected by the concentration of liquid H_2O_2 that is used. The reduction in the MB decay rate in the

treated, unchlorinated water source compared to that in DI water is 62.2% ($\pm$13.1%). This is approximately the same as the percent reduction between DI water and the pre-treatment water sample. This shows that the 50% reduction in background alkalinity between the pre-treatment and treated, unchlorinated water samples does not affect the MB decay rate when liquid H_2O_2 is used as the source of active H_2O_2.

The same leveling off trend of the destruction of MB seen in previous water samples above an active H_2O_2 concentration of approximately 5mg/L was found in the treated, unchlorinated water. The percent reduction of MB decay rate when SPB is used as the source of H_2O_2 in the treated, unchlorinated water source compared to DI water was 49.2% ($\pm$13.4%). In comparison, when SPC is used as the source of H_2O_2, the percent reduction between DI water and treated, unchlorinated water was 30.4% ($\pm$14.8%), approximately twice as much as between DI water and pre-treatment water.

The decay of MB in the practical range of active H_2O_2 concentrations used in the UV/H_2O_2 AOP is shown in greater detail in **Figure 5-21**.
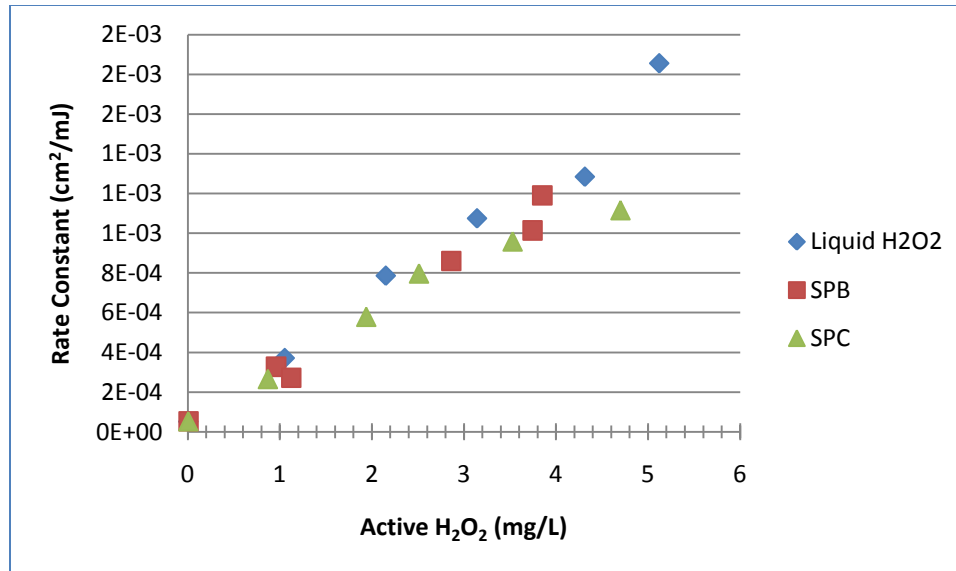
Figure 5-21: MB Decay Rates in Treated, Unchlorinated Water as a Function of Active H_2O_2 up to 5mg/L

The destruction rates of MB when SPB and SPC are used as the source of H_2O_2 are approximately the same as when liquid H_2O_2 is used up to active H_2O_2 concentrations of approximately 5mg/L. This can be attributed to the hydroxyl radical scavenging by background alkalinity present in the water sample. Above this concentration scavenging by carbonate and borate species limit the effectiveness of these reagents. The total scavenging and theoretical percentage of scavenging by H_2O_2 species, NOM, carbonate species and borate species is shown in **Tables 5-12** and **5-13**, respectively.

Table 5-12: Total Scavenging and Theoretical Percent Hydroxyl Radical Scavenging for
SPC Samples in Treated, Unchlorinated Water

Active H_2O_2 Concentration (mg/L)	Total Scavenging (s^{-1})	% Hydroxyl Radical Scavenging by H_2O_2 and HO_2^-	% Hydroxyl Radical Scavenging by SPC derived CO_3^{2-} and HCO_3^-	% Hydroxyl Radical Scavenging by NOM and Background Alkalinity
0	1.88×10^5	0%	0%	100%
1.58	1.91×10^5	0.0%	0.0%	100%
4.92	1.98×10^5	0.7%	1.4%	98.0%
9.67	2.17×10^5	2.0%	3.3%	94.7%
14.11	2.46×10^5	3.5%	10.0%	86.4%

Table 5-13: Total Scavenging and Theoretical Percent Hydroxyl Radical Scavenging for
SPB Samples in Treated, Unchlorinated Water

Active H_2O_2 (mg/L)	Total Scavenging (s^{-1})	% Hydroxyl Radical Scavenging by H_2O_2 and HO_2^-	% Hydroxyl Radical Scavenging by SPB Derived H_3BO_3 and $H_2BO_3^-$	% Hydroxyl Radical Scavenging by NOM and Background Alkalinity
0.01	1.88×10^5	0%	0%	100%
0.96	1.89×10^5	0.41%	0.01%	99.58%
1.12	1.89×10^5	0.48%	0.02%	99.50%
2.86	1.91×10^5	1.27%	0.11%	98.62%
3.74	1.92×10^5	1.77%	0.27%	97.96%
3.85	1.93×10^5	2.11%	0.56%	97.33%
8.45	2.02×10^5	5.25%	1.76%	92.99%
12.31	2.12×10^5	8.31%	2.99%	88.71%

Even though the initial background alkalinity of the treated, unchlorinated water

sample is lower than that of the pre-treatment water sample, NOM still scavenges

hydroxyl radicals at a greater percentage than H_2O_2 and carbonate species. However, the

total scavenging is slightly less in this natural water source compared to the pre-treatment

water. The scavenging by carbonate species is similar for this natural water source compared to the pre-treatment water source. Also, similar to the pre-treatment water source, the scavenging by borate species accounts for a small percentage of the total scavenging that occurs. However, the theoretical percentage of borate scavenging is greater in this water sample at higher active H_2O_2 concentrations, which is indicative of the lower background alkalinity of the water source. Using this information, it can be concluded that both SPB and SPC are practical alternatives to liquid H_2O_2 up to an active H_2O_2 concentration of approximately 5mg/L in waters similar to the pre-treatment water source.

The pH dependence of each reagent in the treated, unchlorinated water source is shown in **Figure 5-22**. Also, **Figure 5-23** shows pH as a function of active H_2O_2 concentration after each reagent is added to the treated, unchlorinated water.
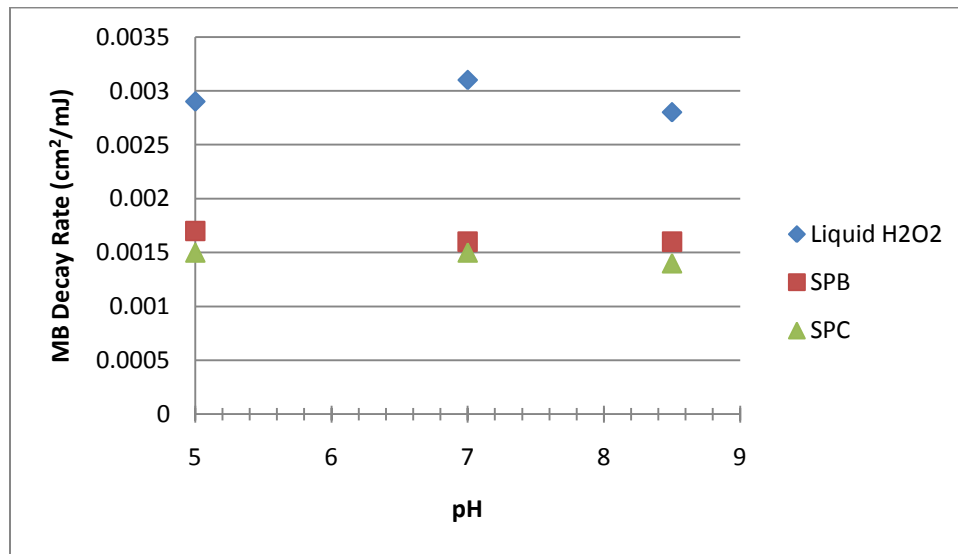
Figure 5-22: MB Decay Rate as a Function of pH in Treated, Unchlorinated Water; All Samples are approximately 10mg/L H_2O_2
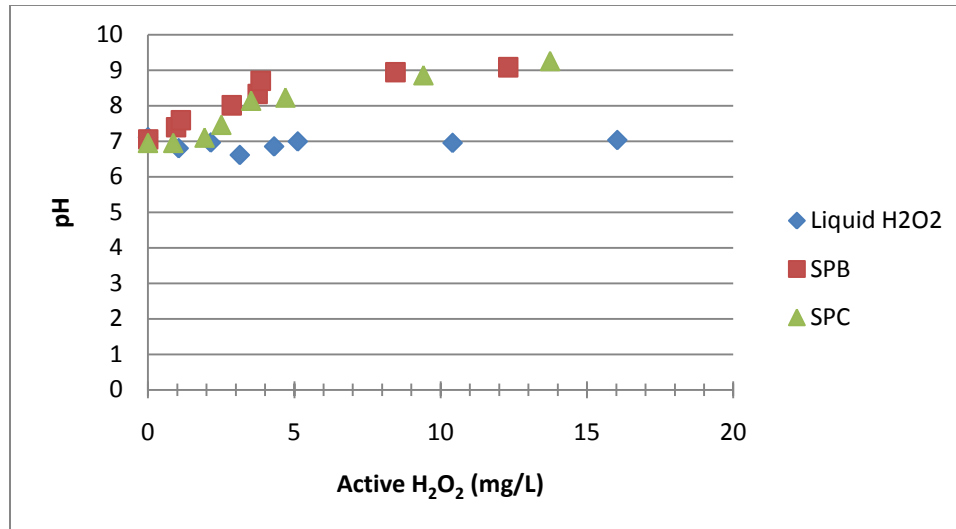
Figure 5-23: pH as a Function of Active H_2O_2 after Addition of Liquid H_2O_2, SPB and SPC to Treated, Unchlorinated Water

The reduced concentration of NOM and background alkalinity in the treated, unchlorinated water explains why there is no pH dependence for liquid H_2O_2, SPB and SPC in the treated, unchlorinated water. Also, similar to the pre-treatment water source, the added buffering capacity of the background alkalinity limits the pH increase after each reagent is added to the water. However, at active H_2O_2 concentrations greater than 5mg/L the pH of the water after SPB and SPC addition increases to undesirable levels. This is another reason why SPB and SPC are viable alternatives to liquid H_2O_2 only when the active H_2O_2 concentration is approximately 5mg/L or less in the treated, unchlorinated water sample.

5.4.3   Post-Treatment Water

The pseudo first order rate constants for the destruction of MB via UV reaction with active H_2O_2 derived from liquid H_2O_2, SPB and SPC in the post-treatment water are shown as a function of active H_2O_2 concentration in **Figure 5-24**.
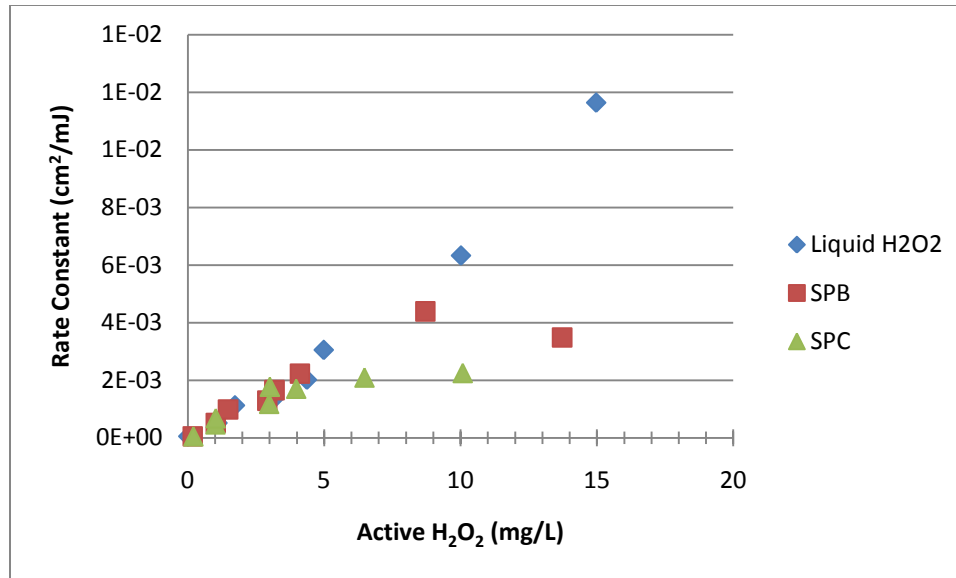
Figure 5-24: MB Decay Rates in Post-Treatment Water as a Function of Active H_2O_2

The same trend seen in the previous water sources, where MB decay is directly proportional to liquid H_2O_2 concentration was found in the post-treatment water sample. Also, a leveling off of MB decay occurred when SPB and SPC were used as the H_2O_2 source. Compared to DI water, the percent reduction in MB decay rate in the post-treatment water when liquid H_2O_2 was used as the H_2O_2 source was 34.9% ($\pm$28.7%). The purity of the post-treatment water sample explains why this is lower than the percent reduction between DI water and pre-treatment and the treated, unchlorinated water samples.

The percent reduction in MB destruction rates when SPB was used as the source of H_2O_2 in the post-treatment water compared to DI water was 31.4% ($\pm$16.4%). This is similar to the pre-treatment water source, and less than the treated, unchlorinated water source. In comparison when SPC was used as the H_2O_2 source, there was a 6.4% ($\pm$30.5%) increase in MB destruction rate in the post-treatment water compared to DI water. The percent increase is misleading because of the high variability between the

samples considered. Thus, it was concluded that the change in MB destruction rate when

SPC was used as the source of H_2O_2 in the post-treatment water compared to DI water

was negligible.

Unlike in DI water, but similar to the pre-treatment and unchlorinated water

sources, at active H_2O_2 concentrations up to approximately 5mg/L the MB destruction

rates using all three reagents as sources of hydroxyl radicals are nearly identical due to

the presence of NOM and background alkalinity scavenging hydroxyl radicals. **Figure 5-**

25 displays these similar destruction rates of MB focusing on active H_2O_2 concentrations
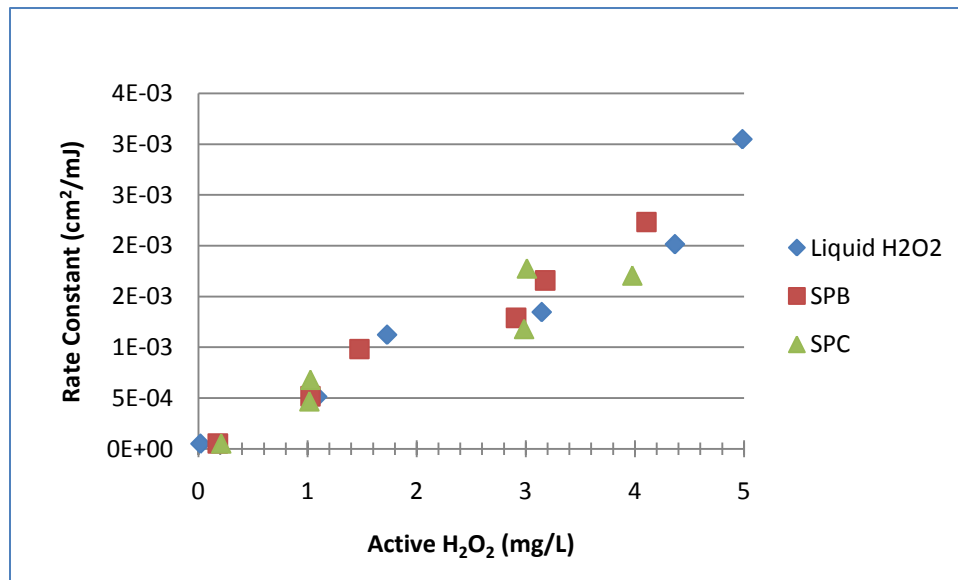
up to 5mg/L.

Figure 5-25: MB Decay Rates in Post-Treatment Water as a Function of Active H_2O_2 up
to 5mg/L

It can be concluded that in post-treatment water sources the rate of production of

hydroxyl radicals by each of the reagents is similar up to an active H_2O_2 concentration of

5mg/L. At active H_2O_2 concentrations higher than 5mg/L the efficiency of hydroxyl

radical production by SPB and SPC decreases due to the effect of radical scavenging.

Tables 5-14 and **5-15** list the total scavenging and theoretical scavenging by carbonate

and borate species, respectively.

Table 5-14: Total Scavenging Theoretical Percent Hydroxyl Radical Scavenging for SPC
Samples in Post-Treatment Water

Active H_2O_2 Concentration (mg/L)	Total Scavenging (s^{-1})	% Hydroxyl Radical Scavenging by H_2O_2 and HO_2^-	% Hydroxyl Radical Scavenging by SPC Derived CO_3^{2-} and HCO_3^-	% Hydroxyl Radical Scavenging by NOM and Background Alkalinity
0.17	5.50×10^5	0.0%	0.0%	100.0%
0.86	5.56×10^5	0.1%	0.9%	99.0%
2.33	5.67×10^5	0.3%	2.7%	97.0%
5.37	5.97×10^5	0.7%	7.2%	92.1%
8.02	6.28×10^5	1.0%	11.4%	87.6%

Table 5-15: Total Scavenging and Theoretical Percent Hydroxyl Radical Scavenging for
SPB Samples in Post-Treatment Water

Active H_2O_2 (mg/L)	Total Scavenging (s^{-1})	% Hydroxyl Radical Scavenging by H_2O_2 and HO_2^-	% Hydroxyl Radical Scavenging by SPB Derived H_3BO_3 and $H_2BO_3^-$	% Hydroxyl Radical Scavenging by NOM and Background Alkalinity
0.18	5.50×10^5	0.03%	0.00%	99.97%
1.03	5.51×10^5	0.15%	0.00%	99.85%
1.47	5.51×10^5	0.22%	0.02%	99.76%
2.91	5.53×10^5	0.46%	0.06%	99.48%
3.18	5.53×10^5	0.54%	0.10%	99.37%
4.11	5.55×10^5	0.72%	0.16%	99.12%
8.71	5.62×10^5	1.69%	0.48%	97.83%
13.72	5.74×10^5	3.13%	1.08%	95.78%

The addition of the sodium bicarbonate buffer to the post-treatment water source

increases the background alkalinity of the water sample, and thus the total scavenging of

hydroxyl radicals that occurs, compared to the other water sources examined. This also results in similar theoretical hydroxyl radical scavenging percentages by H_2O_2, carbonate species and NOM compared to the pre-treatment water sample. However, the added effects of carbonate scavenging via SPC are not seen until concentrations of 5mg/L or greater. Also, the theoretical percentage of scavenging by borate species is similar in the post-treatment water and pre-treatment water. The higher background alkalinity concentrations of these two water samples, (15.0 and 22.0 mg/L as Ca_3CO_3, respectively) limits the effect of scavenging by borate species. It is concluded that SPB and SPC can be used as sources of hydroxyl radicals for use in the UV/H_2O_2 AOP in post-treatment water sources at concentrations of 5mg/L or less. However, in order to increase the performance of the UV/H_2O_2 AOP in this specific water source, a different a pH buffer that would not increase background scavenging effects should be used in finished waters.

The pH dependence of each reagent in the post-treatment water is shown in **Figure 5-26**. **Figure 5-27** shows the pH increase after addition of each reagent to the post-treatment water as a function of active H_2O_2 concentration.
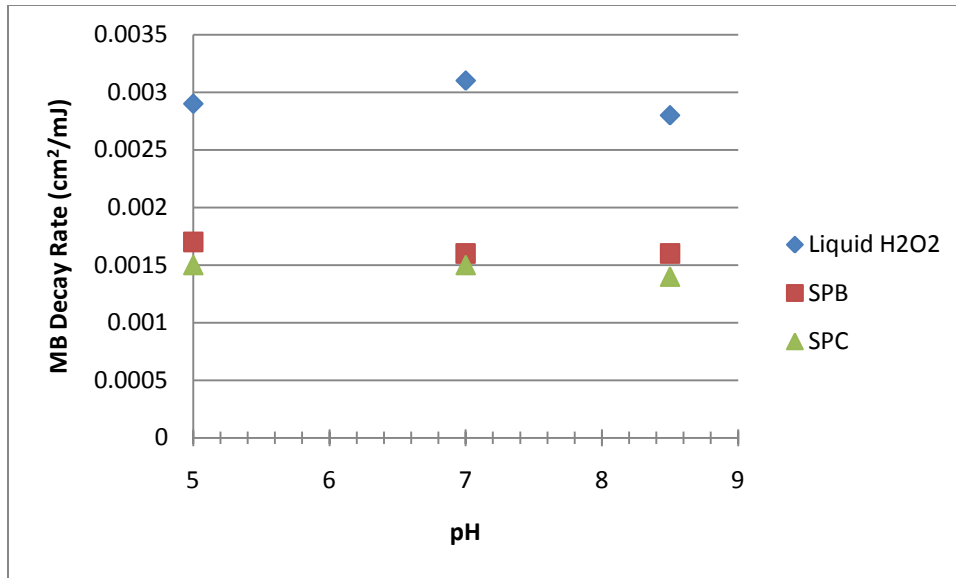
Figure 5-26: MB Decay Rate as a Function of pH in Post-Treatment Water; All Samples are approximately 10mg/L H_2O_2
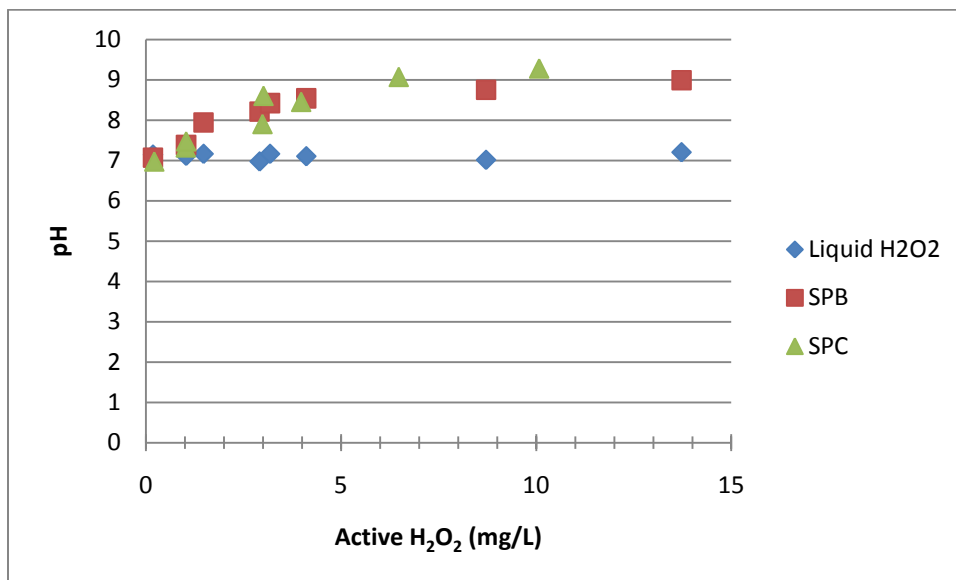
Figure 5-27: pH as a Function of Active H_2O_2 after Addition of Liquid H_2O_2, SPB and SPC to Post-Treatment Water

Similar results on the pH dependence of each reagent in the post-treatment water source were found compared to the other natural water sources. The added buffering capacity of the post-treatment water due to background alkalinity prohibits excessive pH

68

increase from occurring as the active H_2O_2 concentration is increased. This also explains why there was a negligible decrease in MB destruction as the pH of SPB and SPC samples increased. These results validate the conclusion that SPB and SPC are viable alternatives to liquid H_2O_2 in the post-treatment water at active H_2O_2 concentrations of 5mg/L.

CHAPTER 6: COST AND ENERGY ANALYSIS

6.0 Cost Data

Chemical and shipping costs of liquid H_2O_2, SPB and SPC were collected from industrial suppliers of the chemicals on a million gallon of water treated basis. FMC Industrial Chemicals (2010), OCI Chemical Company (2010b) and US Peroxide (2010a,b) provided costs for food grade liquid H_2O_2. The average chemical cost of 30% and 50% liquid H_2O_2 were $1.19 ($\pm$$1.32) and $1.81 ($\pm$$1.89) per liter, respectively. The average shipping costs of 30% and 50% liquid H_2O_2 were $0.46 ($\pm$$0.28) per liter for each grade. The high standard deviation in chemical costs of H_2O_2 can be attributed to varying chemical costs of liquid H_2O_2 from the suppliers. Costs pertaining to SPB were obtained from the Brenntag Group (2010a). The chemical cost of SPB was $2.26 per kilogram and the shipping cost was $0.028 per kilogram. The SPB provided by Brenntag (2010a) is not food grade, and as a result the cost of food grade SPB may be slightly higher. Additionally, Alfa Aesar (2010), the Brenntag Group (2010) and OCI Chemical Company (2010b) supplied information regarding to the costs of food grade SPC. The average chemical and shipping costs of SPC were $2.32 ($\pm$$0.70) per kilogram and $0.027 ($\pm$$0.003) per kilogram, respectively. FMC Chemicals (2010), OCI Chemical Company (2010b) and US Peroxide (2010a) indicated that the provided costs would decrease slightly if higher amounts of reagents are desired. As a result, it was assumed that the costs of the large scale use of these chemicals would not deviate significantly from the presented values.

6.1 Cost Analysis

The required amount of 30% and 50% liquid H_2O_2, SPB and SPC were determined based on the results of the ability of each to produce hydroxyl radicals in the natural water source where the UV/H_2O_2 AOP is typically installed. For this analysis, this corresponded to the results of the treated, unchlorinated water source. Based on those results, the maximum desired concentration of active H_2O_2 concentration for use with the UV/H_2O_2 AOP was 5mg/L. Additionally; the reduction in MB destruction rate of SPB and SPC compared to liquid H_2O_2 was accounted for in the analysis. This was accomplished by dividing the required amount of active peroxide by the percent decrease in MB destruction rate when using SPB and SPC versus liquid H_2O_2. Using this information the required amounts of each reagent per million gallon of treated drinking water per year to achieve 5mg/L of active H_2O_2 were determined (**Table 6-1**). The amounts are presented in mass and volume units, when appropriate.

Table 6-1: Mass and Volume Requirements of Each Reagent to Obtain 5mg/L Active H_2O_2 per Year

Reagent	Mass Required (kg/MG/yr)	Volume Required (L/MG/yr)
30% Liquid H_2O_2	23,000	20,700
50% Liquid H_2O_2	13,800	12,400
SPB	7,800	-
SPC	9,800	-

Using the obtained chemical and shipping cost data from industrial suppliers of each reagent, the total cost of treatment per million gallon of water per year was

determined. **Table 6-2** displays the total cost of treatment and the percentage of the total cost apportioned to chemical and shipping costs.

Table 6-2: Total Treatment Cost and Percentage of Chemical and Shipping Costs for Each Reagent

Reagent	Total Cost ($/MG/yr)	% Chemical Cost	% Shipping Cost
30% Liquid H$_2$O$_2$	$34,000	72%	28%
50% Liquid H$_2$O$_2$	$28,000	80%	20%
SPB	$23,000	99%	1%
SPC	$29,000	99%	1%

The total cost of treatment per million gallon of water is approximately $10,000 greater when 30% liquid H$_2$O$_2$ is used compared to SPB and $5,000 greater compared to SPC. The main reason for this is the low shipping costs of SPB and SPC. This was expected due to the fact that SPB and SPC are solids that can be shipped for much cheaper than liquid H$_2$O$_2$ which is shipped as a solution containing 70% (or 50%) water. For this reason alone, utilizing SPB and SPC as sources of H$_2$O$_2$ is expected to be more cost efficient. The chemical costs per million gallon of water for each reagent are approximately the same (approximately $25,000/MG/yr). Additionally, the cost of shipping 30% liquid H$_2$O$_2$ is approximately 40 times that of SPC and SPB and approximately 25 times as much as 50% liquid H$_2$O$_2$. This is also seen in **Table 6-2** in that the percentage of the total cost apportioned to shipping liquid H$_2$O$_2$ is much higher than that of SPB and SPC. Essentially, the shipping costs of SPB and SPC are negligible compared the total cost of SPB and SPC.

Another way of comparing the shipping costs of liquid H_2O_2 to that of SPB and SPC is by examining the cost per mile of shipment. These costs were determined based on the freight on board (FOB) location of each industrial supplier. The average cost per mile of 30% and 50% liquid H_2O_2, SPB and SPC based on the requirements shown in **Table 6-1**, were \$5.28 ($\pm$\$2.54), \$1.46 ($\pm$\$1.31) and \$1.03 ($\pm$\$1.13) per mile per million gallon, respectively. Clearly, shipping each reagent the same distance will result in much higher costs for liquid H_2O_2 compared to SPB and SPC.

A more practical representation of the savings that occur with using SPB and SPC versus liquid H_2O_2 in the UV/H_2O_2 AOP can be made by comparing the total cost of H_2O_2 for use in actual treatment facilities. Four such facilities were examined; the proposed 21MGD South District Water Reclamation Plant (SDWRP) in Miami-Dade, FL, the 26MGD Cornwall, ON Water Purification Plant, the 70MGD Orange County, CA Water Reclamation Plant and the 50MGD Aurora, CO Reservoir Water Purification Facility. The Miami-Dade and Orange County UV/H_2O_2 AOP systems are post reverse osmosis systems. These systems have high purity source waters, and as a result the results of the MB decay in DI water were used for the analysis of these facilities. On the other hand, the Cornwall and Aurora UV/H_2O_2 AOP systems occur in treated surface waters, therefore, the Northampton, MA treated, unchlorinated water source was assumed to be fairly representative of these systems. **Table 6-3** shows the theoretical total cost per year of active H_2O_2 for use in the UV/H_2O_2 AOPs in place at each of these facilities.

Table 6-3: Theoretical Total Cost of H_2O_2 via Each Reagent in Actual UV/H_2O_2 AOP Facilities

Reagent	Miami-Dade, FL	Orange County, CA	Cornwall, ON	Aurora, CO
30% Liquid H_2O_2	$718,000	$2,393,000	$889,000	$1,710,000
50% Liquid H_2O_2	$593,000	$1,978,000	$735,000	$1,413,000
SPB	$820,000	$2,734,000	$606,000	$1,166,000
SPC	$1,739,000	$5,796,000	$760,000	$1,462,000

It is seen that the use of SPB and SPC has the potential decrease the cost of H_2O_2 for use in the UV/H_2O_2 AOP for the treatment facilities utilizing surface waters as source waters. However, the use of these reagents needs to be tested on a pilot-plant scale to confirm the findings of this research prior to its use in a large-scale facility similar to the ones presented here. On the other hand, the facilities with high purity source water do not see savings with the use of SPB or SPC as alternative sources of H_2O_2. It can be assumed that SPB and SPC are not economically viable sources of H_2O_2 in high purity waters.

6.2 Energy Analysis

The reduction in the consumption energy required to deliver SPB and SPC compared to liquid H_2O_2 was examined through the use of an online Carbon Calculator provided by CSX Transportation (CSXa, 2010). The methodology behind the calculator was validated by Arthur D. Little, a management consulting agency for businesses (CSXb, 2010). Carbon dioxide (CO_2) emissions via freight transport of each reagent are determined by the Carbon Calculator using **Equation 6-1** below.

$$CO_2(tons) = Tons\ of\ Freight \times Shipping\ Distance$$

$$\times Mode\ Specific\ Diesel\ Consumption\ Factor$$

$$\times Mode\ Specific\ Emission\ Factor\ \textbf{Equation\ 6-1}$$

The tons of freight of each reagent per million gallon of treated drinking water were determined using the values presented in **Table 6-1**. CSX (b, 2010) reported that the diesel consumption factor used for truck shipping, 6 miles per gallon, was obtained from The Greenhouse Gas Protocol Initiative (2005). Also, CSX (b, 2010) noted that the CO_2 emission factor used for diesel fuel is the value (10.15 kg CO_2 per gallon) reported by U.S. Energy Information Administration. The Carbon Calculator allows for the input of the one-way distance of the shipment and the tonnage of product being shipped. It also allows for the adjustment of the freight weight per truck, however, this value was kept as the default 18 tons per truck.

Three base case scenarios considering different quantities of treated water were examined for the reduction in CO_2 emissions of shipping liquid H_2O_2, SPB and SPC. The tonnage of product required, number of trucks needed to ship the required amount of product and tons of CO_2 released as the result of shipping the reagents 250, 500 and 1,000 miles for each scenario are shown in **Tables 6-4** to **6-6**.

Table 6-4: CO_2 Emissions for Base Case Scenario 1: 1 MGD of Treated Water

Scenario 1: 1 MGD of Treated Water					
Reagent	Required Amount of Reagent (Tons)	Trucks Needed	CO_2 Emissions (tons) – 250 miles	CO_2 Emissions (tons) – 500 miles	CO_2 Emissions (tons) – 1000 miles
30% Liquid	23	2	0.5	1.0	2.0
50% Liquid	14	1	0.3	0.6	1.2
SPB	8	1	0.2	0.3	0.7
SPC	10	1	0.2	0.4	0.9

Table 6-5: CO_2 Emissions for Base Case Scenario 2: 5 MGD of Treated Water

Scenario 2: 5 MGD of Treated Water					
Reagent	Required Amount of Reagent (Tons)	Trucks Needed	CO_2 Emissions (tons) – 250 miles	CO_2 Emissions (tons) – 500 miles	CO_2 Emissions (tons) – 1000 miles
30% Liquid	115	7	2.6	5.1	10.2
50% Liquid	70	4	1.5	3.1	6.1
SPB	40	3	0.9	1.8	3.6
SPC	50	3	1.1	2.2	4.4

Table 6-6: CO_2 Emissions for Base Case Scenario 3: 10 MGD of Treated Water

Scenario 3: 10 MGD of Treated Water					
Reagent	Required Amount of Reagent (Tons)	Trucks Needed	CO_2 Emissions (tons) – 250 miles	CO_2 Emissions (tons) – 500 miles	CO_2 Emissions (tons) – 1000 miles
30% Liquid	230	13	5.1	10.2	20.4
50% Liquid	140	8	3.1	6.1	12.3
SPB	80	5	1.8	3.6	7.1
SPC	100	5	2.2	4.4	8.9

It was found that the average percent reductions in the shipping CO_2 emissions for each distance considered between SPB and 30% liquid H_2O_2 was 64.9% ($\pm$2.1%) and 57.4% ($\pm$1.4%) for SPC. Similarly, the average percent reductions between SPB and SPC and 50% liquid H_2O_2 was 41.5% ($\pm$3.8%) and 28.9% ($\pm$2.5%), respectively. Based on the results of the base case scenarios, significant CO_2 emissions savings are possible if SPB and SPC are used as alternatives to liquid H_2O_2 in source waters similar to Northampton, MA.

Another method of displaying the potential savings in shipping energy consumption of each reagent is by focusing on the existing and proposed UV/H_2O_2 AOP treatment facilities. Knowledge of the actual production facilities of H_2O_2 that are used by each of the treatment facilities is unknown, and as a result the results of the following scenarios are considered to be true only in theory and not in a practical sense. The production facilities chosen in the analysis are actual production facilities of US Peroxide (2010b) and the Brenntag Group (2010b). These were used to compare the results of

scenarios by varying the distance from the treatment facility considered. The facilities examined were the Miami-Dade, FL SDWRP, the Cornwall, ON Water Purification Plant, the Orange County, CA Water Reclamation Plant and the Aurora, CO Reservoir Water Purification Facility. As was the case with the cost analysis, the results of UV exposure experiments in DI water were used for the Miami-Dade and Orange County Facilities. Similarly, the results of the UV exposure experiments for the treated, unchlorinated water source were used for the Cornwall and Aurora facilities.

Figure 6-1 was generated using Google Maps (2010), and it shows each of the treatment facilities (stars) and the locations of the chosen chemical production facilities that could be used as suppliers of liquid H_2O_2 (circles), SPB and SPC (triangles) for each facility. Corresponding fill patterns of circle and triangles indicate the production facilities used for each facility in the analysis.
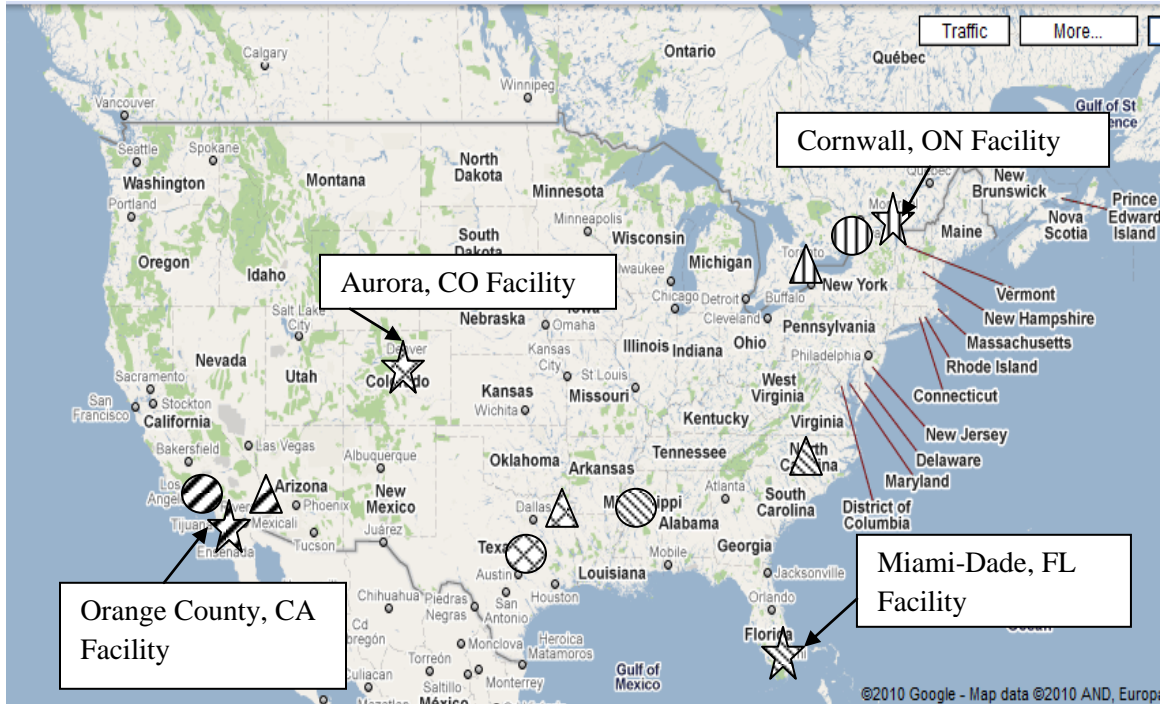
Figure 6-1: Water Treatment Facilities Utilizing the UV/H_2O_2 AOP and Respective Theoretical Locations of Chemical Suppliers (Source: www.maps.google.com)

Table 6-7 shows the reagent requirements of each reagent for each facility to maintain 5mg/L H_2O_2 based on the results of the previously presented UV exposure experiments. Fifty percent liquid H_2O_2 was used for the Miami-Dade and Orange County facilities due to the higher quality of finished water required. Similarly, 30% liquid H_2O_2 was used for the Cornwall and Aurora facilities. Also shown in **Table 6-7** are the distances to the respective production facilities chosen for each facility. **Figure 6-2** shows a comparison of the CO_2 emissions of shipping each reagent to the water treatment facilities. Furthermore, the percent changes in CO_2 emissions between shipping liquid H_2O_2, SPB and SPC are shown in **Table 6-8**. Negative values in **Table 6-8** indicate percent decreases in CO_2 emissions due to shipping H_2O_2.

Table 6-7: Requirements of Each Reagent to Maintain 5mg/L H_2O_2

Facility	Liquid H_2O_2 Required (Tons)	SPB Required (Tons)	SPC Required (Tons)	Distance to Liquid H_2O_2 Supplier (miles)	Distance to SPB and SPC Supplier (miles)
Miami-Dade	294	273	588	845	824
Orange County	980	910	1960	320	23
Cornwall	364	208	260	58	272
Aurora	700	400	500	974	1034
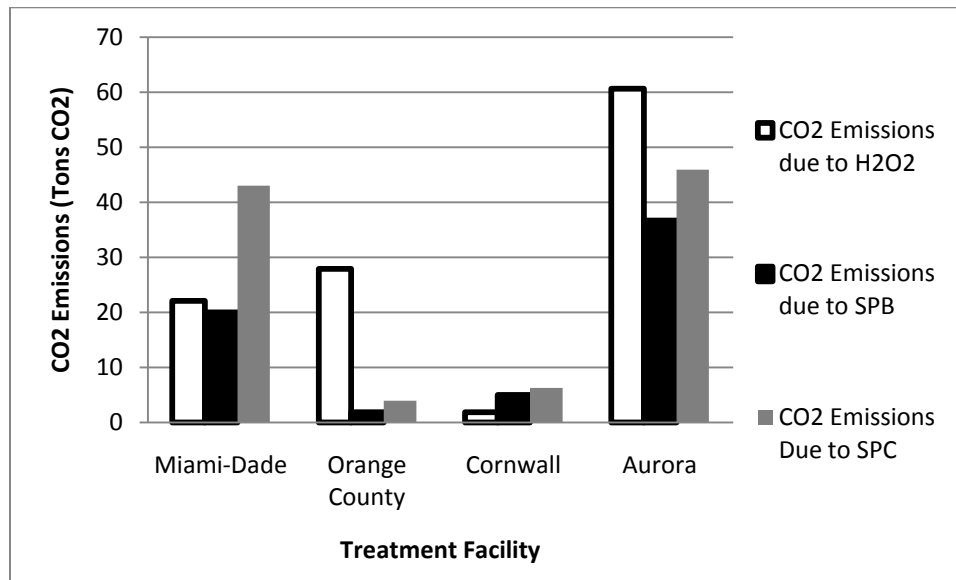
Figure 6-2: CO_2 Emissions for Shipping Each H_2O_2 Source to the Treatment Facilities

Table 6-8: Percent Change in CO_2 Emissions between Liquid H_2O_2 and SPB and SPC

Facility	Percent Change in CO_2 Emissions between SPB and Liquid H_2O_2	%Percent Change in CO_2 Emissions between SPC and Liquid H_2O_2
Miami-Dade	-9.5%	94.6%
Orange County	-93.2%	-85.7%
Cornwall	163.2%	231.6%
Aurora	-39.4%	-24.3%

For the Miami-Dade facility, the chosen production facilities of each reagent were similar distances away from the treatment facility. For this situation, the use of SPB has the ability to slightly decrease the portion of the carbon footprint associated with shipping H_2O_2. The use of SPC on the other hand requires a significantly increased amount of reagent than liquid H_2O_2 which causes a substantial increase in CO_2 emissions. The SPB and SPC production facility for the Orange County facility is in closer proximity to the treatment facility than the liquid H_2O_2 facility. As a result, significant reductions in CO_2 emissions are possible with using SPB or SPC as alternative sources of H_2O_2.

The scenario for the Cornwall treatment plant was essentially the opposite of the Orange County facility. The liquid H_2O_2 production facility is located closer to the treatment plant than the SPB and SPC production facility. This leads to significant increases in CO_2 emissions due to shipping H_2O_2 if SPB or SPC are used despite the greater tonnage requirement of liquid H_2O_2. Furthermore, the production facilities of each reagent associated with the Aurora facility were approximately the same distance from the treatment facility. In this case, there is the potential for a reduction in the CO_2 emissions associated with shipping H_2O_2 if SPB or SPC is used in place of liquid H_2O_2.

The findings of these scenarios on actual treatment facilities indicate that the proximity of the production facilities of each reagent play a significant role in the CO_2 emissions involved with shipping each form of H_2O_2. Additionally, for the situations in which greater amounts of either form of solid H_2O_2 are required, CO_2 emissions may increase if they are chosen as the source of H_2O_2. It can be concluded that quantity of reagent required and location of the each reagent's production facilities needs to be considered by drinking water treatment facilities utilizing the UV/H_2O_2 AOP. Once this

has been done the potential reduction in the shipping H_2O_2 portion of their carbon footprint by using SPB and SPC as alternative sources of H_2O_2 can be determined.

CHAPTER 7: CONCLUSIONS AND RECOMMENDATIONS

7.0 Conclusions

The use of the UV/H_2O_2 AOP for controlling emerging, unregulated contaminants has become a more commonly used AOP by drinking water treatment facilities. This AOP utilizes the formation of the hydroxyl radical by reaction between UV light and H_2O_2. The hydroxyl radical is a powerful oxidant that has the potential to oxidize contaminants into less harmful forms. However, one issue the UV/H_2O_2 AOP is the high costs of treatment. One possible way of decreasing these costs is by using alternative forms of H_2O_2. Two such alternatives are SPB and SPC. The advantage that these species have over liquid H_2O_2 is that they are shipped as solids. In comparison, liquid H_2O_2 for use in drinking water treatment is shipped as 30% (or 50%) solution, indicating that 70% (or 50%) of the solution is water. However, drinking water treatment facilities have plenty of water at hand. This leads to the assumption that solid forms of H_2O_2, such as SPB and SPC, have the potential to significantly decrease the treatment costs associated with the UV/H_2O_2 AOP.

In the analysis presented here, the active H_2O_2 yields of each reagent were examined in DI water and three natural water sources collected from the Northampton, MA Water Filtration Plant. It was found that liquid H_2O_2 produced approximately 100% active H_2O_2 yields in each water sample tested. The active H_2O_2 yield of SPB in each of the water sources ranged from approximately 83% to 93%. Similarly, the active H_2O_2 yield of SPC ranged from approximately 70% to 90%. In natural waters with higher background alkalinity, the active yield H_2O_2 via SPC was reduced. This can be attributed to the fact that as background carbonate concentrations increase, the rate of dissolution of

carbonate species decreases. This was not seen with SPB, and it is assumed that the

background borate concentrations of the natural water samples were minimal as a result.

These results indicate that SPB and SPC addition to water will result in nearly

proportional concentrations of active H_2O_2.

The rate of hydroxyl radical production using each reagent as a source of H_2O_2 in

the UV/H_2O_2 AOP was determined using MB decay as a hydroxyl radical probe. MB

does not decay appreciably in the presence of UV light alone. Hydroxyl radicals formed

via the reaction between UV light and H_2O_2 need to be present for MB decay to occur. A

summary of the percent reduction in hydroxyl radical production rate for each reagent

compared to liquid H_2O_2 is shown in **Table 7-1**. Also, the percent reductions are

presented for active H_2O_2 concentrations up to 5mg/L, which is typical of the UV/H_2O_2

AOP. **Table 7-2** lists the percent reduction MB destruction rate in each of the natural

water sources compared to DI water.

Table 7-1: Percent Reduction in Hydroxyl Radical Production Rate by SPB and SPC in
Each Water Source Compared to Liquid H_2O_2

Water Source	Percent Reduction Hydroxyl Radical Production Rate Compared to Liquid H_2O_2	
	SPB	**SPC**
DI Water	47.2% ($\pm$16.2%)	75.5% ($\pm$12.9%)
Pre-Treatment Water	1.2% ($\pm$11.4%)	17.1% ($\pm$12.8%)
Treated, Unchlorinated Water	22.2% ($\pm$18.5%)	29.2% ($\pm$5.3%)
Post-Treatment Water	12.2% ($\pm$9.5%)	23.6% ($\pm$13.8%)

Table 7-2: Percent Reduction in MB Destruction Rate in Natural Water Sources
Compared to DI Water

Water Source	Percent Reduction in MB Destruction Rate from DI Water		
	Liquid H_2O_2	SPB	SPC
Pre-Treatment Water	60.1% ($\pm$9.9%)	39.1% ($\pm$11.7%)	14.1% ($\pm$13.3%)
Treated, Unchlorinated Water	62.2% ($\pm$13.1%)	49.2% ($\pm$13.4%)	30.4% ($\pm$14.8%)
Post-Treatment Water	34.9% ($\pm$28.7%)	31.4% ($\pm$16.4%)	-6.6% ($\pm$30.5%)

From **Table 7-1** it can be seen that in the presence of radical scavengers (natural waters), the use of SPB as a source of H_2O_2 in the UV/H_2O_2 AOP produces hydroxyl radicals at a rate within approximately 25% of liquid H_2O_2. Similarly, SPC produces hydroxyl radicals within approximately 30% of the rate of hydroxyl radical production via liquid H_2O_2. The reduction in the hydroxyl radical production rate via SPB and SPC compared to liquid H_2O_2 can be attributed to the added effects of scavenging by borate and carbonate species in solution. This is seen specifically in DI water, which initially has a minimal concentration of radical scavengers. In this case the percent reduction in hydroxyl radical production rate is significantly higher than that natural water samples. Therefore, SPB and SPC are not expected to create the same oxidizing power as liquid H_2O_2 in the presence of UV light in high purity waters.

The effect of radical scavengers is also seen in **Table 7-2**. There is a significant decrease in MB destruction rate compared to DI water in each of the natural water sources. However, the post-treatment water sample did show the lowest percent reduction in MB destruction rate compared to DI water. This water has been sufficiently treated to

remove most background radical scavengers initially present in the pre-treatment water. It is expected that this reduction in MB destruction rate would be decreased further if the sodium bicarbonate pH buffer was not added to the water sample. The higher concentration of NOM and background alkalinity in the pre-treatment water makes the use of the UV/H_2O_2 AOP at this point in the treatment process less desirable. Additionally, chlorine is a known quencher of hydrogen peroxide. For this reason and due to the addition of the sodium bicarbonate pH buffer, the UV/H_2O_2 AOP is not recommended to be implemented in post-treatment water source. Based on these results the use of the UV/H_2O_2 AOP is most efficient at the point in the treatment process where NOM and background alkalinity reduction has occurred, and prior to any chlorine addition.

The two main limitations for using SPC in the UV/H_2O_2 AOP are the carbonate concentration of the source water and scavenging by carbonate species added to the water after SPC addition. In waters with reduced C_T, the dissolution of SPC in water forming H_2O_2 is allowed to proceed further to completion, thus increasing the efficiency of the UV/H_2O_2 AOP. It was discovered; however, that the increase in carbonate concentration of the water upon SPC addition did increase the rate of hydroxyl radical scavenging at SPC concentrations greater than approximately 5mg/L. The rate of hydroxyl radical production by SPC in the presence of UV light was found to be unaffected by the pH of the natural water sources. Furthermore, the increase in pH upon SPC addition to the natural water sources was limited to approximately 8.3 at active H_2O_2 concentrations of 5mg/L or less. Based on the research findings presented here, it is concluded that the use

of SPC in the UV/H_2O_2 AOP is most effective in waters with low C_T and at active H_2O_2 concentrations of 5mg/L or less.

In contrast, the only limitation of SPB as a source of H_2O_2 was scavenging by borate species at active H_2O_2 concentrations above approximately 5mg/L. However, the effect of borate scavenging was found to be significantly less than carbonate scavenging. It is also believed that the addition of SPB to natural water samples at concentrations of approximately 5mg/L or less will not violate the health reference level of boron set by the US EPA. Similar to SPC, MB destruction by SPB derived hydroxyl radicals was unaffected by the pH of the natural water samples. Additionally, the pH increase after SPB addition to the natural water sources was limited to approximately 8.3 or less at active H_2O_2 concentrations of 5mg/L or less. Therefore based on the findings of this research, it is concluded that SPB can be used as an alternative to liquid H_2O_2 in the UV/H_2O_2 AOP in a wide range of water sources up to a an active H_2O_2 concentration of approximately 5mg/L.

The theoretical comparison of the chemical and shipping costs of liquid H_2O_2, SPB and SPC was completed utilizing the percent reduction in MB decay rate using SPB and SPC versus liquid H_2O_2 in the treated, unchlorinated water source. It was assumed that the desired active H_2O_2 concentration fur use in the UV/H_2O_2 AOP was 5mg/L. It was found that the chemical costs of each reagent were approximately $25,000/MG/yr. The percentage of the total cost of H_2O_2 attributed to shipping was 28% for 30% liquid H_2O_2, 20% for 50% liquid H_2O_2 and 1% for SPB and SPC. Additionally, the shipping costs of SPB and SPC are 40 times less than 30% liquid H_2O_2 and 25 times less than 50% liquid H_2O_2. The main reason for the decrease in shipping costs of SPB and SPC versus

liquid H_2O_2 is that SPB and SPC are shipped as solids compared to liquid H_2O_2 which is shipped as a 30% (or 50%) solution. The potential approximate savings of the total cost of H_2O_2 by using SPB and SPC compared to 30% liquid H_2O_2 are $5,000 to $10,000 per million gallon of treated water. In contrast, if 50% liquid H_2O_2 is used, the potential savings associated with using SPB and SPC are negligible.

The examination of four treatment facilities that utilize the UV/H_2O_2 AOP (Miami-Dade, FL SDWRP, Cornwall, ON Water Purification Plant, Orange County, CA Water Reclamation Plant and Aurora, CO Reservoir Water Purification Facility) found that the cost of H_2O_2 could be potentially be reduced by for facilities that use surface waters as their source waters. For facilities with high purity source waters, the use of SPB or SPC as an alternative to liquid H_2O_2 would cause an increase in the cost of H_2O_2. Therefore, these treatment facilities will fare better economically speaking with the use of liquid H_2O_2 as their H_2O_2 source.

A comparison of the energy required to ship the three forms of H_2O_2 was completed using CSX Transportation's online Carbon Calculator. This calculator allows for the determination of the tons of CO_2 emitted by shipping a certain number of tons of product a specific distance. Three base case scenarios with varying treatment size were utilized to compare the CO_2 emissions for transporting 30% and 50% liquid H_2O_2, SPB and SPC 200, 500 and 1,000 miles. It was found that the percent reduction in CO_2 emissions of shipping SPB and SPC versus 30% liquid H_2O_2 was approximately 60%. Similarly the percent reduction in CO_2 emissions via SPB and SPC shipping was approximately 35% compared to 50% liquid H_2O_2.

The potential reduction in the portion of the carbon footprints attributed to shipping H_2O_2 of the four water treatment facilities utilizing the UV/H_2O_2 AOP was examined. The results indicated that the reduction in the facility's carbon footprint associated with shipping H_2O_2 depends on the proximity of the treatment plants to the chemical production facilities of each reagent and the amounts of reagent required. When the treatment facilities are approximately equidistant from the chemical production facilities, significant CO_2 emissions savings are possible by shipping SPB and SPC rather than liquid H_2O_2. On the other hand, when the liquid H_2O_2 production facility is located closer to the treatment plant than the SPB and SPC production facilities, the CO_2 emissions associated with shipping H_2O_2 can possibly increase if SPB and SPC are used.

7.1 Recommendations

Based on the results of the experiments presented in this report, SPB and SPC can be used as alternatives to liquid H_2O_2 up to active H_2O_2 concentrations of 5mg/L. At active H_2O_2 concentrations above 5mg/L the effects of hydroxyl radical scavenging by carbonate and borate species reduce the effectiveness of the UV/H_2O_2 AOP. Furthermore, the use of the UV/H_2O_2 AOP is most efficient in waters with reduced background alkalinity concentrations. It is suggested that pilot plant studies examining the efficiency of the UV/SPB and UV/SPC AOPs in a treatment facility's specific source water be completed prior to the use of SPB and SPC. Not only will the use of a pilot plant indicate if SPB and SPC are effective oxidizers in the presence of UV light, but also the potential cost savings (or expenses) associated with the use of SPB and SPC in the UV/H_2O_2 AOP can be realized. Furthermore, an analysis of the proximity of the production facilities of each reagent must be completed in order to realize potential reductions in treatment

facilities' carbon footprints associated with shipping H_2O_2. However, in the ideal

situations, SPB and SPC are expected to be efficient oxidizers in the presence of UV light

and their use can result in significant cost and transportation energy savings.

APPENDIX A: ALTERNATIVE HYDROGEN PEROXIDE DETERMINATION METHODS

There are numerous methods for determining the H_2O_2 concentration of an aqueous solution. The method used in this report is the I_3^- (tri-iodide) Method (Klassen et al., 1994). This method utilizes the spectrophotometric determination of the absorbance of a sample at 352nm. The H_2O_2 in the sample reacts with a solution of potassium iodide (KI) to produce a yellow color. The reaction is catalyzed by a solution of ammonium molybdate tetrahydrate $((NH_4)_6Mo_7O_{24})$. This process is described in earnest in **Section 4.3.1** of this report.

Klassen et al. (1994) also present the $KMnO_4$ Titration Method for the determination of H_2O_2 concentrations. In this method 4mL of sulfuric acid (H_2SO_4) per 100mL of H_2O_2 is added to a flask while keeping the flask at room temperature using a cold water bath. The solution of H_2O_2 and H_2SO_4 is then titrated with 0.1N potassium permanganate $(KMnO_4)$ until the solution turned a permanent light pink color. The reaction between permanganate (MnO_4^-) and H_2O_2 is presented below. (**Reaction A-1**).

$$2MnO_4^- + 5H_2O_2 + 6H^+ \rightarrow 2Mn^{2+} + 8H_2O + 5O_2 \; \textbf{\textit{Reaction A} - 1}$$
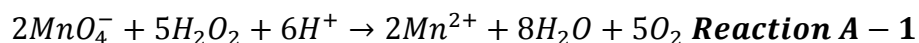
Once the permanent pink color of the sample has been established, the MnO_4^- concentration is determined spectrophotometrically at 525nm. In order to do this Klassen et al. needed to confirm the maximum absorption wavelength (λ_{max}) of MnO_4^-, and the molar absorptivity (ε_{max}) of MnO_4^-. They found experimentally that the λ_{max} was 525nm and the ε_{max} to be $2450M^{-1}cm^{-1}$. Using this information the molar concentration of MnO_4 concentration can be determined using **Equation A-1** below.

$$c\,(MnO_4^-) = \frac{A}{2450 \times b} \; \textbf{\textit{Equation A}} - \textbf{1}$$

Where b is the pathway length of the cuvette used in the spectrophotometer. Once this concentration is determined, the concentration of H_2O_2 can be determined using the stoichiometry shown in **Reaction A-1**. One disadvantage of this method is that an analysis of a sample containing less than 100µM H_2O_2 requires several hundred milliliters of H_2O_2 if 0.1N $KMnO_4$ is used as the titrant. Also with this method, the solution must be acidic and the addition of $KMnO_4$ must be done slowly to prohibit the formation of manganese dioxide, which will decompose H_2O_2.

An earlier method for determining H_2O_2 concentration utilized the photoelectric measurement of color intensities of H_2O_2 solutions treated with titanium sulfate reagent (Eisenberg, 1943). When combining titanium sulfate and H_2O_2, pertitanic acid (H_2TiO_4) is formed which results in a yellow color that can be evaluated using a colorimeter. This reaction is highlighted in **Reaction A-2** below.

$$Ti^{4+} + H_2O_2 + 2H_2O \rightarrow H_2TiO_4 + 4H^+ \; \textbf{\textit{Reaction A}} - \textbf{2}$$
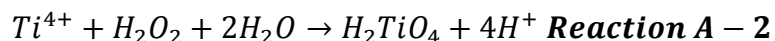
Eisenberg (1943) found that maximum color development occurred when 1 volume of titanium sulfate reagent per 10 volumes of peroxide solution were mixed. Additionally, the color develops instantly and lasts for at least 6 hours. The H_2O_2 concentration can be determined with a calibration curve of H_2O_2 concentrations versus scale readings from the colorimeter. Using this method Eisenberg (1943) tested 11 samples of known H_2O_2 concentrations from 0.18 to 2.7mg/100mL. Compared to the actual H_2O_2 concentrations the average standard deviation of the 11 samples was 0.03mg/100mL.

APPENDIX B: INFORMATION ON OPERATION OF AVASOFT SOFTWARE FROM HROSS (2010)

The following information is quoted from Hross (2010) on the operation of the AvaSoft Software utilized in the methylene blue decay experiments under ultraviolet light presented in this report.

Performing Experiments with AvaSoft

"The AvaSoft Software needs to be installed in order to use the fiber optic spectrometer with a laptop. This software is stored on a CD and can be found with the scavenging measurement system components. Follow the installation dialogue on the CD or refer to the AvaSoft manual to install the software.

Establishing Absorbance Measurements in AvaSoft

Before AvaSoft will provide absorbance measurements of a water sample, the used needs to perform the following:

1. Prepare 40 mL of deionized water in a 50x35 mm exposure dish.
2. Secure this exposure dish in the collimating piece using the three teflon screws. Try to center the dish within the collimating piece as precisely as possible. Also, be sure no printed text on the surface of the exposure dish interferes with light transmission through the water.
3. With the scavenging measurement system assembled, open AvaSoft.
4. Click the green 'Start' button on the task bar at the top of the software. A spectrum with vertical and horizontal axes of counts and wavelength, respectively, should be shown.

5. Adjust the integration time on the top task bar, such that the maximum count over the wavelength range is approximately 90% of the full count axis (or about 56,000 counts).

6. When this has been satisfied turn on the halogen light source. Save the "dark data" by clicking on the black square on the top task bar.

7. Turn the halogen light source back on. Save the "reference data" by clicking the white square on the top task bar.

8. This procedure opens new view modes of both absorbance and transmittance. Absorbance and transmittance data may now be viewed by clicking the A and T buttons, respectively, on the top task bar.

Realize that if the user adjusts the integration time or position of the light attenuator during an experiment this procedure will ne to be repeated, since the measurement and delivery of light will have been altered.

Configuring Excel Output in AvaSoft

The most convenient way to collect data in AvaSoft is by using the Excel output option. Of course, this requires having Excel installed in addition to AvaSoft. For other means of obtaining data please refer to the AvaSoft manual.

1. Under the Application menu select Excel Output and then Settings.

2. For the purpose of measuring MB degradation select "Export a fixed number of time scans to Excel" under the select mode.

3. Under Export Mode enter the desired number of scans and the interval time between scans. This is convenient for recording absorbance measurements at incremental UV doses (i.e. every 5 mJ).

4. Return to the Application menu and select Enable under Excel Output to activate the settings.

5. Under the Application menu select History and then Function Entry. This is where the used may define the type of data to be exported to Excel.

6. Up to eight functions may be defined. For measuring MB degradation, absorbance data is desired. On the first function entry tab, F1, select View Spectrum under Function Type and Absorbance under Measure Mode.

7. Under Function Definition enter the desired wavelength range to record data. Leave the Spectrometer Channel as Master. No peaks need to be displayed for the purpose of measuring MB degradation.

8. If desired, up to seven additional function may be defined with tabs F2-F8.

Running an Experiment in AvaSoft

At this point the ability to measure absorbance should be established and the Excel output functions should be defined. MB degradation experiments may now be performed and recorded.

1. To begin recording data select Start Measuring under History from the Application Menu.

2. AvaSoft will begin collecting data by creating new Excel spreadsheets. For example, when recording only absorbance measurements, AvaSoft will open a

blank workbook in Excel. AvaSoft will rename Sheet1 "F1", corresponding to the absorbance function entry.

3. Rows 1 and 2 in sheet "F1" will be the time of recording and the elapsed time since the last recording, respectively. Each subsequent row will be the range of wavelengths defind in the function entry at approximately 0.5cm increments. Each column is a scan with the total number of columns equaling the number of scans defined in the Excel Output Settings. Since one Excel sheet can only contain up to 256 columns, additional sheets will be created by AvaSoft for an experiment with scans totaling greater than 256.

4. Sensitivity has been observed when trying to view Excel while AvaSoft is recording scans. At times, AvaSoft aborts scanning when trying to view Excel as scans are entered. Instead, it is advised to let AvaSoft run the number of scans to completion before trying to view Excel. The orange "scan" light on the fiber optic spectrometer will pulse each time a scan is recorded in Excel. When this light stops pulsing and remains lit, all of the scans have been entered and it is safe to view Excel without risk of aborting AvaSoft.

The data recorded in Excel may now be saved and used as desired by the user. Of course, AvaSoft contains many other function and options. The aforementioned represents the simplest means of recording data of MB degradation for the use of calculating the overall background ·OH scavenging of a water. For further information regarding the capabilities of AvaSoft, please refer to the AvaSoft manual."

APPENDIX C: RELATIVE CONCENTRATION PLOTS OF METHYLENE BLUE DECAY

Figures C-1 to **C-5** show the decay of MB in DI water as a function of UV fluence at each theoretical concentration of H_2O_2 considered. The MB decay due to each source of H_2O_2 (liquid H_2O_2, SPB and SPC) are shown in the figures.
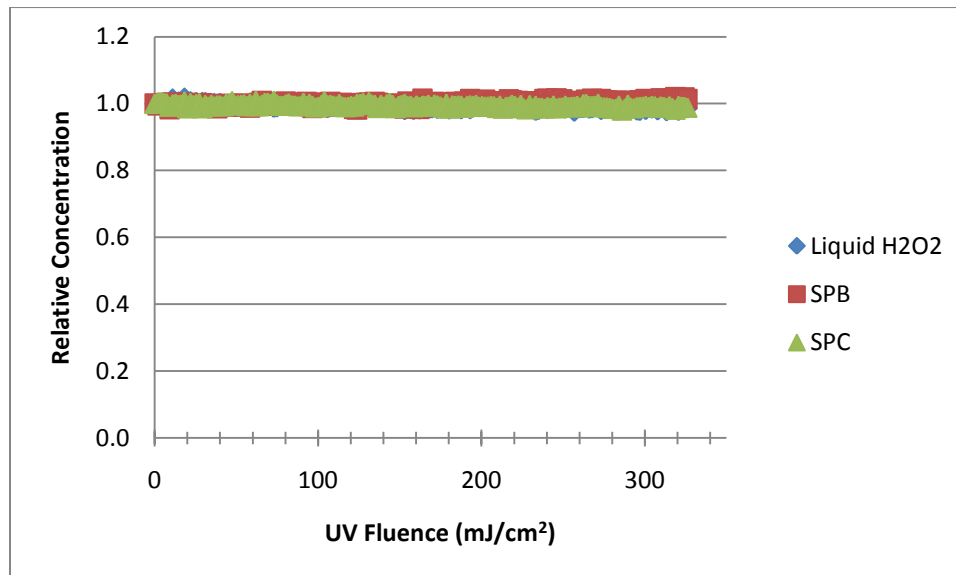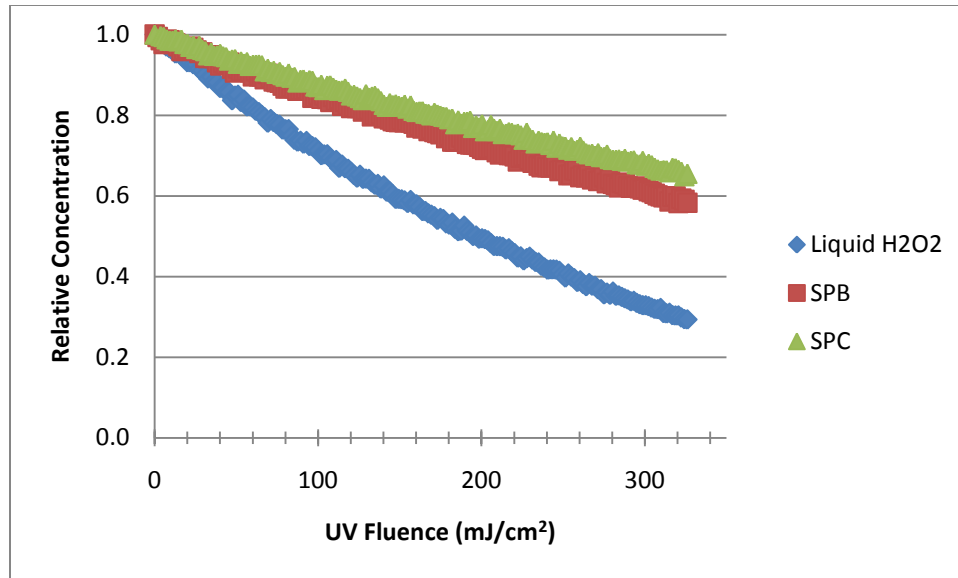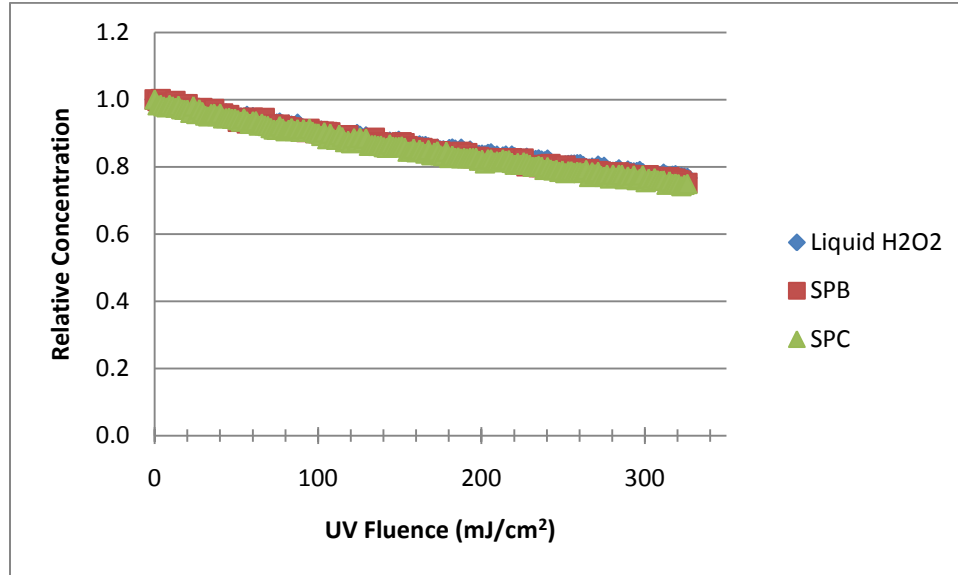

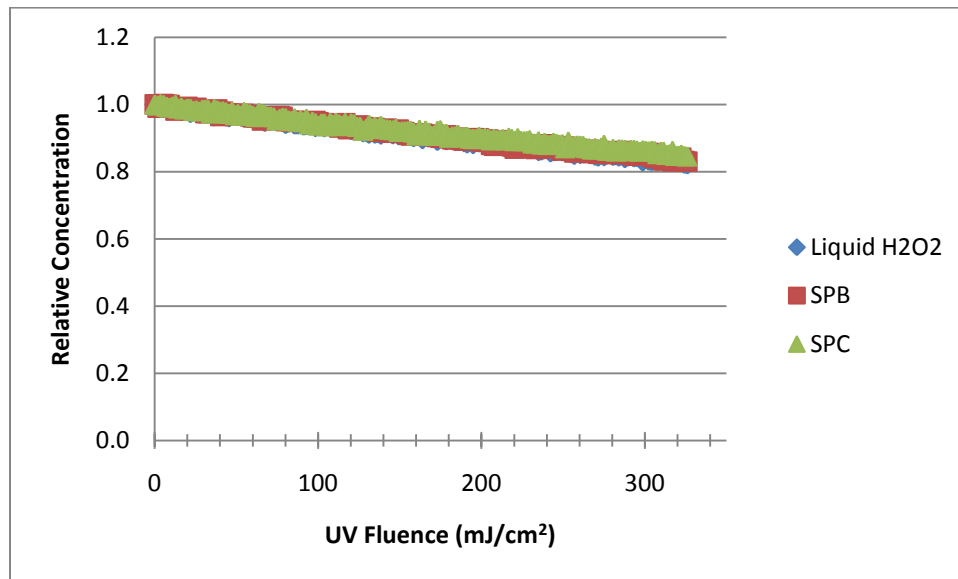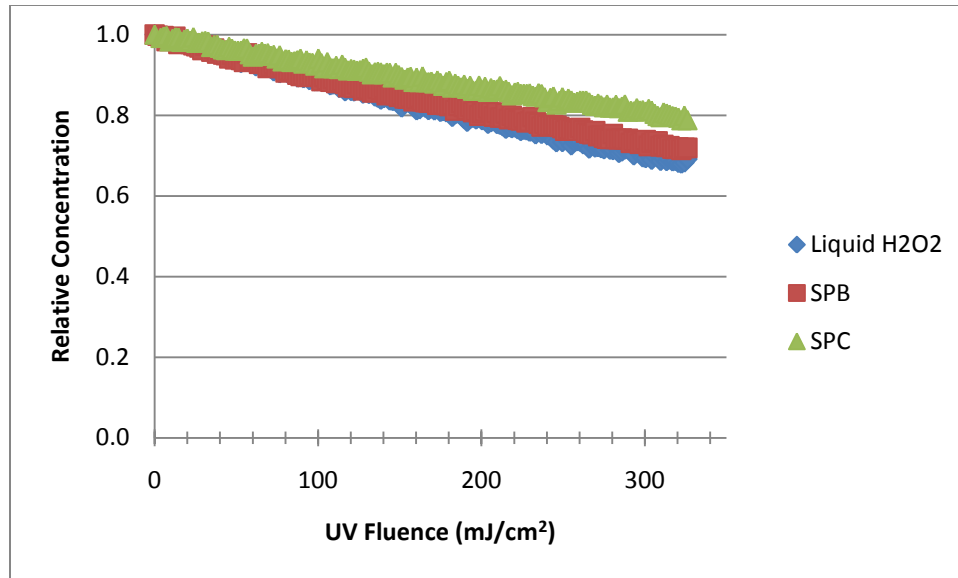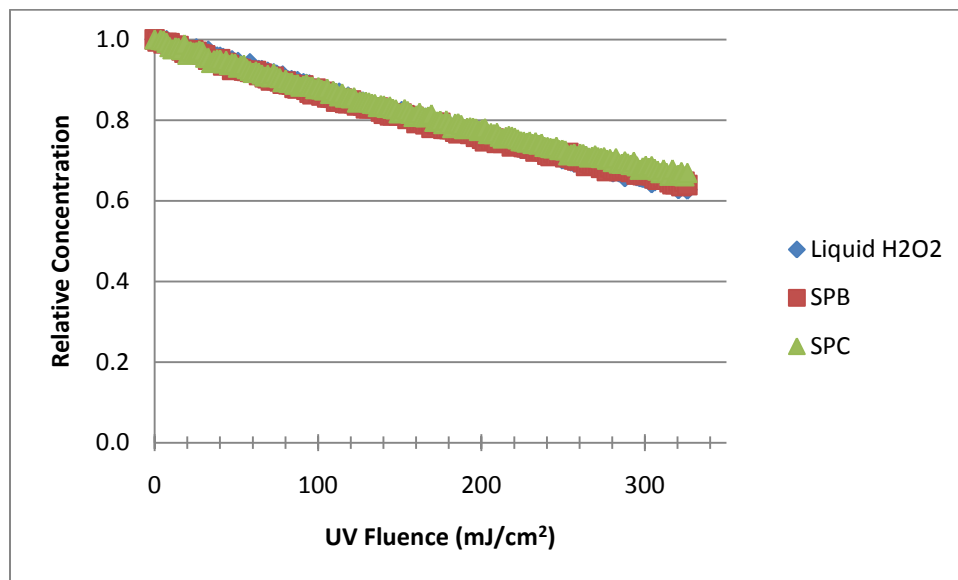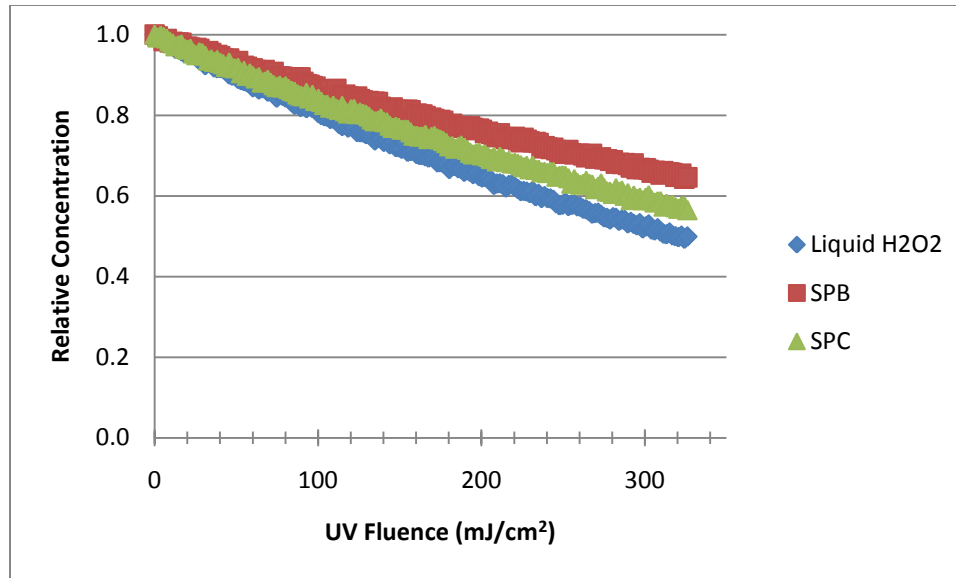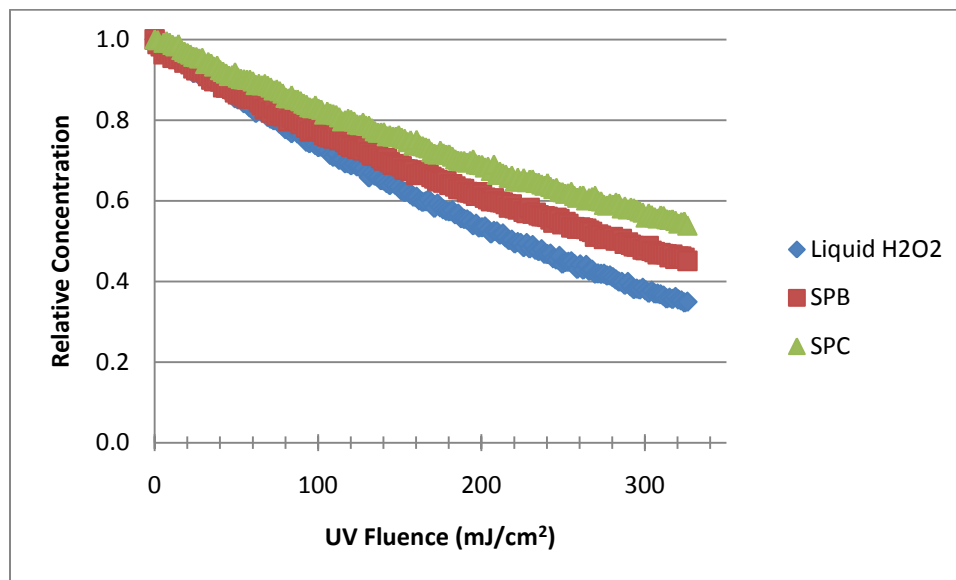Figure C-3: MB Decay as a Function of UV Dose; Sample in DI Water; Reagents are Theoretical 0mg/L H_2O_2
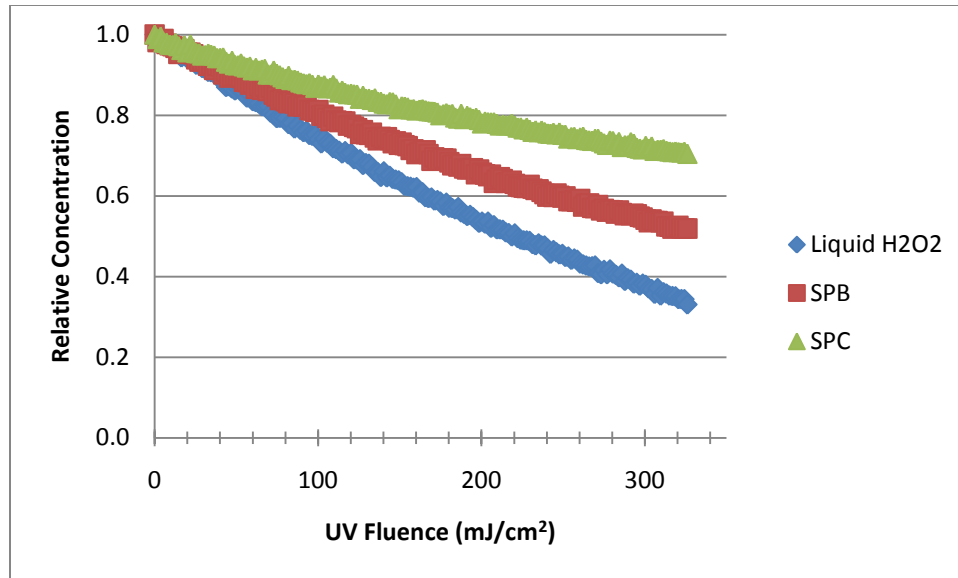
Figure C-4: MB Decay as a Function of UV Dose; Sample in DI Water; Reagents are Theoretical 2mg/L H_2O_2
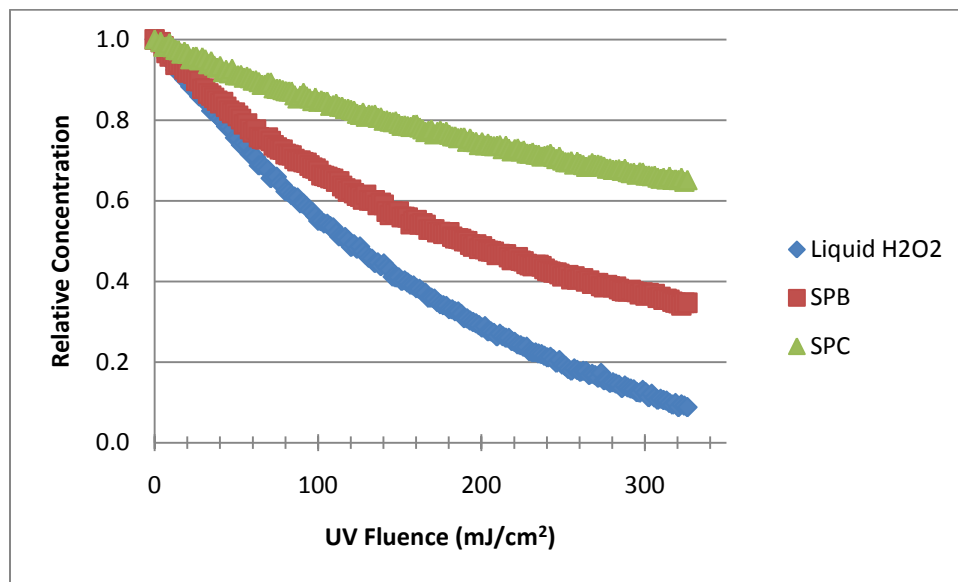
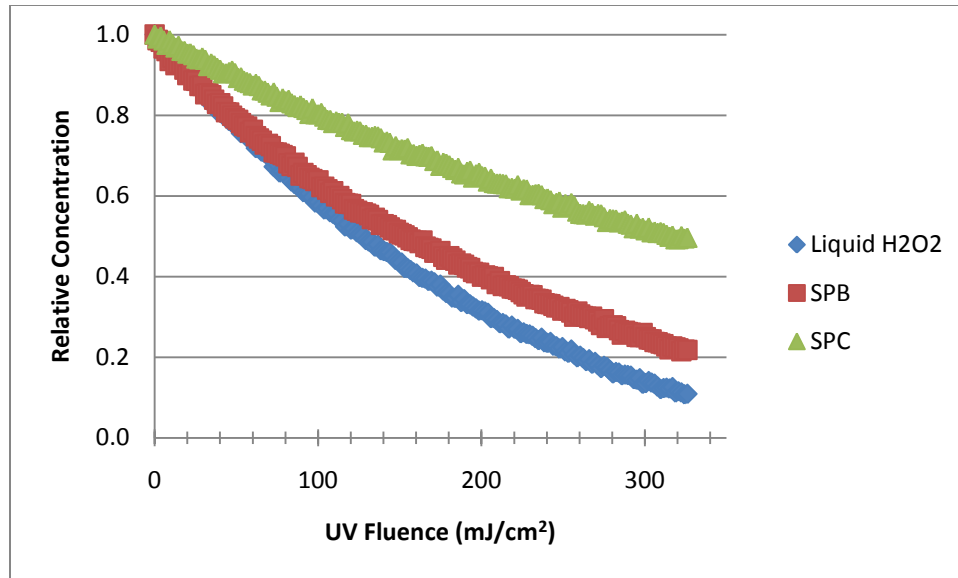Figure C-5: MB Decay as a Function of UV Dose; Sample in DI Water; Reagents are Theoretical 5mg/L H_2O_2
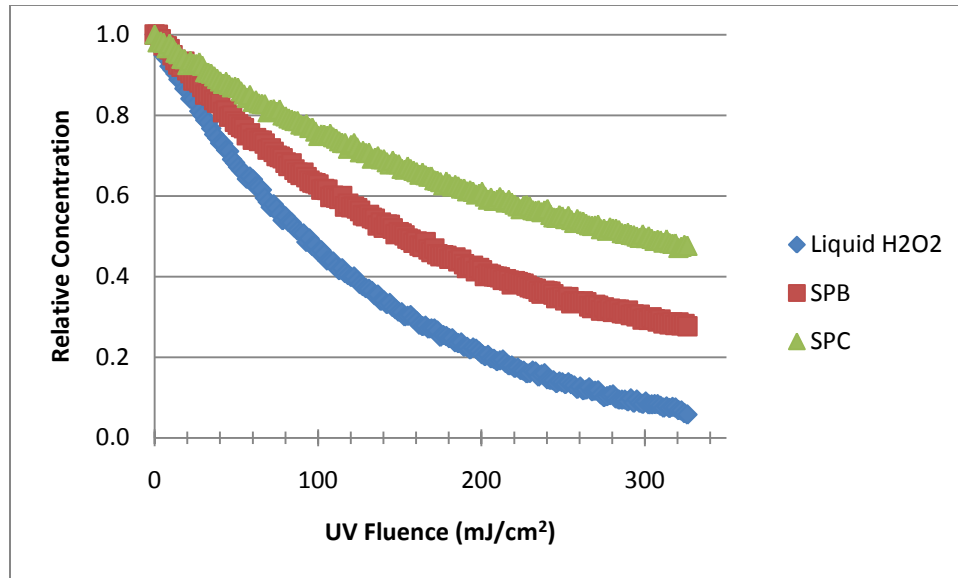
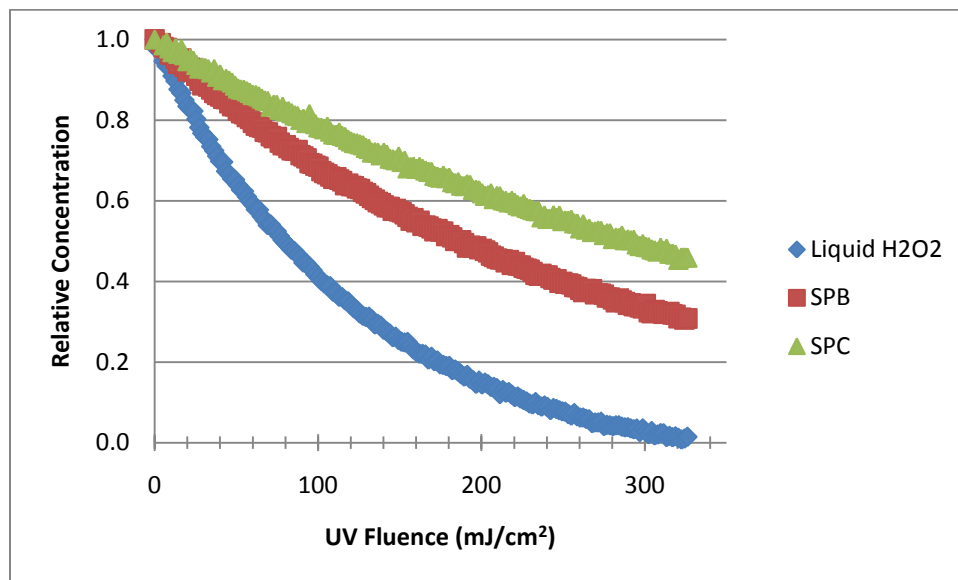Figure C-6: MB Decay as a Function of UV Dose; Sample in DI Water; Reagents are Theoretical 10mg/L H_2O_2
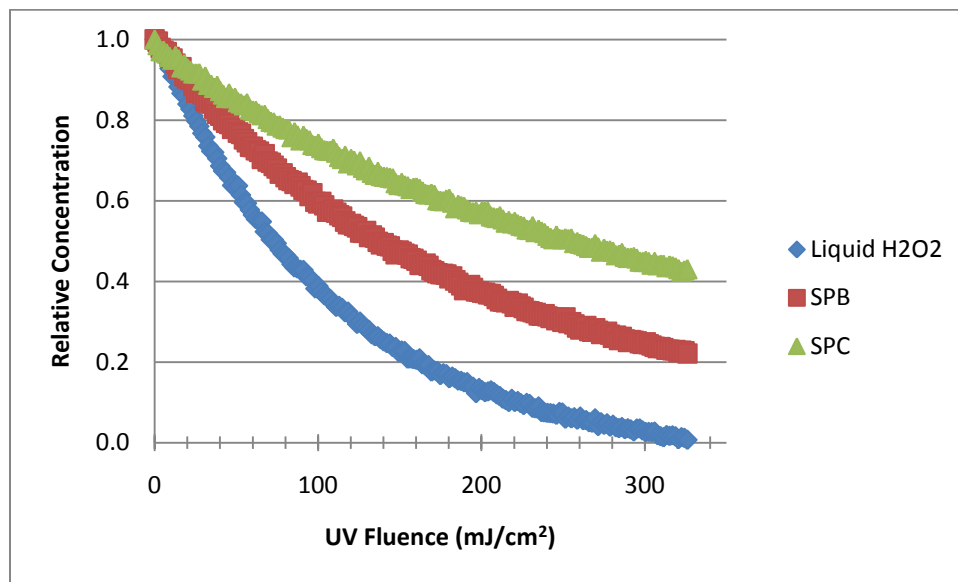
Figure C-7: MB Decay as a Function of UV Dose; Sample in DI Water; Reagents are Theoretical 15mg/L H_2O_2

Figures C-6 to **C-13** show the decay of MB in the pre-treatment water from the

Northampton, MA Water Filtration Plant as a function of UV fluence at each theoretical

concentration of H_2O_2 considered. The MB decay due to each source of H_2O_2 (liquid H_2O_2, SPB and SPC) are shown in the figures.
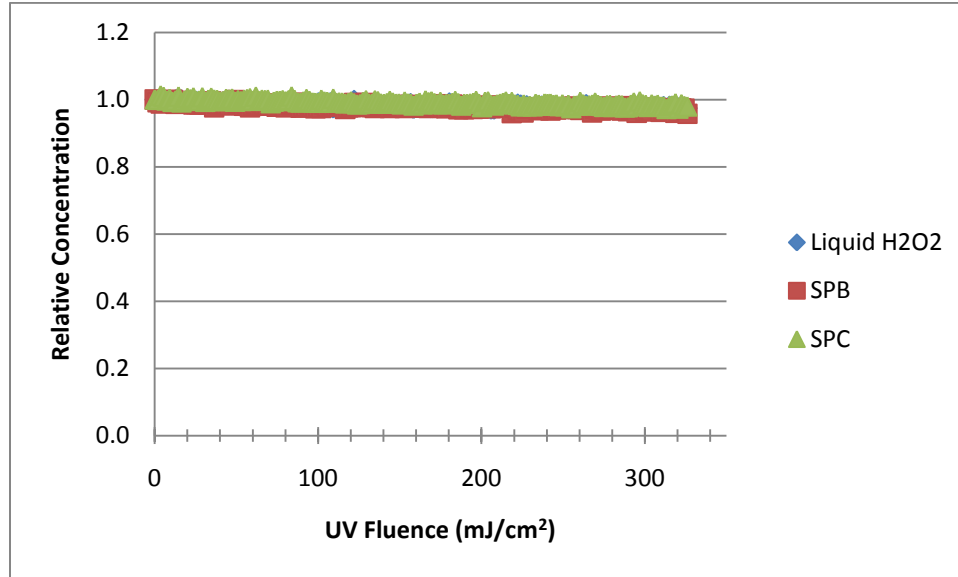
Figure C-8: MB Decay as a Function of UV Dose; Sample in Pre-Treatment Water; Reagents are Theoretical 0mg/L H_2O_2
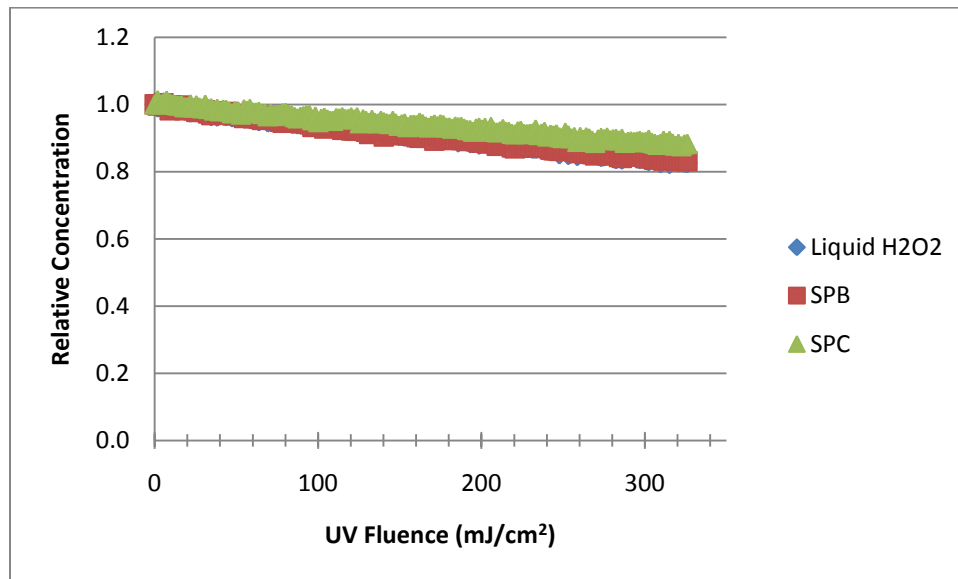
Figure C-9: MB Decay as a Function of UV Dose; Sample in Pre-Treatment Water; Reagents are Theoretical 1mg/L H_2O_2
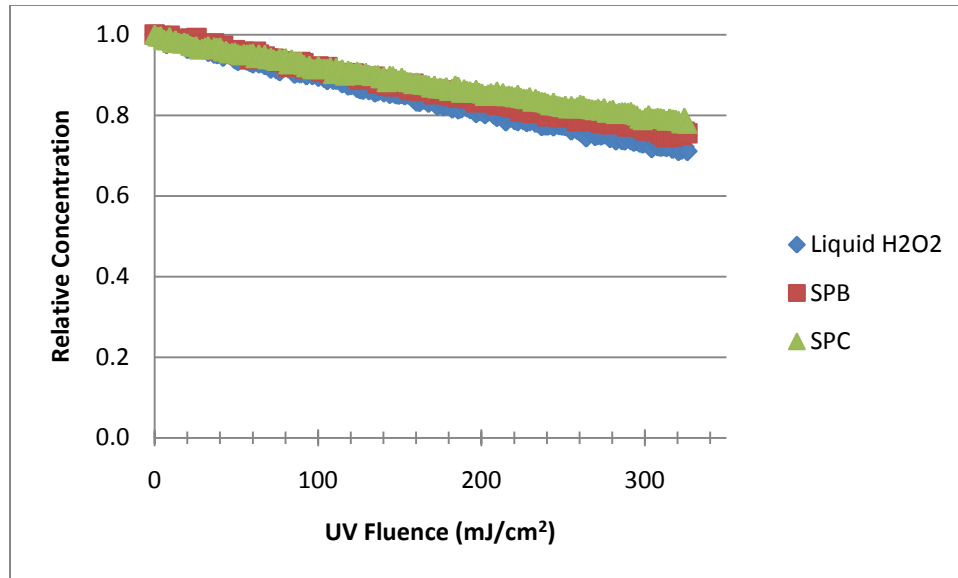
Figure C-10: MB Decay as a Function of UV Dose; Sample in Pre-Treatment Water; Reagents are Theoretical 2mg/L H_2O_2
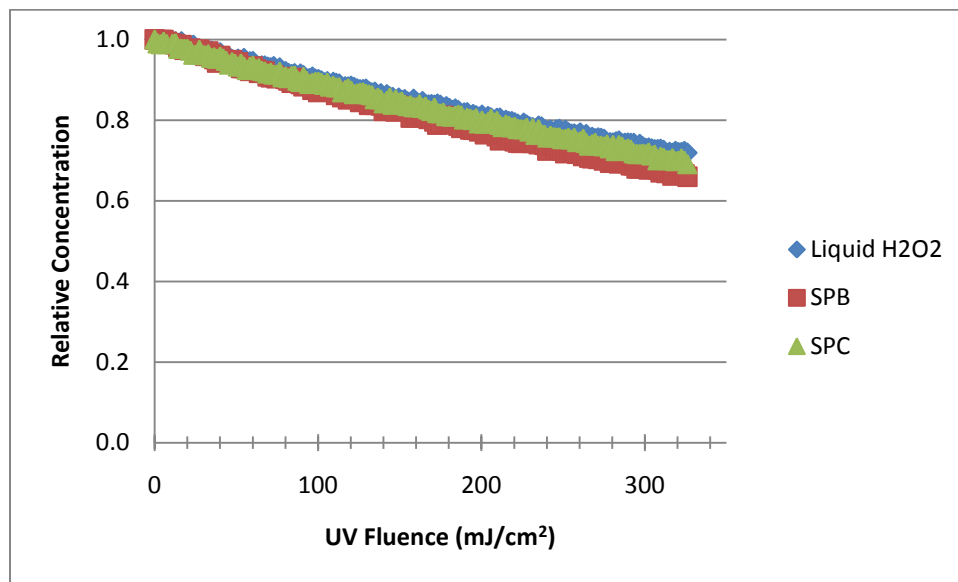
Figure C-11: MB Decay as a Function of UV Dose; Sample in Pre-Treatment Water; Reagents are Theoretical 3mg/L H_2O_2
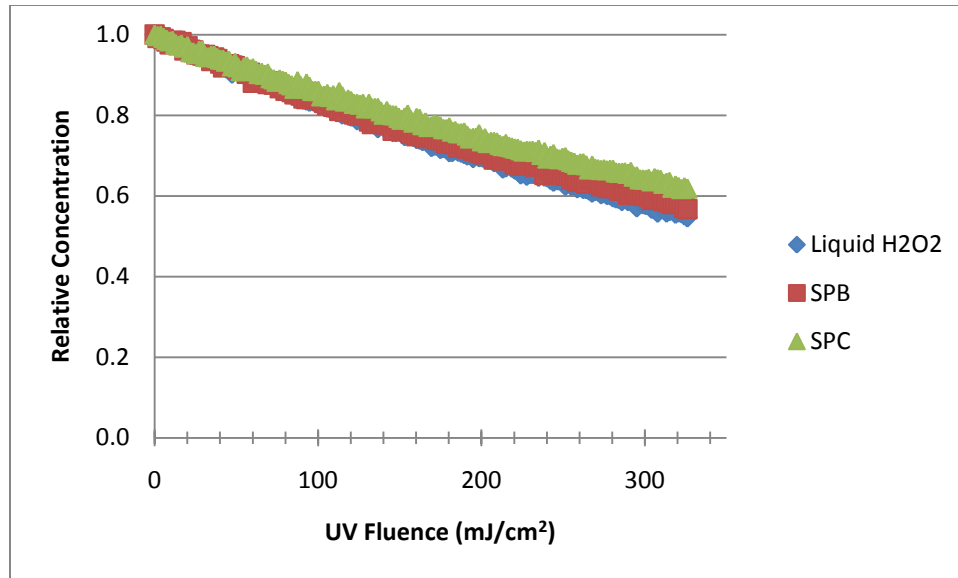
Figure C-12: MB Decay as a Function of UV Dose; Sample in Pre-Treatment Water;
Reagents are Theoretical 4mg/L H_2O_2
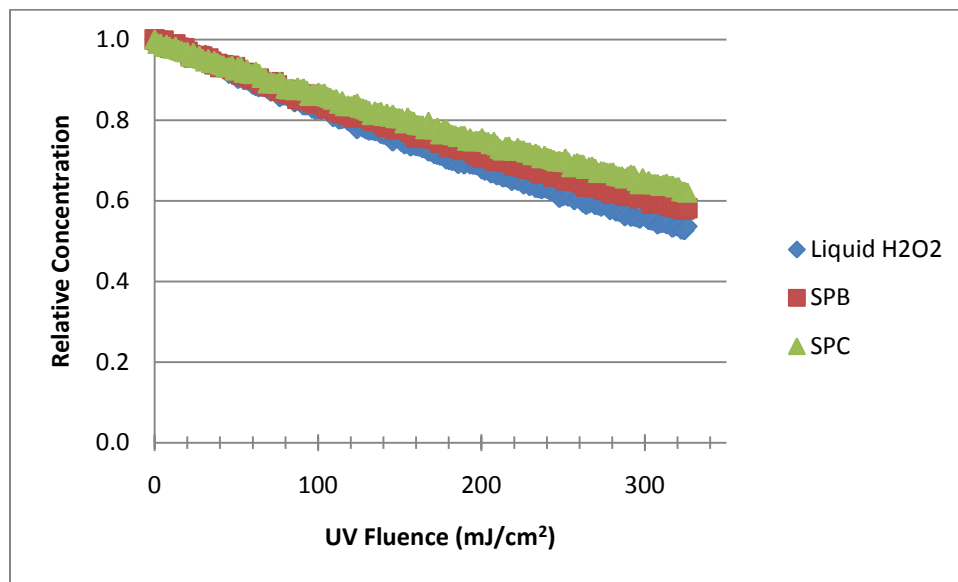
Figure C-13: MB Decay as a Function of UV Dose; Sample in Pre-Treatment Water;
Reagents are Theoretical 5mg/L H_2O_2
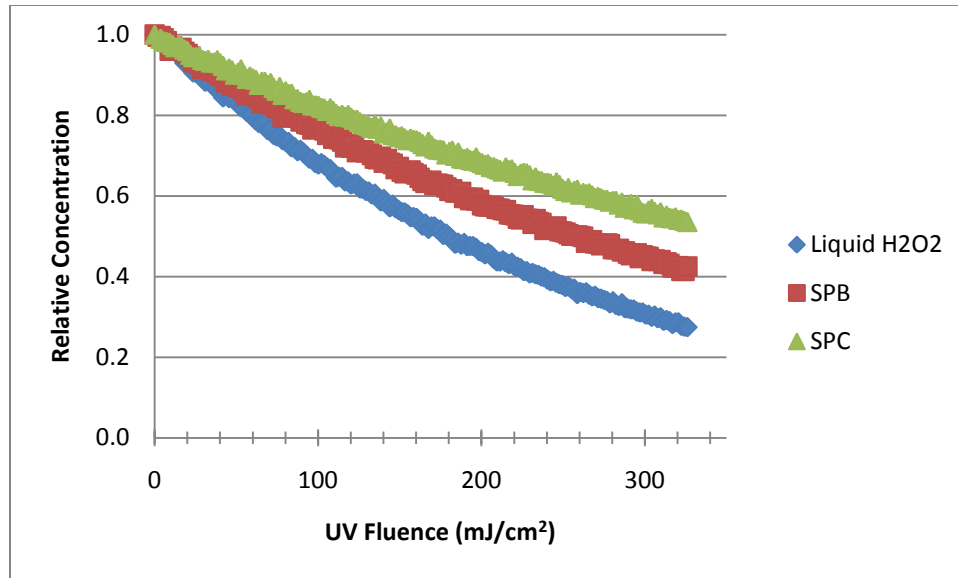
Figure C-14: MB Decay as a Function of UV Dose; Sample in Pre-Treatment Water; Reagents are Theoretical 10mg/L H_2O_2
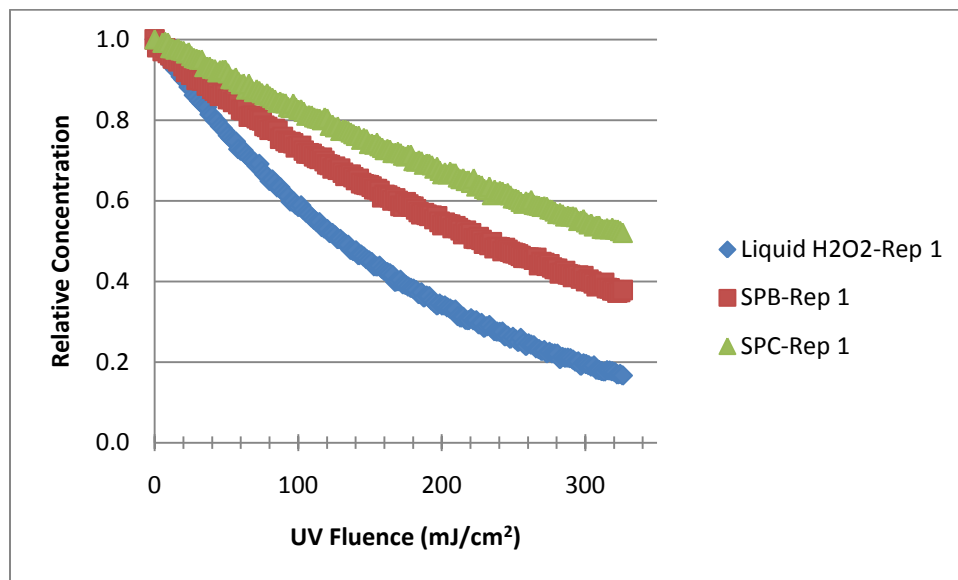
Figure C-15: MB Decay as a Function of UV Dose; Sample in Pre-Treatment Water; Reagents are Theoretical 15mg/L H_2O_2

Figures C-14 to **C-21** show the decay of MB in the treated, unchlorinated water

from the Northampton, MA Water Filtration Plant as a function of UV fluence at each

theoretical concentration of H_2O_2 considered. The MB decay due to each source of H_2O_2 (liquid H_2O_2, SPB and SPC) are shown in the figures.
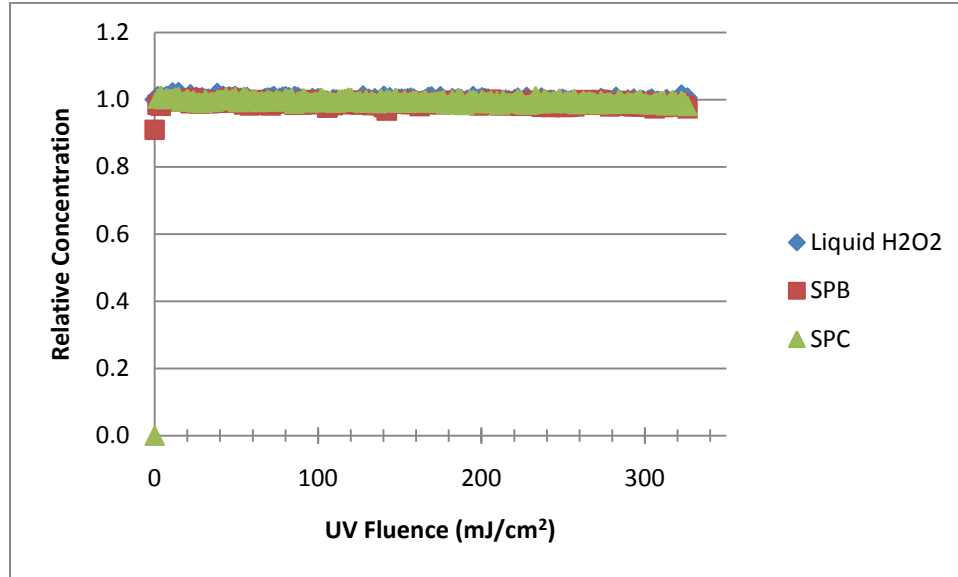
Figure C-16: MB Decay as a Function of UV Dose; Sample in Treated, Unchlorinated Water; Reagents are Theoretical 0mg/L H_2O_2
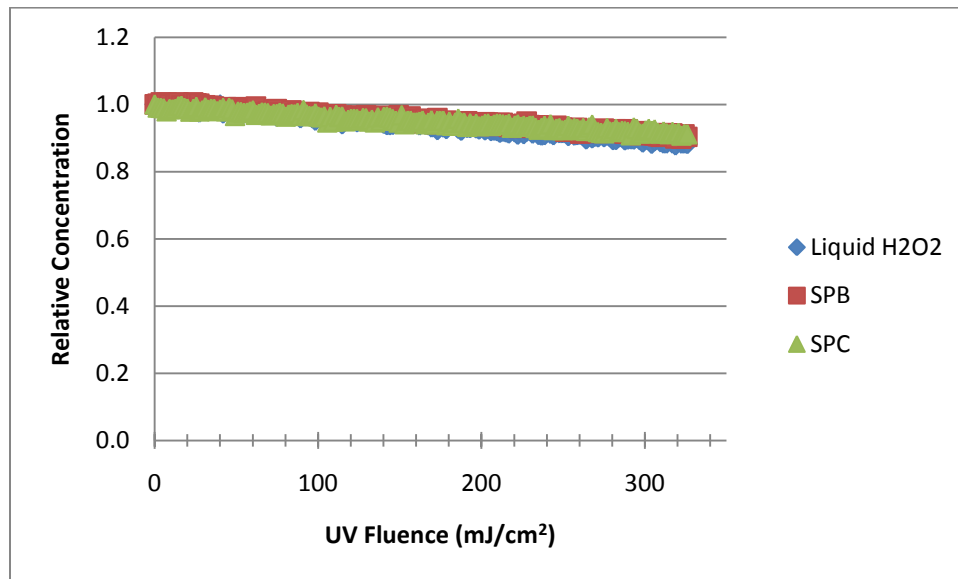
Figure C-17: MB Decay as a Function of UV Dose; Sample in Treated, Unchlorinated Water; Reagents are Theoretical 1mg/L H_2O_2
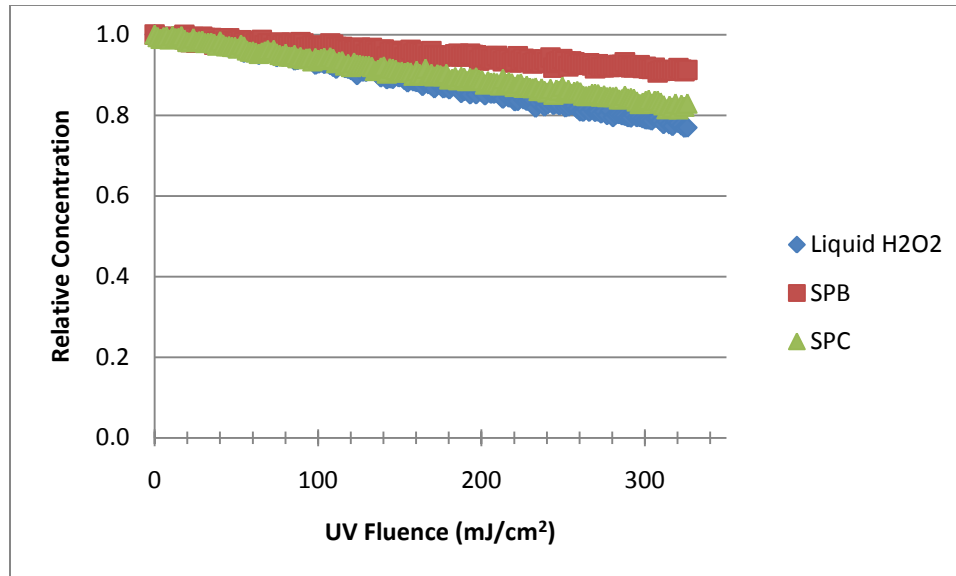
Figure C-18: MB Decay as a Function of UV Dose; Sample in Treated, Unchlorinated Water; Reagents are Theoretical 2mg/L H_2O_2
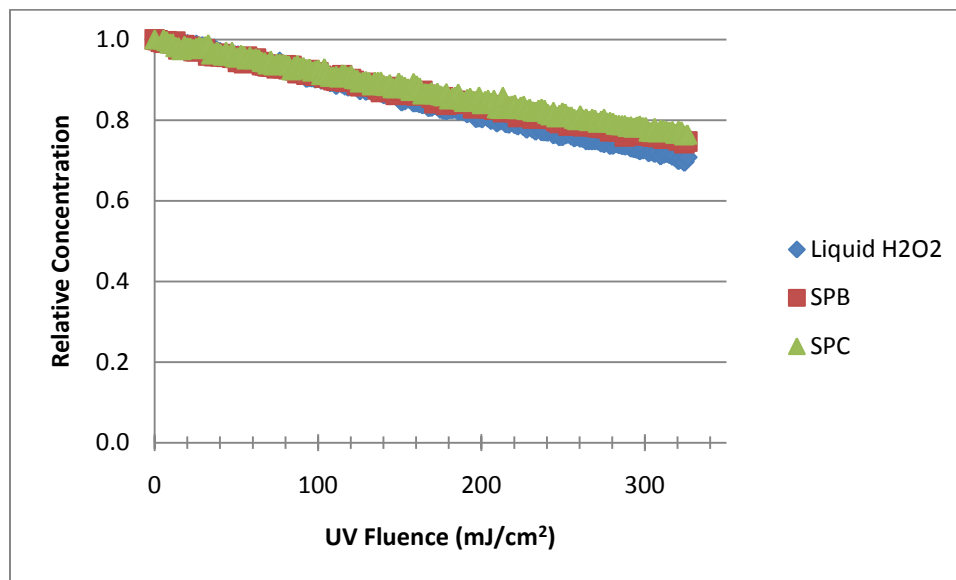
Figure C-19: MB Decay as a Function of UV Dose; Sample in Treated, Unchlorinated Water; Reagents are Theoretical 3mg/L H_2O_2
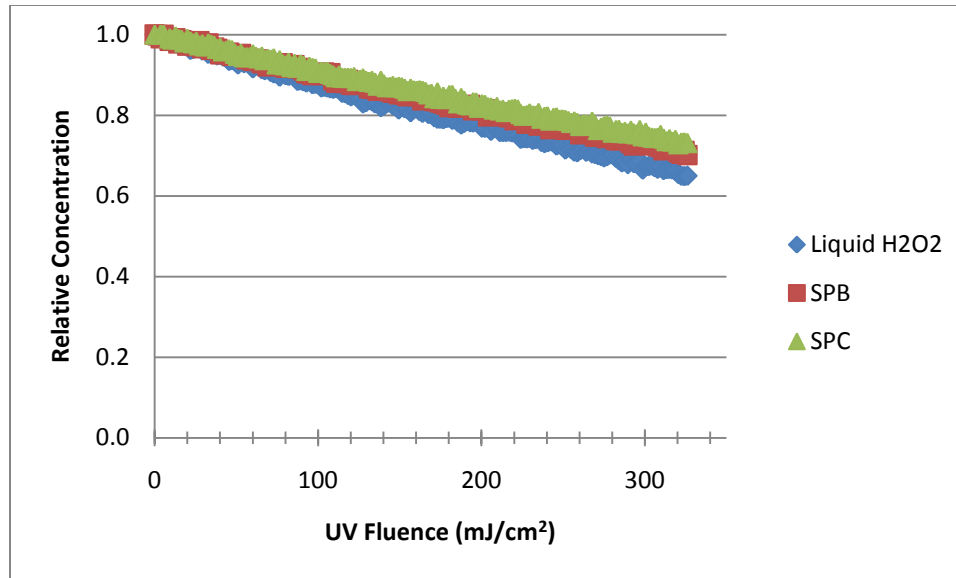
Figure C-20: MB Decay as a Function of UV Dose; Sample in Treated, Unchlorinated Water; Reagents are Theoretical 4mg/L H_2O_2
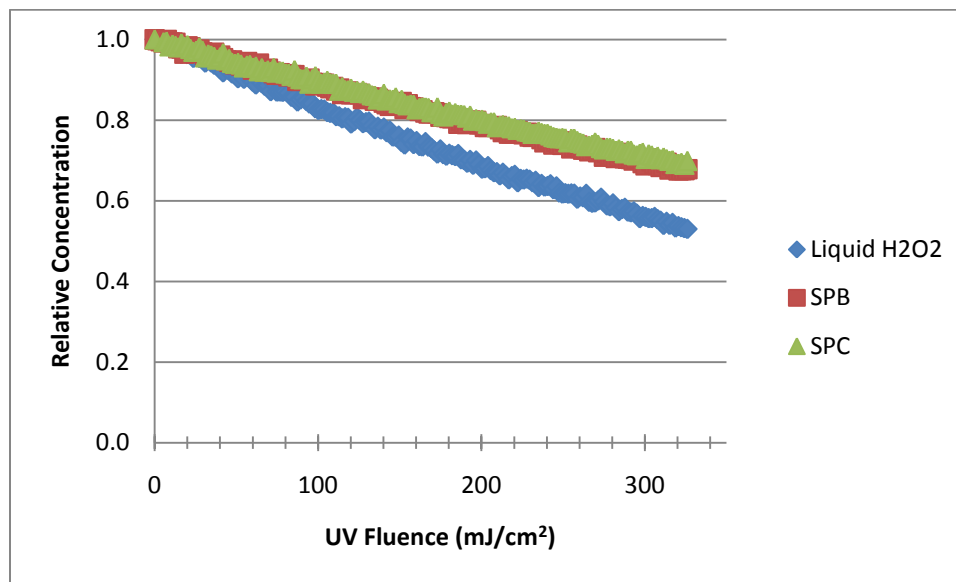
Figure C-21: MB Decay as a Function of UV Dose; Sample in Treated, Unchlorinated Water; Reagents are Theoretical 5mg/L H_2O_2

Figure C-22: MB Decay as a Function of UV Dose; Sample in Treated, Unchlorinated Water; Reagents are Theoretical 10mg/L H_2O_2
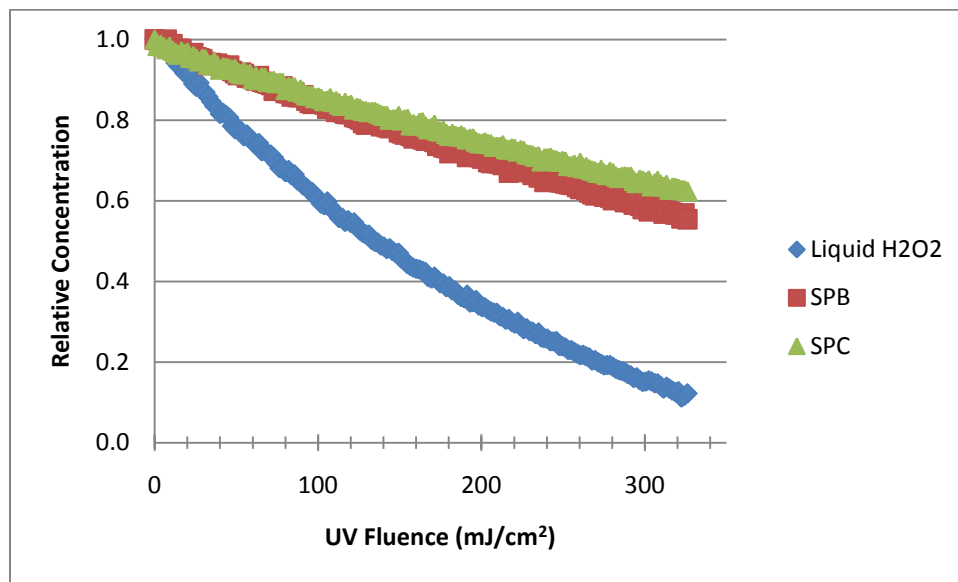
Figure C-23: MB Decay as a Function of UV Dose; Sample in Treated, Unchlorinated Water; Reagents are Theoretical 15mg/L H_2O_2

Figures C-22 to **C-29** show the decay of MB in the treated, unchlorinated water

from the Northampton, MA Water Filtration Plant as a function of UV fluence at each

theoretical concentration of H_2O_2 considered. The MB decay due to each source of H_2O_2 (liquid H_2O_2, SPB and SPC) are shown in the figures.

Figure C-24: MB Decay as a Function of UV Dose; Sample in Post-Treatment Water; Reagents are Theoretical 0mg/L H_2O_2

Figure C-25: MB Decay as a Function of UV Dose; Sample in Post-Treatment Water; Reagents are Theoretical 1mg/L H_2O_2

Figure C-26: MB Decay as a Function of UV Dose; Sample in Post-Treatment Water; Reagents are Theoretical 2mg/L H_2O_2

Figure C-27: MB Decay as a Function of UV Dose; Sample in Post-Treatment Water; Reagents are Theoretical 3mg/L H_2O_2

Figure C-28: MB Decay as a Function of UV Dose; Sample in Post-Treatment Water; Reagents are Theoretical 4mg/L H_2O_2

Figure C-29: MB Decay as a Function of UV Dose; Sample in Post-Treatment Water; Reagents are Theoretical 5mg/L H_2O_2

Figure C-30: MB Decay as a Function of UV Dose; Sample in Post-Treatment Water; Reagents are Theoretical 10mg/L H_2O_2

Figure C-31: MB Decay as a Function of UV Dose; Sample in Post-Treatment Water; Reagents are Theoretical 15mg/L H_2O_2

APPENDIX D: FIGURES USED IN METHYLENE BLUE DECAY RATE CONSTANT DETERMINATION

Figures D-1 to **D-5** are plots of the natural logarithm of the methylene blue concentration as a function of the UV fluence each sample was subject to. The negative of the slope of the linear best fit line is equal to the pseudo-first order decay rate constant (k') of methylene blue in DI water for liquid H_2O_2 as the source of H_2O_2.
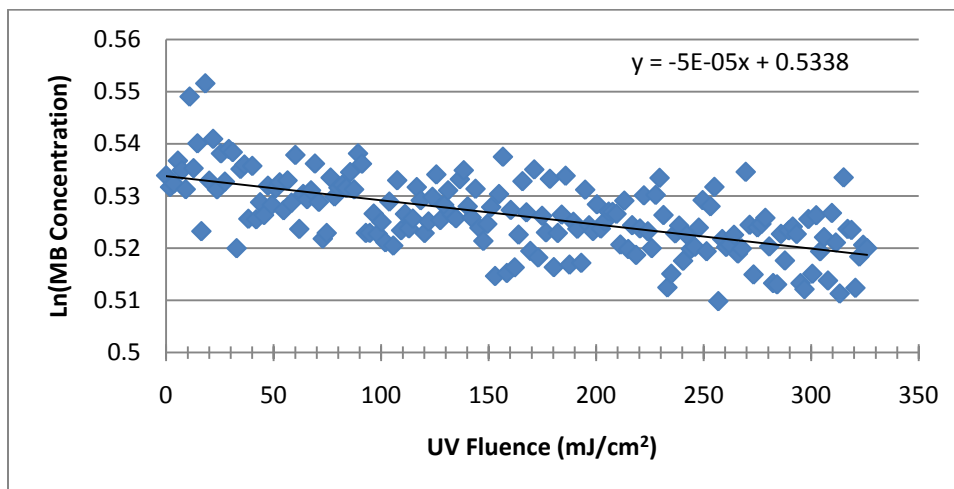
Figure D-32: Natural Logarithm of MB Decay as a Function of UV Fluence; Sample Theoretical 0mg/L Liquid H_2O_2 in DI Water
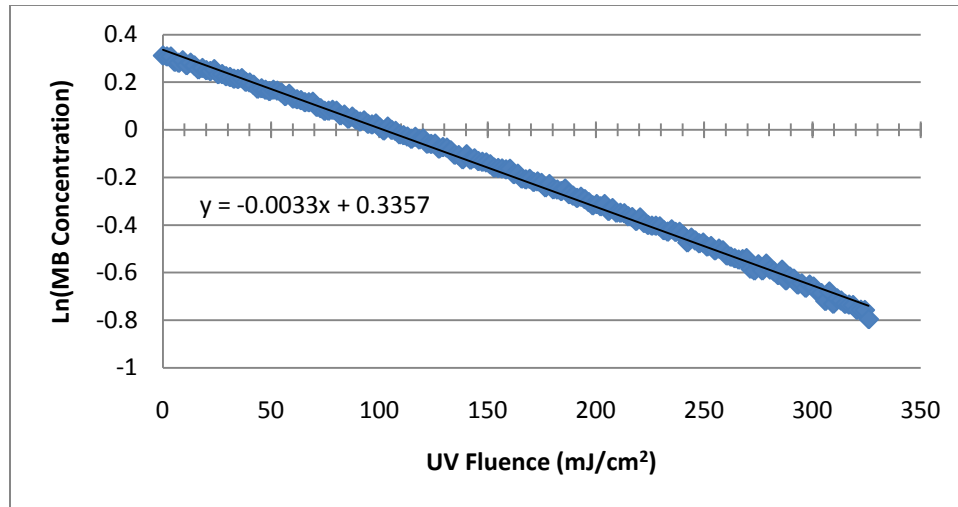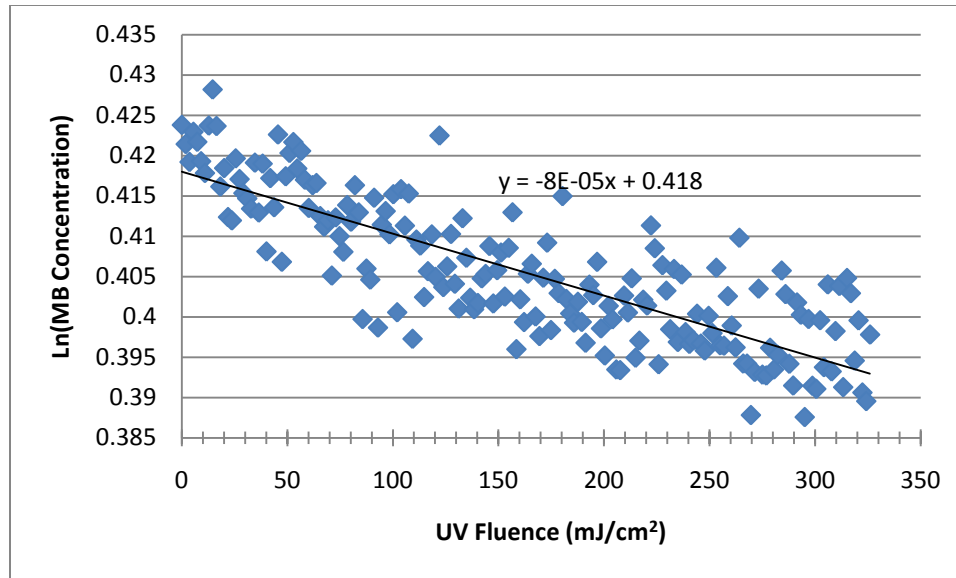
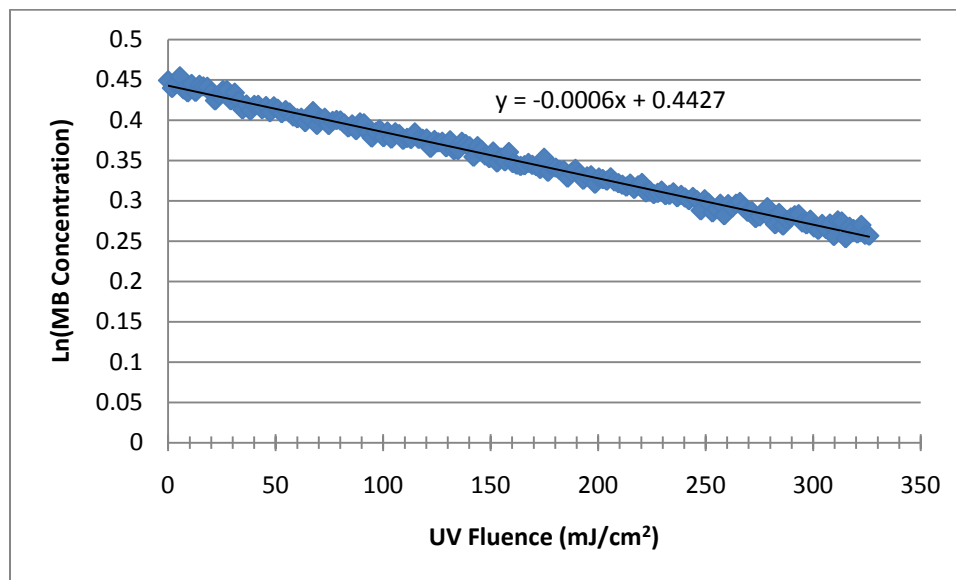Figure D-33: Natural Logarithm of MB Decay as a Function of UV Fluence; Sample Theoretical 2mg/L Liquid H_2O_2 in DI Water
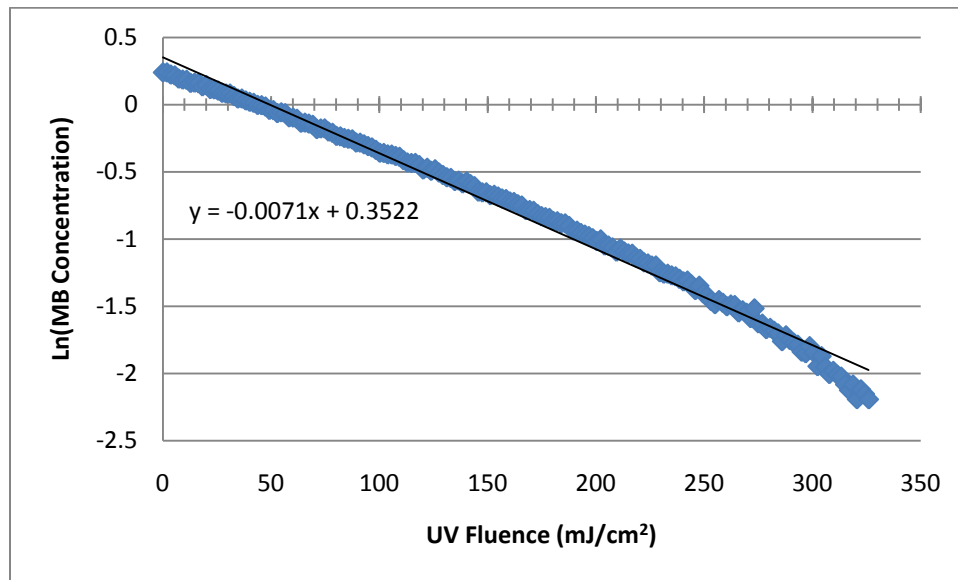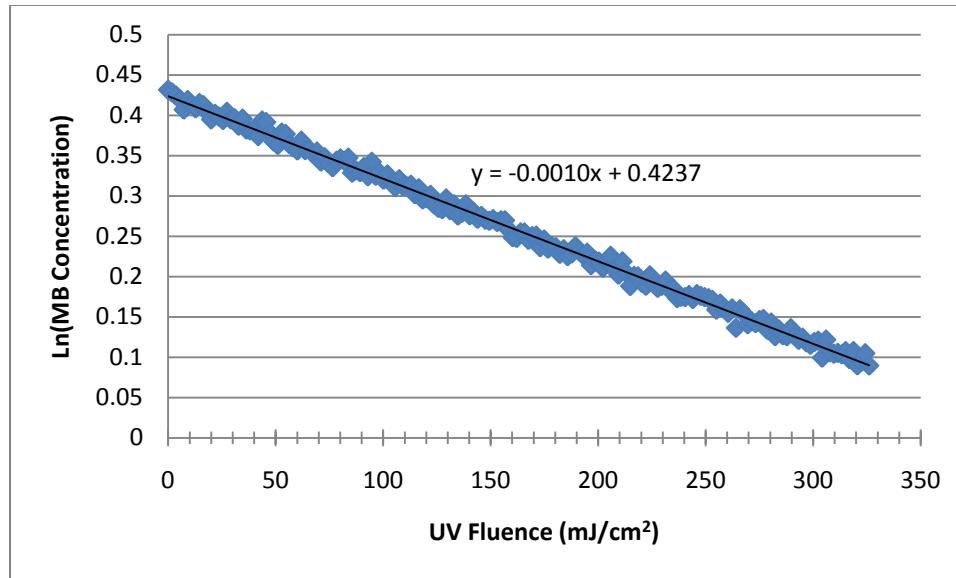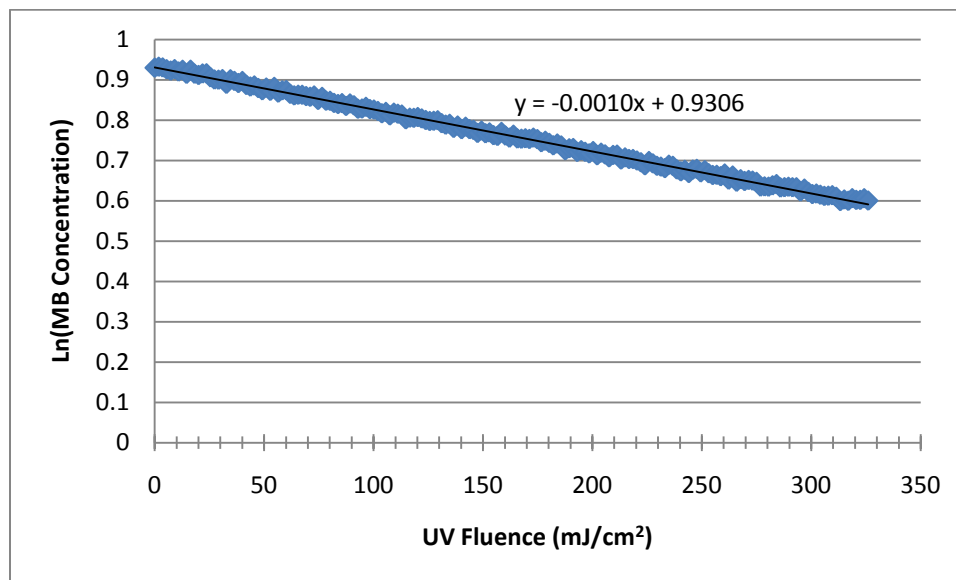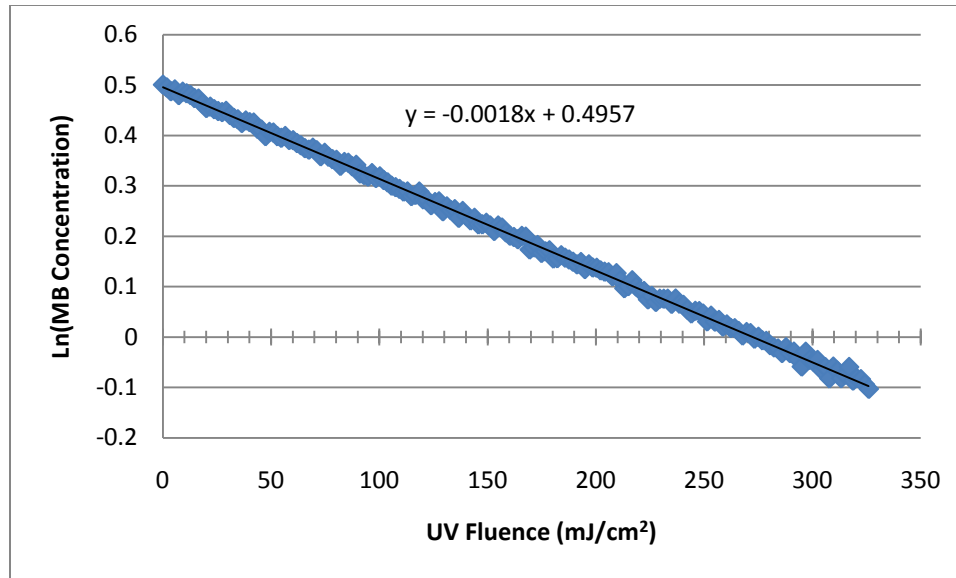

Figure D-34: Natural Logarithm of MB Decay as a Function of UV Fluence; Sample Theoretical 5mg/L Liquid H_2O_2 in DI Water
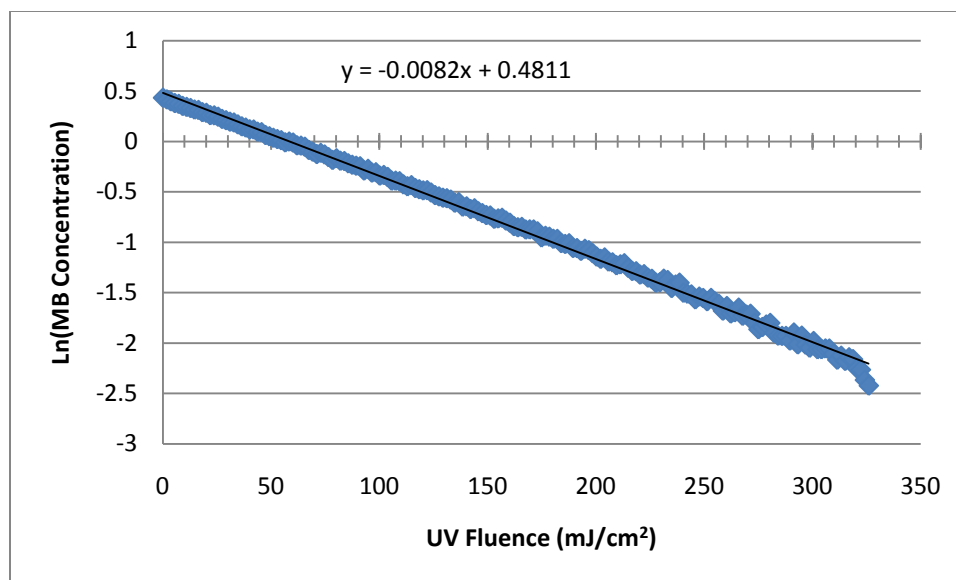
Figure D-35: Natural Logarithm of MB Decay as a Function of UV Fluence; Sample Theoretical 10mg/L Liquid H_2O_2 in DI Water
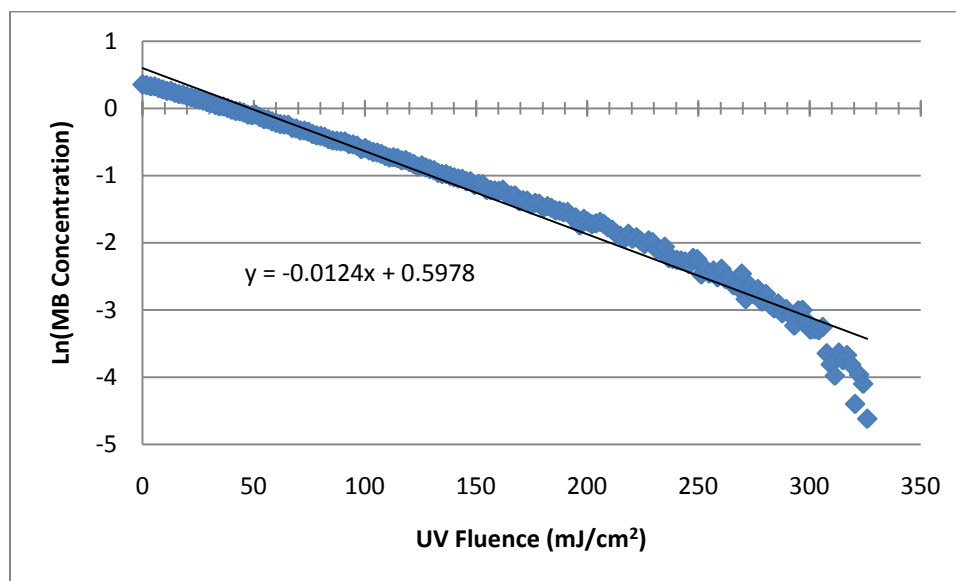
Figure D-36: Natural Logarithm of MB Decay as a Function of UV Fluence; Sample Theoretical 15mg/L Liquid H_2O_2 in DI Water

Figures D-6 to **D-10** are plots of the natural logarithm of the methylene blue concentration as a function of the UV fluence each sample was subject to. The negative of the slope of the linear best fit line is equal to the pseudo-first order decay rate constant (k') of methylene blue in DI water for SPB as the source of H_2O_2.
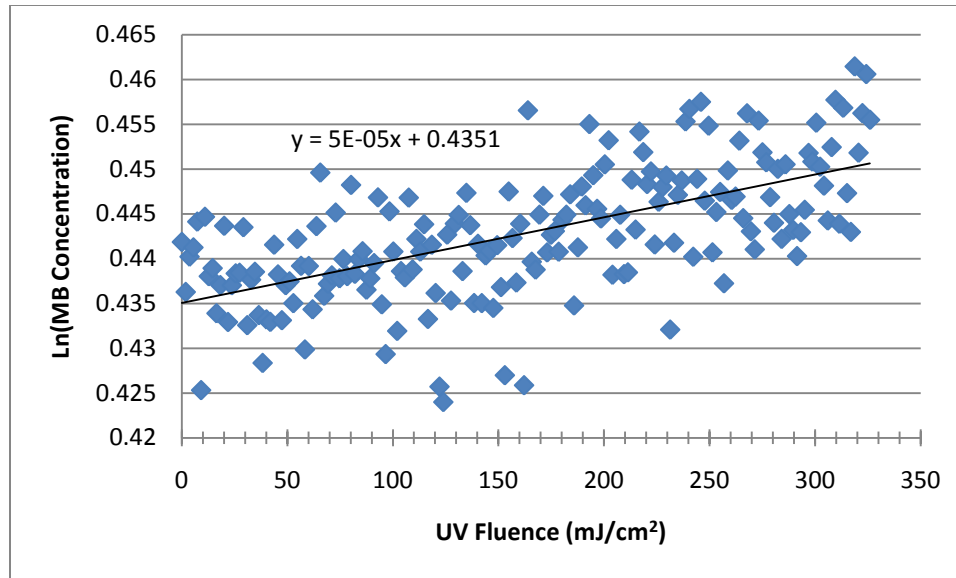
Figure D-37: Natural Logarithm of MB Decay as a Function of UV Fluence; Sample Theoretical 0mg/L SPB in DI Water
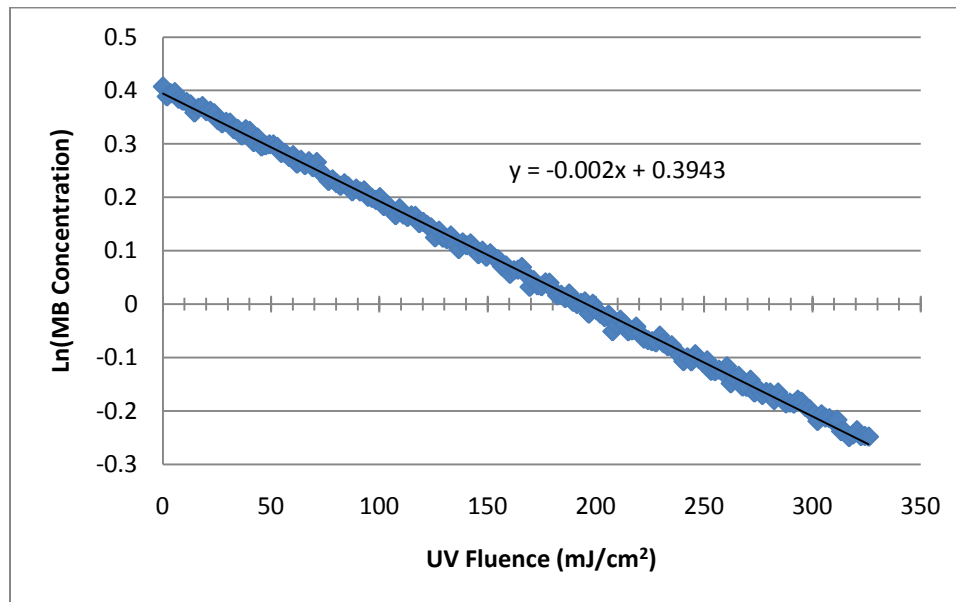
Figure D-38: Natural Logarithm of MB Decay as a Function of UV Fluence; Sample Theoretical 2mg/L SPB in DI Water
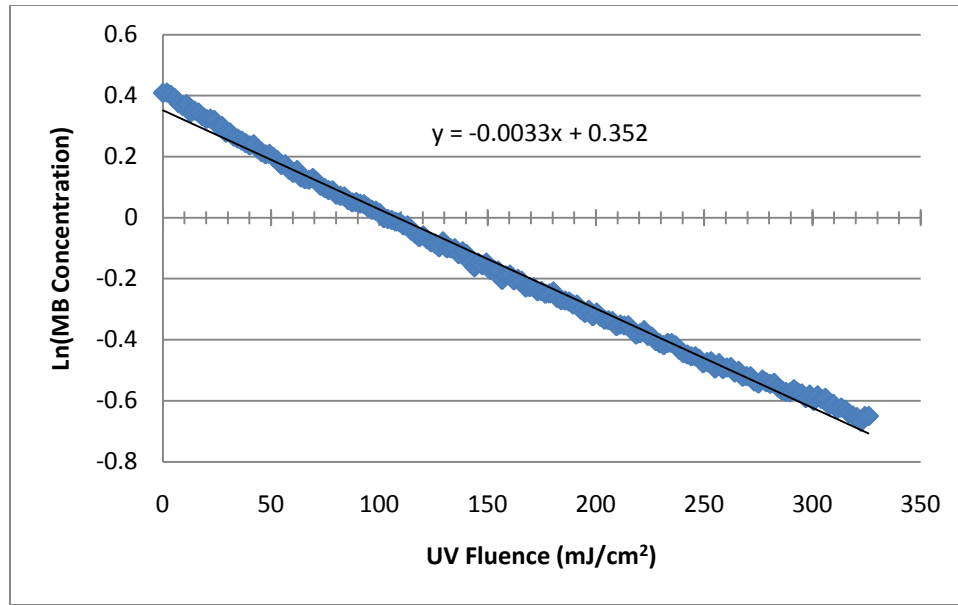
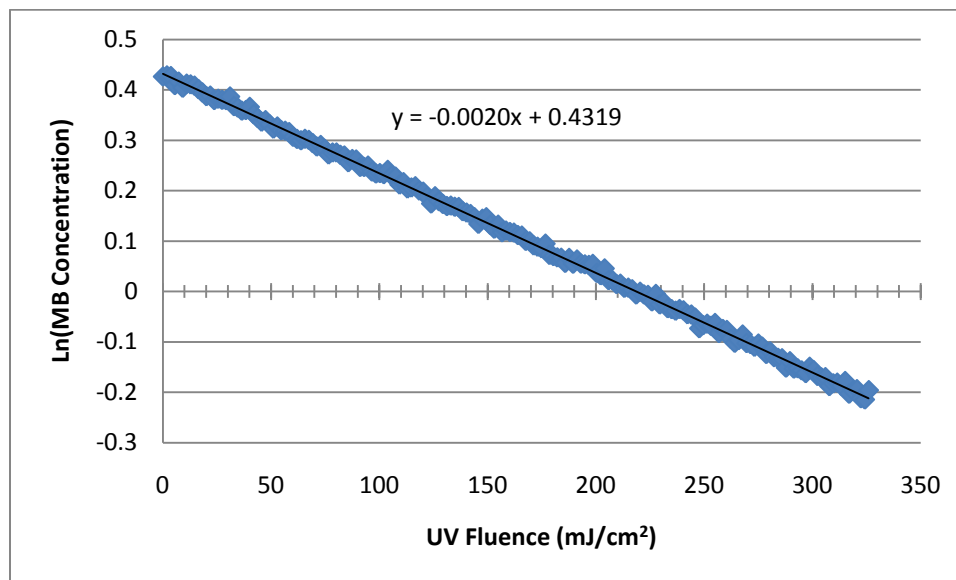Figure D-39: Natural Logarithm of MB Decay as a Function of UV Fluence; Sample Theoretical 5mg/L SPB in DI Water
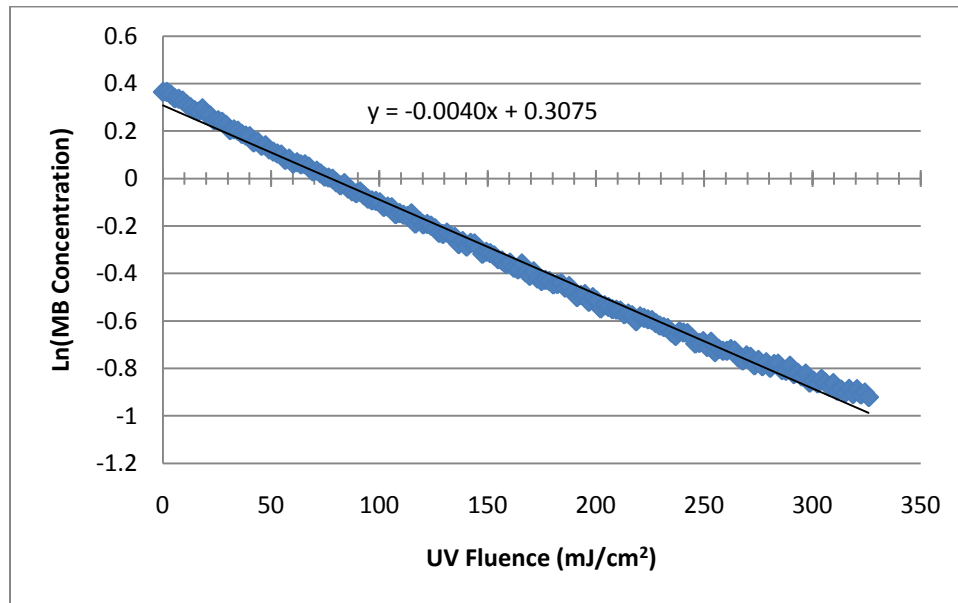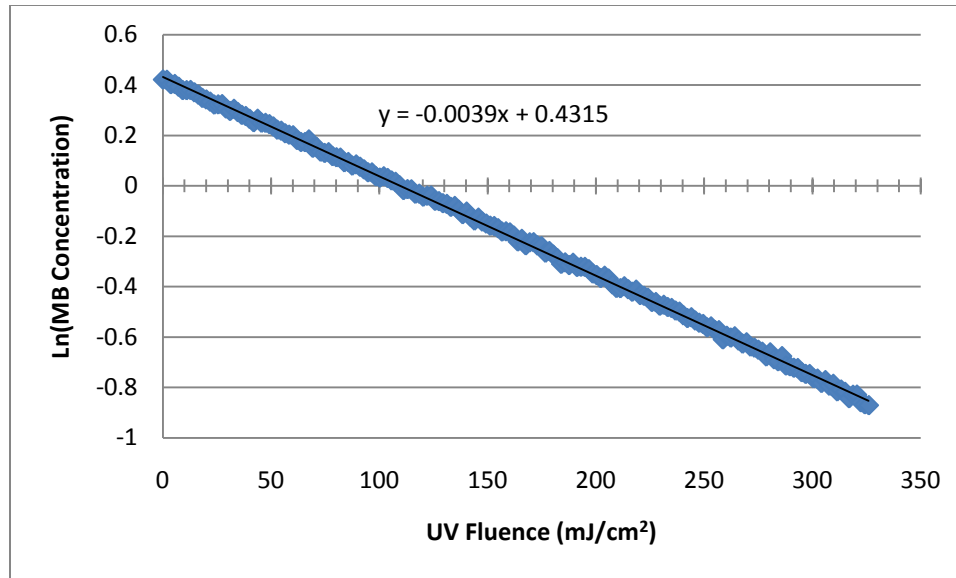

Figure D-40: Natural Logarithm of MB Decay as a Function of UV Fluence; Sample Theoretical 10mg/L SPB in DI Water
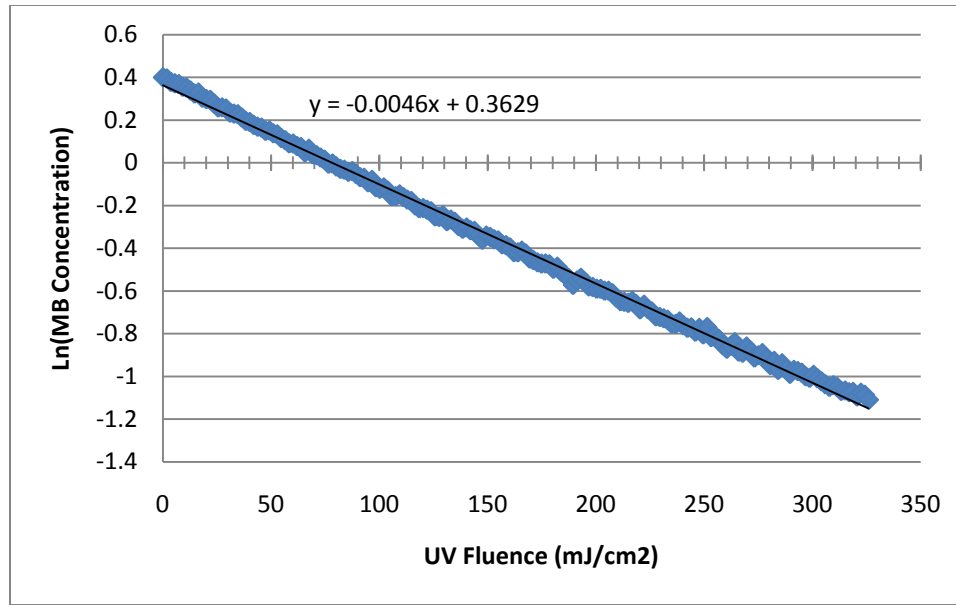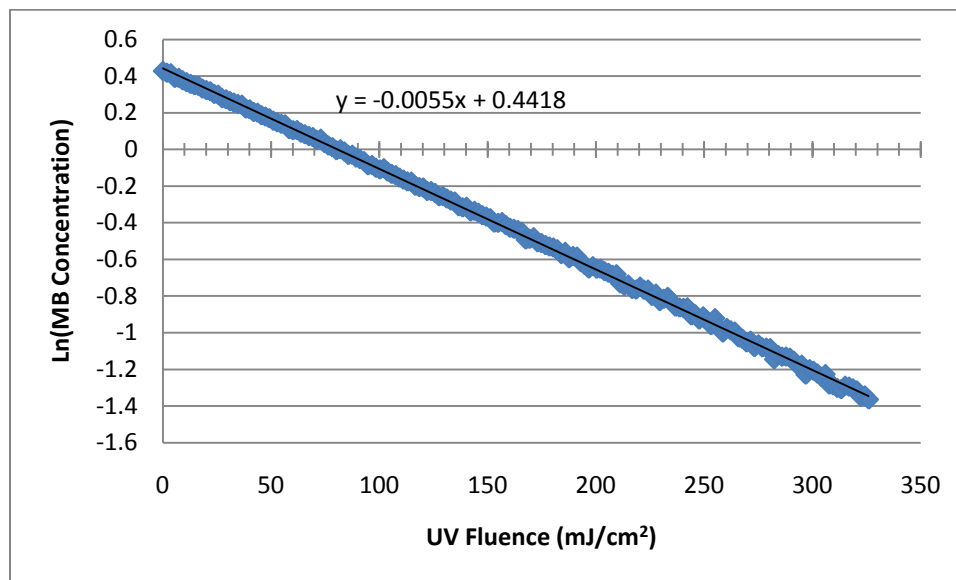
Figure D-41: Natural Logarithm of MB Decay as a Function of UV Fluence; Sample
Theoretical 15mg/L SPB in DI Water

Figures D-11 to **D-15** are plots of the natural logarithm of the methylene blue

concentration as a function of the UV fluence each sample was subject to. The negative

of the slope of the linear best fit line is equal to the pseudo-first order decay rate constant

(k') of methylene blue in DI water for SPC as the source of H_2O_2.
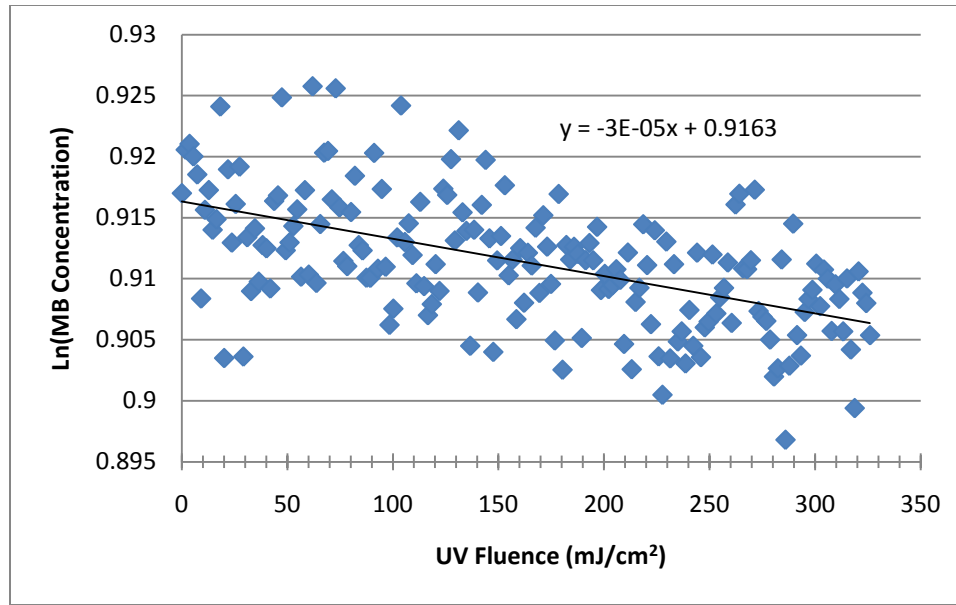
Figure D-42: Natural Logarithm of MB Decay as a Function of UV Fluence; Sample Theoretical 0mg/L SPC in DI Water
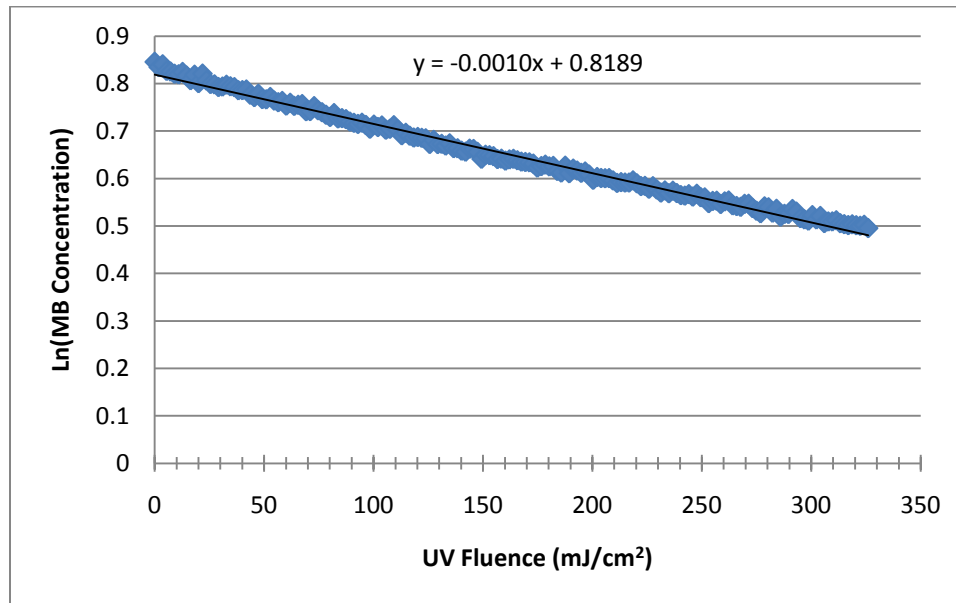
Figure D-43: Natural Logarithm of MB Decay as a Function of UV Fluence; Sample Theoretical 2mg/L SPC in DI Water
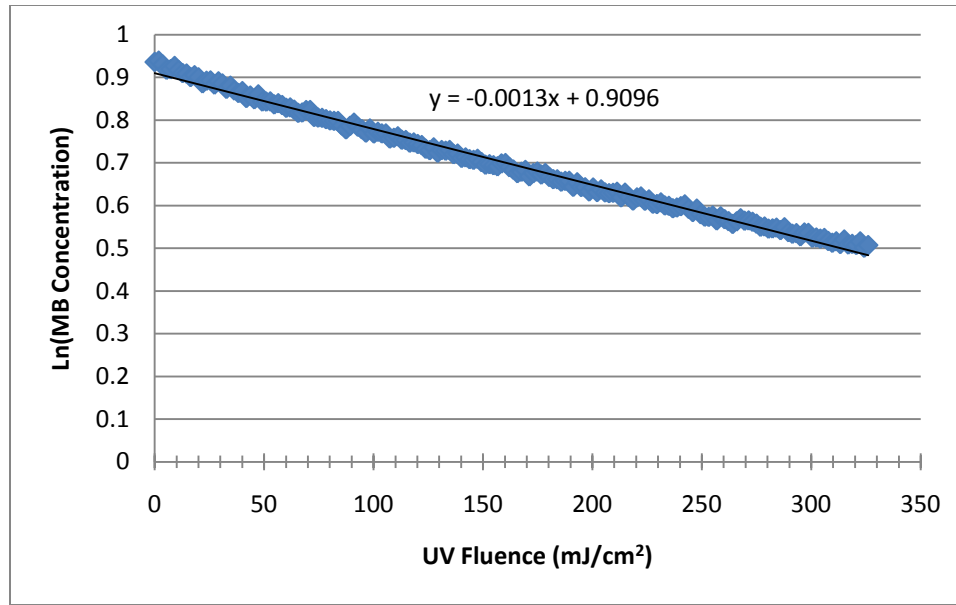
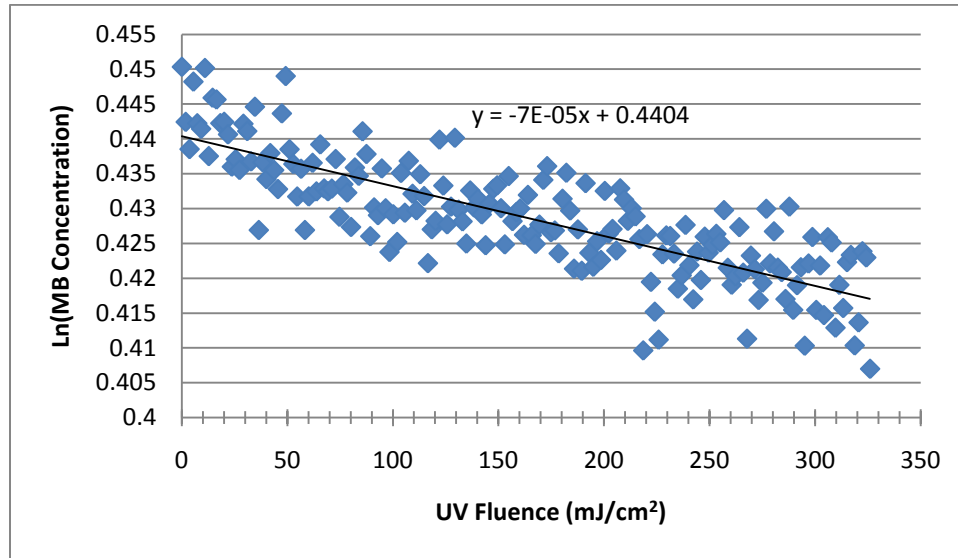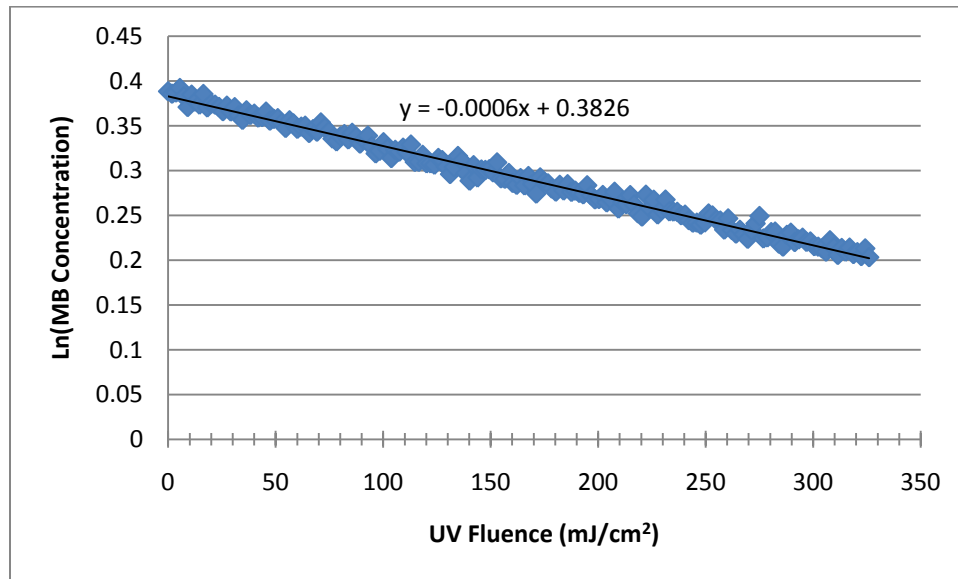Figure D-44: Natural Logarithm of MB Decay as a Function of UV Fluence; Sample Theoretical 5mg/L SPC in DI Water
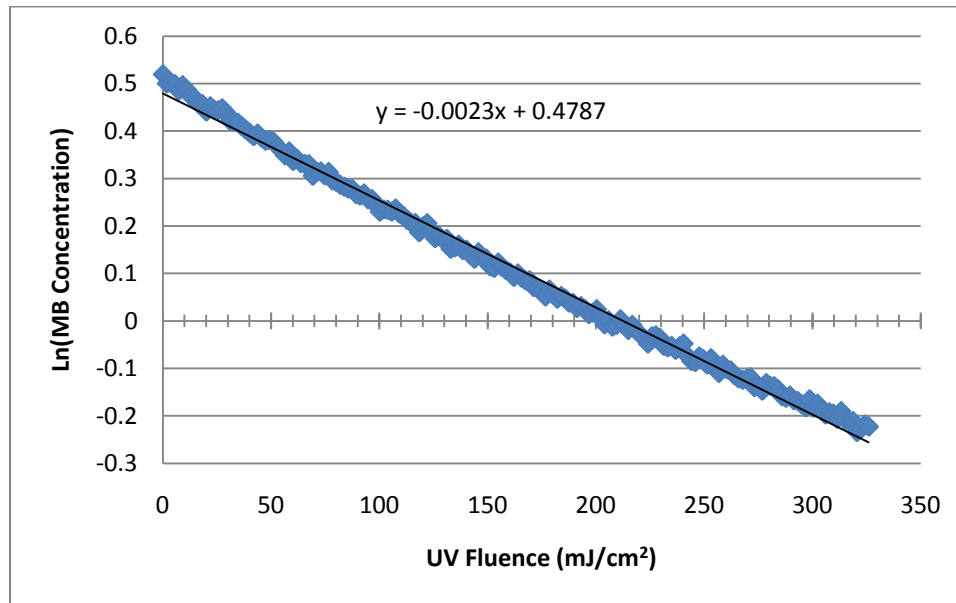
Figure D-45: Natural Logarithm of MB Decay as a Function of UV Fluence; Sample Theoretical 10mg/L SPC in DI Water
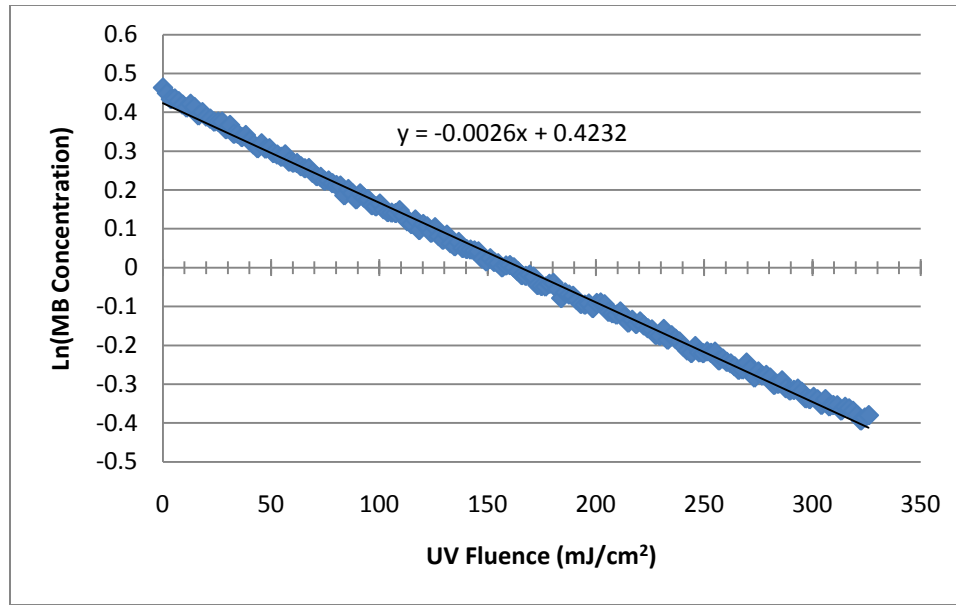
Figure D-46: Natural Logarithm of MB Decay as a Function of UV Fluence; Sample
Theoretical 15mg/L SPC in DI Water

Figures D-16 to **D-23** are plots of the natural logarithm of the methylene blue

concentration as a function of the UV fluence each sample was subject to. The negative

of the slope of the linear best fit line is equal to the pseudo-first order decay rate constant

(k') of methylene blue in the pre-treatment water source for liquid H_2O_2 as the source of
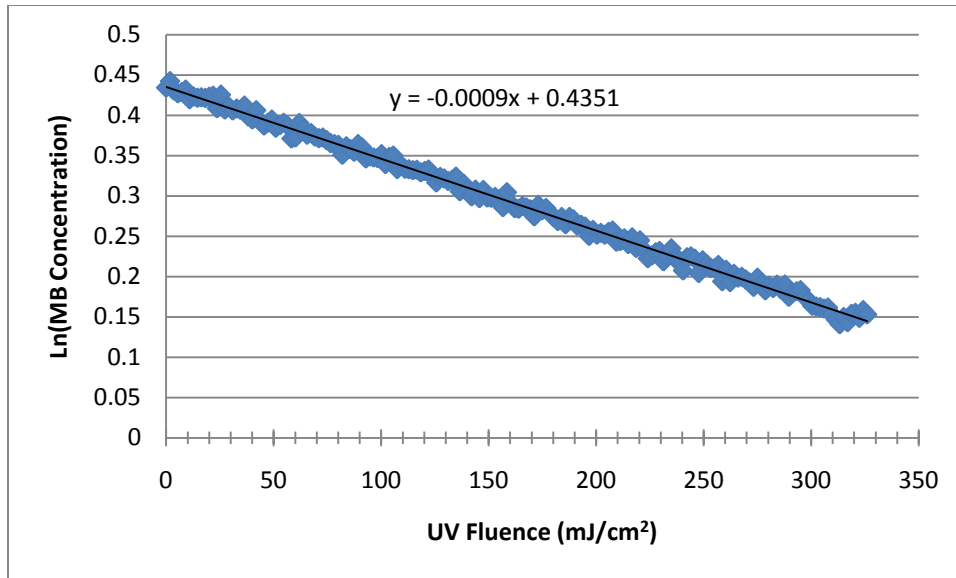
H_2O_2.

Figure D-47: Natural Logarithm of MB Decay as a Function of UV Fluence; Sample Theoretical 0mg/L Liquid H_2O_2 in Pre-Treatment Water
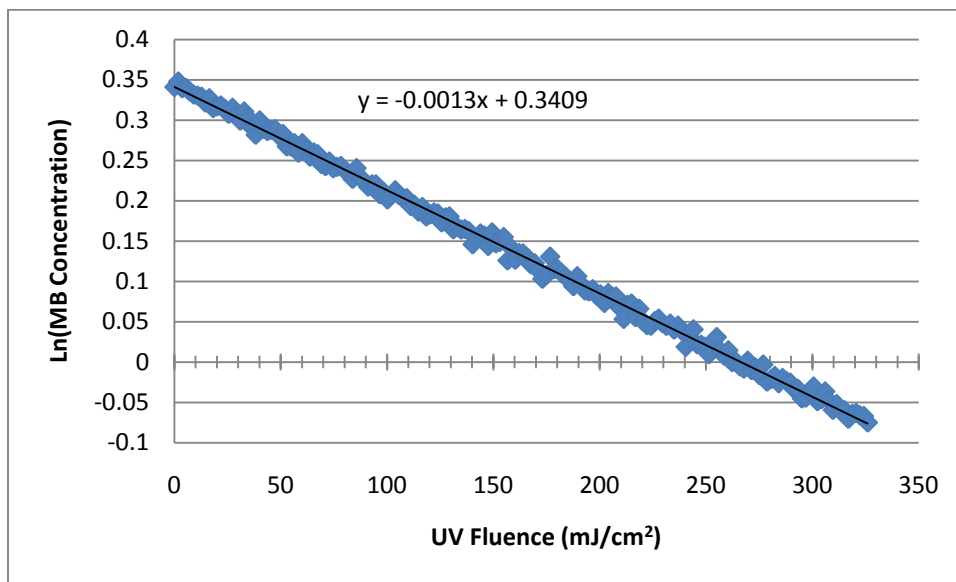

Figure D-48: Natural Logarithm of MB Decay as a Function of UV Fluence; Sample Theoretical 1mg/L Liquid H_2O_2 in Pre-Treatment Water
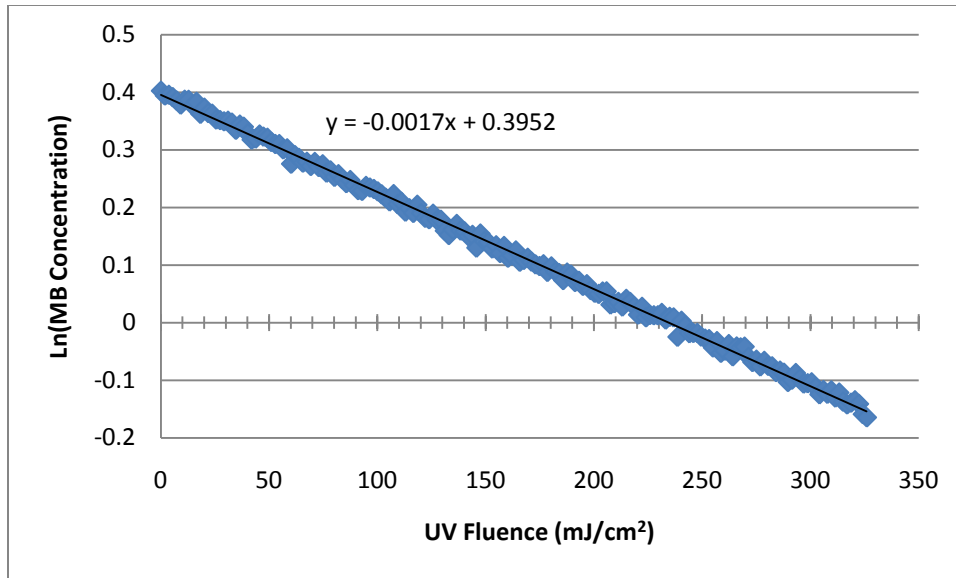
Figure D-49: Natural Logarithm of MB Decay as a Function of UV Fluence; Sample Theoretical 2mg/L Liquid H_2O_2 in Pre-Treatment Water
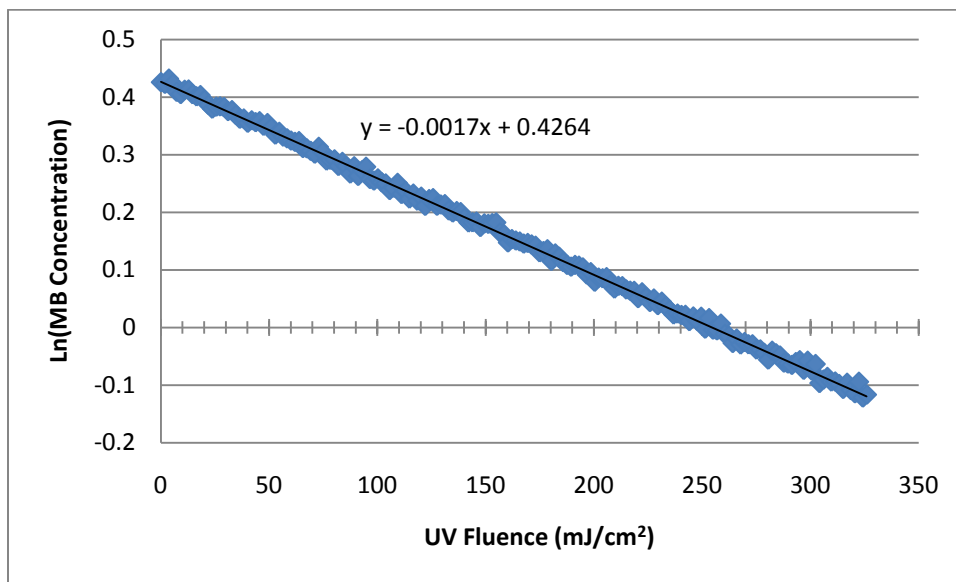

Figure D-50: Natural Logarithm of MB Decay as a Function of UV Fluence; Sample Theoretical 3mg/L Liquid H_2O_2 in Pre-Treatment Water
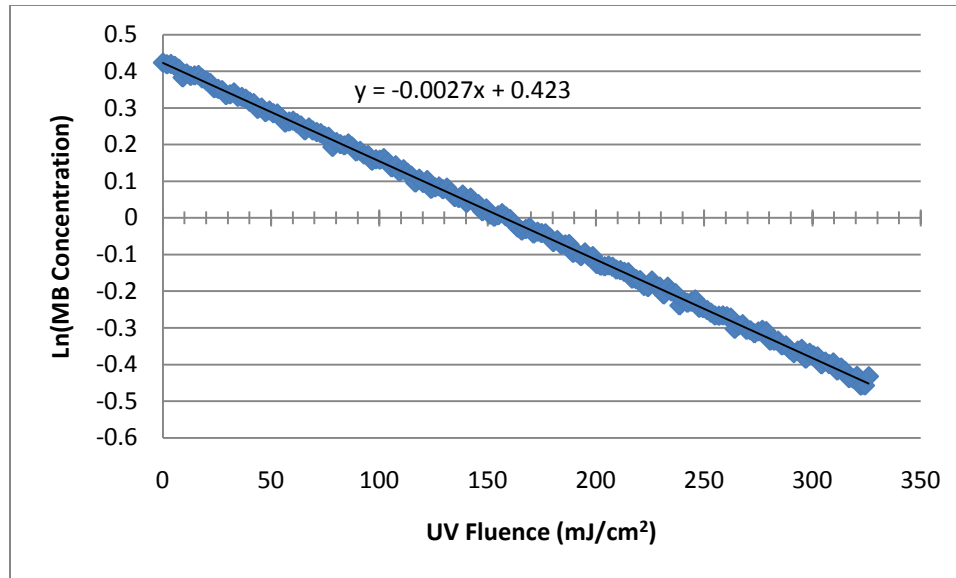
Figure D-51: Natural Logarithm of MB Decay as a Function of UV Fluence; Sample Theoretical 4mg/L Liquid H_2O_2 in Pre-Treatment Water

Figure D-52: Natural Logarithm of MB Decay as a Function of UV Fluence; Sample Theoretical 5mg/L Liquid H_2O_2 in Pre-Treatment Water

Figure D-53: Natural Logarithm of MB Decay as a Function of UV Fluence; Sample Theoretical 10mg/L Liquid H_2O_2 in Pre-Treatment Water
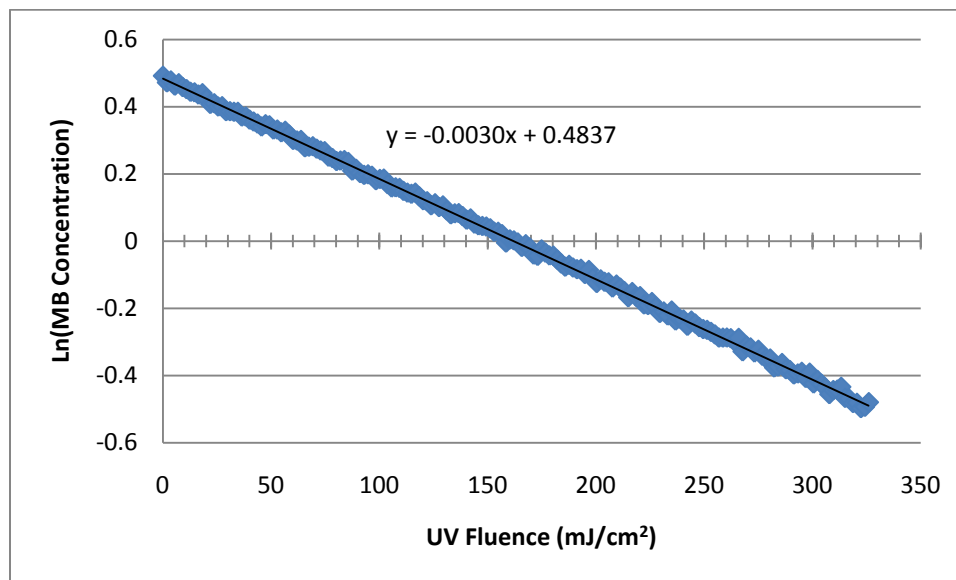

Figure D-54: Natural Logarithm of MB Decay as a Function of UV Fluence; Sample Theoretical 15mg/L Liquid H_2O_2 in Pre-Treatment Water

Figures D-24 to **D-31** are plots of the natural logarithm of the methylene blue

concentration as a function of the UV fluence each sample was subject to. The negative

of the slope of the linear best fit line is equal to the pseudo-first order decay rate constant (k') of methylene blue in the pre-treatment water source for SPB as the source of H_2O_2.
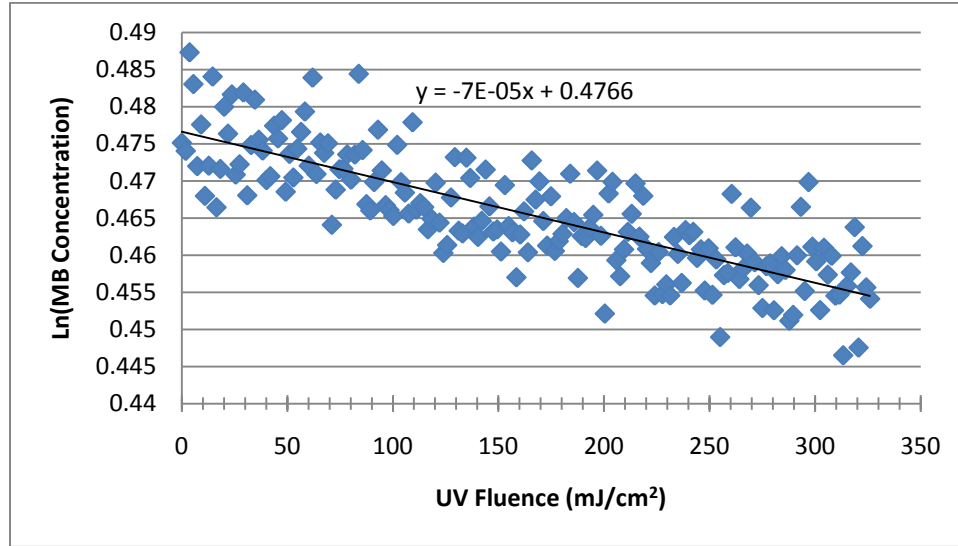

Figure D-55: Natural Logarithm of MB Decay as a Function of UV Fluence; Sample Theoretical 0mg/L SPB in Pre-Treatment Water
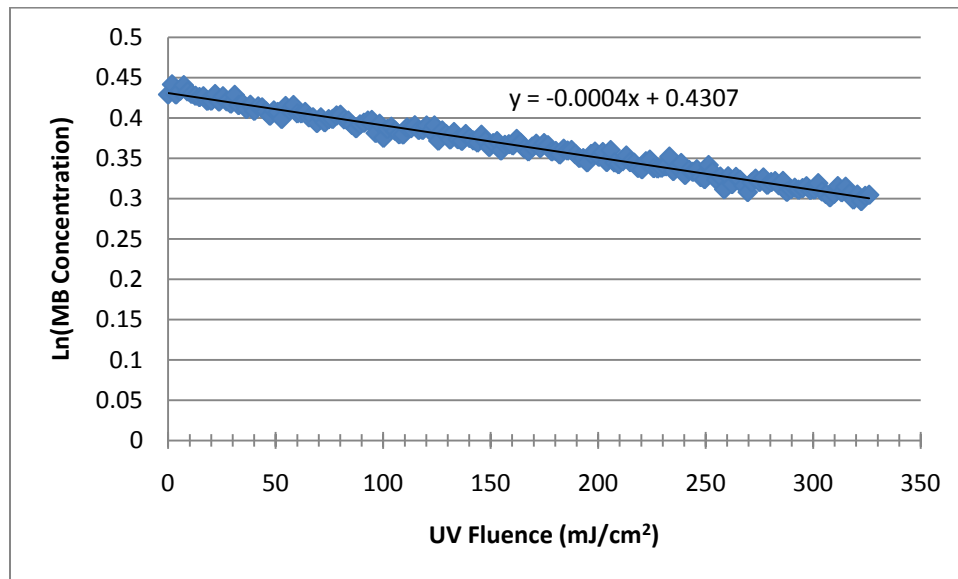

Figure D-56: Natural Logarithm of MB Decay as a Function of UV Fluence; Sample Theoretical 1mg/L SPB in Pre-Treatment Water
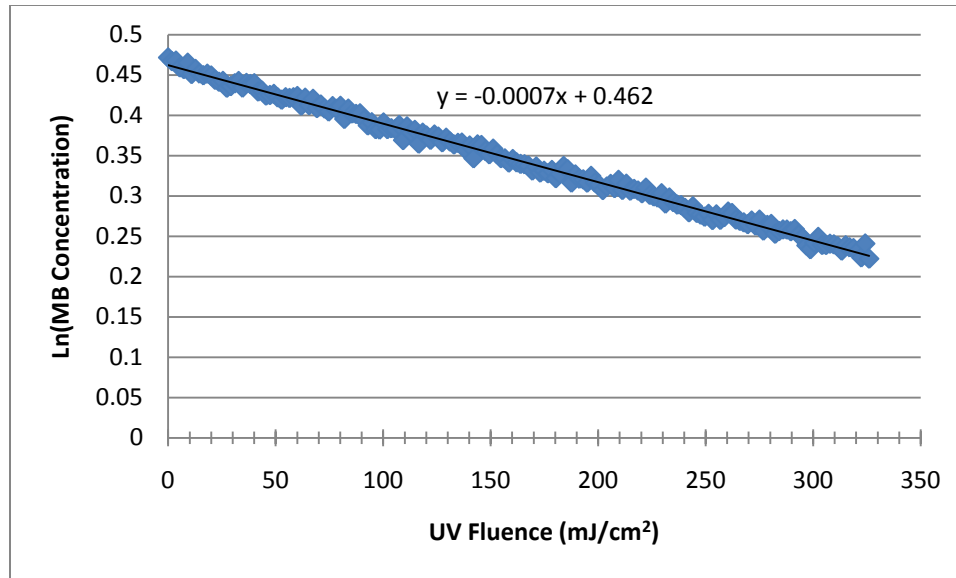
Figure D-57: Natural Logarithm of MB Decay as a Function of UV Fluence; Sample Theoretical 2mg/L SPB in Pre-Treatment Water

Figure D-58: Natural Logarithm of MB Decay as a Function of UV Fluence; Sample Theoretical 3mg/L SPB in Pre-Treatment Water

Figure D-59: Natural Logarithm of MB Decay as a Function of UV Fluence; Sample Theoretical 4mg/L SPB in Pre-Treatment Water
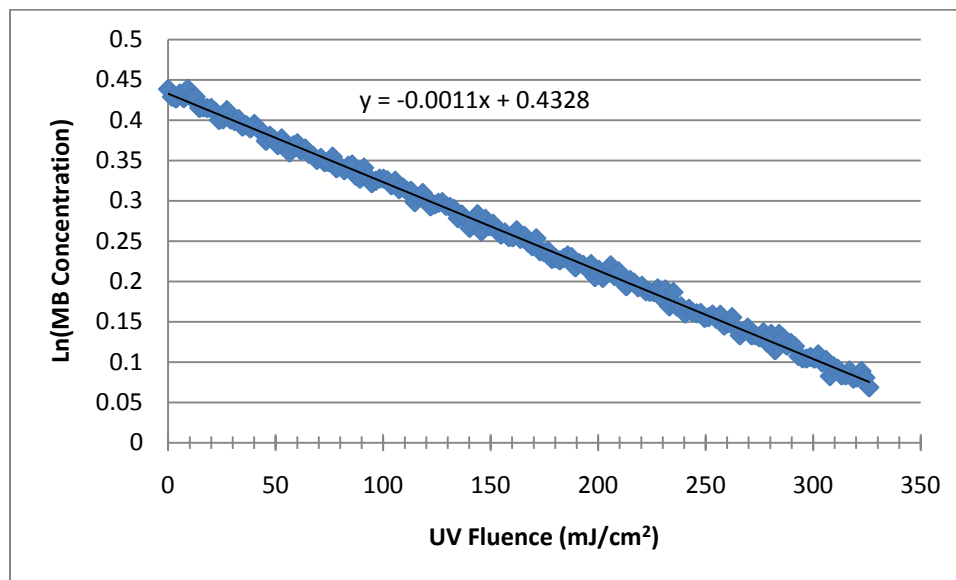

Figure D-60: Natural Logarithm of MB Decay as a Function of UV Fluence; Sample Theoretical 5mg/L SPB in Pre-Treatment Water
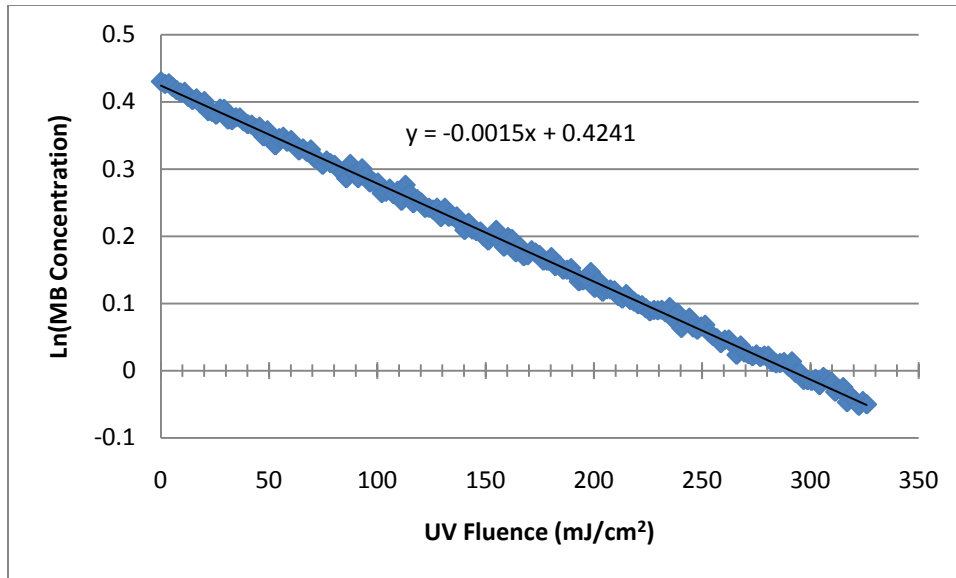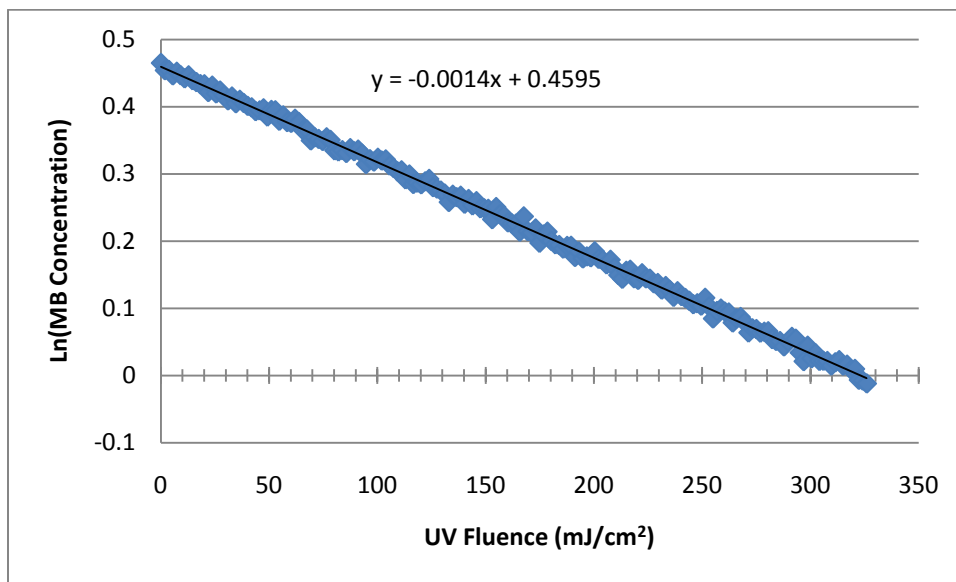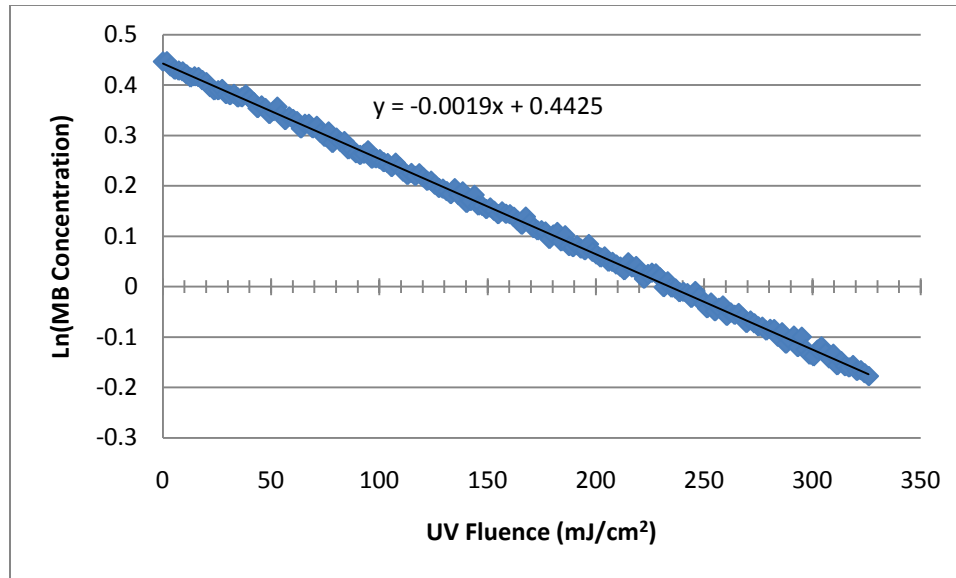
Figure D-61: Natural Logarithm of MB Decay as a Function of UV Fluence; Sample Theoretical 10mg/L SPB in Pre-Treatment Water

Figure D-62: Natural Logarithm of MB Decay as a Function of UV Fluence; Sample Theoretical 15mg/L SPB in Pre-Treatment Water

Figures D-32 to **D-39** are plots of the natural logarithm of the methylene blue

concentration as a function of the UV fluence each sample was subject to. The negative

of the slope of the linear best fit line is equal to the pseudo-first order decay rate constant (k') of methylene blue in the pre-treatment water source for SPC as the source of H_2O_2.

Figure D-63: Natural Logarithm of MB Decay as a Function of UV Fluence; Sample Theoretical 0mg/L SPC in Pre-Treatment Water

Figure D-64: Natural Logarithm of MB Decay as a Function of UV Fluence; Sample Theoretical 1mg/L SPC in Pre-Treatment Water
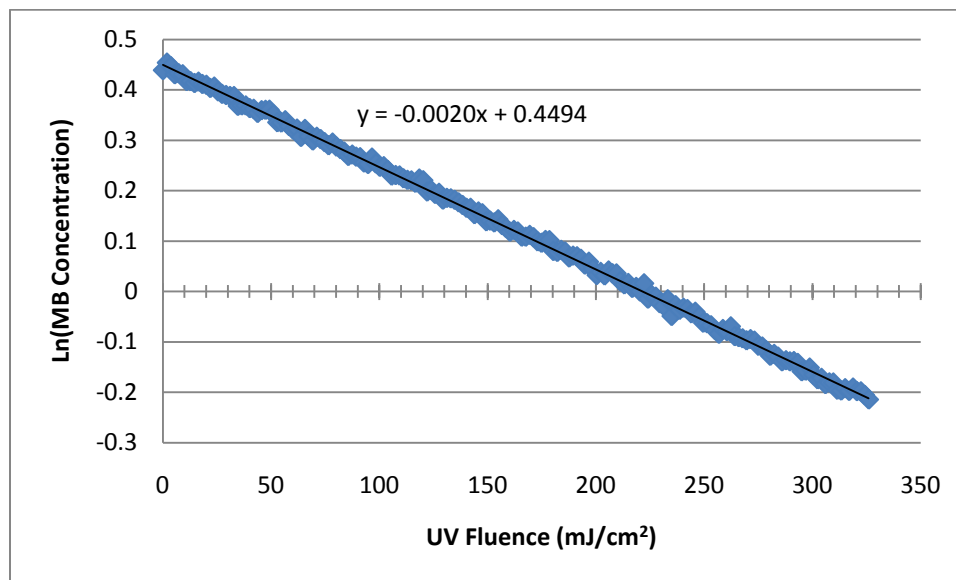
Figure D-65: Natural Logarithm of MB Decay as a Function of UV Fluence; Sample
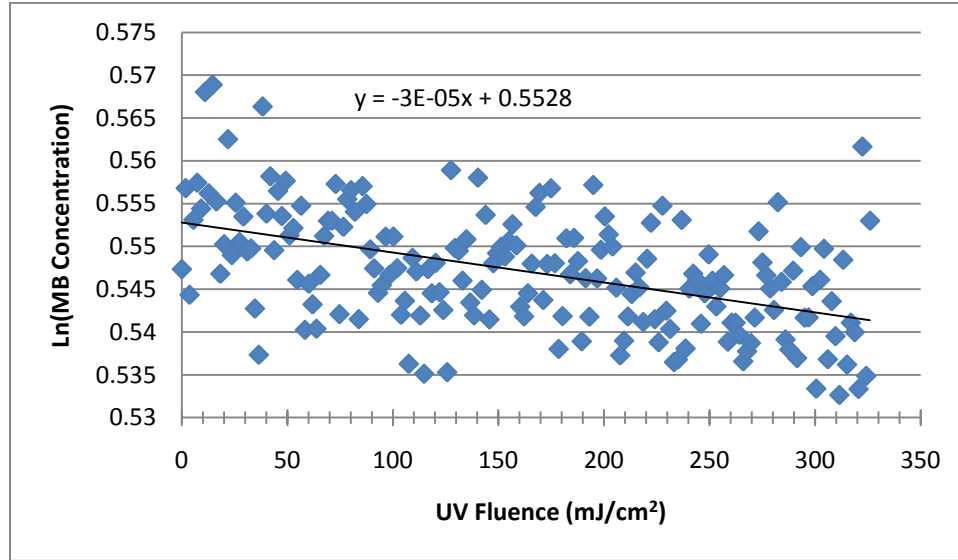Theoretical 2mg/L SPC in Pre-Treatment Water

Figure D-66: Natural Logarithm of MB Decay as a Function of UV Fluence; Sample
Theoretical 3mg/L SPC in Pre-Treatment Water

Figure D-67: Natural Logarithm of MB Decay as a Function of UV Fluence; Sample
Theoretical 4mg/L SPC in Pre-Treatment Water

Figure D-68: Natural Logarithm of MB Decay as a Function of UV Fluence; Sample
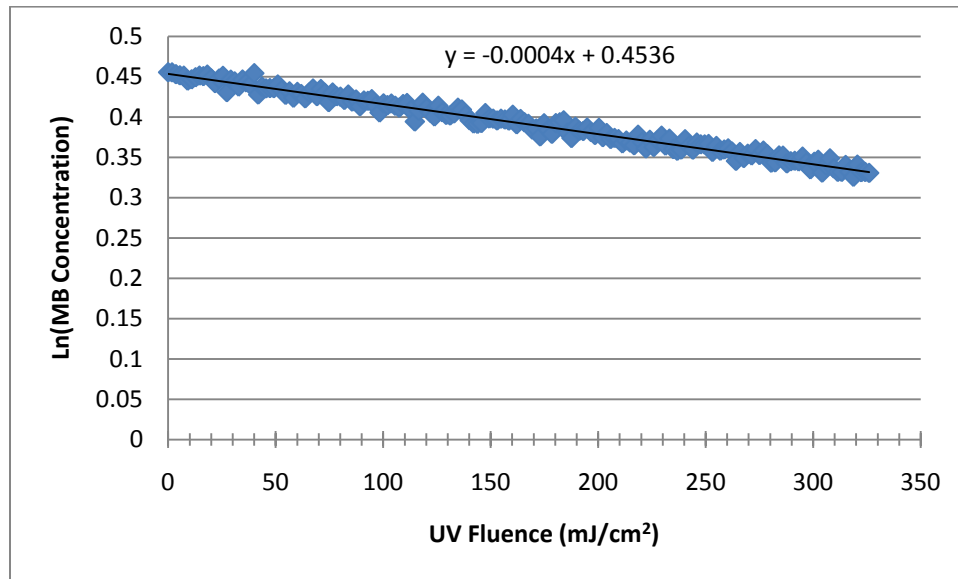Theoretical 5mg/L SPC in Pre-Treatment Water

Figure D-69: Natural Logarithm of MB Decay as a Function of UV Fluence; Sample Theoretical 10mg/L SPC in Pre-Treatment Water

Figure D-70: Natural Logarithm of MB Decay as a Function of UV Fluence; Sample Theoretical 15mg/L SPC in Pre-Treatment Water

Figures D-40 to D-47 are plots of the natural logarithm of the methylene blue concentration as a function of the UV fluence each sample was subject to. The negative of the slope of the linear best fit line is equal to the pseudo-first order decay rate constant

(k') of methylene blue in the treated, unchlorinated water source for liquid H_2O_2 as the source of H_2O_2.

Figure D-71: Natural Logarithm of MB Decay as a Function of UV Fluence; Sample Theoretical 0mg/L Liquid H_2O_2 in Treated, Unchlorinated Water

Figure D-72: Natural Logarithm of MB Decay as a Function of UV Fluence; Sample Theoretical 1mg/L Liquid H_2O_2 in Treated, Unchlorinated Water
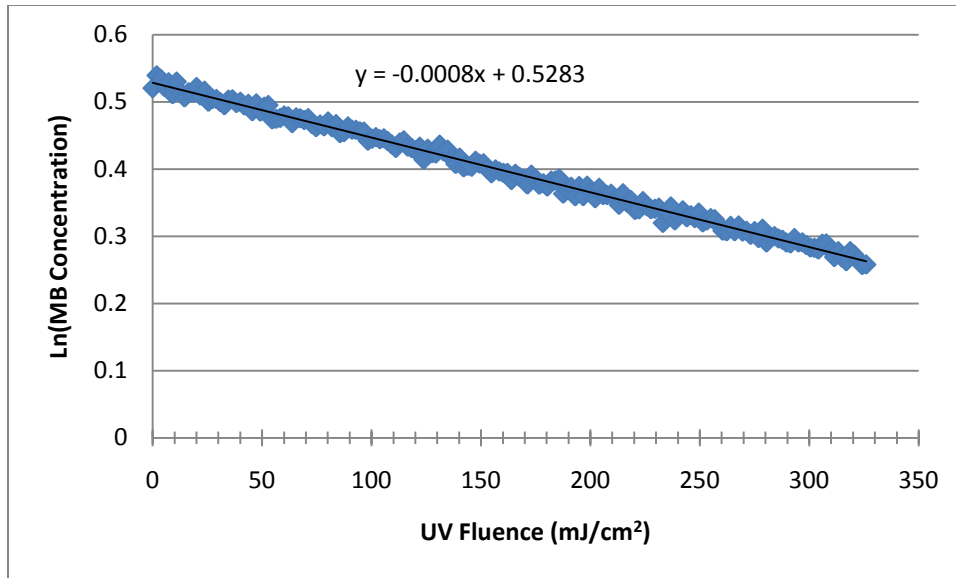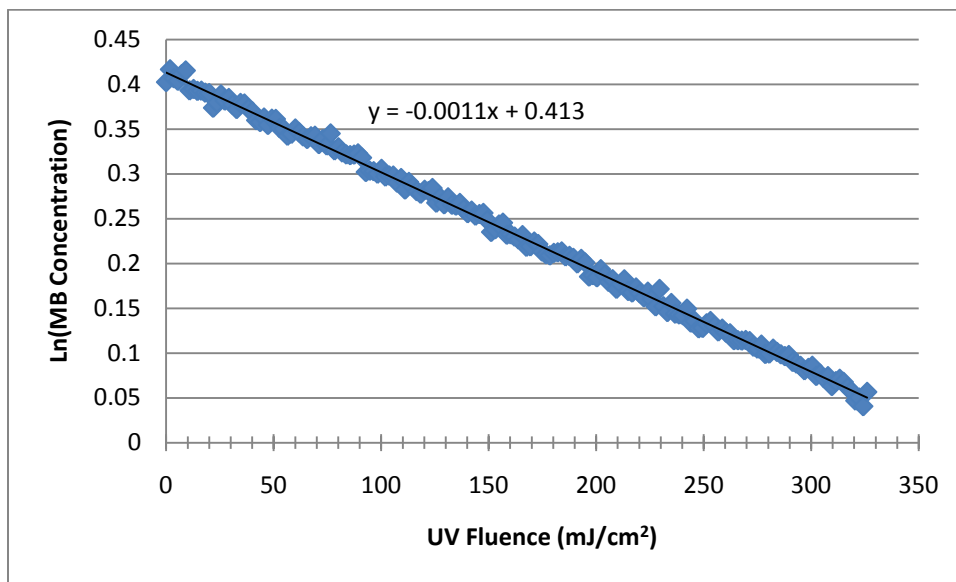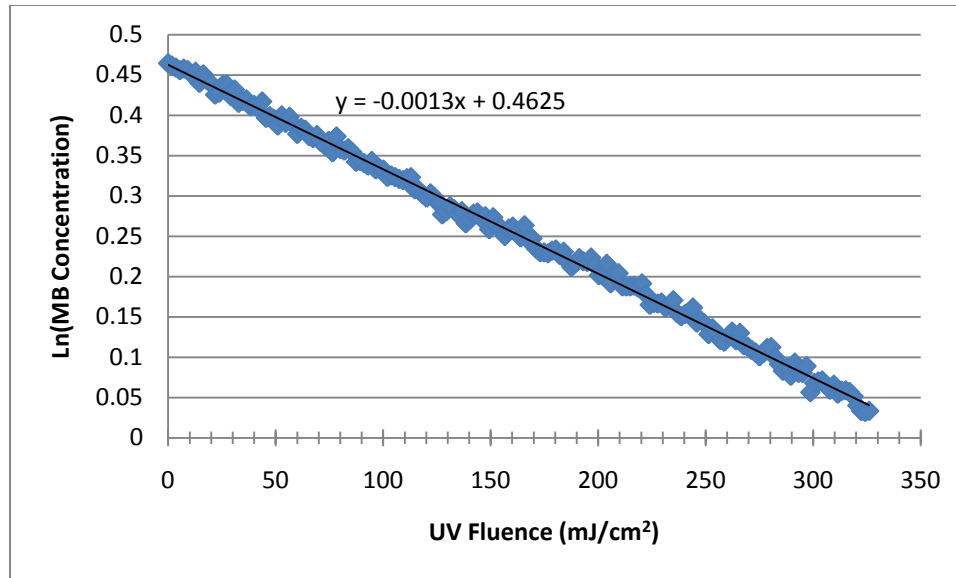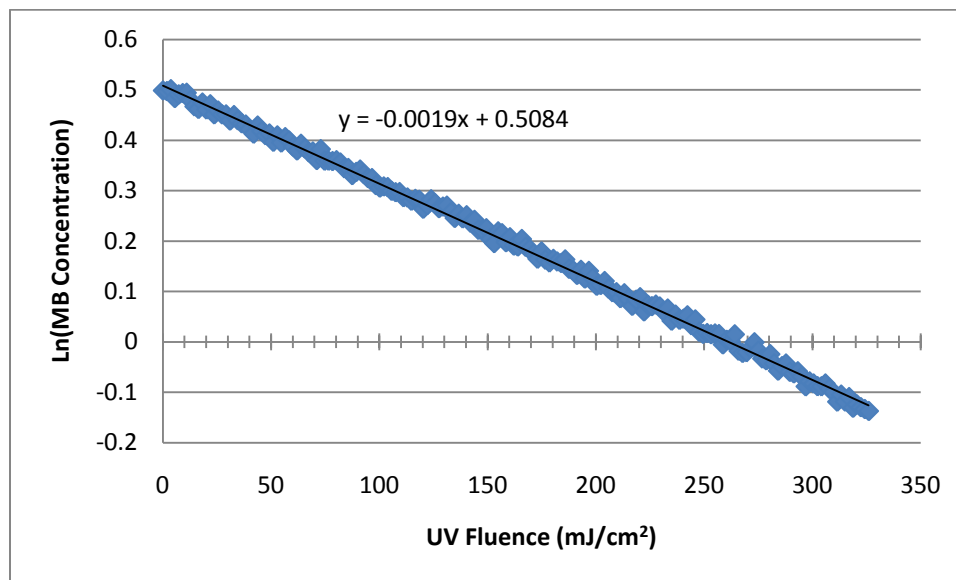
Figure D-73: Natural Logarithm of MB Decay as a Function of UV Fluence; Sample Theoretical 2mg/L Liquid H_2O_2 in Treated, Unchlorinated Water

Figure D-74: Natural Logarithm of MB Decay as a Function of UV Fluence; Sample Theoretical 3mg/L Liquid H_2O_2 in Treated, Unchlorinated Water
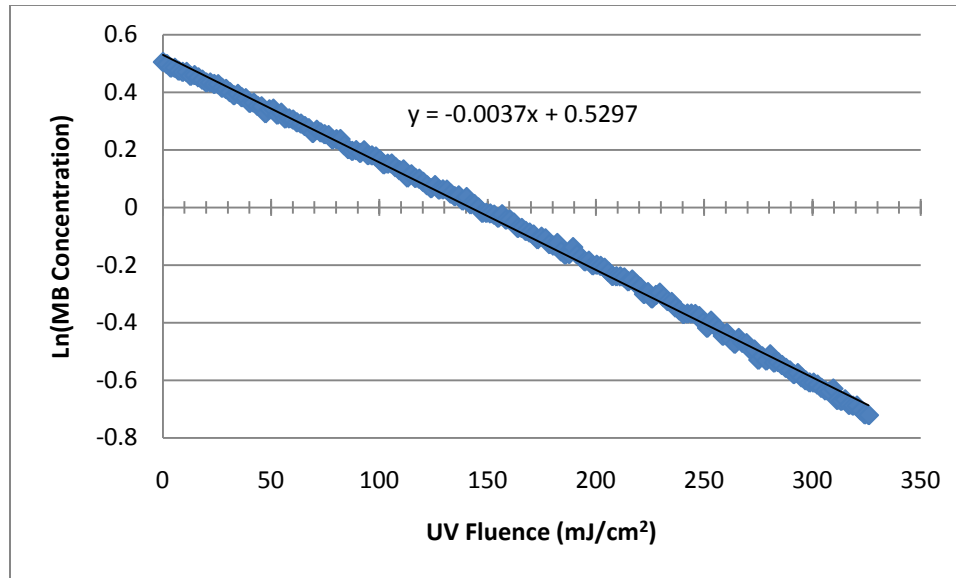
Figure D-75: Natural Logarithm of MB Decay as a Function of UV Fluence; Sample Theoretical 4mg/L Liquid H_2O_2 in Treated, Unchlorinated Water
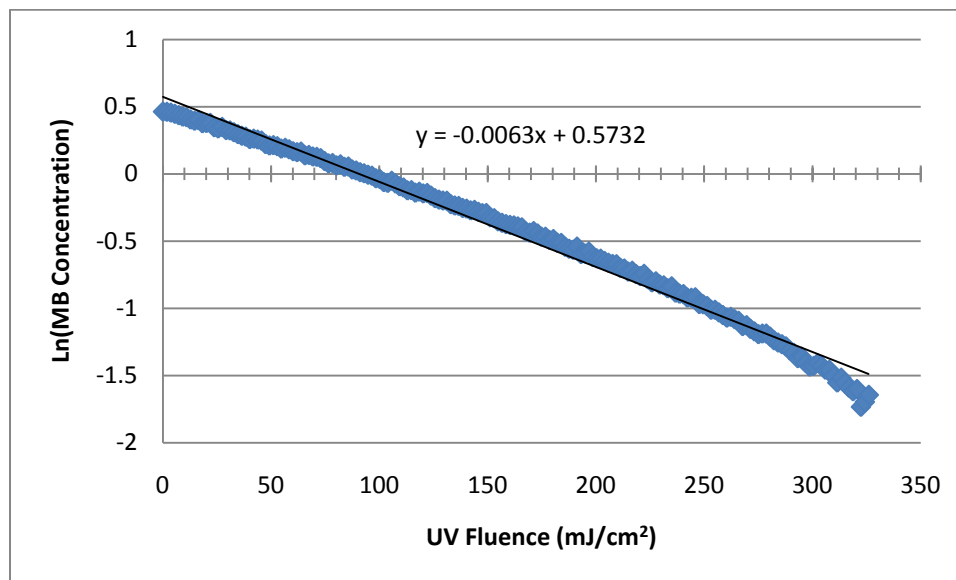

Figure D-76: Natural Logarithm of MB Decay as a Function of UV Fluence; Sample Theoretical 5mg/L Liquid H_2O_2 in Treated, Unchlorinated Water

Figure D-77: Natural Logarithm of MB Decay as a Function of UV Fluence; Sample Theoretical 10mg/L Liquid H_2O_2 in Treated, Unchlorinated Water

Figure D-78: Natural Logarithm of MB Decay as a Function of UV Fluence; Sample Theoretical 15mg/L Liquid H_2O_2 in Treated, Unchlorinated Water

Figures D-48 to **D-55** are plots of the natural logarithm of the methylene blue concentration as a function of the UV fluence each sample was subject to. The negative of the slope of the linear best fit line is equal to the pseudo-first order decay rate constant

(k') of methylene blue in the treated, unchlorinated water source for SPB as the source of H_2O_2.
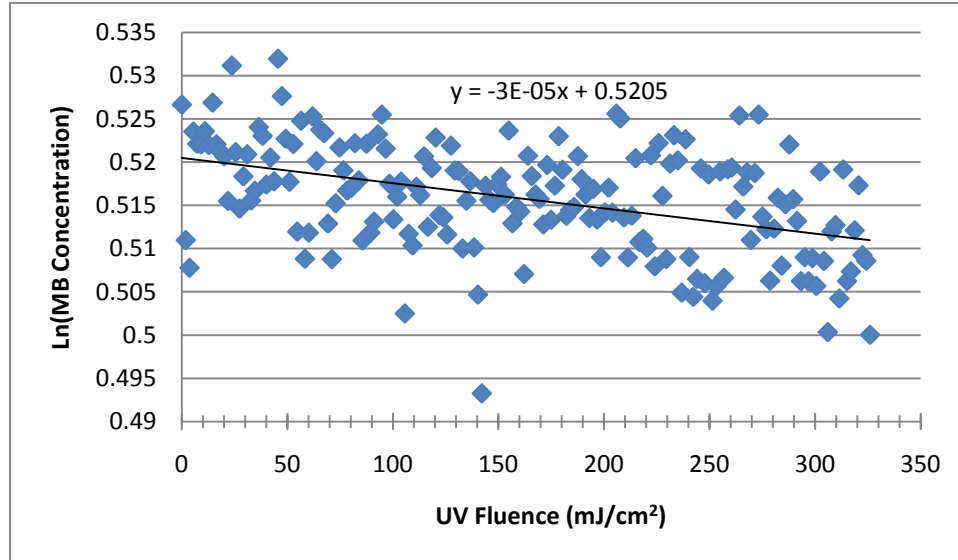

Figure D-79: Natural Logarithm of MB Decay as a Function of UV Fluence; Sample
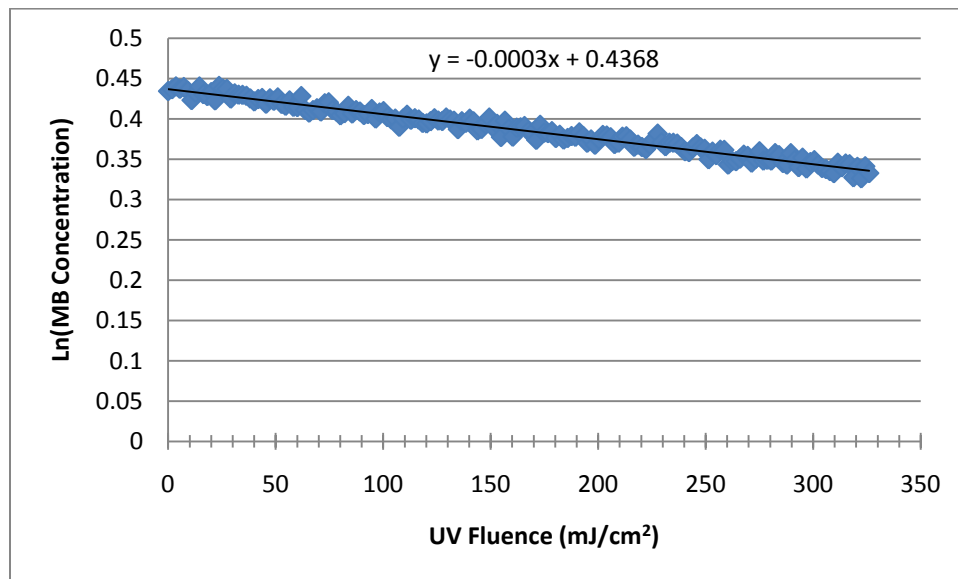Theoretical 0mg/L SPB in Treated, Unchlorinated Water

Figure D-80: Natural Logarithm of MB Decay as a Function of UV Fluence; Sample
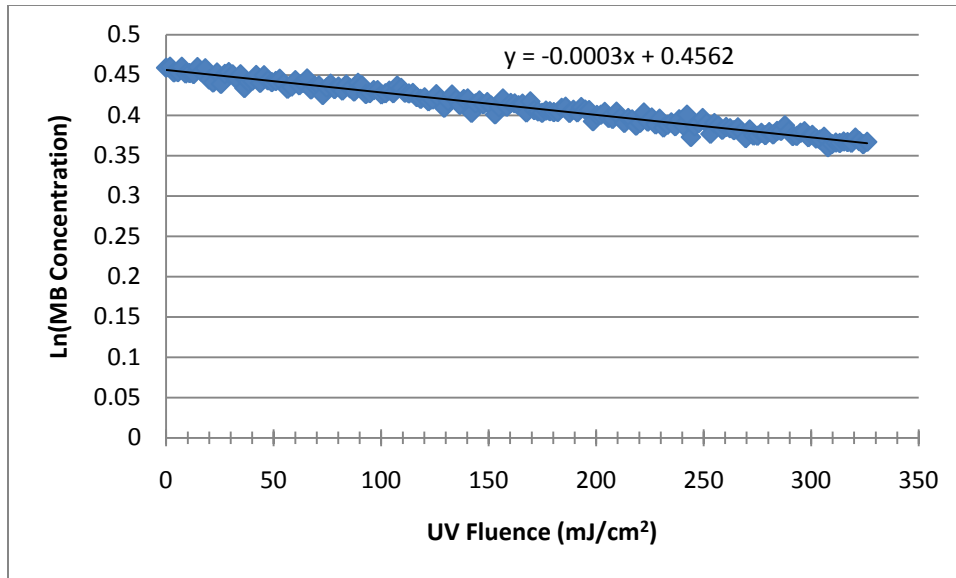Theoretical 1mg/L SPB in Treated, Unchlorinated Water

Figure D-81: Natural Logarithm of MB Decay as a Function of UV Fluence; Sample Theoretical 2mg/L SPB in Treated, Unchlorinated Water
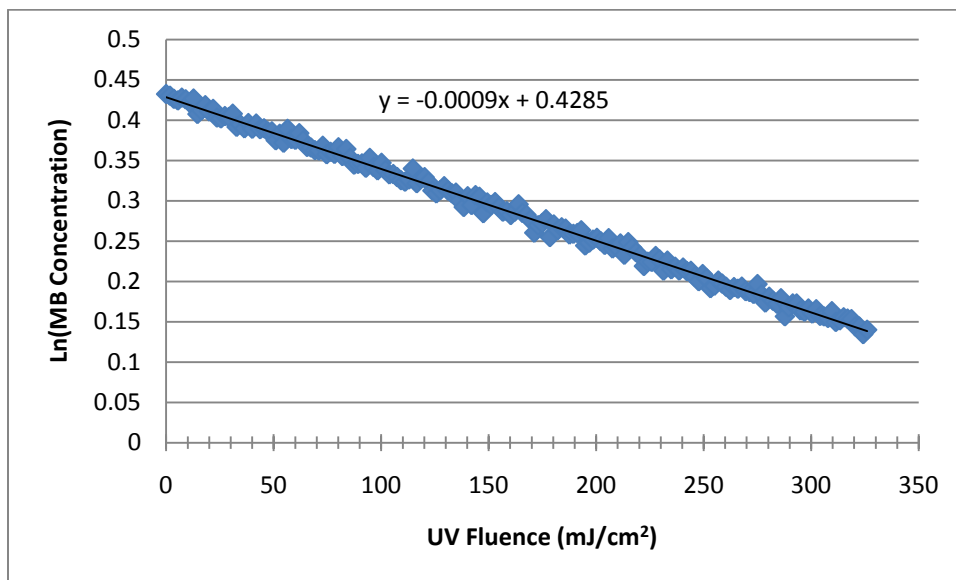

Figure D-82: Natural Logarithm of MB Decay as a Function of UV Fluence; Sample Theoretical 3mg/L SPB in Treated, Unchlorinated Water
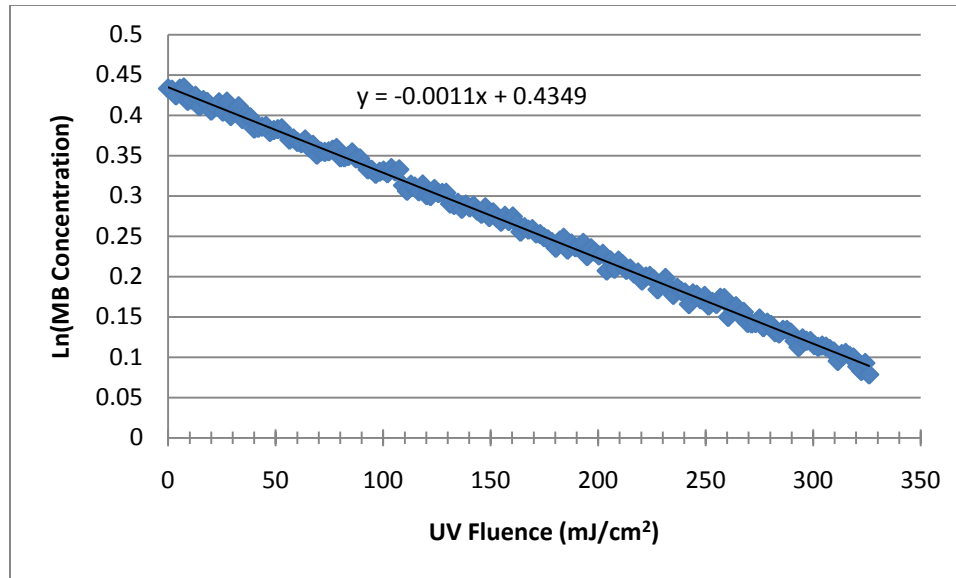
Figure D-83: Natural Logarithm of MB Decay as a Function of UV Fluence; Sample Theoretical 4mg/L SPB in Treated, Unchlorinated Water
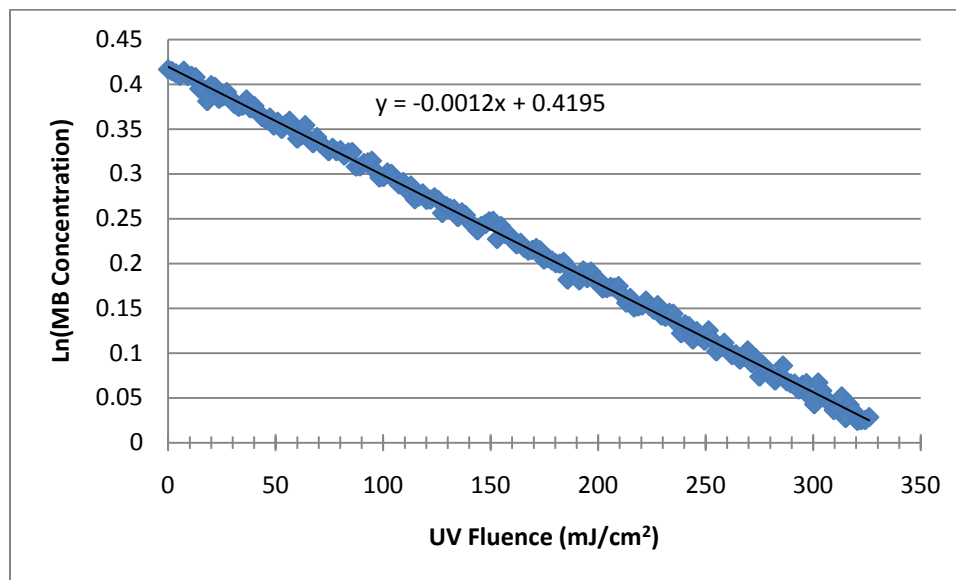

Figure D-84: Natural Logarithm of MB Decay as a Function of UV Fluence; Sample Theoretical 5mg/L SPB in Treated, Unchlorinated Water
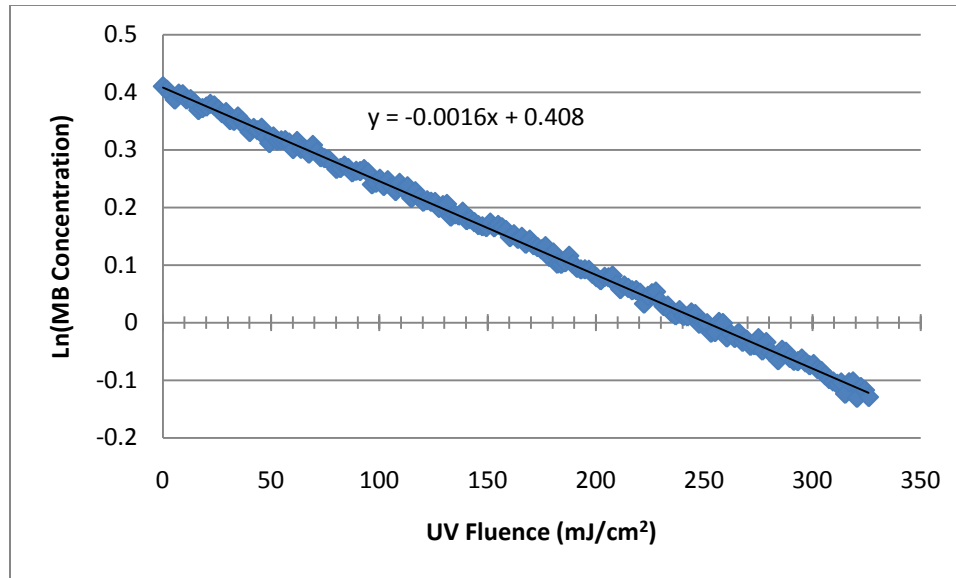
Figure D-85: Natural Logarithm of MB Decay as a Function of UV Fluence; Sample Theoretical 10mg/L SPB in Treated, Unchlorinated Water
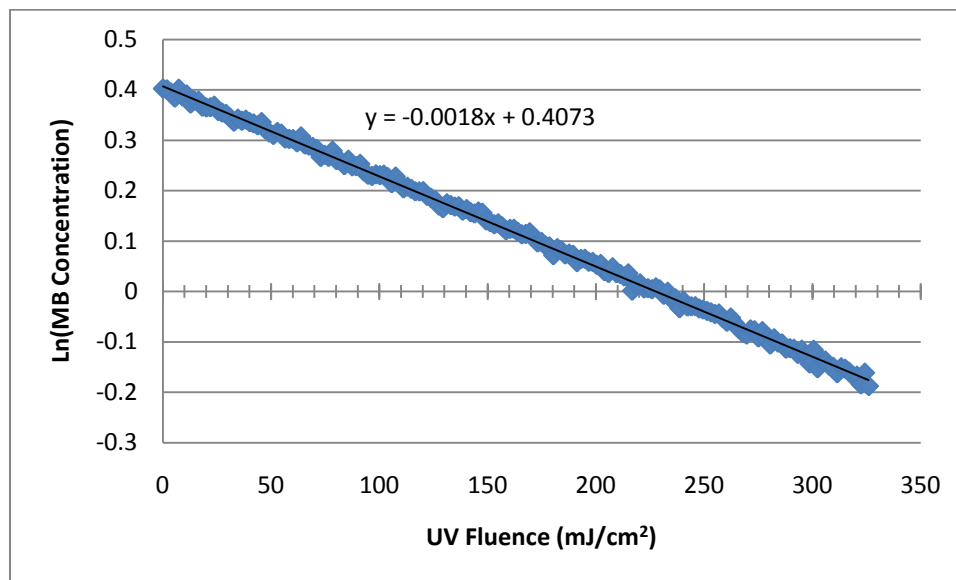

Figure D-86: Natural Logarithm of MB Decay as a Function of UV Fluence; Sample Theoretical 15mg/L SPB in Treated, Unchlorinated Water

Figures D-56 to **D-63** are plots of the natural logarithm of the methylene blue

concentration as a function of the UV fluence each sample was subject to. The negative

of the slope of the linear best fit line is equal to the pseudo-first order decay rate constant

140

(k') of methylene blue in the treated, unchlorinated water source for SPC as the source of H_2O_2.

Figure D-87: Natural Logarithm of MB Decay as a Function of UV Fluence; Sample Theoretical 0mg/L SPC in Treated, Unchlorinated Water

Figure D-88: Natural Logarithm of MB Decay as a Function of UV Fluence; Sample Theoretical 1mg/L SPC in Treated, Unchlorinated Water
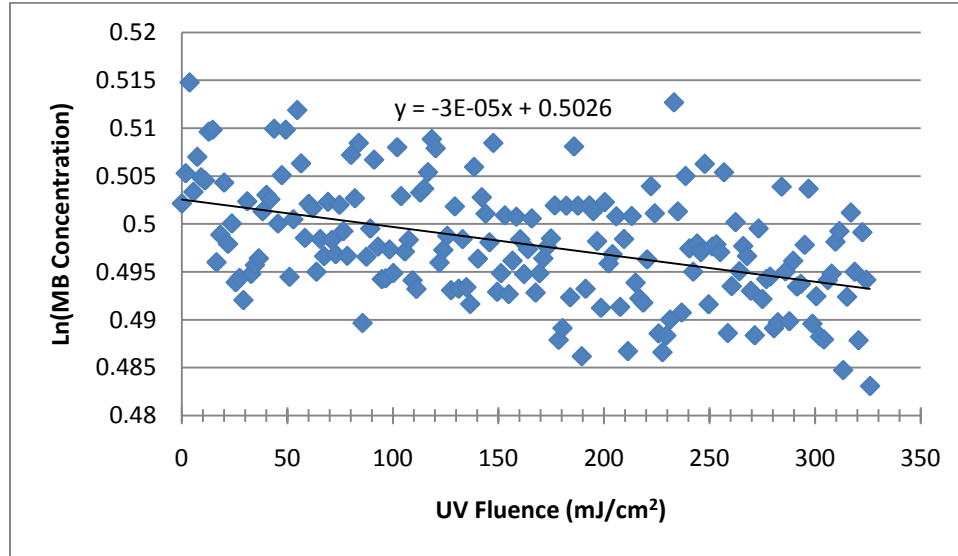
Figure D-89: Natural Logarithm of MB Decay as a Function of UV Fluence; Sample Theoretical 2mg/L SPC in Treated, Unchlorinated Water
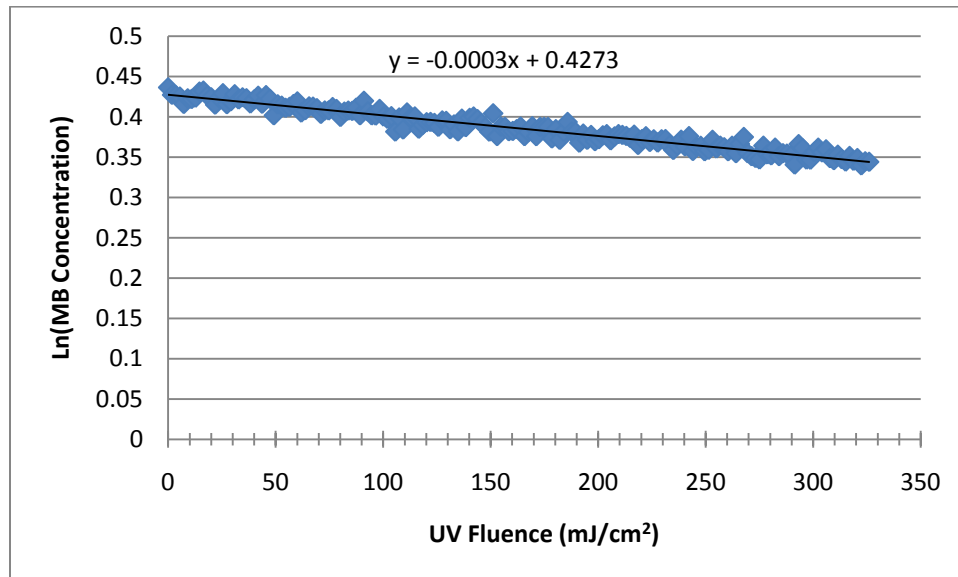

Figure D-90: Natural Logarithm of MB Decay as a Function of UV Fluence; Sample Theoretical 3mg/L SPC in Treated, Unchlorinated Water
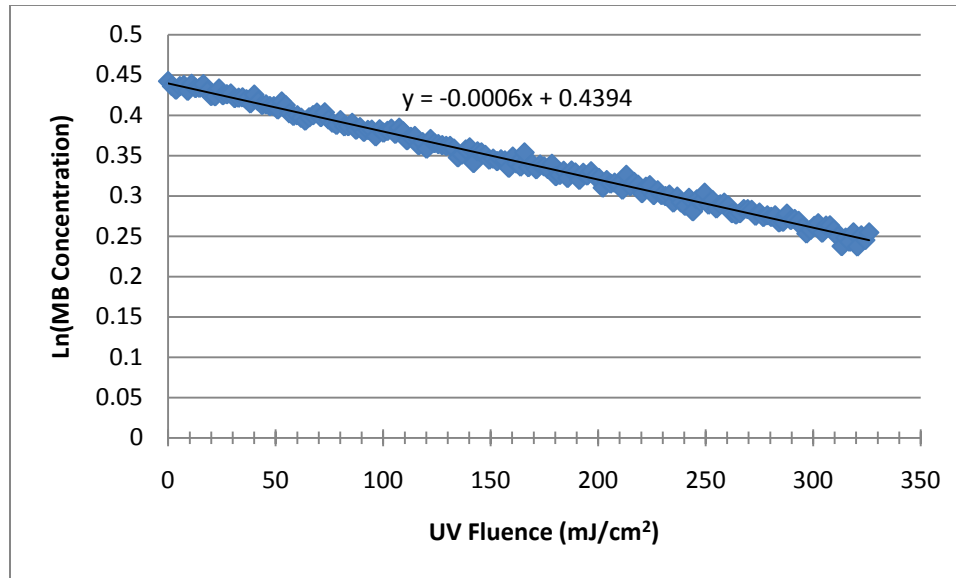
Figure D-91: Natural Logarithm of MB Decay as a Function of UV Fluence; Sample Theoretical 4mg/L SPC in Treated, Unchlorinated Water
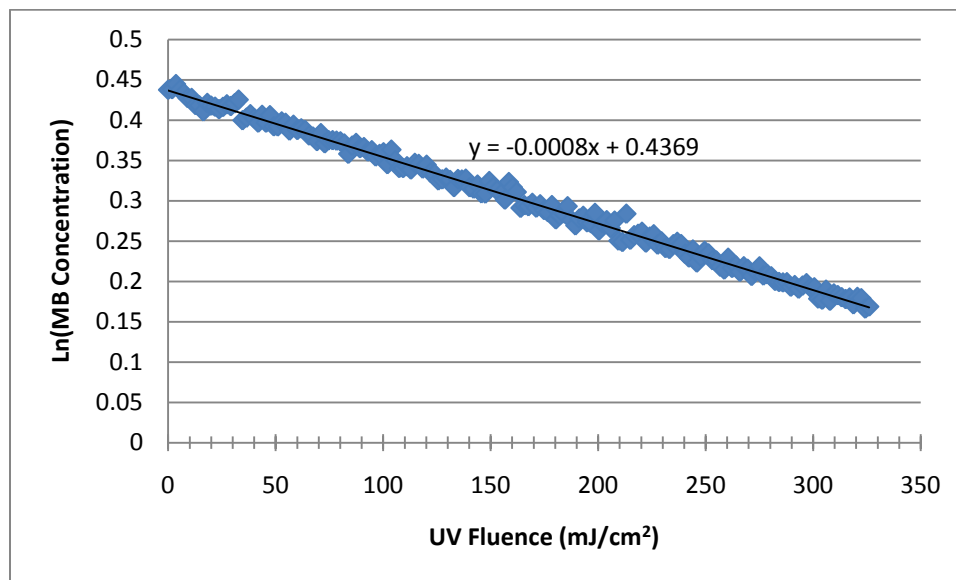

Figure D-92: Natural Logarithm of MB Decay as a Function of UV Fluence; Sample Theoretical 5mg/L SPC in Treated, Unchlorinated Water

Figure D-93: Natural Logarithm of MB Decay as a Function of UV Fluence; Sample Theoretical 10mg/L SPC in Treated, Unchlorinated Water
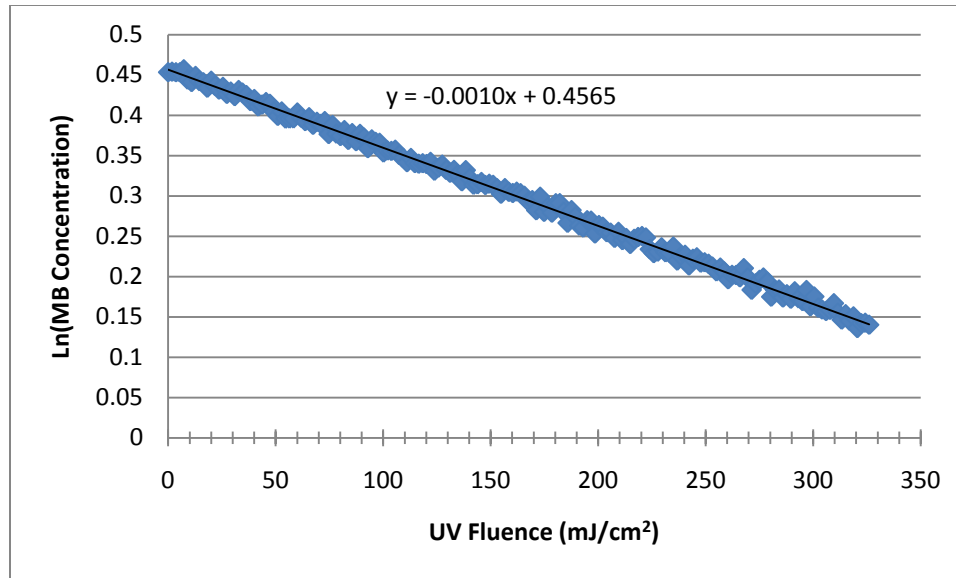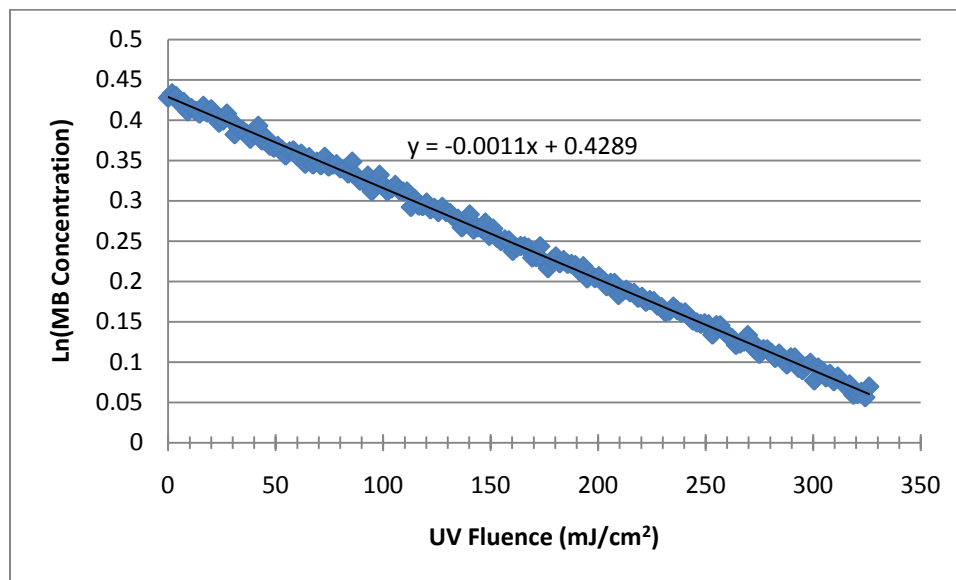

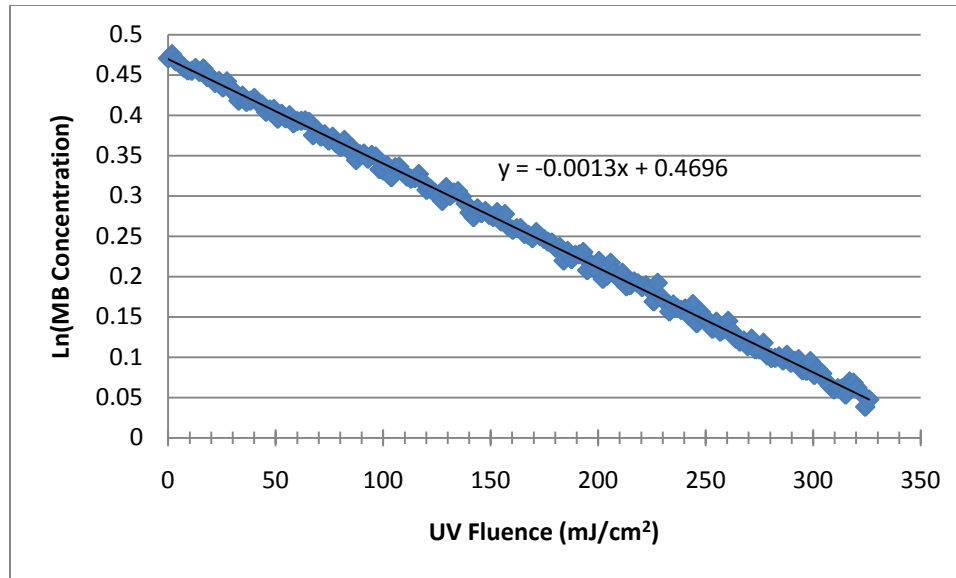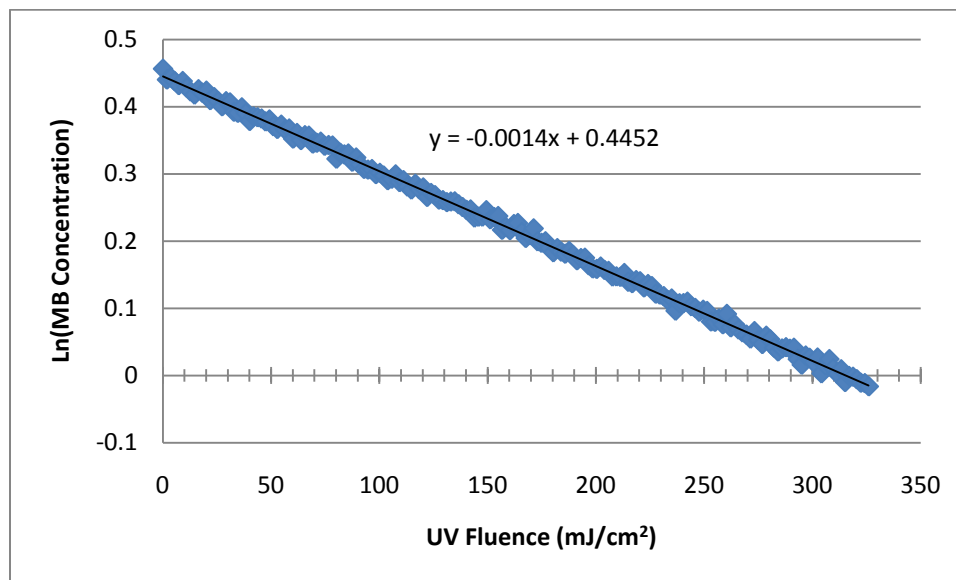Figure D-94: Natural Logarithm of MB Decay as a Function of UV Fluence; Sample Theoretical 15mg/L SPC in Treated, Unchlorinated Water

Figures D-64 to **D-71** are plots of the natural logarithm of the methylene blue

concentration as a function of the UV fluence each sample was subject to. The negative

of the slope of the linear best fit line is equal to the pseudo-first order decay rate constant

(k') of methylene blue in the post-treatment water source for liquid H_2O_2 as the source of H_2O_2.

$$y = -0.0008x + 0.3683$$

Figure D-95: Natural Logarithm of MB Decay as a Function of UV Fluence; Sample
Theoretical 0mg/L Liquid H_2O_2 in Post-Treatment Water

$$y = -0.0006x + 0.4971$$

Figure D-96: Natural Logarithm of MB Decay as a Function of UV Fluence; Sample
Theoretical 1mg/L Liquid H_2O_2 in Post-Treatment Water

Figure D-97: Natural Logarithm of MB Decay as a Function of UV Fluence; Sample Theoretical 2mg/L Liquid H_2O_2 in Post-Treatment Water
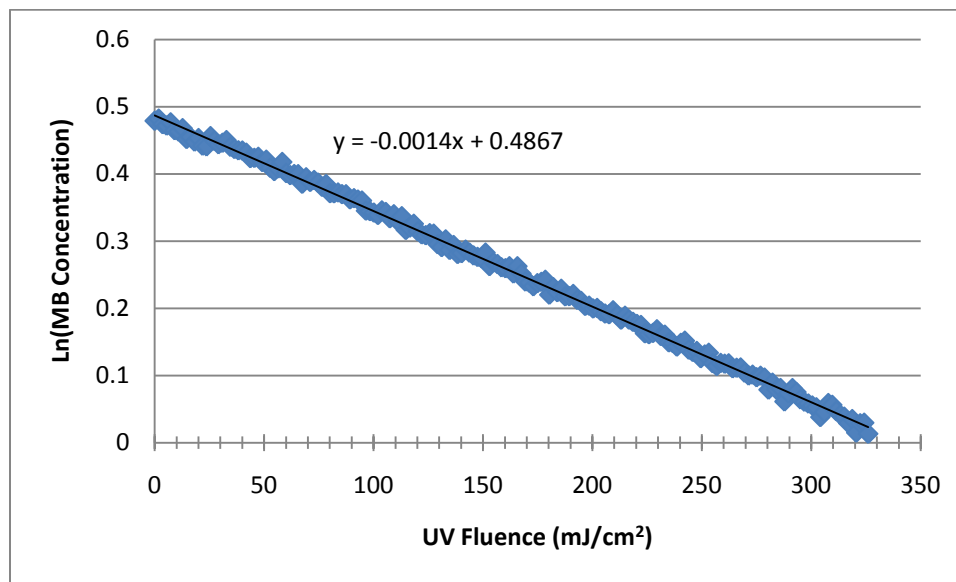
Figure D-98: Natural Logarithm of MB Decay as a Function of UV Fluence; Sample Theoretical 3mg/L Liquid H_2O_2 in Post-Treatment Water

Figure D-99: Natural Logarithm of MB Decay as a Function of UV Fluence; Sample Theoretical 4mg/L Liquid H_2O_2 in Post-Treatment Water

Figure D-100: Natural Logarithm of MB Decay as a Function of UV Fluence; Sample Theoretical 5mg/L Liquid H_2O_2 in Post-Treatment Water
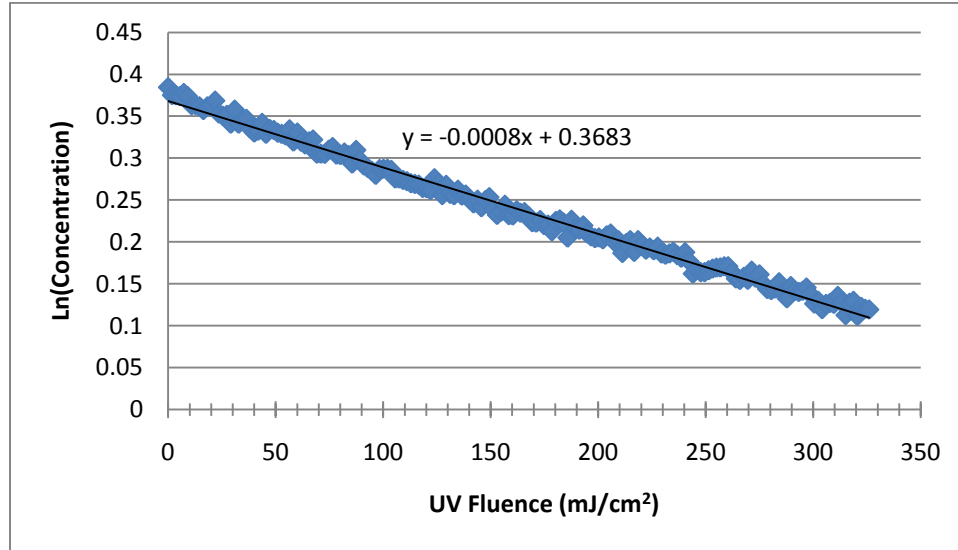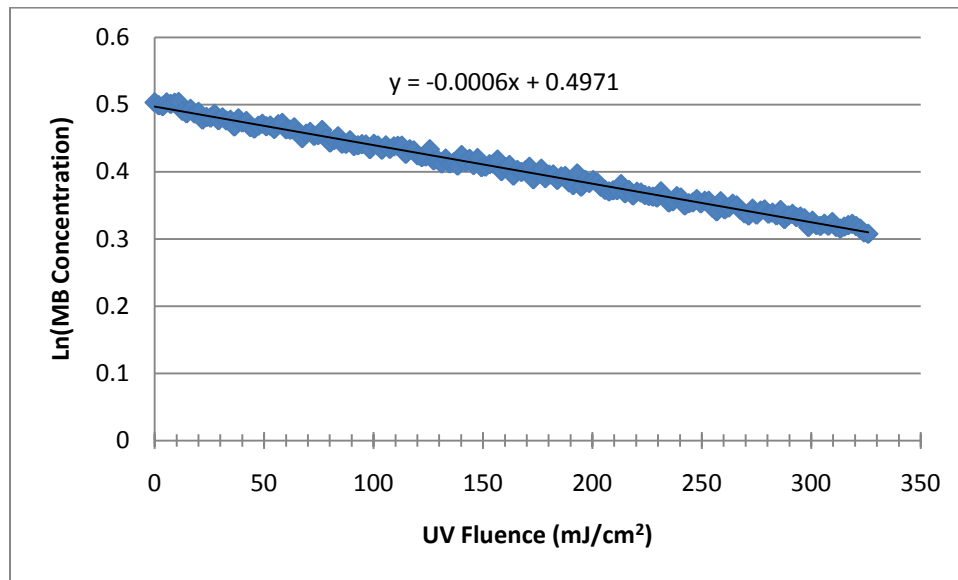
Figure D-101: Natural Logarithm of MB Decay as a Function of UV Fluence; Sample Theoretical 10mg/L Liquid H_2O_2 in Post-Treatment Water
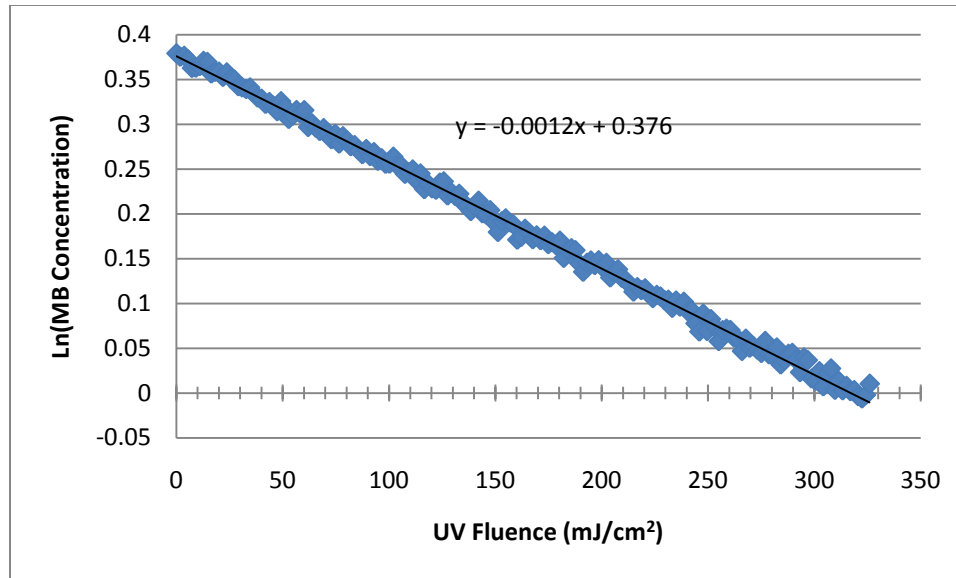

Figure D-102: Natural Logarithm of MB Decay as a Function of UV Fluence; Sample Theoretical 15mg/L Liquid H_2O_2 in Post-Treatment Water

Figures D-72 to **D-79** are plots of the natural logarithm of the methylene blue

concentration as a function of the UV fluence each sample was subject to. The negative

of the slope of the linear best fit line is equal to the pseudo-first order decay rate constant (k') of methylene blue in the post-treatment water source for SPB as the source of H_2O_2.

Figure D-103: Natural Logarithm of MB Decay as a Function of UV Fluence; Sample Theoretical 0mg/L SPB in Post-Treatment Water

Figure D-104: Natural Logarithm of MB Decay as a Function of UV Fluence; Sample Theoretical 1mg/L SPB in Post-Treatment Water

Figure D-105: Natural Logarithm of MB Decay as a Function of UV Fluence; Sample Theoretical 2mg/L SPB in Post-Treatment Water

Figure D-106: Natural Logarithm of MB Decay as a Function of UV Fluence; Sample Theoretical 3mg/L SPB in Post-Treatment Water

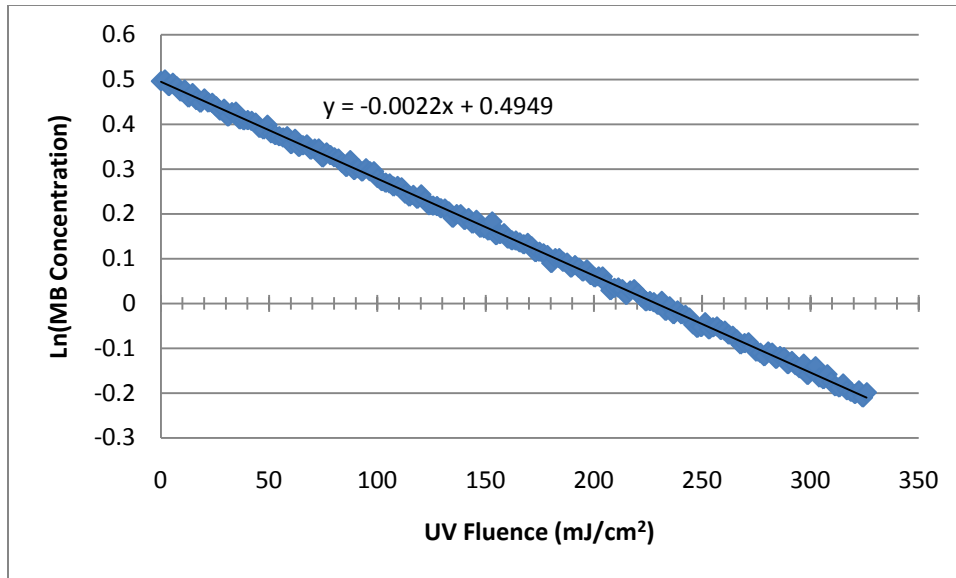Figure D-107: Natural Logarithm of MB Decay as a Function of UV Fluence; Sample Theoretical 4mg/L SPB in Post-Treatment Water
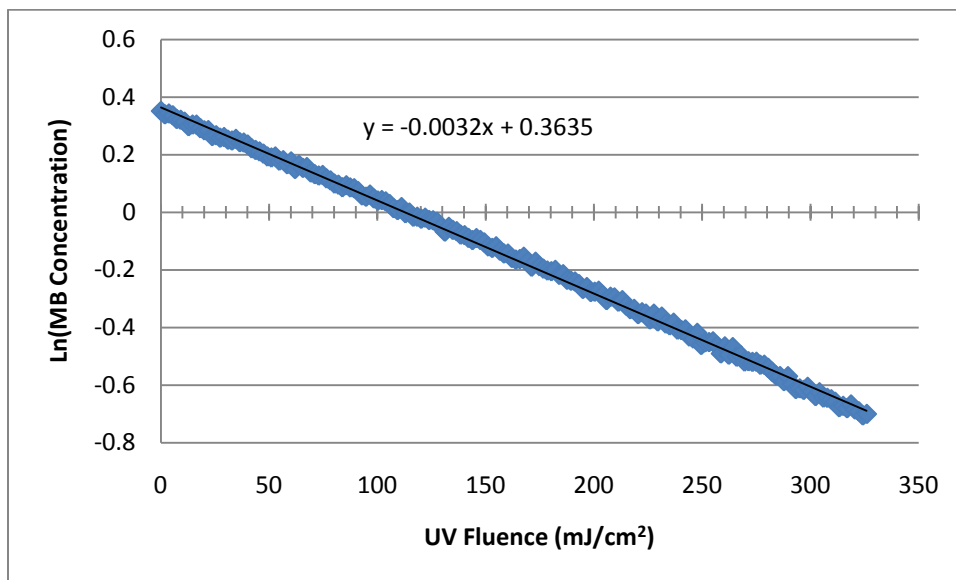

Figure D-108: Natural Logarithm of MB Decay as a Function of UV Fluence; Sample Theoretical 5mg/L SPB in Post-Treatment Water
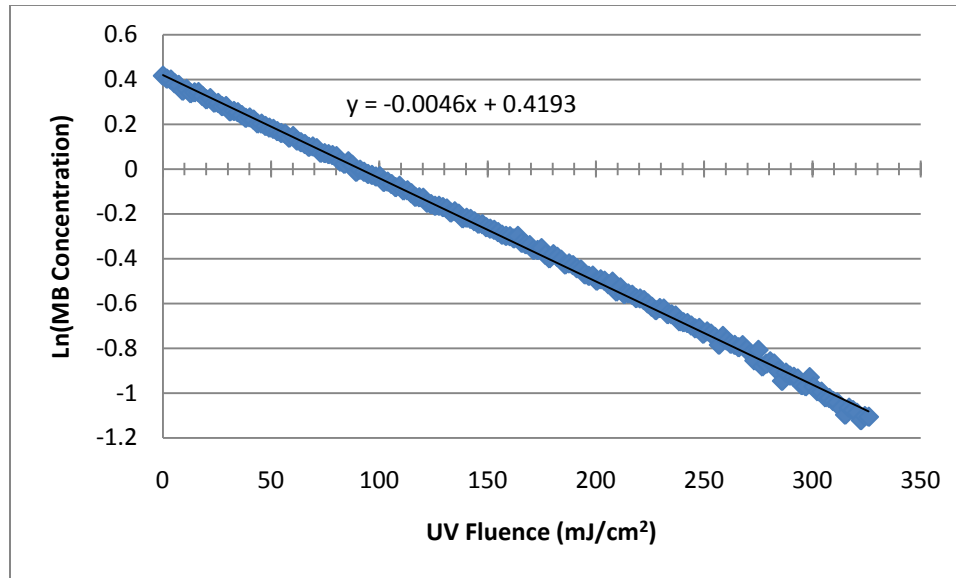
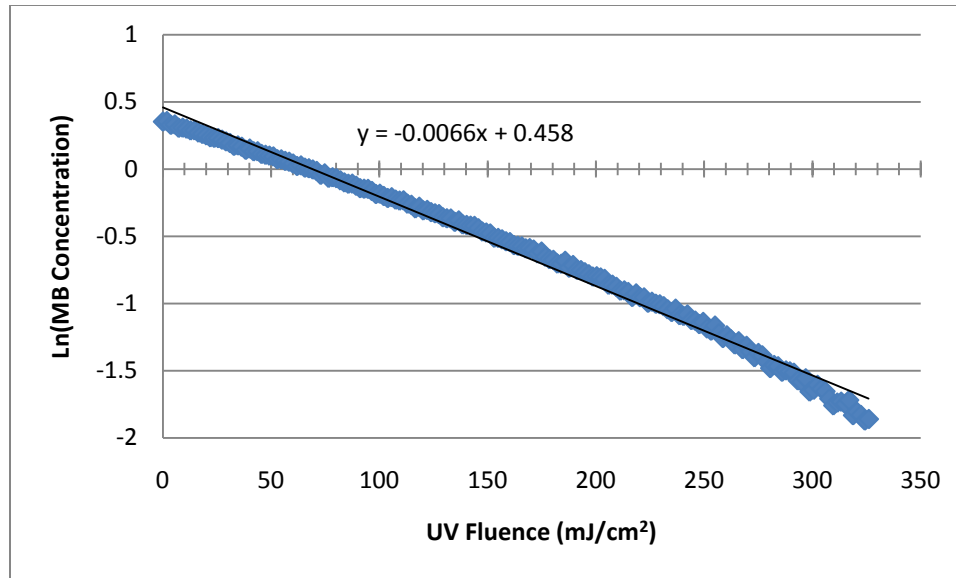Figure D-109: Natural Logarithm of MB Decay as a Function of UV Fluence; Sample
Theoretical 10mg/L SPB in Post-Treatment Water
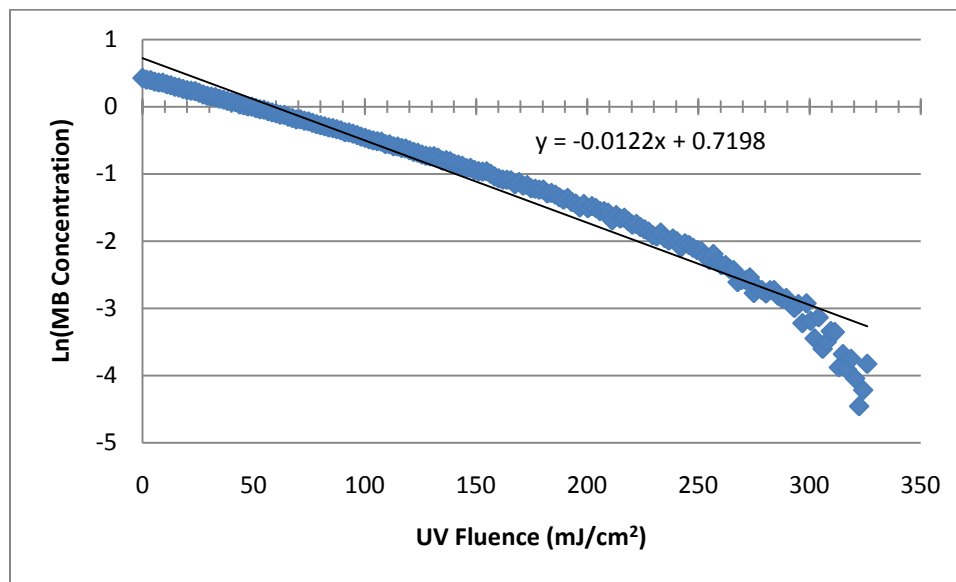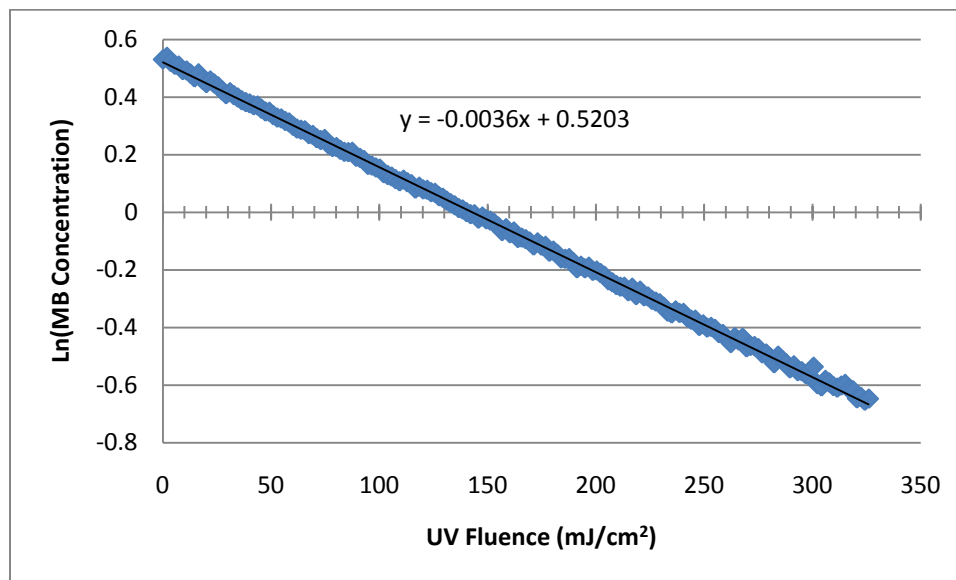

Figure D-110: Natural Logarithm of MB Decay as a Function of UV Fluence; Sample
Theoretical 15mg/L SPB in Post-Treatment Water

Figures D-80 to **D-87** are plots of the natural logarithm of the methylene blue

concentration as a function of the UV fluence each sample was subject to. The negative

of the slope of the linear best fit line is equal to the pseudo-first order decay rate constant (k') of methylene blue in the post-treatment water source for SPC as the source of H_2O_2.
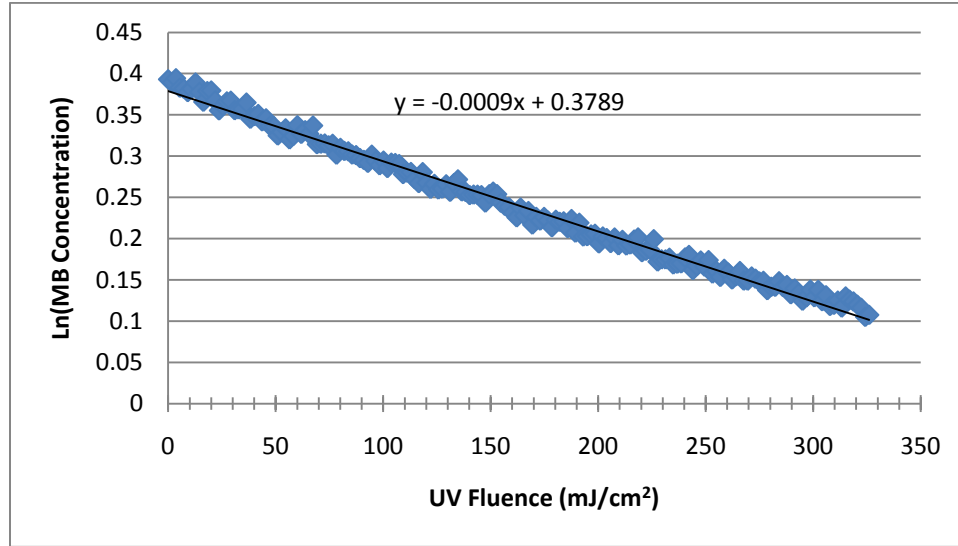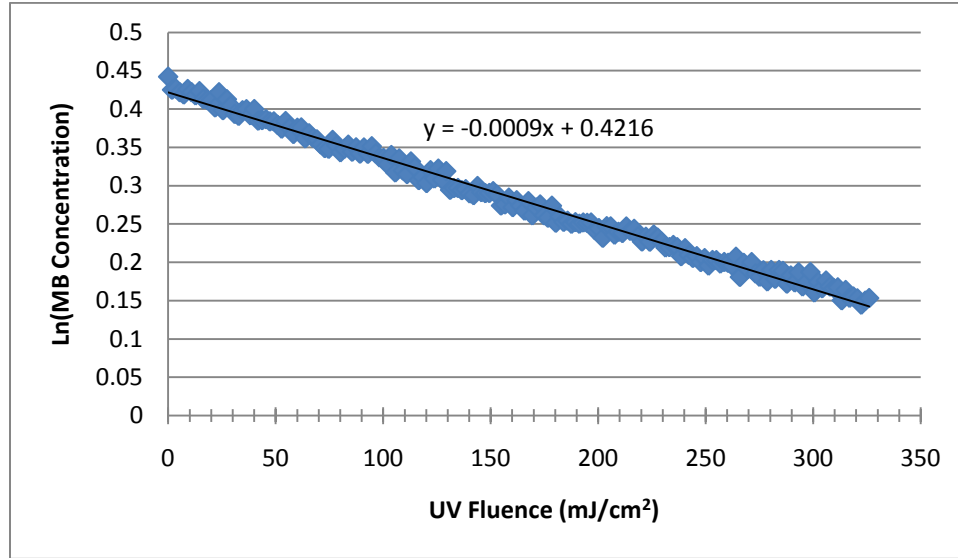

Figure D-111: Natural Logarithm of MB Decay as a Function of UV Fluence; Sample Theoretical 0mg/L SPC in Post-Treatment Water
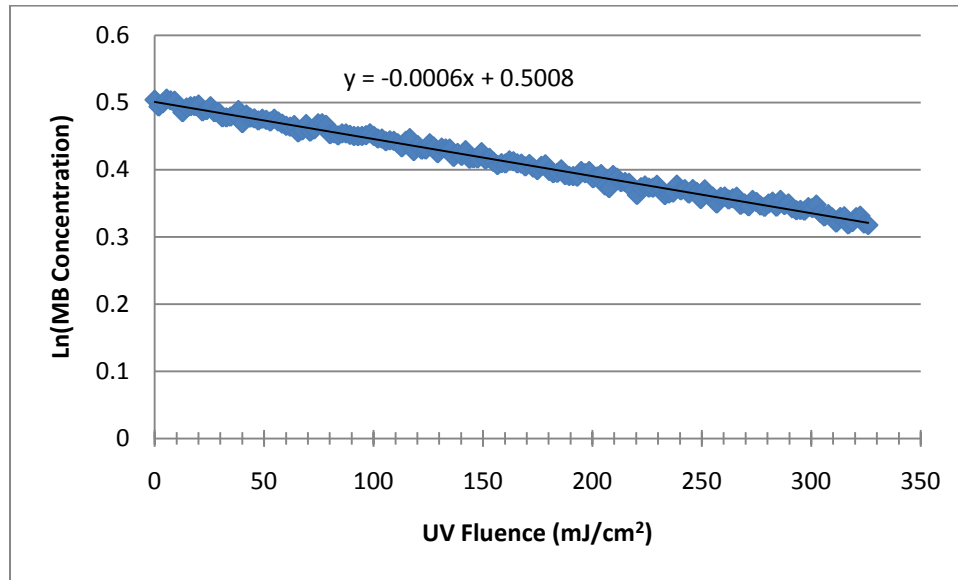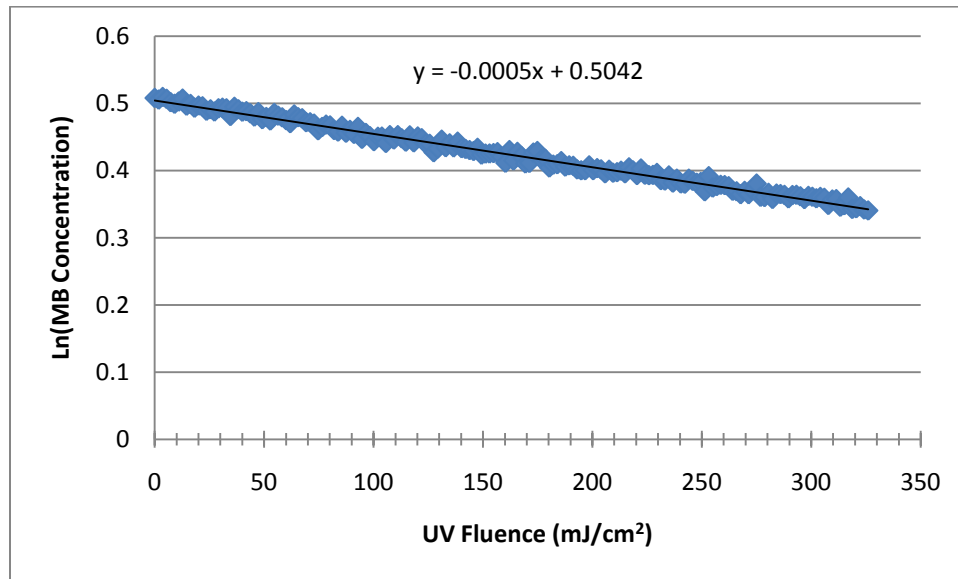

Figure D-112: Natural Logarithm of MB Decay as a Function of UV Fluence; Sample Theoretical 1mg/L SPC in Post-Treatment Water
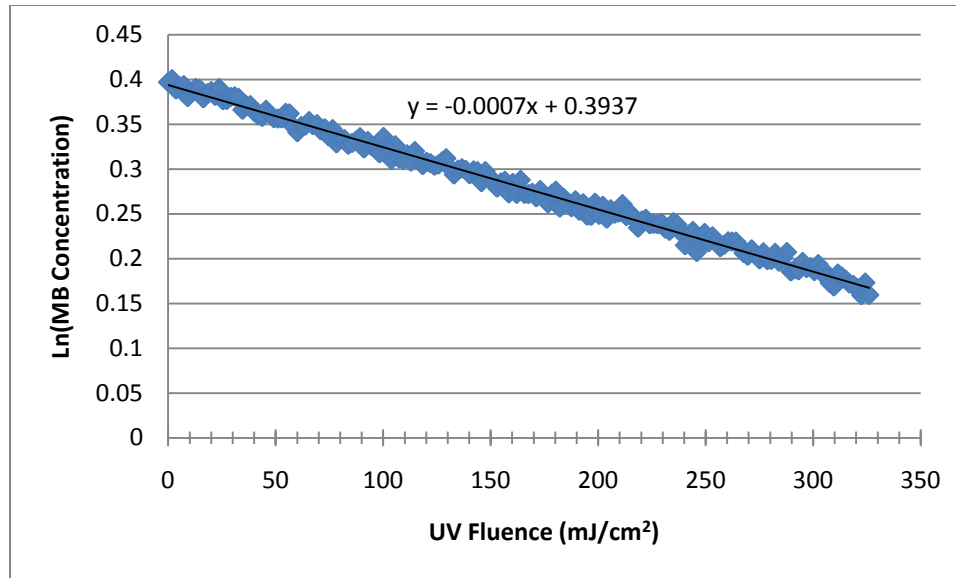
Figure D-113: Natural Logarithm of MB Decay as a Function of UV Fluence; Sample Theoretical 2mg/L SPC in Post-Treatment Water
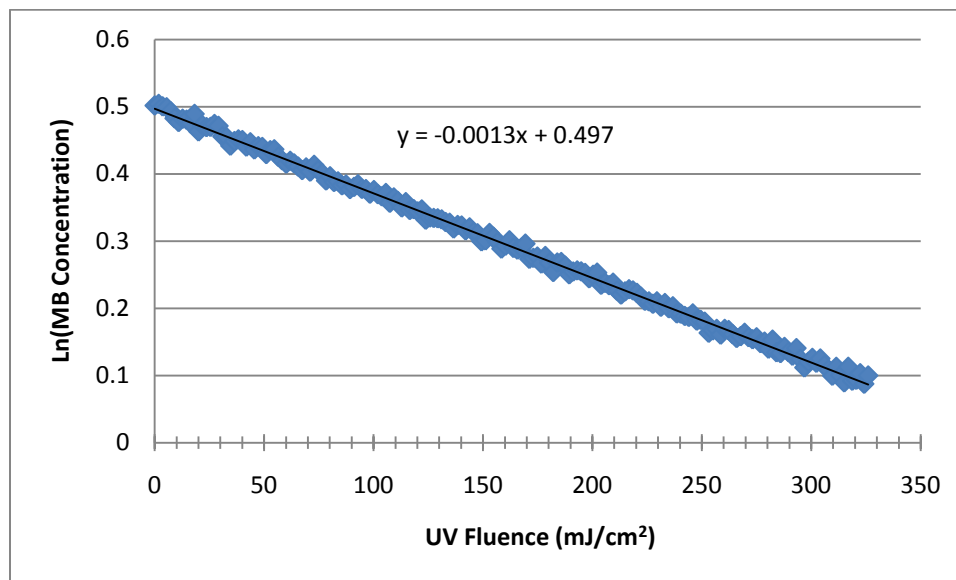
Figure D-114: Natural Logarithm of MB Decay as a Function of UV Fluence; Sample Theoretical 3mg/L SPC in Post-Treatment Water
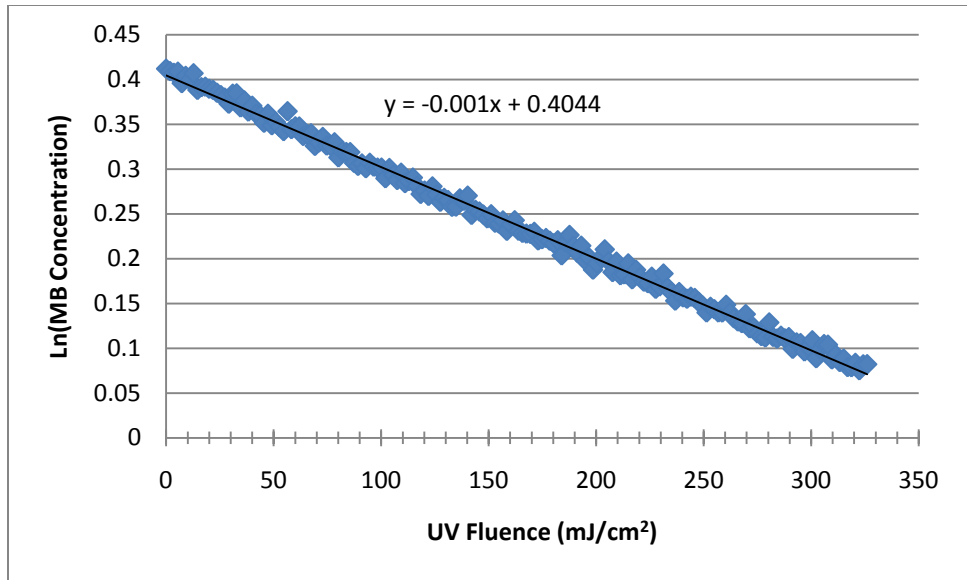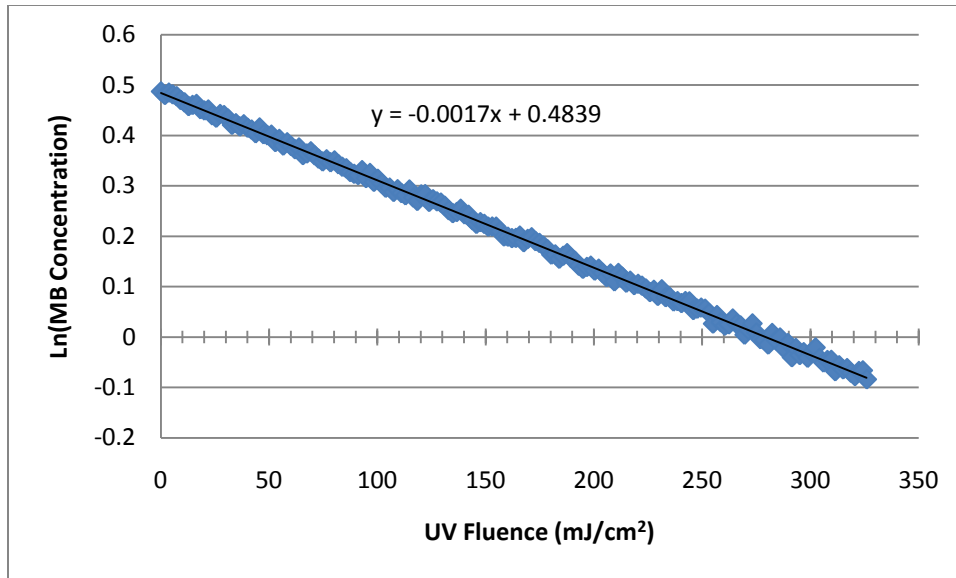
4Figure D-115: Natural Logarithm of MB Decay as a Function of UV Fluence; Sample Theoretical 4mg/L SPC in Post-Treatment Water
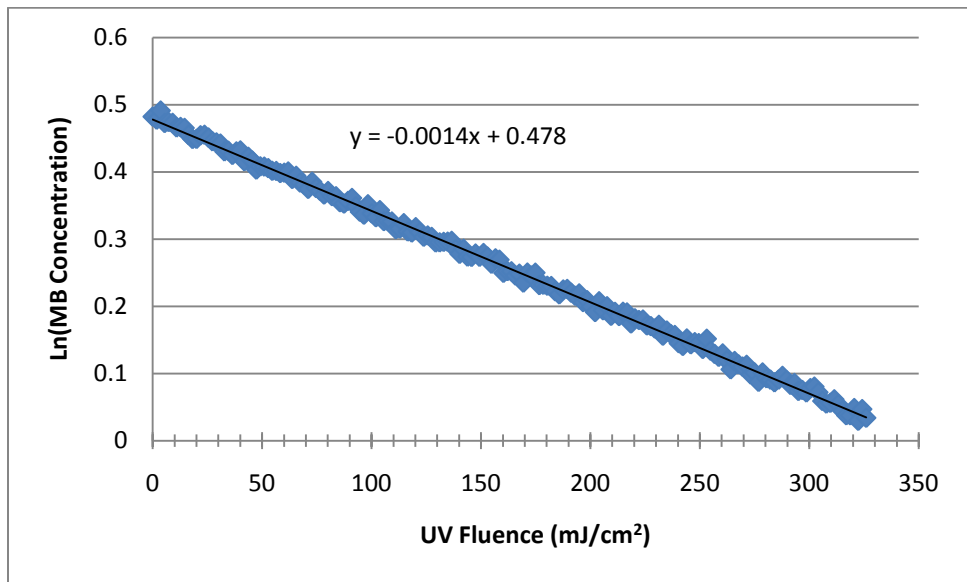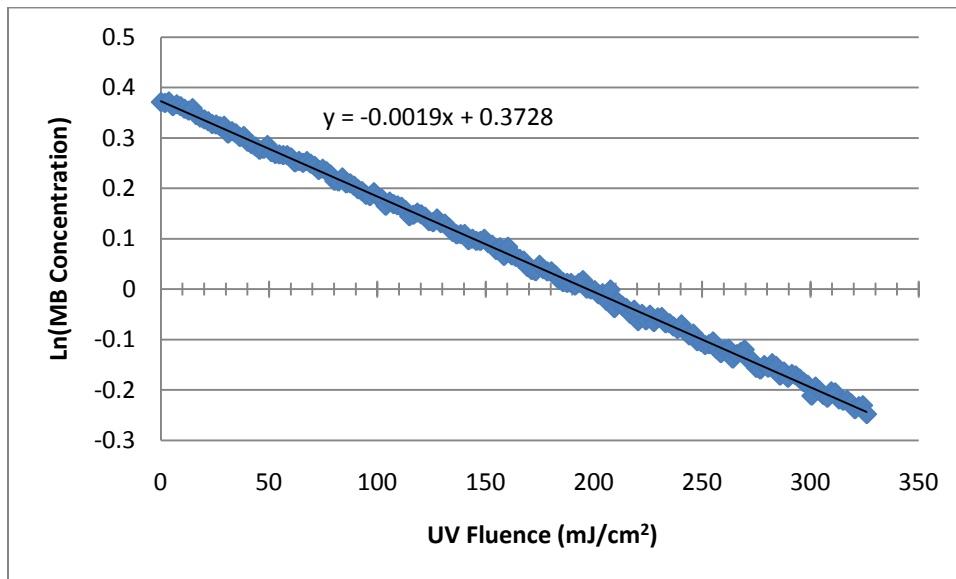

Figure D-116: Natural Logarithm of MB Decay as a Function of UV Fluence; Sample Theoretical 5mg/L SPC in Post-Treatment Water
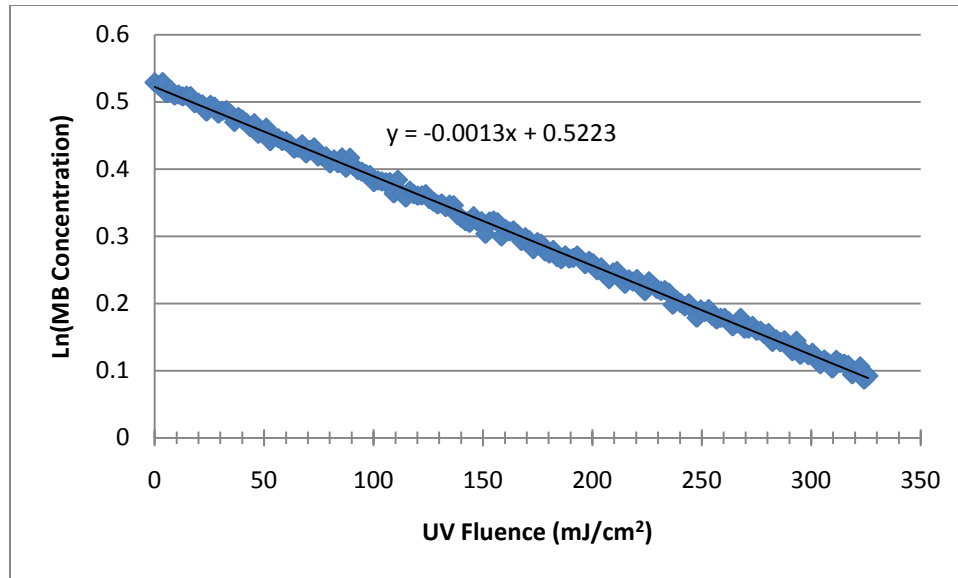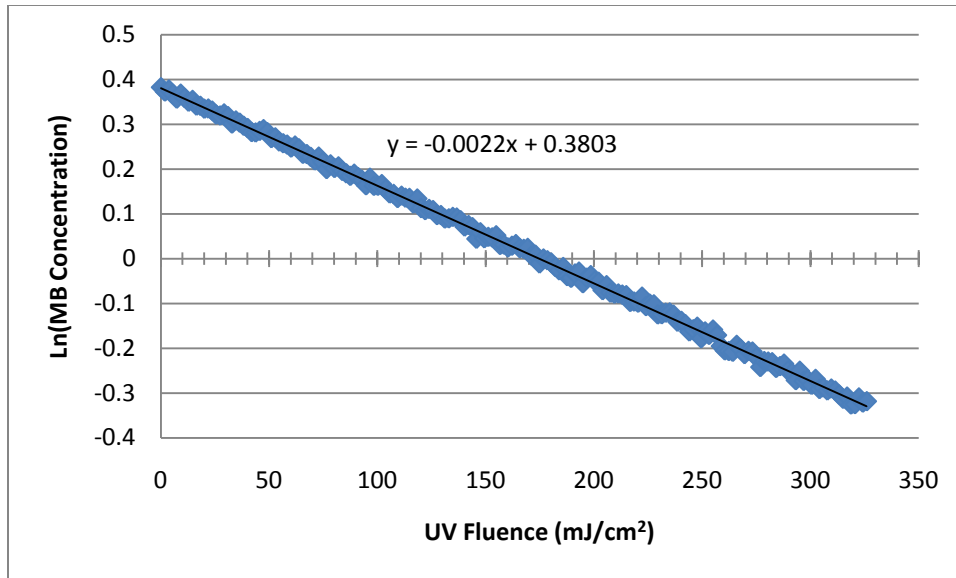
Figure D-117: Natural Logarithm of MB Decay as a Function of UV Fluence; Sample Theoretical 10mg/L SPC in Post-Treatment Water
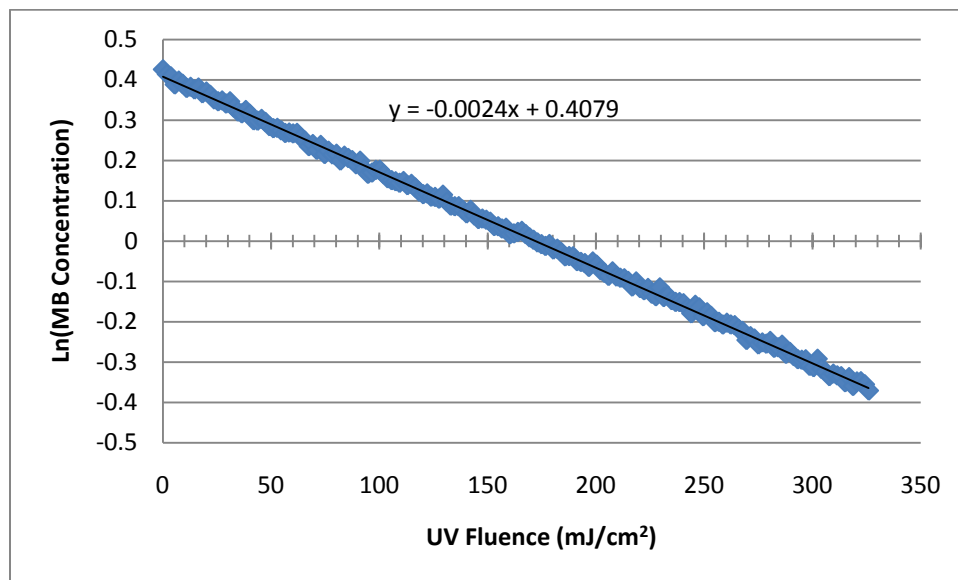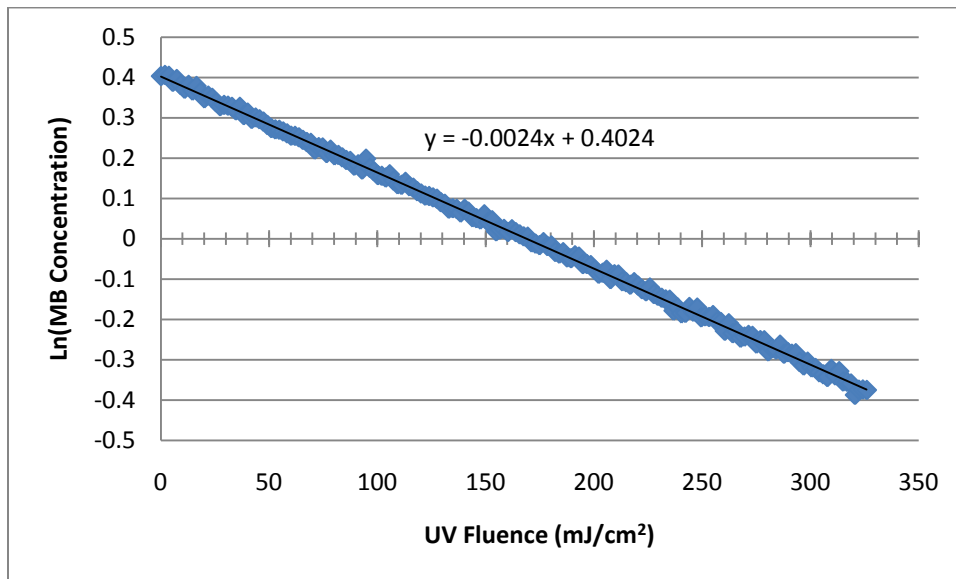

Figure D-118: Natural Logarithm of MB Decay as a Function of UV Fluence; Sample Theoretical 15mg/L SPC in Post-Treatment Water

APPENDIX E: REPLICATE COMPARISON PLOTS OF UV EXPOSURES

Figures E-1 and **E-2** are replicate analyses of methylene blue decay in for theoretical H_2O_2 concentrations of 2mg/L and 15mg/L via addition of liquid H_2O_2, SPB and SPC to DI water. The results of the replicate analysis gives validation to the methods used to measure methylene blue decay.
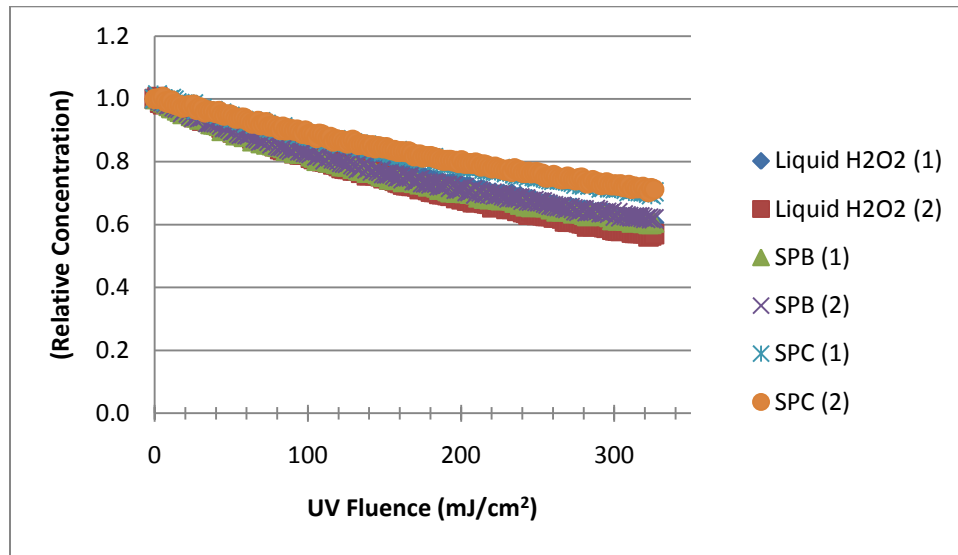
Figure E-119: Replicate Analysis of UV Exposures; Samples are Theoretical 2mg/L H_2O_2 in DI Water
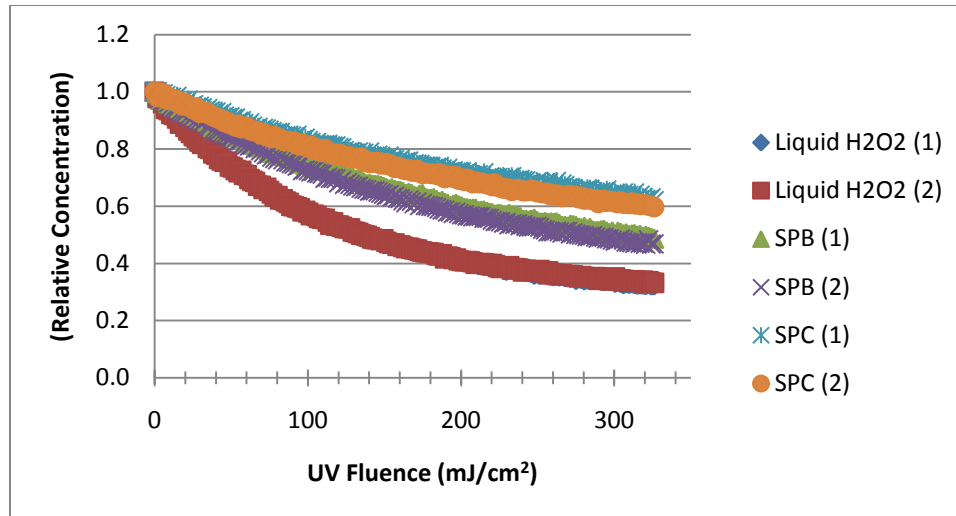
Figure E-120: Replicate Analysis of UV Exposures; Samples are Theoretical 15mg/L H_2O_2 in DI Water

Figures E-3 and **E-4** are replicate analyses of methylene blue decay in for

theoretical H_2O_2 concentrations of 2mg/L and 15mg/L via addition of liquid H_2O_2, SPB

and SPC to the pre-treatment water source.
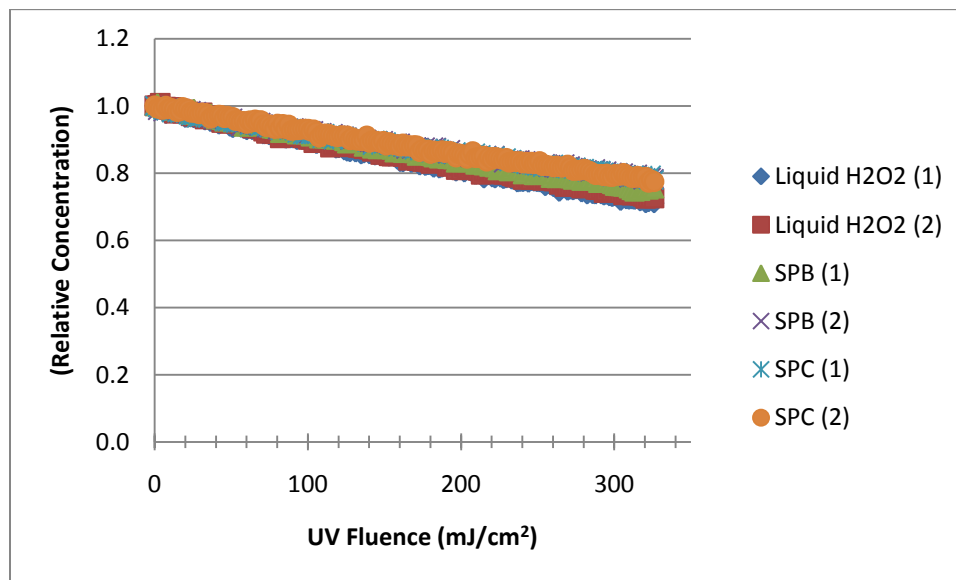
Figure E-121: Replicate Analysis of UV Exposures; Samples are Theoretical 2mg/L H_2O_2 in Pre-Treatment Water
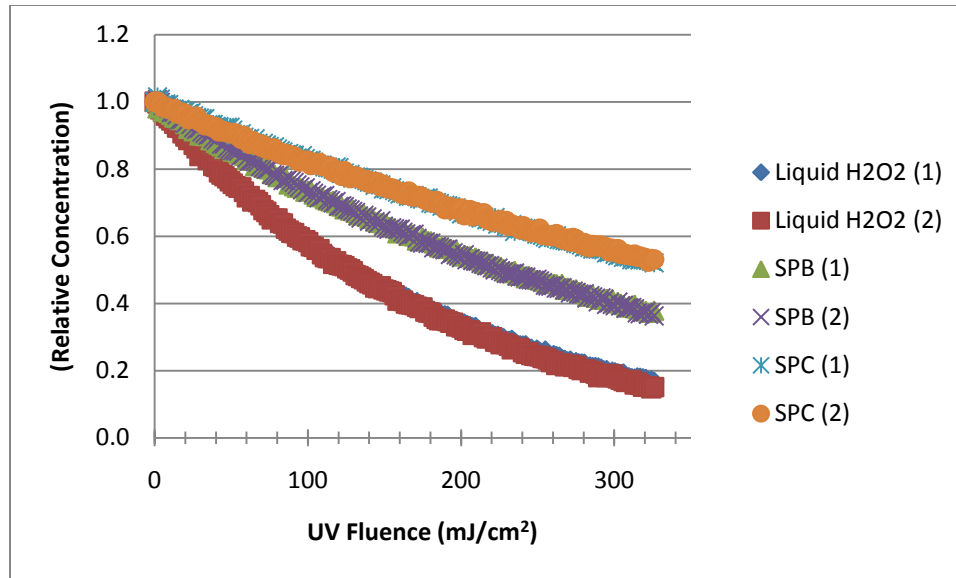
Figure E-122: Replicate Analysis of UV Exposures; Samples are Theoretical 15mg/L H_2O_2 in Pre-Treatment Water

Figures E-5 and **E-6** are replicate analyses of methylene blue decay in for

theoretical H_2O_2 concentrations of 2mg/L and 15mg/L via addition of liquid H_2O_2, SPB

and SPC to the treated, unchlorinated water source.
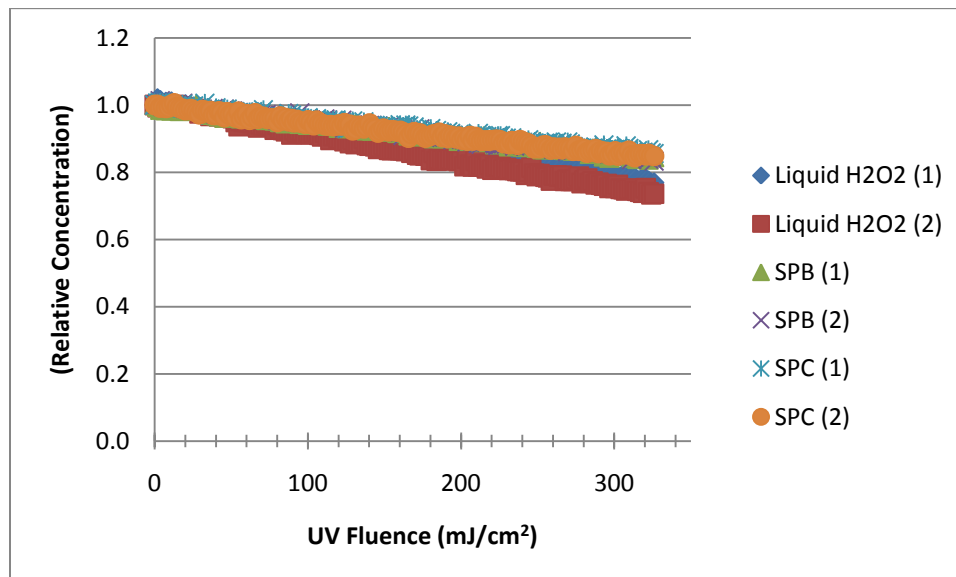
Figure E-123: Replicate Analysis of UV Exposures; Samples are Theoretical 2mg/L H_2O_2 in Treated, Unchlorinated Water
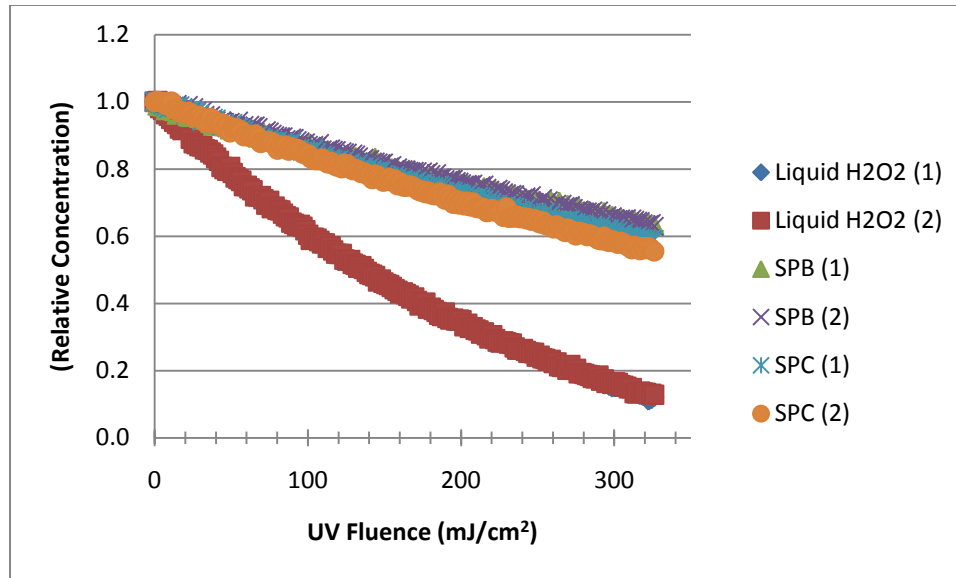
Figure E-124: Replicate Analysis of UV Exposures; Samples are Theoretical 15mg/L H_2O_2 in Treated, Unchlorinated Water

Figures E-7 and **E-8** are replicate analyses of methylene blue decay in for

theoretical H_2O_2 concentrations of 2mg/L and 15mg/L via addition of liquid H_2O_2, SPB

and SPC to the post-treatment water source.
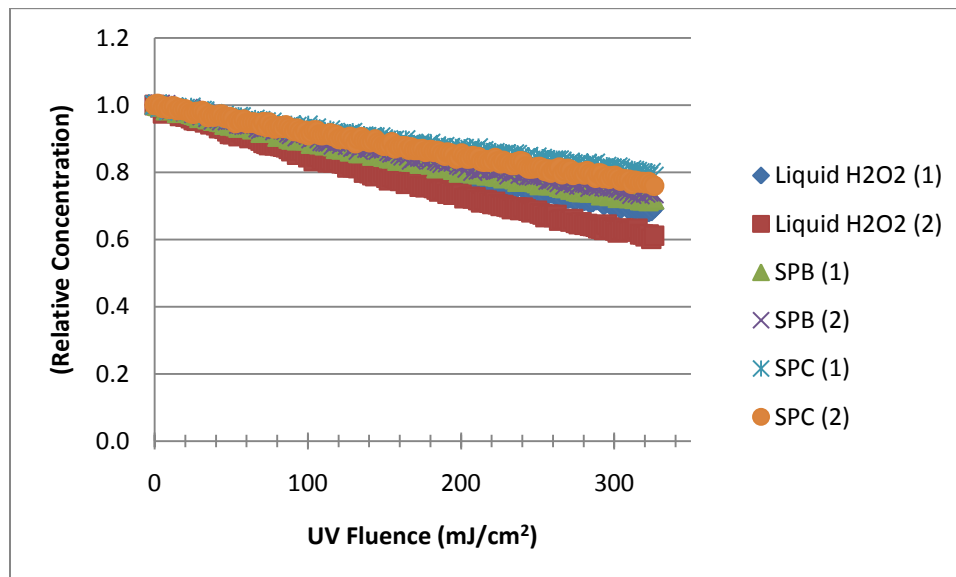
Figure E-125: Replicate Analysis of UV Exposures; Samples are Theoretical 2mg/L H_2O_2 in Post-Treatment Water
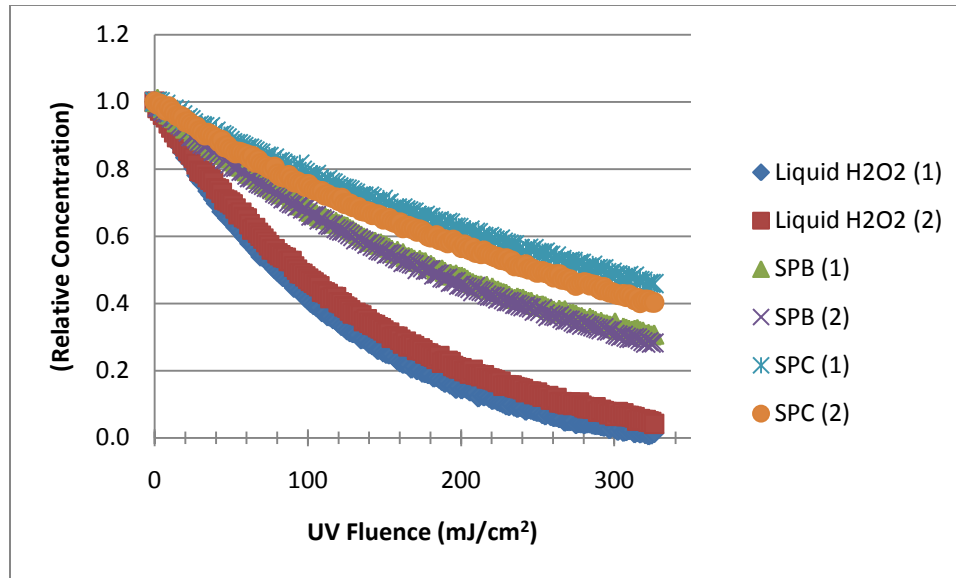
Figure E-126: Replicate Analysis of UV Exposures; Samples are Theoretical 15mg/L H_2O_2 in Post-Treatment Water

BIBLIOGRAPHY

Acros Organics. (2009). "Sodium Perborate monohydrate MSDS." Updated as of 7/20/2009.

Acros Organics. (2009). "Sodium Percarbonate MSDS." Updated as of 7/20/2009.

Alfa Aesar. (2010). Communcation with Debora Fatello regarding costs of sodium perborate and sodium percarbonate on 28 SEP 2010.

Andreozzi, R., Campanella, L. Fraysse, B., Garric, J., Gonnella, A., Lo Guidice, R., Marrotta, R. Pinto, G. and Pollio, A. (2004). "Effects of advanced oxidation processes (AOPs) on the toxicity of a mixture of pharmaceuticals." *Wat Sci. and Tech.* **50**. (2004), pp. 23-28.

APHA. (1992). "Standard Methods of Water and Wastewater." 18th ed. American Public Health Association, American Water Works Association, Water Environment Federation publication. Washington DC.

Argonne National Library (Undated). "Proper Segregation of Chemical Classes." US Department of Energy, Office of Science. Viewed at <http://www.aps.anl.gov/Safety_and_Training/User_Safety/chemstorage.html> on 29 NOV 2010.

Bolton, J.R. (2010). "Ultraviolet Applications Handbook." Edmonton: Bolton Photosciences, Inc.

Borax. (2005). "Bleaching with Sodium Perborate." Viewed at <http://www.borax.com/detergents/bleaching.html> on 14 SEP 2010.

Brenntag Group. (2010a). Communication with Brian Bartashus, Inside Sales/New Accountant Specialist regarding sodium perborate and sodium percarbonate costs on 14 OCT 2010.

Brenntag Group. (2010b). "Brenntag Group – North America." Viewed at <http://www.brenntag.com/en/pages/BrenntagWorldwide/Regions/Nordamerika/index.html> on 27 OCT 2010.

Buxton, G.V. and Sellers, R.M. (1987). "Reactivity of the Hydrated Electron and the Hydroxyl Radical with Boric Acid in Aqueous Solutions." *International Journal of Radiation Applications and Instrumentation*. **29**. (1987), pp. 137-140.

Buxton, G.V., Greenstock, C.L., Helman, W.P. and Ross, A.B. (1988). "Critical Review of Rate Constants for the Reactions of Hydrated Electrons, Hydrogen Atoms and

Hydroxyl Radicals in Aqueous Solutions." *J. Phys. Chem. Ref. Data.* **17**. (1988), pp. 513-886.

Caldeira, K. and Rau, G.H. (2000). "Accelerating carbonate dissolution to sequester carbon dioxide in the ocean: Geochemical implications." *Geochemical Research Letters*. **27**. (2000), pp. 225-228.

Carlson, D.A., Seabloom, R.W., DeWalle, F.B., Wetzler, T.F., Engeset, J., Butler, R., Wangsuphachart, S., and Wang, S. (1985). "Ultraviolet Disinfection of Water for Small Water Supplies." US EPA Report No. EPA/600/S2-85/092.

Chang, M-W., Chung, C-C., Chern, J-M. and Chen, T-S. (2010). "Dye composition kinetics by UV/H_2O_2: Initial rate analysis by effective kinetic modeling methodology." *Chemical Engineering Science*. **65**. (2010), pp. 135-140.

CSX (2010a). "Carbon Calculator." Viewed at <http://www.csx.com/index.cfm/customers/tools/carbon-calculator/> on 27 OCT 2010.

CSX (2010b). "Carbon Calculator Calculation Methodology and Arthur D. Little Validation Statement." Viewed at <http://www.csx.com/index.cfm/customers/tools/carbon-calculator/methodology/> on 27 OCT 2010.

Doom, T. (2008). "Characterizing Hydrogen Peroxide Degradation By Granular Activated Carbon For Advanced Oxidation Processes In Water Treatment." Department of Civil, Environmental and Architectural Engineering, University of Colorado at Boulder.

Drink H_2O_2. (Undated). "Hydrogen Peroxide Therapy: Drinking Hydrogen Peroxide." Viewed at < http://drinkh2o2.com/#hydrogen-peroxide-grades> on 22 SEP 2010.

Eisenberg, G.M. (1943). "Colorimetric Determination of Hydrogen Peroxide." *Ind. Eng. Chem. Anal. Ed.* **15**. (1943), pp. 327-328.

European Chemical Industry Council. (1997). "Ecoprofile of Perborates." Viewed at <http://www.cefic.org/sector/peroxy/ecoperb/tc.htm#tc> on 14 SEP 2010.

Frey, M.M., Seidel, C., Edwards, M., Parks, J. and McNeill, L. (2004). "Occurrence Survey for Boron and Hexavalent Chromium." AWWARF Report No. 90144F.

FMC Chemicals. (2010). Communication with Steven Yuan, Commercial Development Manager of the FMC Chemicals Peroxygens Division regarding hydrogen peroxide costs on 21 OCT 2010.

General Kinetics, LLC. (1999). "A Brief History of Concentrated Hydrogen Peroxide Uses." AIAA-1999-2739. Presented by M. Ventura and C. Garboden.

Georgiou, D., Melidis, P., Aivasidis, A. and Gimouhopoulos, K. (2001). "Degradation of azo-reactive dyes by ultraviolet radiation in the presence of hydrogen peroxide." *Dyes and Pigments*. **52**. (2002), pp. 69-78.

GHG Protocol. (2005). "Calculation Tool for Direct Emissions from Transport or Mobile Sources." Version 1.3. Updated as of 21 MAR 2005.

Glaze, W.H., Kang, J. and Chapin, D. (1987). "The Chemistry of Water Treatment Processes Involving Ozone, Hydrogen Peroxide and Ultraviolet Radiation." *Ozone Science and Engineering*. **9**. (1987), pp. 335-352.

Glaze, W.H., Lay, Y., and Kang, J. (1995). "Advanced Oxidation Processes. A Kinetic Model for the Oxidation of 1,2-Dibromo-3-chloropropane in Water by the Combination of Hydrogen Peroxide and UV Radiation." *Ind. Eng. Chem. Res.* **34.** (1995), pp 2314-2323.

Goel, N. (2007). "Pharmaceutical Chemistry: Pharmaceutical Acids and Necessities." Maharaja Surajmal Institute of Pharmacy, New Dehli, India.

Google Maps. (2010). Used as a Map Generation Tool. Viewed at <http://maps.google.com/> on 27 OCT 2010.

Gultekin, I. and Ince, N.H. (2004). "Degradation of Reactive Azo Dyes by UV/H_2O_2: Impact of Radical Scavengers." *J. Envir. Sci. and Heal.*. **A39.** (2004), pp. 1069-1081.

Hross, M.H. (2010). "Rapid Measurement of Background Hydroxyl Radical Scavenging in Water." Masters Project. University of Massachusetts – Amherst, Department of Civil and Environmental Engineering.

Ince, N.H. and Apikyan, I.G. (1999). "Combination of Activated Carbon Adsorption with Light-Enhanced Chemical Oxidation via Hydrogen Peroxide." *Wat. Res.* **34**. (2000), pp. 4169-4176.

Illinois Department of Public Health. (Undated). "Commonly Found Substances in Drinking Water and Available Treatment." Viewed at <http://www.idph.state.il.us/envhealth/pdf/DrinkingWater.pdf> on 19 OCT 2010.

ITT Water and Wastewater. (Undated). "Advanced Oxidation Processes." Viewed at <http://www.wedeco.com/us/index.php?id=91313> on 16 SEP 2010

Klassen, N.V., Marchington, D. and McGowan, H.C.E. (1994). "H_2O_2 Determination by the I_3^- Method and $KMnO_4$ Titration." *Anal. Chem.* **66**. (1994), pp. 2921-2925.

Legrini, O., Oliveros, E. and Braun, A.M. (1993). "Photochemical Processes for Water Treatment." *Chem. Rev.* **93**. (1993), 671-698.

Liao, C. and Gurol, M. (1995). "Chemical Oxidation by Photolytic Decomposition of Hydrogen Peroxide." *Envrion. Sci. Technol*. **29**. (1995), pp. 3007-3014.

Liao, C., Kang, S. and Wu, F. (2000). "Hydroxyl radical scavenging role of chloride and bicarbonate ions in the H_2O_2/UV process." *Chemosphere.* **44**. (2001), pp. 1193-1200.

Magnussen, N. (1997). "Oxidizing Materials." College of Science, Texas A&M University. Viewed at <http://safety.science.tamu.edu/oxidizers.html> on 29 NOV 2010.

McKillop, A. and Sanderson, W.R. (1995). "Sodium Perborate and Sodium Percarbonate: Cheap, Safe and Versatile Oxidising Agents for Organic Synthesis." *Tetrahedron*. **51**. (1995), pp. 6145-6166.

McKillop, A. and Sanderson, W.R. (1999). "Sodium perborate and sodium percarbonate: further applications in organic synthesis." *J. Chem. Soc., Perkin Trans*. **1**. (2000), pp. 471-476.

Modrzejewska, B., Guwy, A.J., Dinsdale, R. and Hawkes, D.L. "Measurement of hydrogen peroxide in an advanced oxidation process using an automated biosensor." *Water Research*. **41**. (2007), pp. 260-268.

Muzart, J. (1995). "Sodium Perborate and Sodium Percarbonate in Organic Synthesis." *Synthesis*. **11**. (1995), pp. 1325-1347.

National Research Council (1995). "Prudent Practices in the Laboratory: Handling and Disposal of Chemicals." Committee on Prudent Practices for Handling, Storage and Disposal of Chemicals in Laboratories.

National Research Council. (1999). "Identifying Future Drinking Water Contaminants." 1998 Workshop on Emerging Drinking Water Contaminants. *National Academies Press.*

OCI Chemical Company. (2010a). "Sodium Percarbonate Logistics." Viewed at <http://www.ocichemical.com/sodium_percarbonate/sp_logistics.asp?SubnavID=24> on 15 SEP 2010.

OCI Chemical Company (2010b). Communication with Joshua Smith, Territory Sales Rep. – Northeast regarding the costs of hydrogen peroxide and sodium percarbonate on 7 SEP 2010.

Pantin, S. (2009). "Impacts of the UV-H_2O_2 Treatment for Taste and Odour Control on Secondary Disinfection." Master's Thesis. Department of Civil Engineering, University of Toronto.

Perelygin, Y.P. and Chistyakov, D.Y. (2006). "Boric Acid." *Russian Journal of Applied Chemistry.* **79**. (2006), pp. 2041-2042.

Rosenfeldt, E.J., Linden, K.G., Canonica, S. and von Guten, U. (2006). "Comparison of the efficiency of ·OH radical formation during ozonation and the advanced oxidation processes O_3/H_2O_2 and UV/H_2O_2. *Water Research*. **40**. (2006), pp 3695-3704.

Rosenfeldt, E.J., Linden, K.G., Canonica, S. and von Guten, U. (2008). "Erratum to Comparison of the efficiency of ·OH radical formation during ozonation and the advanced oxidation processes O_3/H_2O_2 and UV/H_2O_2. *Water Research*. **42**. (2008), pp 2836-2838.

Solvay Chemicals. (2005). "Hydrogen Peroxide: Safety and Handling." Technical Data Sheet. Updated as of MAR 2005.

Swinehart, D.F. (1962). "The Beer-Lambert Law." *J.Chem. Educ.* **39**. (1962), pp. 333.

Tayade, R.J., Natarajan, T.S. and Bajaj, H.C. (2009). "Photocatalytic Degradation of Methylene Blue Dye Using Ultraviolet Light Emitting Diodes." *Ind. Eng. Chem. Res.* **48**. (2009), pp. 10262-10267.

Toor, R. and Mohseni, M. (2006). "UV-H_2O_2 based AOP and its integration with biological activated carbon treatment for DBP reduction in drinking water." *Chemosphere*. **66**. (2007), pp. 2087-2095.

US Peroxide (2009). "Hazard Classes." Viewed at <http://www.h2o2.com/technical-library/default.aspx?pid=76&name=Hazard-Classes> on 29 NOV 2010.

US Peroxide. (2010a). Communication with Paris Neofotistos, Regional Manager, Eastern Division regarding the costs of hydrogen peroxide on 27 OCT 2010.

US Peroxide (2010b). "How much does H_2O_2 Cost?" Viewed at <http://www.h2o2.com/faqs/FaqDetail.aspx?fId=25> on 27 OCT 2010.

Vela, M.E., Vilche, J.R. and Arvia, A.J. (1986). "The dissolution and passivation of polycrystalline iron electrodes in boric acid-borate buffer solutions in the 7.5-9.2 pH range." *Journal of Applied Electrochemistry*. **16**. (1986), pp. 490-504.

US Department of Health and Human Services. (2010). "Household Products Database – Sodium Percarbonate" Updated as of June 2010. Viewed at <http://householdproducts.nlm.nih.gov/cgi-

bin/household/brands?tbl=chem&id=2888&query=sodium+percarbonate&searchas= TblChemicals> on14 SEP 2010.

US EPA. (1976). "Toxic Substances Control Act."

US EPA. (2007). "Ultraviolet (UV) Disinfection Systems for Secondary Wastewater Effluent and Water Reuse." Environmental Technology Verification Program.

US EPA. (2008a). "Regulatory Determinations Support Document for Selected Contaminants from the Second Drinking Water Contaminant Candidate List (CCL2): Chapter 3: Boron." EPA Report No. EPA/815/R-08/012.

US EPA. (2008b). "Drinking Water Health Advisory for Boron." EPA Report No. EPA/882/R-08/013.

Walling, Cheves. (1975). "Fenton's Reagent Revisited." *Acc. Chem. Res.* **8** (1975), pp. 125-131.

Wang, G., Liao, C. and Wu, F. (1999). "Photodegradation of humic acids in the presence of hydrogen peroxide." *Chemosphere*. **42** (2001), pp. 379-387.

Wernimont, E.J. and Durant, D. (2004). "Development of a 250lbfv Kerosene – 90% Hydrogen Peroxide Thruster." General Kinetics, Inc. Presented to 40th AIAA/ASME/SAE/ASEE Joint Propulsion Conference and Exhibit. July 2004.

Wernimont, E.J. and Ventura, M.C. (2009). "Low Temperature Operation of Hydrogen Peroxide Gas Generators: Verification Testing & Possible Applications." General Kinetics, Inc. Presented to 7th International Energy Conversion Engineering Conference. August 2009.

Yao, J. and Wang, C. (2010). "Decolorization of Methylene Blue with TiO_2 Sol via UV Irradiation Photocatalytic Degradation." *International Journal of Photoenergy*. **2010**, 6 pages.